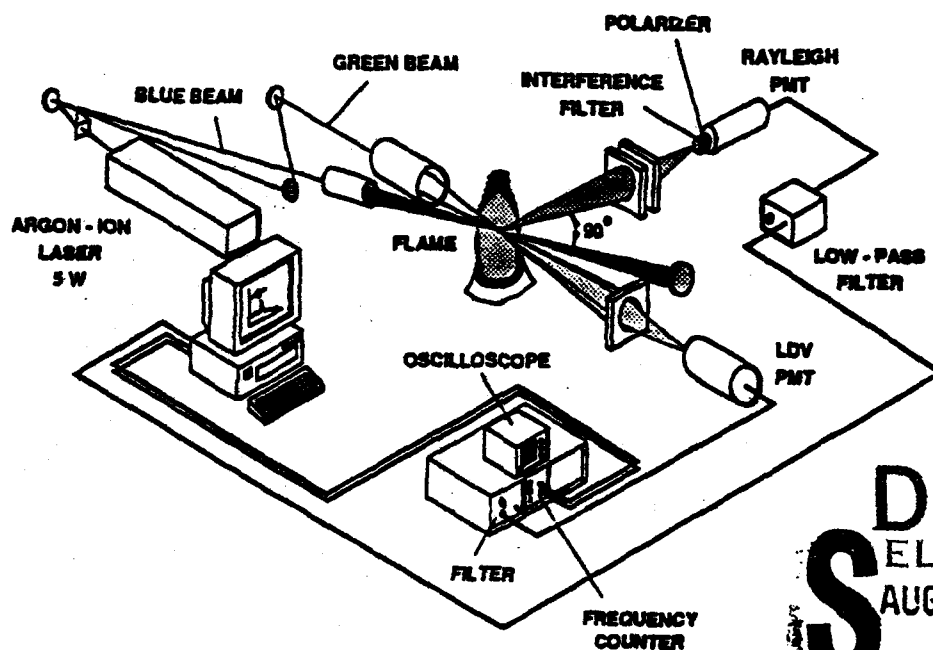


THE THIRD INTERNATIONAL SYMPOSIUM ON  
SPECIAL TOPICS IN CHEMICAL PROPULSION:

NON-INTRUSIVE COMBUSTION  
DIAGNOSTICS

May 10-14, 1993  
Scheveningen, The Netherlands

AD-A267 595



DTIC  
ELECTE  
AUG 05 1993  
S B D

Co-sponsored by:

TNO Prins Maurits Laboratory, The Netherlands

The Pennsylvania State University, USA

European Space Agency

European Research Office of U.S. Army

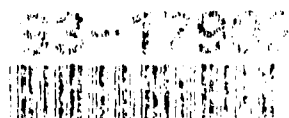
SNPE, France

EOARD of U.S. Air Force

Symposium Organizers:

Prof. Kenneth K. Kuo, PSU  
Symp. Chairman and Co-Organizer

Dr. Ir. Hans J. Pasman, TNO  
Co-organizer



93 8 4 125

DISTRIBUTION STATEMENT A

Approved for public release  
Distribution Unlimited

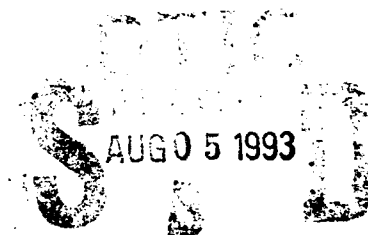
1

# **NON-INTRUSIVE COMBUSTION DIAGNOSTICS**

## **The Third International Symposium on Special Topics in Chemical Propulsion**

**May 10-14, 1993**

**Europa Hotel  
Scheveningen, The Netherlands**



### **Co-Sponsors:**

**TNO Prins Maurits Laboratory, The Netherlands**

**The Pennsylvania State University, USA**

**European Research Office of U.S. Army**

**European Space Agency**

**SNPE, France**

**EOARD of U.S. Air Force**



## **REGISTRATION AND WELCOME RECEPTION**

**MONDAY, 10 May, 1993**

**4:00 PM-7:00 PM**

**Registration in the Lobby of the Europa Hotel  
Zwolsestraat 2  
2587 VJ Scheveningen, Holland  
4:00 - 7:00 p.m.**

**Registration will be continued during the symposium period**

**Welcome reception at the Europa Hotel  
5:00 - 7:00 p.m.**

## SYMPOSIUM ORGANIZATION

**Symposium Chairman and  
Co-organizer:**

**Dr. Kenneth K. Kuo**  
Distinguished Professor and Director of the  
High Pressure Combustion Lab  
140 Research Building East  
The Pennsylvania State University  
University Park, PA 16802 USA

**Co-Organizer:**

**Dr. Ir. Hans J. Pasman, TNO**  
Director of Marketing and Programme  
TNO Defence Research  
Schoemakerstraat 97  
P.O. Box 6070, 2600 JA Delft  
The Netherlands

**Steering Committee:**

**Prof. Ezra, Bar-Ziv, NRC**  
**Dr. Richard A. Beyer, ARL**  
**Prof. Franz Durst, University of Erlangen-Nürnberg**  
**Dr. Alan C. Eckbreth, UTRC**  
**Prof. Ronald K. Hanson, Stanford Univ.**  
**Prof. Manuel V. Heitor, IST**  
**Dr. Wen H. Hsieh, PSU**  
**Dr. Katharina Kohse-Höinghaus, DLR**  
**Ir. P.A.O.G. Korting, TNO-PML**  
**Prof. Kenneth K. Kuo, PSU**  
**Dr. Robert P. Lucht, Sandia Lab**  
**Dr. Andrzej W. Miziolek, ARL**  
**Dr. Tim Parr, NAWC**  
**Dr. Ir. Hans J. Pasman, TNO**  
**Dr. Roland Pein, DLR**  
**Dr. Henk J. Reitsma, TNO-PML**  
**Mr. Jean-Paul Reynaud, SNPE**  
**Dr. Herman F. R. Schoeyer, ESA**  
**Dr. Klaus Schadow, NAWC**  
**Dr. Jean-Pierre Taran, ONERA**  
**Dr. Stefan Thynell, PSU**  
**Dr. James H. Whitelaw, Imperial College**  
**Dr. Tark Wijchers, TNO-PML**  
**Prof. Vladimir E. Zarko, Inst. of Chem. & Kinetics**

**Local Arrangements:**

**Dr. Tark Wijchers, TNO-PML**

iii

DTIC QUALITY INSPECTED 3

Accession For	
NTIS	<input checked="" type="checkbox"/>
DTIC	<input type="checkbox"/>
U.S. Govt.	<input type="checkbox"/>
perform 50	
A-1	



## Symposium Program

**TUESDAY 11 MAY 1993 - 8:00 AM - 12:00**

Registration in the Lobby of the Europa Hotel

**8:30**

**INTRODUCTION and ANNOUNCEMENTS**

Professor Kenneth K. Kuo  
and  
Dr. Ir. Hans J. Pasman

**8:50**

**WELCOMING REMARKS**  
Mr. E. Slachmuylders  
Head of the Mechanical Systems Department  
ESTEC

**TUESDAY 11 May, 1993 - 9:00 AM-5:00 PM**

**Page**  
**No.**

**9:00 SESSION I-1: Invited Talk by Professor Ronald K. Hanson,  
Quantitative Absorption and Fluorescence Diagnostics in  
Combustion Systems," (Introduced by Session Chair: Dr. K. Kohse-  
Höinghaus)**

**2**

**10:00 Coffee Break**

### **SESSION R-1: LIF and PLIF Diagnostics**

**Co-Chairs: Prof. R. K. Hanson and Dr. T. Parr**

**10:30 Species Concentration and Temperature Measurements by Single-Pulse  
Spontaneous Raman Scattering in a Turbulent H<sub>2</sub>/air Flame, W. Meier, S.  
Prucker, and W. Stricker**

**13**

**11:00 Quantitative Two-Dimensional Single Pulse Measurements of Temperature  
and Species Concentrations Using LIF, K. Kohse-Höinghaus and U. E. Meier**

**14**

**11:30 Laser Induced Fluorescence Thermometry of Burning and Evaporating Fuel  
Droplets, T. Kadota, K. Miyoshi., M. Tsue and K. Miyoshi**

**16**

**12:00 Lunch**

- 1:00 SESSION I-2: Invited Mini Review by Professor Franz Durst, "Particle Diagnostics for Combustion Systems", (Introduced by Session Chair: Dr. W. Calarese)** **3**

**SESSION R-2: Particle Diagnostics**

**Co-Chairs: Dr. R. A. Beyer and Dr. H. J. Pasman**

- 1:40 Phase Doppler Particle Sizing Inside a Production Gas Turbine Combustor, R. Kneer, M. Willmann, R. Zeitler, S. Wittig and K. H. Collin** **20**
- 2:10 Characterization and Diagnostics of Single Particles Oxidized in an Electrodynamic Chamber, Y. Weiss and E. Bar-Ziv** **22**
- 2:40 Coffee Break**
- 3:00 Ignition and Combustion of Mg-Coated and Uncoated Boron Particles, C. L. Yeh, W.H.Hsieh, K. K. Kuo and W. Felder** **23**
- 3:30 Rocket Exhaust Particles Sizing and Combustion Diagnostics of Metallic Species from Solid Propellants, J. Souletis and V. Bodart** **26**
- 4:00 Computerized Video Image Processing Technique for Droplet Combustion Studies, I. Hadar and A. Gany** **28**
- 4:30 Holographic Investigation of Solid Propellant Combustion Particle Field with Spatial Filtering Imaging System, S. Chen, X. Zhang and J. Wang** **30**

- 8:00 SESSION I-3: Invited Talk by Drs. John H. Stufflebeam and Alan C. Eckbreth, "CARS Temperature and Species Measurements in Propellant Flames," (Introduced by Session Chair: Dr. J. P. Taran ) 4**

**SESSION R-3: CARS Measurements**

**Co-Chairs: Dr. J. H. Stufflebeam and Dr. K. Kohse-Höinghaus**

- 9:00 CARS Temperature Measurements in a Subsonic Combustion Chamber, W. Clauß, R. Söntgen, A. Rudolph and M. Böhm 32**
- 9:30 Measurements of the Flame Temperature of Solid Propellants Using the Single-Shot CARS Technique, D.M. Chen, H. C. Wang, H. C. Perng, Y. T. Hsu and Y. P. Lee 35**
- 10:00 Coffee Break**
- 11:00 Quantitative Nitric Oxide CARS Spectroscopy in Propellant Flames, A. Kurtz, D. Brüggemann, U. Giesen and S. Heshe 39**
- 12:00 Lunch**

**WEDNESDAY 12 MAY, 1993 - 1:00 PM-7:30 PM**

**Page**  
**No.**

- 1:00 SESSION I-4: Invited Talk by Dr. Katharina Kohse-Höinghaus,  
"Quantitative LIF Diagnostics in Flames and Chemical Reactors,"  
(Introduced by Session Chair: Dr. H. F. R. Schoeyer )** **5**

**SESSION R-4: LIF and PLIF Diagnostics**

**Co-Chairs: Prof. E. Bar-Ziv and Dr. H. B. Levinsky**

- 2:00 Measurements of Rotational Energy Transfer in OH A  $v' = 0$  at Elevated  
Temperatures, M.P. Lee, R. Kienle and K. Kohse-Höinghaus** **42**
- 2:30 Collisional Energy Transfer in OH ( $A^2\Sigma^+$ ): Investigations for Quantitative LIF  
Combustion Diagnostics, R. Kienle, M. P. Lee, U. Meier and K. Kohse-  
Höinghaus** **43**
- 3:00 Two Degenerate Four-Wave Mixing Techniques for Measurement of OH in  
Flat Flames from 1 to 9 Bar Compared with Laser-Induced Fluorescence  
and Absorption Measurements, E. Domingues, M.-J. Cottureau and D.  
Feikema** **45**
- 3:30 Coffee Break**

**4:00- POSTER SESSION I.  
6:30**

**Co-Chairs: Dr. H. J. Pasman and Dr. T. Wijchers**

**7:30 Symposium Banquet**

**THURSDAY, 13 MAY, 1993 - 8:00 AM-12:00 PM**

**Page  
No.**

- 8:00 SESSION I-5: Invited Talk by Professors Vladimir E. Zarko and Kenneth K. Kuo, "Critical Review of Methods for Regression Rate Measurements of Condensed Phase Systems," (Introduced by Session Chair: Dr. R. Pein )**

**6**

**SESSION R-5: Combustion Diagnostics of Solid Propellants**

**Co-Chairs: Dr. A. Davenas and Dr. R. S. Miller**

- 9:00 Study on the Subatmospheric Burning Rate Characteristics of Composite Propellants, K. Kato, M. Kimura, M. Kohno, and K. Kobayashi**

**48**

- 9:30 Transient Burning Behavior of a Solid Propellant, K. K. Kuo, Y. C. Lu, Y. J. Yim, and F. Schwam**

**49**

**10:00 Coffee Break**

- 10:30 Diagnostic Tools for Studies on Burn Rate Behavior of Advanced Solid Propellants, S.N. Asthana, A. N. Nazare, S. S. Dhar, P. G. Shrotri and H. Singh**

**52**

- 11:00 Determination of Solid Propellant Burning Rate Sensitivity to the Initial Temperature by the Ultrasonic Method, F. Cauty, J. Cl. Démarais and Ch. Erades**

**53**

- 11:30 Investigation on Solid Rocket Propellant Combustion by Laser Doppler Anemometry, A. Volpi, and C. Zanotti**

**55**

**12:00 Lunch**

**THURSDAY 13 May, 1993 - 9:00 AM-12:00 PM**

**Page  
No.**

**SESSION R-6: Quantitative Spectroscopic and Interferometer Measurements**

**Co-Chairs: Dr. R. Pein and Dr. T. Wijchers**

<b>9:00</b>	<b>Temperature Measurements in Hostile Combusting Flows Using Multichannel Absorption Spectroscopy, J.A. Vanderhoff, A. J. Kotlar and R. A. Beyer</b>	<b>59</b>
<b>9:30</b>	<b>Study of Relation Between Characteristic Length and Plasma Jet by Measuring the Electron Temperature, K. Yoshida, and A. Saima</b>	<b>61</b>
<b>10:00</b>	<b>Coffee Break</b>	
<b>10:30</b>	<b>The Preflame Reaction in a Spark Ignition Engine, H. Shoji, A. Saima, and H. Watanabe</b>	<b>67</b>
<b>11:00</b>	<b>Vacuum-UV cw-Resonance Fluorescence Studies on Laser Photodissociation of Hydrazine Fuels, G. L. Vaghjani</b>	<b>78</b>
<b>11:30</b>	<b>Development of a Broadband Microwave Interferometer for Diagnostic Measurements of Detonations, J. J. Lee, T. J. F. Pavlasek, J. H. S. Lee, and R. Knystautas</b>	<b>80</b>
<b>12:00</b>	<b>Lunch</b>	

**THURSDAY 13 May, 1993 - 1:00 PM-6:45 PM**

**Page  
No.**

- 1:00 SESSION I-6: Invited Mini Review by Professor Thomas B. Brill, "FTIR Spectroscopy for Flame Diagnostics and Surface Pyrolysis Phenomena," (Introduced by Session Chair: Prof. K. K. Kuo)**

**7**

**SESSION R-7: Diagnostics in Propellant Combustion**

**Co-Chairs: Prof. V. E. Zarko and Ir. P.A.O.G. Korting**

- 1:40 Temperature Sensitivity Studies on Nitramine Based Propellant, L. Ramachandran, T. E. Krishnan, A. J. Kurian, S. S. Rao and K. N. Ninan** **82**
- 2:10 Method to Derive Solid Propellant Erosive Burning Rate Using Reactive Motor Pressure Diagram, I. G. Assovskii** **85**
- 2:50 Laser Assisted High-Speed Shutter TV Camera for Investigations on Aluminized Propellants Combustion, R. Akiba, M. Kohno, A. Volpi, T. Shibata, and S. Tokudome** **87**
- 3:20 Coffee Break**
- 3:50 Non-Intrusive Temperature Measurement of Propellant Flames and Rocket Exhausts Analyzing Band Profiles of Diatomic Molecules, W. Eckl, N. Eisenreich and W. Liehmann** **89**
- 4:00 Experimental Studies on Rocket Exhaust Plumes: Support for Computed Simulation, V. Bodart, and J. C. Chastenot** **90**
- 4:30- 6:45 Poster Session II:**

**Co-Chairs: Dr. H. J. Reitsma and Ir. P.A.O.G. Korting**

**FRIDAY, 14 MAY, 1993 - 8:00 AM - 12:15 PM**

**Page  
No.**

<b>8:00</b>	<b>SESSION I-7: Invited Talk by Drs. Timothy Parr and D.M. Hanson-Parr, "Solid Propellant Flame Chemistry and Structure", (Introduced by Session Chair: Dr. H. J. Reitsma)</b>	<b>8</b>
	<b>SESSION R-8: Flame Visualization and Measurements</b>	
	<b>Co-Chairs: Dr. K. Schadow and Prof. V. S. Abruikov</b>	
<b>9:00</b>	<b>Planar Mie Scattering Visualization of Reacting and Nonreacting Supersonic Coaxial Jets, K. Yu, T. Parr, and K. Schadow</b>	<b>92</b>
<b>9:30</b>	<b>Imaging of Impinging Jet Breakup and Atomization Processes Using Copper-Vapor Laser Sheet Illuminated Photography, M. C. Kline, R. D. Woodward, R. L. Burch, F. B. Cheung, and K. K. Kuo</b>	<b>95</b>
<b>10:00</b>	<b>Coffee Break</b>	
<b>10:15</b>	<b>Soot Diagnostics Based on Simultaneous Measurements of Soot Particle Size and of its Temperature Dependent Optical Constant in Flames, B. Ineichen, and B. Mandel</b>	<b>98</b>
<b>10:45</b>	<b>FTIR Spectrometry of Laminar, Premixed Hydrocarbon/Air Flames, I. T. Huang, S. T. Thynell and K. K. Kuo</b>	<b>100</b>
<b>11:15</b>	<b>Optical Methods for the Determination of Relative Radical Concentration and Soot Temperature, T. Wijchers</b>	<b>104</b>
<b>11:45</b>	<b>The Use of Non-Intrusive Combustion Diagnostics to Correction of Probing Measurements in Flames, O.P. Korobeinichev, E. Yu. Fedorov, K. P. Kutsenogii, and P. A. Mavliev</b>	<b>107</b>
<b>12:15</b>	<b>Lunch</b>	



- 1:00 SESSION I-8: Invited Talk by Professor Robert Dibble, "Molecular Probes of Mixing Rates and Kinetic Rates in Turbulent Flows"**  
**(Introduced by Session Chair: Prof. J. H. Whitelaw)** **10**

**SESSION R-9: Flow Field Measurements and Observation**

**Co-Chairs: Prof. F. Durst and Prof. M. V. Heitor**

- 2:00 Application of Non-Intrusive Diagnostic Methods to Sub-and Supersonic H<sub>2</sub> - Air Combustion, M. Haibel, F. Mayinger, and G. Strube** **109**
- 2:30 Investigation of the Flowfield of a Scramjet Combustor with Parallel H<sub>2</sub> - Injection Through a Strut by Particle Image Displacement Velocimetry, M. Oswald, R. Guerra and W. Waidmann** **113**
- 3:00 Optical Analysis of Turbulent Heat Transfer in Disc-Stabilized Flames, P. Ferdo and M. V. Heitor** **116**
- 3:30 Coffee Break**
- 3:50 UV Raman Measurements of Temperature and Concentrations with 308 nm In Turbulent Diffusion Flames, F. Lipp, E. P. Hassel, and J. Janicka** **120**
- 4:15 Doppler Velocity Measurements Using a Phase Stabilized Michelson Spectrometer, G. Smeets** **126**
- 4:40 Development of Laser Diagnostic Techniques for Full-Field Velocity Measurements, B. Ineichen and R. Müller** **129**
- 5:05 Temperature Measurement in Flat Laminar Premixed Gas/Air Flames by Laser Doppler Velocimetry, A. van Maaren, L. P. H. de Goey, and R. van de Velde** **131**
- 5:30 Interferometry Techniques in Combustion Research, V.S. Abruikov, S. V. Ilyin, V. M. Maltsev** **134**

**FRIDAY, 14 May, 1993 - 2:00 PM - 5:00 PM**

**Page  
No.**

**SESSION R-10: X-Ray Diagnostic and Image Analysis of Combustion of Liquids and Solids**

**Co-Chairs: Mr. J. P. Reynaud and Dr. Th. H. Van der Meer**

- |             |   |            |
|-------------|---|------------|
| <b>2:00</b> | <b>The Application of Color Image Analysis in Studies of Dense Monopropellant Spray Combustion, <i>A. Birk and M. J. McQuaid</i></b>  | <b>138</b> |
| <b>2:30</b> | <b>Real-Time X-Ray Radiography Study of Liquid Jet Breakup from Rocket Engine Coaxial Injectors, <i>R. D. Woodward, R. L. Burch, K. K. Kuo and F. B. Cheung</i></b>                       | <b>139</b> |
| <b>3:00</b> | <b>X-Ray Diagnostics Methods for Closed Liquid Metal Combustion: Real-Time Radiographic Experiments and Simulations, <i>L. A. Parnell, R. S. Nelson, K. A. Kodimer and T.R. Ogden</i></b> | <b>142</b> |
| <b>3:30</b> | <b>Coffee Break</b>   |            |
| <b>4:00</b> | <b>Analysis of Solid Propellant Behavior During Firing Test Using X-Ray Radioscopy, <i>P. Lamarque, Y. Deniges and M. Gimbre-Celerg</i></b>   | <b>143</b> |
| <b>4:30</b> | <b>Laser Mie Scattering for the Characterization of Diesel Injection Processes, <i>K. U. Münch and A. Leipertz</i></b>  | <b>145</b> |

## POSTER SESSION PAPERS:

Presented at Two Time Period

WEDNESDAY, 12 May 1993 from 4:00 to 6:30 PM

and

THURSDAY, 13 May 1993 from 4:30 to 6:45 PM

POSTER SESSION: AREA 1

### Non-Intrusive Temperature Measurements

	<u>Page No.</u>
PP-1.1 Comparison of Turbulent Diffusion Flame Stress Model Prediction, A. A. Neuber, E. P. Hassel, and J. Janicka	150
PP-1.2 CARS Temperature Measurements in a Lean, Turbulent, 120 kW Natural Gas Flame, R. Bombach, B. Hemmerling, and W. Kreutner	153
PP-1.3 CARS Temperatures up to 3200 K, Data Evaluation of Single-Shot Broadband Nitrogen Spectra, M. Fischer, E. Mogens, and A. Winandy	154
PP-1.4 Measurement of three-dimensional Temperature Fields by Heterodyne Holographic Interferometry, B. Ineichen and R. Müller	156
PP-1.5 Holographic Temperature Measurement on Axisymmetric Propane-Air, Fuel-Lean Flame, S. M. Tieng, W. Z. Lai and T. Fujiwara	158
PP-1.6 Temperature Measurements by CARS: State of the Art, Limitations and Objectives, P. Bouchardy, G. Collin, F. Grisch, P. Magre and M. Péalat	160

## POSTER SESSION PAPERS:

Presented at Two Time Periods

WEDNESDAY, 12 MAY 1993 from 4:00 to 6:30 PM

and

THURSDAY, 13 MAY 1993 from 4:30 to 5:45 PM

### Diagnostics in Gaseous Flames

		<u>Page No.</u>
PP-2.1	A Study on the Emissivity Prediction of Open Propane Flame with Infrared Image, <i>J.-M. Char and J.-H. Yeh</i>	162
PP-2.2	Determination of Radiation Properties of the Gas Flame, <i>J. Nadziakiewicz</i>	165
PP-2.3	Observation of Flow Instability in the Cone of Bunsen Flames by LIF, <i>A. A. Konnov, I. V. Dyakov, and E. V. Belozero</i>	168
PP-2.4	Planar Laser Imaging of Species in a Novel Pulsating Burner, <i>B. A. Mann, I. G. Pearson, and D. Proctor</i>	171
PP-2.5	Schlieren Method of Optical Registration of Combustion-to-Detonation Transition in Gaseous Mixtures, <i>N. N. Smirnov, and M. V. Tyurnikov</i>	172
PP-2.6	Laser Doppler Velocimetry Measurements in a Laminar Counter Flow Premixed Double Flame: Comparison with Numerical Calculations, <i>M.H. Sennoun, E. Djavdan, N. Darabiha and J.C. Rolon</i>	173
PP-2.7	New Applications of Shock Tubes for Studies of Combustion and Explosion Processes, <i>B. E. Gelfand, S. P. Medvedev, S. M. Frolov, and A. N. Polenov</i>	176
PP-2.8	Tomographic Reconstruction of Velocity and Pressure Fields of Ignition and Explosion Gas Flows Based on Interferometry Measurements, <i>S.A.Abrukov, V.S.Abrukov, and S.V.Ilyin</i>	177

## POSTER SESSION PAPERS:

Presented at Two Time Periods

WEDNESDAY, 12 May 1993 from 4:00 to 6:30 PM

and

THURSDAY, 13 May 1993 from 4:30 to 6:45 PM

### POSTER SESSION: AREA 3

#### Diagnostics of Combustion Processes of Condensed Phase Systems

	<u>Page No.</u>
PP-3.1 The Agglomeration of Aluminum and Combustion of Agglomerates in Laser Radiation Field, V. A. Bezprozvannykh, V. A. Yermakov, and A. A. Razdobreev	179
PP-3.2 Emission Spectroscopy and Pyrometry of Propellant Flames and Rocket Plumes, W. Eckl, N. Eisenreich, V. Gröbel, W. Liehmann, and H. Schneider	182
PP-3.3 The Comparative Analysis of Methods of Measuring the Non-Stationary Solid Propellant Burning Rate, V. A. Arkhipov, and V. N. Vilyunov	183
PP-3.4 Critical Phenomena by Interaction of Laser Irradiation with Reactive Substances, I. G. Assovskii	185
PP-3.5 Instantaneous Burning Rate Measurement of Solid Propellant Strand in 2-D Motor by Means of Laser Scanning Device, S. Chen and J. Huang	186
PP-3.6 Influence of Internal Refractive Index Gradients on Size Measurements of Spherically Symmetric Particles by Phase Doppler Anemometry, M. Schneider and E. Hirtleman	187
PP-3.7 Determination of Explosive Transformation Energy Under Transition from Combustion to Explosion of High-Energy Materials, I. V. Kondakov, B. G. Loboiko, and V. A. Rygalov	188
PP-3.8 Experimental Investigation of the Transition from Combustion to Explosion of High-Energy Explosive Materials in a Shell, I.V. Kondakov, B.G. Loboiko, B.V. Litvinov and V.A. Pestrichihin	190

## POSTER SESSION PAPERS:

Presented at Two Time Periods

WEDNESDAY, 12 May 1993 from 4:00 to 6:30 PM

and

THURSDAY, 13 May 1993 from 4:30 to 6:45 PM

POSTER SESSION: AREA 3

(Continued)

### Diagnostics of Combustion Processes of Condensed Phase Systems

	<u>Page No.</u>
PP-3.9 Use of Acoustic Emission for Investigation into Ignition and Combustion of High-Energy Materials, <i>I. V. Kondakov, B. V. Litvinov, B. G. Loboiko, and V. V. Shaposhnikov</i>	192
PP-3.10 Sizing Tolerance of Non-Spherical Particles Using a Scattered Light Instrument Compared with Measurements of Aerodynamic Diameter, <i>Y. Hardalupas, N. G. Orfanoudakis, A.M.K.P. Taylor and J. H. Whitelaw</i>	194
PP-3.11 Electrical Diagnostics of Condensed Fuels Combustion, <i>A. N. Zolotko, I. S. Al'tman, A. V. Florko, and V.G. Shevchuk</i>	200
PP-3.12 The Method of the End Products of Al and Mg Combustion Dispersability Determination by Radiation Spectrum, <i>A.V. Florko, I.S. Al'tman and A.N. Zolotko</i>	202

## POSTER SESSION PAPERS:

Presented at Two Time Periods

WEDNESDAY, 12 May 1993 from 4:00 to 6:30 PM

and

THURSDAY, 13 May 1993 from 4:30 to 6:45 PM

POSTER SESSION: AREA 4

### Diagnostics in Practical Combustion Systems

	<u>Page No.</u>
PP-4.1 Effect of the Ambient Pressure on Droplet Heating in Diesel Sprays, <i>M. Haug and M. Megahed</i>	205
PP-4.2 2D-LIF Measurements of NO in a Running Diesel Engine, <i>Th. Brugman, R. Klein-Douwel, J. J. ter Meulen, G. Huigen and E. van Walwijk</i>	207
PP-4.3 A Comparison of Some Optical and Spectroscopic Non-Intrusive Diagnostic Methods in Combustion Systems, <i>Y. M. Timnat</i>	208
PP-4.4 Analysis of the Ignition Sequence of a Multiple Injector Combustor Using PLIF Imaging, <i>K. McManus, F. Aguerre, B. Yip and S. Candel</i>	213
PP-4.5 Diesel Soot Characterization Based on Simultaneous Measurement of Polychromatic Scattering and Extinction, <i>F. E. Corcione, O. Monda, and B. M. Vaglieco</i>	214

# INVITED PAPERS

- I-1: **Professor Ronald K. Hanson** - Quantitative Absorption and Fluorescence Diagnostics in Combustion Systems  
Session Chair: Dr. K. Kohse-Höinghaus
- I-2: **Professor Franz Durst** - Particle Diagnostics for Combustion Systems  
Session Chair: Dr. W. Calarese
- I-3: **Drs. John H. Stufflebeam and Alan C. Eckbreth** - CARS Temperature and Species Measurements in Propellant Flames  
Session Chair: Dr. J. P. Taran
- I-4: **Dr. Katharina Kohse-Höinghaus** - Quantitative LIF Diagnostics in Flames and Chemical Reactors  
Session Chair: Dr. H. F. R. Schoeyer
- I-5: **Professors Vladimir E. Zarko and Kenneth K. Kuo** - Critical Review of Methods for Regression Rate Measurements of Condensed Phase Systems  
Session Chair: Dr. R. Pein
- I-6: **Professor Thomas B. Brill** - FTIR Spectroscopy for Flame Diagnostics and Surface Pyrolysis Phenomena  
Session Chair: Prof. K. K. Kuo
- I-7: **Drs. Timothy Parr and D.M. Hanson-Parr** - Solid Propellant Flame Chemistry and Structure  
Session Chair: Dr. H. J. Reitsma
- I-8: **Professor Robert Dibble** - Molecular Probes of Mixing Rates and Kinetic Rates in Turbulent Flows  
Session Chair: Prof. J. H. Whitelaw



## **Quantitative Absorption and Fluorescence Diagnostics in Combustion Systems**

**Ronald K. Hanson**  
**High Temperature Gasdynamics Laboratory**  
**Department of Mechanical Engineering**  
**Stanford University, Stanford, CA, USA 94305**

Laser diagnostics offer important potential for nonintrusive measurements in combustion and propulsion research. Diagnostics research in the High Temperature Gasdynamics Laboratory (HTGL) at Stanford University is currently focussed on two complementary approaches: spectrally resolved lineshape strategies, and 2-d imaging strategies. The methods concerned with resolving spectral lineshapes are conducted with rapidly tunable narrow-linewidth cw laser sources, either ring dye or semiconductor lasers, and are suitable for either line-of-sight absorption (LOSA) or single-point laser-induced fluorescence (LIF). These measurements, which represent one form of wavelength modulation spectroscopy, are capable of simultaneously measuring multiple flowfield properties, including velocity, temperature, species concentration, pressure, and density, as well as quantities derived from these parameters such as mass flux and momentum flux (thrust). The measurements can be made accurately at relatively high repetition rates: up to 4 kHz with a ring dye laser and up to about 100 kHz with a diode laser. When performed with diode laser, this relatively new measurement strategy offers real promise for simple, rugged, compact and economical diagnostics based on spectroscopic principles. Compatibility with optical fibers suggests that these diagnostics will find use in remote or hostile environments, including flight instrumentation. LOSA results to be presented include uv ring dye laser measurements of OH (306 nm) and NO (225 nm) and diode laser measurements of H<sub>2</sub>O (1.4 microns). Single-point LIF results include uv ring dye laser measurements of OH (306 nm) in subsonic and supersonic combustion gases.

Our research on 2-d imaging is based on planar laser-induced fluorescence (PLIF). Here the laser source is a tunable pulsed dye laser or narrow-linewidth excimer laser and the detector is an intensified CCD camera interfaced with an image processing computer. The PLIF method is now over ten years old, and good progress has been made in developing strategies for monitoring combustion species and other parameters such as temperature and velocity. The obvious advantage of PLIF is that an entire 2-d field can be measured with a single laser pulse; in essence this is a modern, species-specific form of flowfield visualization. The method is particularly well-suited for studies of mixing of gaseous streams and for measurements of complex flow structures. Limitations of PLIF, other than cost, have been associated with: uncertainties in quench rates (i.e, fluorescence yield), which inhibit quantitative measurements of species concentration and temperature; low signal-to-noise ratios, especially in large or luminous flows; and the fact that the method is not suitable for all combustion species of interest. In this paper we report our most recent efforts to obtain quantitative PLIF results for temperature, concentration and velocity using various two laser - two camera strategies. Examples of recent experiments to be described include: temperature and species imaging in a shock tube study of mixing and combustion of a fuel jet in supersonic crossflow; temperature and velocity imaging in a shock tunnel to examine hypersonic flows with vibrational nonequilibrium; and multiple-species imaging in a reacting supersonic mixing layer.

## "Particle Diagnostics for Combustion Systems"

by

Franz Durst,  
Lehrstuhl für Strömungsmechanik  
Universität Erlangen-Nürnberg  
Cauerstr. 4  
D - 8520 Erlangen

---

Reliable measurements in fluid flows with combustion require the application of well designed equipment which takes in account the special features combusting flows show. The lecturer introduces miniaturized laser-Doppler-anemometers based on semi-conductor lasers and detectors and shows their utilization to study diffusion and premixed flames. Main velocity measurements are presented, together with turbulence quantities that characterize the flow, especially near the combustion region.

Phase-Doppler-anemometry is described as an extension of laser-Doppler-anemometry and conventional phase-Doppler-anemometers are applied to various spray study. The resultant size and velocity distributions are described by log-hyperboloid functions in order to reduce the data to be stored for sprays to an acceptable minimum. From the stored data, this actual size and velocity distributions can be recomputed. This will be demonstrated through measurements and their comparison with log-hyperboloid discriptions of the measured distributions.

It is pointed out that spray measurements in combustion systems require the special attention when size measurements are carried out with phase-Doppler-anemometers. The size of the spray droplets can only be evaluated from conventional phase-Doppler-measurements, if the refractive index of the droplet fluid is known. In combusting flows, the temperature might change and hence, the refractive index of the particle material is not known. Extended phase-Doppler-anemometry is described that measures the refractive index of every particle that passes the measuring control volume. Utilizing this information, the droplet size can be evaluated in the entire spray. Measurements are presented that show the reliability of extended phase-Doppler-measurements for studies of particulate two-phase flows with combustion.

## **CARS Temperature and Species Measurements in Propellant Flames<sup>a</sup>**

John H. Stufflebeam and Alan C. Eckbreth

*United Technologies Research Center  
East Hartford, Connecticut 06108*

### **Abstract**

Measurements of combustion species, temperature, and their gradients are necessary for accurate modeling of solid propellant reaction mechanisms and their effect on the combustion characteristics of the propellant. The very difficult experimental problems posed by solid propellant combustion environments challenge even the most modern diagnostic techniques. CARS (coherent anti-Stokes Raman scattering) and DFWM (degenerate four-wave mixing) are nonlinear, laser-based, optical diagnostics with high spatial and temporal resolution that are used for measurement of temperature and species concentrations. CARS measurements at our laboratory confirmed the equilibrium chemistry (temperature and species concentration) of nitramine propellant formulations burning at elevated pressures. A 1-D imaging configuration, realized with cylindrical optics and a 2-D detector, provided enhanced spatial resolution and single shot data on species and temperature gradients adjacent to the strand surface during high pressure combustion. An experimental program is currently underway to obtain CARS and DFWM measurements near the surface of energetic material combustion systems at atmospheric pressure.

The experiment uses a motorized strand burner, servo-controlled by a diode laser, which advances the regressing propellant strand at its burn rate to maintain the surface fixed in the laboratory frame. The burner has an internal heater to preheat the strands if necessary to allow combustion at low pressure. CARS spectra can be acquired arbitrarily close to the burning surface throughout the combustion process with this facility. Alternately, the motor can drive the strand slightly faster than its regression rate and slowly force the surface up through the laser focus from which sequential CARS spectra will map temperature and species gradients. A Nd:YAG pumped, broadband Stokes system is resonant with Raman transitions of combustion products. The CARS spectra are dispersed and imaged onto a 1000-intensified channel, diode array detector. Results are presented from CARS experiments that utilize single-shot, species and temperature measurements from the combustion of propellants and pressed pellets of pure nitramine.

---

<sup>a</sup> Supported in part by the Office of Naval Research and the U. S. Army Research Office.

## QUANTITATIVE LIF DIAGNOSTICS IN FLAMES AND CHEMICAL REACTORS

Katharina Kohse-Höinghaus

DLR-Institut für Physikalische Chemie der Verbrennung,  
Stuttgart, Germany

### ABSTRACT

The talk will give an overview over the activities at DLR Stuttgart concerning the quantitative detection of intermediate species and the accurate measurement of temperature in reactive systems.

LIF investigations in several systems will be presented and discussed. One major line of research is the measurement of coefficients for collisional energy transfer, their representation by suitable scaling and fitting relations and their integration - together with recommended values from the literature - into a dynamic model for OH excitation and detection which is used to develop and examine measurement procedures and strategies. By systematic parameter variations, experimental approaches can be tailored to match the requirements of specific experimental environments. Results of the model are exploited in two-dimensional LIF experiments for the determination of concentrations and temperatures in turbulent flames. Besides LIF applications, alternative techniques for detection of minority species in chemically reactive systems are briefly discussed.

## Critical Review of Methods for Regression Rate Measurements of Condensed Phase Systems

V.E.Zarko\* and K.K.Kuo#

\* Institute of Chemical Kinetics and Combustion  
Russian Academy of Sciences, Novosibirsk 630090, Russia

# The Pennsylvania State University  
University Park, PA 16802, U.S.A.

Measurement of instantaneous burning rate of solid propellants and other energetic materials yields unique information which can be effectively used for checking various combustion theories and substantiating the design of different kinds of gas generators and rocket motors. However, there are problems associated with the adequacy of the results of physical measurements and theoretical calculations as well as the accuracy and reliability of experimental data. Up to present, the majority of theoretical results were obtained based upon one-dimensional approaches by considering condensed phase material to be quasi-homogeneous and the whole system to be adiabatic. In the meantime, investigators deal with realistic samples of heterogeneous structure with finite dimensions. The heterogeneous nature of the condensed phase material is responsible for physical and chemical inhomogeneity; and finite dimensions of samples often invalidate the assumed adiabatic condition. One of the main combustion parameters is the linear burning rate (or regression rate,  $r$ ) of the condensed matter.

Spatial and temporal resolution required for instantaneous burning rate measurements can be estimated with the help of thermal wave profile variations in the solid, as described by combustion theory. In general, the detection of burning rate variation during burn out of a layer, whose thickness is equal to that of reaction zone (approximately 20% of the thermal layer thickness), requires a characteristic measurement time  $t^*$  ( $= 0.2 \alpha / r^2$ ), where  $\alpha$  is the average thermal diffusivity of the reaction layer and  $r$  is the linear regression rate of the condensed material. Taking a typical  $\alpha$  value of  $1.5 \times 10^{-3} \text{ cm}^2/\text{s}$  and a typical  $r$  value of 1 cm/s at high pressures (e.g. 100 atm), the characteristic time is as short as  $3. \times 10^{-4} \text{ s}$ . The characteristic time increases as pressure decreases. Near one atmospheric condition, the required spatial and mass resolution for a typical sample of 1 cm in diameter are on the order of 0.003 cm and 3.5 mg, respectively. At high pressures, the required values are lower than these values by one order of magnitude. The operating frequency range of the measurement system must be at least 0-200 Hz at low pressures and about a few kHz at high pressures.

The paper gives a brief survey of various existing burning rate measurement techniques employed by different groups of researchers. These methods include the use of high-speed movie cameras, real-time X-ray radiography, microwave Doppler shift detection system, ultrasonic transducers, volume determination by measurement of dielectric constants, mass determination by tuning fork principle, instantaneous weight determination by tensile transducer, recorded time variation of reactive force, gas efflux velocity measurement tools, etc. Methods based on indirect reduction of  $r$  from measured  $p$ - $t$  traces are also described. Important parameters of various methods are estimated from theoretical and practical view points. Advantages and disadvantages of various techniques are discussed. Recommendations for special applications of certain methods are also provided.

## FTIR Spectroscopy for Flame Diagnostics and Surface Pyrolysis Phenomena

Thomas B. Brill  
Department of Chemistry  
University of Delaware  
Newark, DE 19716

FTIR spectroscopy can play a major function in the combustion and explosion field by serving as the technique that outlines the overall combustion process into which fast kinetics studies of elementary steps can be fit. This is because FTIR spectroscopy is usable in both the absorption and emission modes to identify and quantify the IR active gas products generated by pyrolysis of the condensed phase of energetic materials. These products are the reactants for the early stages of the flame chemistry. Within reason realistic combustion conditions can be employed. The main strength of FTIR spectroscopy is that all of the species are recorded with high sensitivity in a single spectrum. Temporal resolution, which is maximum of about 50 msec, is traded to gain this advantage. However, the large amount of information acquired in a moderately short time increment makes FTIR spectroscopy one of the most powerful techniques for studying very complicated, multistep processes.

In recent years the development of rapid thermolysis methods coupled to rapid-scan FTIR spectroscopy has advanced understanding about pyrolysis processes representative of a burning surface. This is a relatively unique niche for the technique. In particular, the stoichiometric reactions and overall heat balance are resolved in time for propellant components at a temperature approximating that of the burning surface. Elementary steps are imbedded in the stoichiometric reaction schemes and are not determined because of the time resolution available. The role of FTIR is to develop the global reaction framework into which elementary data can be fit

Recent advances in understanding the mid-IR emission characteristics of propellant flames makes FTIR spectroscopy a good technique for quantifying stable molecules in premixed and propellant flames. Tomographic principles make volume resolution of the gas phase species feasible in propellant flames.

## "SOLID PROPELLANT FLAME CHEMISTRY AND STRUCTURE"

Tim Parr and Donna Hanson-Parr  
Code C02392, Research Department  
Naval Air Warfare Center, Weapons Division  
China Lake, CA 93555-6001

The mixing and evaluation of trial propellant formulations is a very expensive process so a-priori calculations of propellant performance are of utmost importance. Specific impulse, flame temperature, and other thermodynamically controlled parameters are easily predicted using computer codes. Kinetically controlled ballistic properties, such as burning rate, pressure exponent, temperature sensitivity, catalysis, ignition delays, combustion instabilities, and the sensitivity to hazard processes, are *not* presently easy to calculate or predict. However, the first steps to understanding and modeling the kinetic mechanism of solid propellant combustion are currently being taken.

In addition to values for detailed gas phase reaction rate constants and a model of the physio-chemical and kinetic processes taking place at and below the surface of the propellant, these efforts require *guidance* in understanding the gas phase combustion mechanism as well as *validation* of predicted combustion behavior. Advanced laser diagnostics can help in this process via measurements of species and temperature profiles under varying combustion conditions.

Solid propellant combustion, however, presents a challenging environment to all diagnostic techniques. The relevant length scales are extremely small; to microns at the deflagration pressures typically found in rocket motors (about 7 MPa). Complicating this is the fact that the deflagration surface can often be non-flat, or even indistinct because of the presence of a foam layer. Also, the entire burn event is often over in less than a second requiring all the data to be taken on a time scale shorter than this so multi-parameter and/or multi-dimensional diagnostic techniques are preferable. Solid propellant flames also can have very high adiabatic flame temperatures, sometimes above 3000K, and this complicates intrusive probing. Finally, the chemistry of propellant flames is often quite different from hydrocarbon flames, due to the presence of large quantities of fuel nitrogen, and this makes it harder to extrapolate the understanding of hydrocarbon flames to propellant ones.

We have made use of the Planar Laser Induced Fluorescence (PLIF) technique to study the structure and chemistry of solid propellant flames. A Nd<sup>3+</sup>-YAG pumped tunable dye laser beam is formed into a thin sheet and directed through the flame. Fluorescence from a chosen species is selected with an interference filter and imaged using an image-intensified CCD camera. This gives an instantaneous 2D picture of relative concentration of the chosen species with spatial resolution approaching 20  $\mu$ m by 20  $\mu$ m and temporal resolution of 6 nsec. Since the laser can be tuned to specific quantum states, it is possible to determine temperature via state population distributions. The technique is applicable to a wide range of flame species, mostly radicals. We have measured CN, CH, OH, CH, C<sub>2</sub>, NO, NO<sub>2</sub>, NCO, and H<sub>2</sub>CO as well as OH, CN, and NO rotational temperatures and NO vibrational temperatures.

As with all diagnostic techniques there are disadvantages with PLIF. It is limited in the number of species it can monitor; for example, species important to nitramine combustion such as HCN and N<sub>2</sub>O are not measurable using LIF nor are large molecular decomposition fragments of the starting energetic material. There are complementary diagnostic techniques however, such as Raman, CARS, or micro probe or molecular beam mass spectral measurements, that can monitor these species. There is also the problem of flame opacity at the UV wavelengths used for some species. Finally severe collisional quenching of excited states makes quantitative measurements of species concentrations from LIF signal intensities very difficult or impossible, even using saturated LIF.

To alleviate the quenching problem we make use of transient UV-Visible absorption measurements to calibrate PLIF profiles. The effective 'path length' for the absorption experiment is calculated from the

shape of the PLIF profile. The absorption along this path then leads to an absolute average concentration, and this is used to place the PLIF profile on an absolute scale. The apparatus consists of a Xenon arc lamp and a multi-pass mirror arrangement to increase low absorptions from low concentration radicals. The spectra is measured using a 0.25 m spectrograph and optical multi-channel analyzer (OMA). This has the added benefit of allowing rotational or vibrational temperatures to be measured by fitting the absorption spectral shape.

We have applied these techniques to both composite propellant as well as neat energetic ingredient flames. A CO<sub>2</sub> laser is used as an ignition source as well as a source of heat flux during supported deflagration. This is adjustable up to heat flux levels seen by solid propellants during self deflagration at realistic rocket motor pressures. The absorption of the 10.6  $\mu$ m radiation occurs within a few microns of the surface (small compared to the thermal profile depth) so it is an adequate mimic for the conductive heat flow that the propellant normally sees from its own flame. The pulse shape of the CO<sub>2</sub> laser can be easily controlled allowing transient ignition mechanisms to be studied and placing a more constrictive validation control on modeling results. It also allows low temperature intermediate products to be monitored before the flame fully develops. Much of our work is done at 0.1 MPa as this slows the kinetics and stretches out the flame structure.

The ignition of the energetic ingredient HMX at 0.1 MPa using a heat flux of 150 cal/cm<sup>2</sup>sec proceeds as follows. The first products seen by our diagnostics are NO and NO<sub>2</sub> (recall we are insensitive to N<sub>2</sub>O, HCN and nitramine fragments, but we do not see H<sub>2</sub>CO at our heating rates). These plumes grow in height and concentration until the secondary flame is ignited in the gas phase away from the surface as indicated by the consumption of NO<sub>2</sub> and NO and the production of a spherical ignition kernel showing CN and NH radicals (very little or no CH is formed). This spherical ignition kernel rapidly forms into a flame sheet which then moves closer to the surface. All this happens on a time scale shorter than 10 msec. At this point a quasi-steady state laser supported deflagration is formed and the flame structure remains relatively constant beyond 15 msec.

The centerline species profiles during laser supported deflagration are as follows: the NO<sub>2</sub> concentration peaks at the surface and dies off rapidly within the 'dark zone'. NO is at a large concentration within the dark zone and is consumed quickly just below the final flame sheet. CN and NH profiles are thin gaussian like profiles centered on the flame sheet at about 3.8 mm above the surface, and the OH concentration rises to a peak just beyond the flame sheet and stays high in the burnt gas region above it. The temperature, as measured by thermocouples within and just above the surface, and by OH rotational measurements within the gas phase, rises sharply within 140  $\mu$ m of the surface to a dark zone plateau of approximately 1300K and then rises again through the secondary flame sheet to a value close to the adiabatic temperature of 2922K just at or beyond the peak of the CN profile. Profiles measured during self deflagration, i.e. without the benefit of additional heat flux from the laser, were similar except somewhat closer to the surface (2.2 mm vs 3.8). Transient UV-Visible absorption measurements indicated peak concentrations of NO<sub>2</sub> to be about 7 mole percent, NO to be 22 mole % and CN to be about 320 ppm.

Measurements made at elevated pressures indicated that the flame height decreased approximately inversely with pressure. At realistic rocket motor pressures the flame would be only 27  $\mu$ m off the surface; a value unlikely to be successfully profiled by any diagnostic technique.

We have also found the PLIF technique ideal for studying the diffusion flame structure in composite sandwich solid propellants.



"Molecular Probes of Mixing Rates and  
of Kinetic Rates in Turbulent Flows"

Professor Robert Dibble  
Department of Mechanical Engineering  
University of California, Berkeley

ABSTRACT

Much of our understanding of turbulent nonpremixed flames is based on a standard model that assumes equilibrium chemistry, adiabatic flow, and equal diffusivities of mass and energy (unity Lewis number). Deviations from these idealizations have been recent research topics. Much attention has been focused on the need for 'real chemistry', meaning chemical models that have finite-rate chemical kinetics. Such models are becoming very sophisticated in that flame extinction (a 'large' departure from equilibrium) and nitric oxide predictions are increasingly common. Moreover, much effort has been focused on 'reduced mechanisms'; chemical mechanisms that retain the desired features and discard unneeded mechanisms and rates.

While much progress has been made in improving the chemical kinetics, the corresponding progress in relaxing the assumptions of unity Lewis number or the assumption of adiabaticity (often in the form of radiative energy losses), has lagged. In this paper we explore the effects of differential diffusion in turbulent jets, nonreacting and reacting. Pulsed Raman scattering spectroscopy is used to measure temperature and species concentrations in reacting jets, of H<sub>2</sub> diluted with CO<sub>2</sub>, into air over a range of Reynolds numbers from 1,000 to 30,000, and in nonreacting jets of H<sub>2</sub> diluted with CO<sub>2</sub>, at Reynolds numbers from 1,000 to 64,000. Measurements are also made in nonreacting strained laminar opposed flows of H<sub>2</sub> diluted with CO<sub>2</sub> against air, where differential diffusion effects are observed to be independent of strain rate.

Results from nonreacting experiments are presented which demonstrate that differential diffusion of H<sub>2</sub> and CO<sub>2</sub> has a significant effect upon instantaneous and average species concentrations in laminar opposed flows and in low Reynolds number jet flows ( $Re=1,000$ ). At higher jet Reynolds numbers, average differential diffusion effects are observed only when the local concentrations of H<sub>2</sub> and CO<sub>2</sub> are very small, although the ratios CO<sub>2</sub>/H<sub>2</sub> continue to fluctuate in all regions of the flow. (In the absence of differential diffusion, the ratio CO<sub>2</sub>/H<sub>2</sub> would be invariant, anywhere in the flow!).

Results from chemically reacting experiments indicate that differential diffusion strongly affects hydrogen element mixture fractions  $Xi_H$  in nonpremixed turbulent jet flames at all Reynolds numbers measured. Differential diffusion of H and H<sub>2</sub>O creates a net flux of hydrogen element toward the stoichiometric contour on the rich side of the flame. This allows for an unexpected maximum in  $Xi_H$  (calculated from the mass fraction of hydrogen atoms in all hydrogen containing species) to occur near stoichiometric burning. Small values of  $Xi_H$  at large values of  $Xi_C$ , the carbon element mixture fraction, are observed at all Reynolds numbers, and indicate that there is a depletion of elemental

hydrogen from fuel rich mixtures due to differential diffusion of H<sub>2</sub> and CO<sub>2</sub>. In turbulent flames differential diffusion also creates local fluctuations in the hydrogen mixture fraction perturbation variable  $z_H$ , defined as the difference between  $X_{i,H}$  and  $X_{i,C}$ . This results from fluctuations in instantaneous values of  $z_H$  at a given value of mixture fraction, as well as from local fluctuations in mixture fraction.

Strained laminar opposed flow flame calculations with differential diffusion are compared to experimentally measured results in turbulent nonpremixed jet flames of H<sub>2</sub> diluted with CO<sub>2</sub> fuel. Values of  $X_{i,H}$  in the nonpremixed jet flames are much lower than values of  $X_{i,H}$  in strained laminar flames, of the same H<sub>2</sub> diluted with CO<sub>2</sub> fuel, when values of  $X_{i,H}$  are the same. The notion that a turbulent flame is an ensemble of laminar strained flames is challenged.

## **SESSION R-1: LIF and PLIF Diagnostics**

**Co-Chairs: Prof. R. K. Hanson and  
Dr. T. Parr**

# Species Concentration and Temperature Measurements by Single-Pulse Spontaneous Raman Scattering in a Turbulent H<sub>2</sub>/air Flame

W. Meier, S. Prucker, W. Stricker

DLR-Institut für Physikalische Chemie der Verbrennung  
Pfaffenwaldring 38  
W-7000 Stuttgart 80  
Fed. Rep. Germany

Spontaneous Raman scattering allows the simultaneous determination of the temperature and all major species concentrations and thus, in a single-pulse technique, the acquisition of correlated data from turbulent flames. Due to the very low scattering cross section, this technique requires high power lasers and efficient detection devices. We have set up a single-pulse spontaneous Raman scattering system based on a commercially available flashlamp-pumped dye laser with pulse energies up to 4 J. So far, 7 flame species can be measured simultaneously by individual photomultiplier tubes. The temperature is deduced from the total density via the ideal gas law. The characteristics of this system will be demonstrated.

The system is used for the investigation of turbulent H<sub>2</sub>/air diffusion flames. Series of typical 500 single-pulse measurements of H<sub>2</sub>, O<sub>2</sub>, N<sub>2</sub>, and H<sub>2</sub>O concentrations and the temperature are performed to determine the mean values and fluctuations of these quantities. Data sets from an adequate number of measuring positions, which yield the basis for the characterization of an individual flame, will be presented. Such data sets can be used for improvements in model calculations.

One of our main objectives is to study the potential of combined single-pulse Raman/LIF measurements. In contrast to spontaneous Raman scattering, the LIF technique is able to detect minor species concentrations (e.g. OH, NO,...) and, applied in a 2D configuration, to provide information about the flame structure (e.g. the shape of the reaction zone or fuel distribution). Thus, a more complete data base can be achieved.

The importance of the Raman data for the quantitative evaluation of 2D LIF images will be demonstrated and discussed elsewhere (see "Quantitative Two-Dimensional Single Pulse Measurements of Temperature and Species Concentrations Using LIF" by K. Kohse-Höinghaus and U.E. Meier). In this contribution, examples will be given how the structural information from 2D LIF measurements are used to optimize the quality of the Raman measurements. Concentration and temperature gradients as well as turbulence length scales within different regions of the flame can be assessed from 2D LIF images. In this way, the density of Raman measuring locations can be chosen adequately. Furthermore, the required spatial resolution for the Raman technique can be adjusted in order to avoid spatial averaging effects.

## Quantitative Two-Dimensional Single Pulse Measurements of Temperature and Species Concentrations Using LIF

Katharina Kohse-Höinghaus, Ulrich E. Meier  
DLR-Institut für Physikalische Chemie der Verbrennung  
Pfaffenwaldring 38-40, D-7000 Stuttgart 80, Germany

The merit of two-dimensional techniques for the visualization of concentration and/or temperature fields, particularly in turbulent combustion, has been demonstrated in various experiments. For a more detailed understanding of the combustion process, especially for comparison with numerical simulations, it is highly desirable to develop these techniques to a point where they yield reliable quantitative information. This includes also the knowledge of remaining systematic uncertainties due to incomplete data on, e.g., the influence of collision processes etc. Based on previous pointwise measurements of temperatures and OH radical concentrations using laser-induced fluorescence (LIF)<sup>1</sup>, we investigated the potential of 2D-LIF for quantitative concentration and temperature imaging in a turbulent H<sub>2</sub>/air diffusion flame.

In order to obtain structural information on this flame, we added NO to the hydrogen as a marker for the fuel. Using two lasers for the excitation of NO and OH, respectively, as well as two image-intensified CCD cameras for fluorescence detection, we obtained simultaneous single-shot images of the distribution of the unburnt fuel and the flame front, indicated by OH; a pair of correlated NO and OH images is shown in Fig. 1.

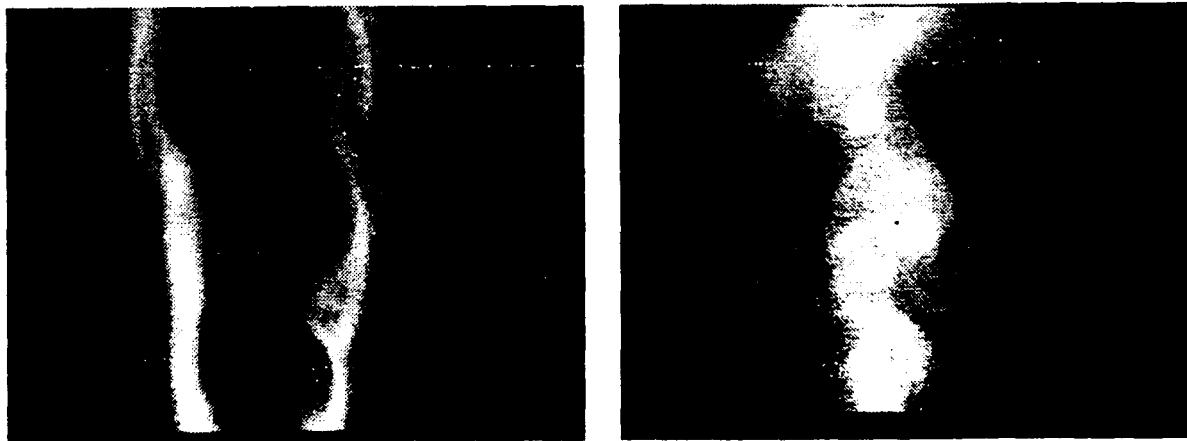


Fig. 1: Simultaneous single-shot two-dimensional fluorescence signal distribution of OH (left) and doped NO (right) in a turbulent H<sub>2</sub>/air diffusion flame

For the interpretation of measured signals in terms of concentrations, basically two factors need to be known: The effect of the local temperature on the population fraction in the initial state, and the local effect of collisions, which affects the fluorescence quantum yield from the excited state.

The temperature effect can be reduced to some degree by choosing an initial state with minimum temperature sensitivity of the population in the relevant temperature range. The choice of the optimum excitation line therefore requires at least some knowledge about the temperature distribution. This information was provided by Raman measurements<sup>2</sup> at some representative points.

To account for collisional effects, we calculated approximate quenching rates for OH and NO for gas compositions ranging from unburnt gas via flame front to burnt gas in laminar flames at different equivalence ratios. These calculations were based on species concentrations resulting from a chemical-kinetic model<sup>3</sup> for premixed flames and literature data on quenching cross sections from different sources. The calculations show a variation of 25% of the overall quenching rate throughout the entire flame for NO, and a factor of two for OH, with very little effect of the stoichiometry.

An experimental approach to the problem of varying fluorescence quantum yields is currently pursued, which yields correlated concentration and temperature information as well: Single pulse LIF measurements of OH are performed simultaneously with measurements of major species concentrations by Raman<sup>2</sup>. This experiment allows correction of the LIF signals with respect to collisional quenching using the actual local gas composition, and therefore does not rely on the theoretical result that the quenching rate is not strongly dependent on chemical environment.

- 1 A. Lawitzki, I. Plath, W. Stricker, J. Bittner, U. Meier, K. Kohse-Höinghaus, Appl. Phys. **B50**, 513 (1990); K. Kohse-Höinghaus, Appl. Phys. **B50**, 455 (1990) and references therein
- 2 S. Prucker, W. Meier, I. Plath, W. Stricker  
To appear in: Berichte der Bunsengesellschaft 96, Oct. 1992
- 3 J. Warnatz, Institut für Technische Verbrennung, Universität Stuttgart; One-Dimensional Flame Code, 1991 version

LASER INDUCED FLUORESCENCE THERMOMETRY  
OF BURNING AND EVAPORATING FUEL DROPLETS

T. Kadota

Department of Mechanical Engineering  
University of Osaka Prefecture  
Gakuen-cho, Sakai Osaka 593 JAPAN

K. Miyoshi

Mazda Motor Corporation  
Fuchu-cho, Hiroshima 730-91 JAPAN

M. Tsue

Department of Mechanic Engineering  
University of Osaka Prefecture

The temperature of atomized fuel droplets in a spray flame is one of the important factors in estimating the heat transfer, the extent of mixing of droplets with ambient gas and the rate constant of evaporation. However, there has been no direct measurement of this key factor for the fuel droplets which move through a heated gaseous medium.

The primary objective of the present study is the development of a diagnostic technique which allows remote, nonintrusive, instantaneous and point thermometry of fuel droplets. Among a large variety of diagnostic tools potentially applicable for this purpose, the laser induced fluorescence technique was selected. The effects of various parameters on the thermometry were studied for a fuel droplet evaporating or burning in a stream of gaseous mixture as well as an evaporating fuel spray.

As shown in Fig.1, a fuel droplet of diameter approximately 1.8 mm suspended at the tip of fine quartz fiber was allowed to evaporate or to burn in a steady free stream of a heated gaseous mixture of oxygen, nitrogen, carbon dioxide and water vapor with uniform velocity and temperature profiles. The liquid fuels tested were n-heptane, n-decane, n-hexadecane doped with small amount of naphthalene and tetramethyl-p-phenylene diamine (TMPD). A fine thermocouple was installed to monitor the droplet temperature.

The excitation source for the fluorescence is a nitrogen laser emitting monochromatic radiation at a wavelength of 337.1 nm with a pulse energy of 5 mJ/P and a pulse width of 5 ns. The fluorescence emission spectra from the fuel droplet were collected with an optical multichannel analyzer. The spectral band contour of the fluorescence emission spectra were used for the determination of droplet temperature. The fluorescence emission intensities were monitored at two different wavelengths and the resultant intensity ratio was correlated with the droplet temperature determined using the fine thermocouple.

An attempt was also made to apply the present technique for the thermometry of atomized fuel droplets in a spray which was injected intermittently into a heated gaseous nitrogen in a constant volume combustion chamber.

The primary conclusions reached in the present study are as follows.

- (1) The remote thermometry of a fuel droplet evaporating and burning in a stream of gaseous mixture is possible from the measured ratio of fluorescence emission intensities at two different wavelengths(Fig.2).
- (2) Among four species in the ambient gas tested in the present study, oxygen is the only one to affect the thermometry of evaporating droplets(Fig.3).
- (3) The thermometry is sensitive to the concentration of naphthalene and TMPD doped in the liquid fuel.
- (4) The ambient gas velocity relative to the fuel droplet has no appreciable influence on the thermometry(Fig.4).
- (5) The thermometry of a droplet burning in air is possible by using the data for a droplet evaporating in nitrogen(Fig.2).
- (6) The present technique is potentially applicable for the thermometry of atomized fuel droplets in a spray.

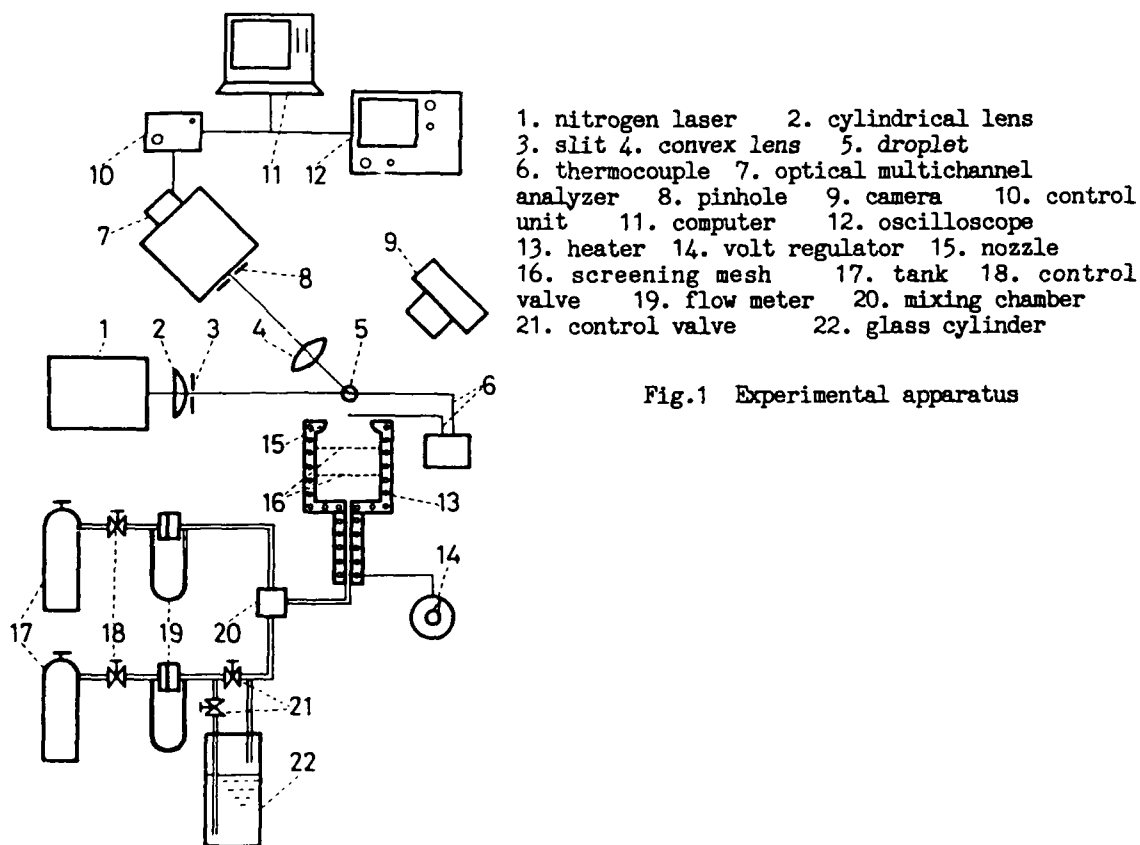


Fig.1 Experimental apparatus



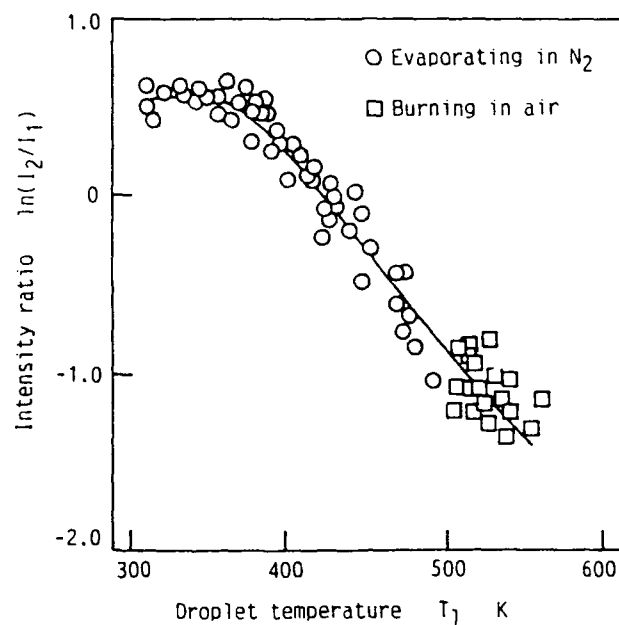


Fig. 2 Relationship between intensity ratio and droplet temperature (n-Hexadecane burning in air and evaporating in N<sub>2</sub>)

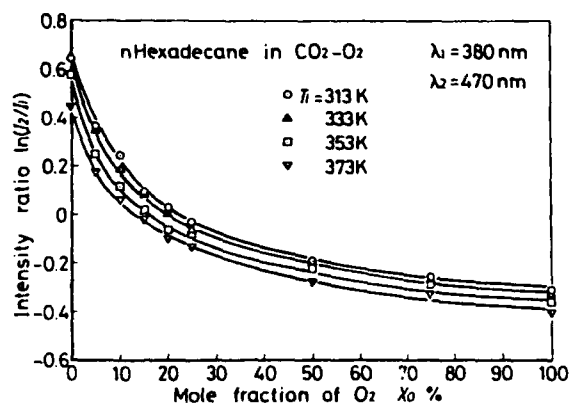


Fig. 3 Relationship between intensity ratio and Oxygen concentration (n-Hexadecane in CO<sub>2</sub>-O<sub>2</sub>)

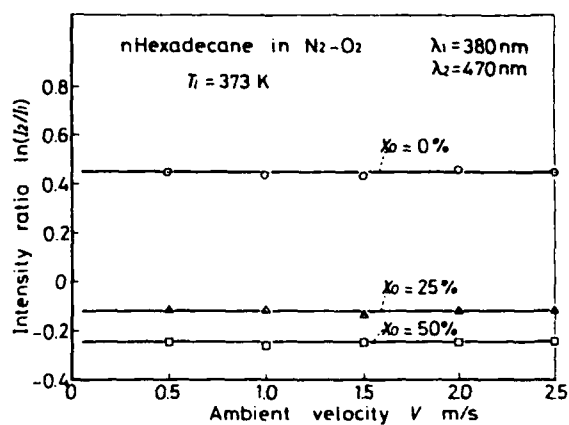


Fig. 4 Relationship between intensity ratio and gas velocity (n-Hexadecane in N<sub>2</sub>-O<sub>2</sub>)

## **SESSION R-2: Particle Diagnostics**

**Co-Chairs: Dr. R. A. Beyer and  
Dr. H. J. Pasman**

# PHASE DOPPLER PARTICLE SIZING INSIDE A PRODUCTION GAS TURBINE COMBUSTOR

R. Kneer, M. Willmann, R. Zeitler, S. Wittig

Lehrstuhl und Institut  
für  
Thermische Strömungsmaschinen  
Universität Karlsruhe

K.-H. Collin

BMW-Rolls Royce, Oberursel

A segmented BMW - Rolls Royce prevaporizing combustor has been adapted to the high pressure - high temperature test facility of the 'Institut für Thermische Strömungsmaschinen' (ITS) and run under several operating conditions. This production engine combustor is designed as prevaporizing combustor in order to separate the fuel vaporization process from the subsequent combustion. From literature this is known as a well-suited measure for  $\text{NO}_x$  emission reduction. Original studies concerning the prevaporizing concept were initiated by the CEC 'BRITE/EURAM - Low Emission Combustor Technology' program. Therefore, simultaneous measurements of droplet sizes in the primary zone of this combustor as well as temperature, pressure and species concentration profile measurements at the flame tube exit have been performed. For the primary zone droplet sizing, as reported here, a two-component phase Doppler system has been applied.

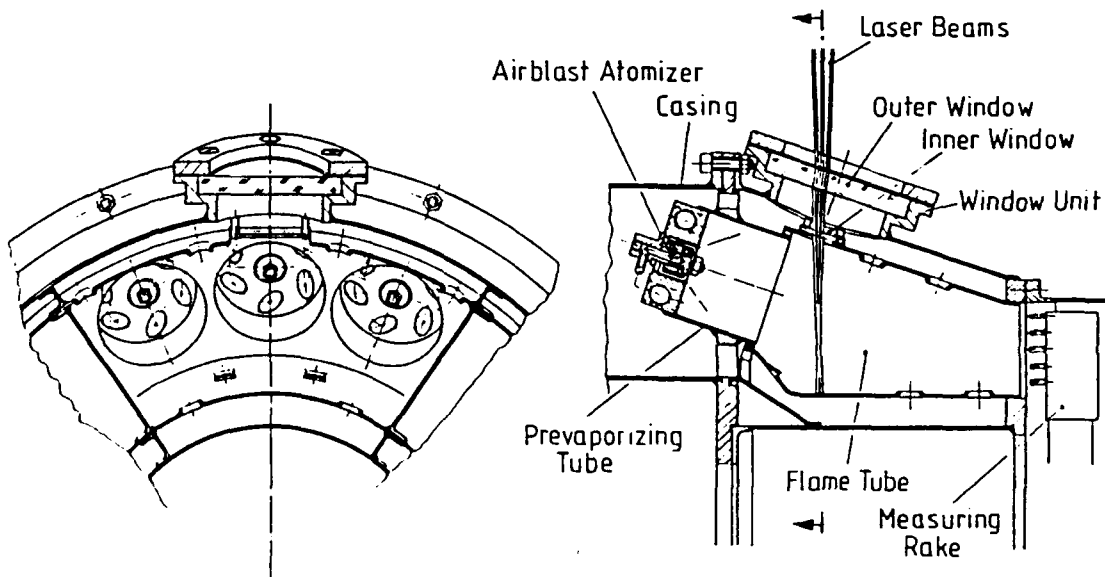


Figure 1. Combustor segment with window unit

Due to the complex combustor geometry and its small dimensions, optical access has been possible within a small angular sector only, as shown in fig. 1. This required a backscatter arrangement of the PDPA system. Theoretical scattering calculations revealed the possibility to size the kerosene fuel spray at an  $160^\circ$  off-axis angle.

The combustor consists of two concentric annular tubes. The inner flame tube covers the reacting flow regime, whereas cold mixing air is guided by the channel formed between the outer casing and the flame tube. Thus, two openings have been necessary to achieve optical access to the primary zone. Therefore, a two-window unit, meeting both optical and mechanical requirements has been designed.

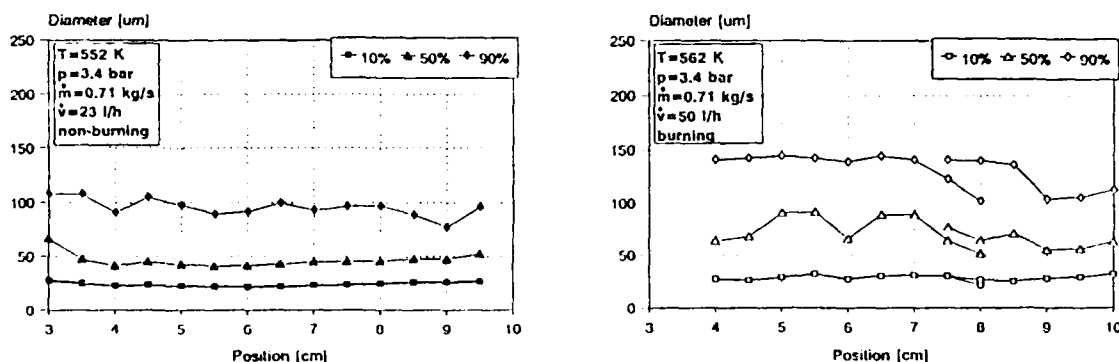


Figure 2: Characteristic diameters with regard to the volume distribution

Employing burning and non-burning conditions increased droplet axial velocities have been clearly detectable indicating the acceleration of the gas flow in the burning case. This is caused by the severe interaction between the heat release from combustion and the flow field. A comparison of the droplet sizes in fig. 2 determined with and without combustion shows the increase of the drop size spectrum due to the faster evaporation of smaller droplets. Moreover, a non-stationary displacement of the spray has been found for the burning case.

Characterization and Diagnostics of Single  
Particles Oxidized in an Electrodynamic Chamber

Ezra Bar-Ziv  
Nuclear Research Center - Negev, P.O.Box 9001  
Beer-Sheva, Israel

ABSTRACT

We have further developed characterization and diagnostic methods of single particles oxidized in an electrodynamic chamber (EDC). The EDC has been developed and applied for kinetic studies of single particle combustion. It was previously pointed out that the main advantages of the EDC are: (1) The ability to study combustion kinetics of a single particle in well controlled conditions. (2) The ability to characterize the particle prior to reaction and monitor the important quantities needed for kinetic understanding in real time. (3) The ability to study the kinetics of single particle combustion in regimes I, II, and III. (4) The elimination of heat and mass transfer limitations existing in other methods that restrict kinetic measurements to slow burning rates. (5) The ability to study particle to particle variations.

The following methods were either developed or improved for higher accuracy: (1) Shadowgraphy for size and shape measurements. (2) Two-dimensional Mie scattering for sizing and determining optical properties. (3) Drag force measurements (by forced convection) for the determination of the density. (4) Optical pyrometry using wide-band detectors in the visible and infrared for temperature determination. The quantities to be measured for modeling of the combustion kinetics of a single particle are: (1) weight, (2) size, (3) density, (4) temperature, (5) heat capacity, and (6) surface area.

In this study, synthetic char particles, spherically shaped (Spherocarb), as well as spherical polystyrene particles were oxidized in atmospheric air and pure oxygen. The particles were suspended in the center of the EDC and heated by a CO<sub>2</sub> laser beam. The particles were characterized prior to reaction by the above methods. Mass and size changes as well as the particle temperature were measured as a function of time during the oxidation process. The particles were consumed in the following manner: First they were consumed uniformly, following previous shrinkage observations. At about 60% conversion non-uniform shrinkage was observed, always preferential shrinkage from the top of the particle. At 70% conversion a clear cut on the top of the particle was monitored. At 80% conversion preferential consumption from the other side of the was established, showing a clear disk configuration. At 95% conversion a hole in the center of the disk was developed. The explanation of this preferential consumption is not yet clear, however it is possible that the non symmetrical boundary layer around the particle, caused by free convection, generated a temperature difference where high temperature is always at the top of the particle. It is perhaps due to the capability of the EDC that enabled us to observe this unique phenomenon due to its ability to suspend a particle at the center of the chamber motionless.

## IGNITION AND COMBUSTION OF Mg-COATED AND UNCOATED BORON PARTICLES<sup>1</sup>

C. L. Yeh, W. H. Hsieh, K. K. Kuo  
Department of Mechanical Engineering  
The Pennsylvania State University  
University Park, PA 16802

and

W. Felder  
AeroChem Research Laboratories, Inc.  
Princeton, NJ 08542

An experimental study of ignition delay and combustion time of Mg-coated and uncoated boron particles was performed in the post-flame region of a flat-flame burner or Meker burner at atmospheric pressure. The overall objective of this research is to study the effect of thin Mg coating, applied using a novel method, on the ignition and combustion behavior of boron particles. The experiments were carried out in four different premixed flames (using  $\text{CH}_4/\text{O}_2/\text{N}_2$ ,  $\text{CO}/\text{O}_2/\text{N}_2$ ,  $\text{H}_2/\text{O}_2/\text{N}_2$ , and  $\text{N}_2\text{O}/\text{O}_2/\text{N}_2$  mixtures) over a wide range of flame temperature and gas compositions.

In the experiments, coated or uncoated boron particles, fed from a fluidized bed particle feeder, were injected individually into the flames through a feeding tube. An optical diagnostic system, shown in Figure 1, was used to detect the first appearance of the boron particle at the exit port of the feeding tube, its instantaneous locations and velocity, the ignition delay, and the total burning time. This optical diagnostic system consists of either an He-Ne laser or an  $\text{Ar}^+$  laser, a photomultiplier tube, an electronic triggering unit, a function generator, an Xybion intensified CCD camera, and a digital image processing system. The He-Ne (or  $\text{Ar}^+$ ) laser beam was aligned and focused on the exit port of the particle feeding tube. When the boron particle started to appear at the exit port of the feeding tube, the particle scattered the laser beam. The photomultiplier tube was used to detect the scattered laser light. The output of the photomultiplier tube, signifying the first appearance of the boron particle at the exit of the particle feeding tube, was sent to the triggering unit. Once the magnitude of photomultiplier output reached a level between the preset lower and upper trigger levels on the triggering unit, a trigger pulse was generated and sent to the function generator. Then, the function generator produced a gating signal to control the Xybion intensified CCD camera for measuring either combustion time based upon the length of an illuminated streak, or particle velocity based upon its instantaneous locations.

In the particle velocity measurements, multi-exposure pictures were recorded by the Xybion camera. The exposure time and the time between exposures of the Xybion camera, were controlled by the gating signal generated by the function generator. The particle velocity was then calculated from the images. In the combustion time measurement, a complete streak of burning was recorded. Ignition delay time and combustion time were deduced from the recorded images.

A typical multi-exposure picture recorded by the Xybion camera for particle velocity measurement is shown in Figure 2. In this picture, 6 exposures were made and the exposure time and the time between exposures were 20  $\mu\text{sec}$  and 1 msec, respectively. Five images are shown in

---

<sup>1</sup> This work represents part of the results obtained from the research project sponsored by Naval Surface Warfare center under the contract No. 60921-92-C-0036. The encouragement and support of the Technical Monitor, Mr. Carl Gotzmer of NSWC are highly appreciated.

this picture, it is believed that the boron particle has not been ignited during the first exposure. The gating signal and deduced particle trajectory are shown in Figure 3. In this representative test, the bulk gas velocity of the burned gases is 95 cm/s, the gas velocity at the exit of the particle feeding tube is 940 cm/s and the height of the camera viewing area is 5 cm. By measuring the distance between two consecutive images, the average particle velocity for the five images is found to be 525 cm/s.

Comparison of ignition and combustion behavior of coated and uncoated boron particles will be given in the full paper in terms of their ignitability in different test conditions as well as the particle life time in the combustion zone.

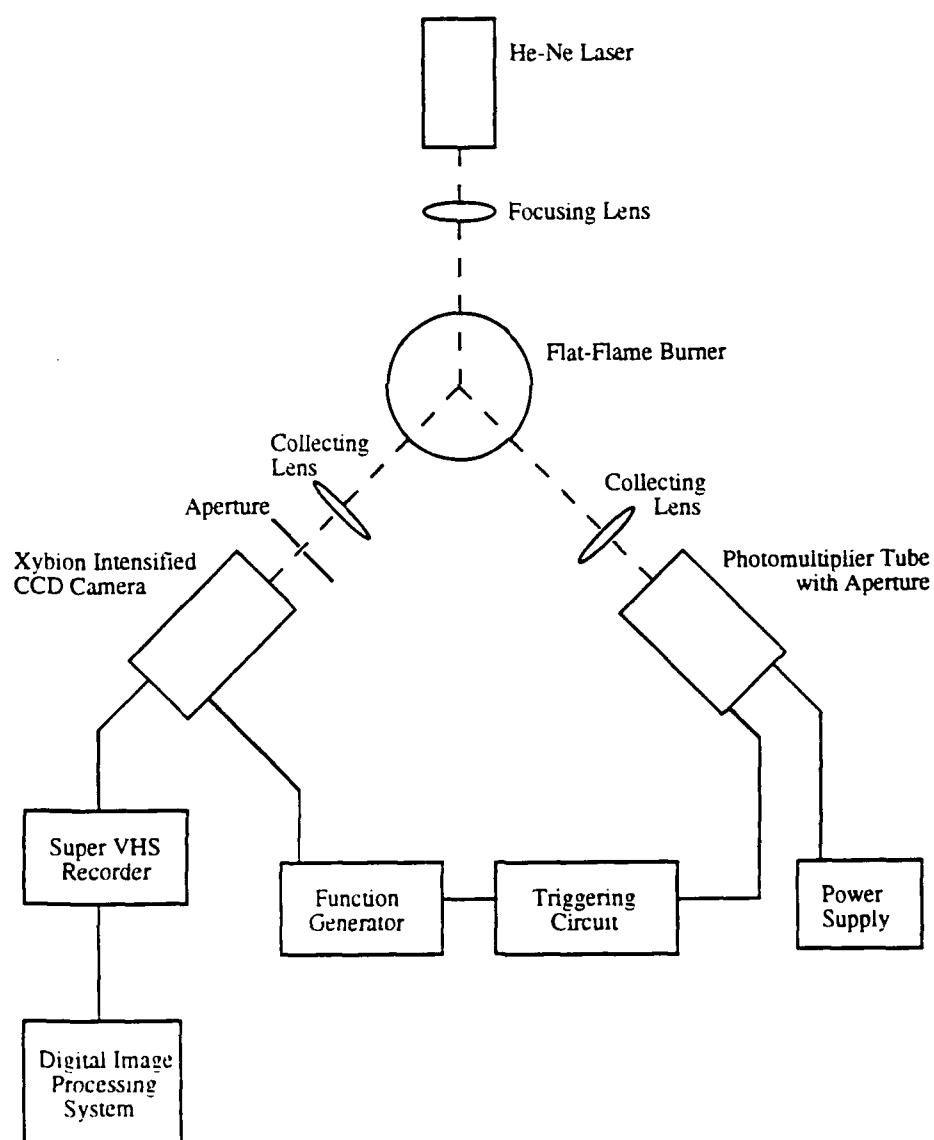


Figure 1 Optical Diagnostic Setup

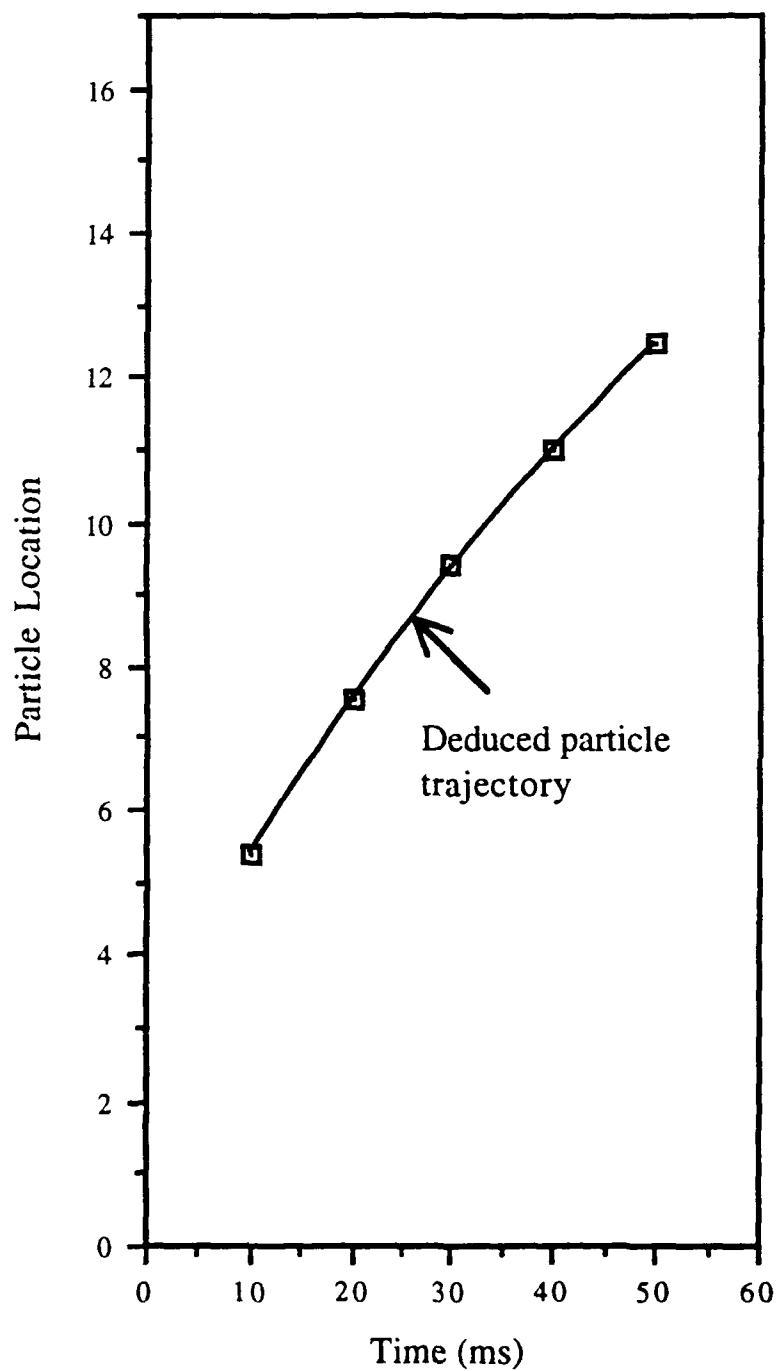
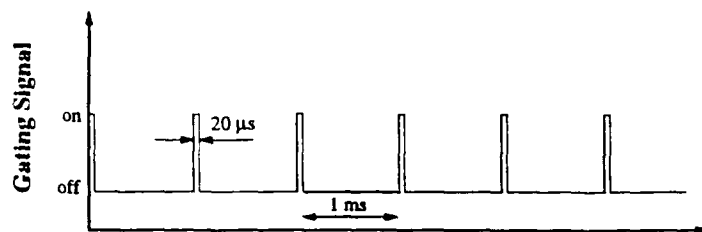
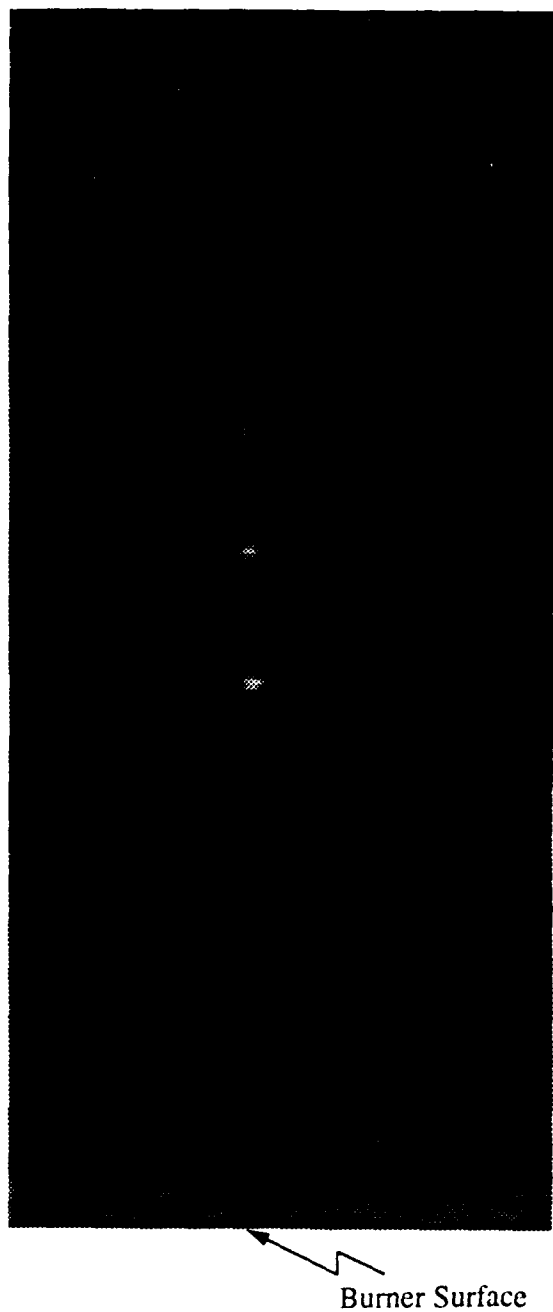


Fig. 2 Xybian Camera Image of Instantaneous Locations of a Moving Particle in the Vertical Direction

Fig. 3 Gating Signal and Particle Trajectory Deduced from Xybian Film Image



# **ROCKET EXHAUST PARTICLES SIZING, AND COMBUSTION DIAGNOSTICS**

## **OF METALLIC SPECIES FROM SOLID PROPELLANTS**

**J. SOULETIS - CELERG 33166 Saint Médard en Jalles - France**

**V. BODART - SNPE 91710 Vert la Petit - France**

**-=-=-=-=-=-=-**

The exhaust from a solid propellant rocket usually contains condensed species, mostly metal compounds, which can be found as raw metal, hydroxides and more often as oxides, chlorides or fluorides. The methodology we develop lies on the measurement of the optical transmission across the exhaust plume, completed in any cases with diffraction recordings close to the light beam in the central lobe of scattering.

The first part of the paper describes the optical method to assess the smoke. It uses a laser system and a single or multiple detector based reception system, and a movie camera observing the laser light scattered by particles for the optical path definition. The transmittance, result of the measurement, can be reduced by means of various hypotheses to obtain the Mic parameter  $Q/\phi$  representative of the interaction of light with mean particles along the optical path. A comparison with a calculation based on the equations of Mie gives then an average size of particles. Direct measurement of the scattered light around the optical beam allows to complete the description of the spherical assumed particles by giving their size without need of the optical index. The latter can be obtained in case of combination of both methods by comparison of results.

Method is then validated from sampling techniques associated with observations by SEM, detections of the metallic elements by X-ray spectrometry, micrographs computer analyses and statistical treatments. Sensitivity of the transmittance to the nature of the metallic additive is then showed both experimentally and theoretically. A given XLDB propellant with the same amount (2 or 3% by mass) of various additives so gives very different results of transverse transmission : a variation by 50% abs in transmission can be obtained for the same configuration.

The condensed species properties, which are very important from the point of view of visible/near infrared detection, are used for the combustion diagnostics of metallic species from the propellant.

If the additive remains inert in the combustion process, a good correlation can be obtained between the sizes distributions in the propellant and in the exhaust plume. The measurement allows then the restitution of particles size distribution inside the chamber and the description of the two-phase mixture for modelization or motor acoustic balance purposes. In the opposite case, any correlation cannot be found between both distributions. The study is illustrated with energetic or reactive additives (Aluminized, copper composed) and with zirconium which remains unburnt in the combustion process. A method for thin layers analysis (Rutherford back-scattering spectrometry) allows the identification of carbon or oxygen in depth of collected particles and confirm the optical results.

Finally, continuous measurements of the transverse transmission along the plume axis give fruitful informations upon the chemical evolution of solid species, particularly as they cross the afterburning flame : changes of state or oxidations can be predicted and confirm diagnostics applied to the nature of the examined species.

# COMPUTERIZED VIDEO IMAGE PROCESSING TECHNIQUE FOR DROPLET COMBUSTION STUDIES

Ilan Hadar and Alon Gany  
Faculty of Aerospace Engineering  
Technion - Israel Institute of Technology  
Haifa 32000, Israel

## ABSTRACT

The combustion characteristics of single (fuel or oxidizer) droplets, particularly in the vicinity of critical thermodynamic conditions, are of great significance in the development of devices, using spray combustion at high pressure and temperature. The lack of essential information concerning some of the basic mechanisms controlling the liquid gasification, leads to recent experimental researches utilizing image analysis, in attempt to help answering some of the questions.

This paper presents a computerized video image processing system which has been developed and built in order to study the behavior of a gasifying/burning liquid droplet at high pressures. The system can automatically compare the variation in the droplet size and shape in consecutive pictures, thereby deriving the burning rate as well as other phenomena.

Unlike other video based image analysis procedures reported in the literature (in which test events are recorded on VCR followed by a later analysis), the data (images) acquired via the present system during the test can be analyzed on-line and stored digitally in the computer memory for a further investigation. Schematic of the system can be seen in figure 1.

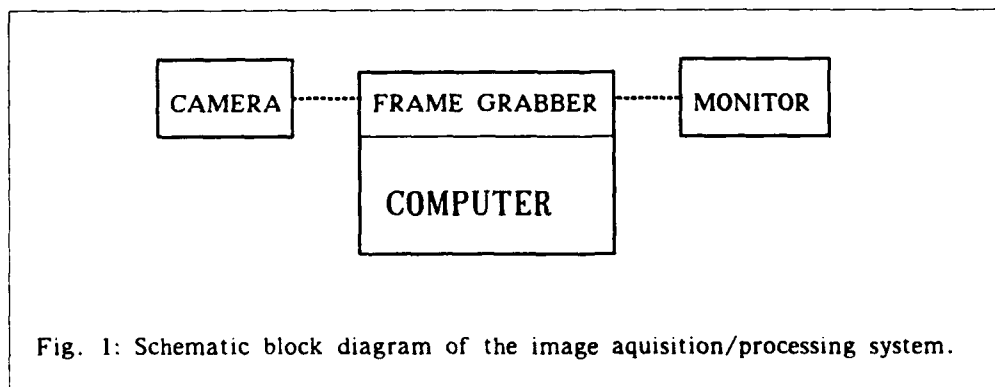


Fig. 1: Schematic block diagram of the image acquisition/processing system.

The hardware components consist of a 486 IBM compatible, 33 MHz computer, a frame grabber, a monitor and a camera. The frame grabber, installed in one of the PC slots, transfers the video signals, arriving from the camera, into digital signals. The monitor is used for the on-line original picture as well as the processed image presentation, while the computer is used to run the software. The system can be connected to any instrument containing charge transfer detectors (e.g., CCD or CID cameras).

A powerful software, named CUE-2, developed in Galai Production Ltd., Israel, is the heart of the system. Each Image (256X256 pixels) contains 0.25 MB, so a relatively large memory is required to store multi-image tests. Some of the features of the user-friendly software which conducts complex image analyses are listed below:

- ☐ Acquisition of 8-bit B/W images (256 gray levels)
- ☐ Image enhancement (filtering, noise removal, etc.)
- ☐ Up to 64 images recalled from memory
- ☐ Build-in flexible analysis of single and multiple images
- ☐ Creation of results files for improved analysis and presentation using different software.

Since the software was developed to meet specific requirements for droplet combustion tests, it enables the following:

- △ Storing up to 42 images in the RAM in a video rate (30 frames or 60 fields per second; typical time: 1-s burning of a 1-mm-diameter droplet).
- △ Combining the images in an overlap mode ("onion rings") to enable presentation of burning rate.

Preliminary results suggest that the system, although designed for droplet burning tests, can serve as a powerful non-intrusive tool for measurements in various combustion and non-combustion environments. The use of the unique capabilities of the hardware/software combination is not restricted to short duration tests. Automatic "Job-programs" enable usage in long tests at the expense of lowering the sampling rate.

HOLOGRAPHIC INVESTIGATION OF SOLID PROPELLANT COMBUSTION  
PARTICLE FIELD WITH SPATIAL FILTERING IMAGING SYSTEM

CHEN SHUXIANG<sup>\*</sup>, ZHANG XIAOWEI<sup>\*\*</sup>, LANG JINGCHAO<sup>#</sup>

Shaanxi Power Machinery Research Institute  
P.O. box 169, Xian, Postal Code 710000  
Shaanxi, People's Republic of China

ABSTRACT

The purpose of this research work is to record, reconstruct and view holograms of solid propellant combustion particle field near burning surface.

The ruby pulsed laser and recording system used are introduced. Problems of elimination of light from stimulating lamp of the ruby laser and from propellant combustion flame are discussed in this paper. In order to improve the quality of solid propellant combustion particle field hologram, a spatial filter is used in the spectral plane of the coherent light imaging system. Other parameters, such as far field number, the intersection angle of scene beam and reference beam, the ending frequency of the propellant combustion vessel window, exposure energy of the holographic film, etc., are discussed also.

Photographs of holographic images of solid propellant combustion particle field near burning surface at different combustion vessel pressures are presented in the paper, which give high contrast.

## **SESSION R-3: CARS Measurements**

**Co-Chairs: Dr. J. H. Stufflebeam and  
Dr. K. Kohse-Höinghaus**

# CARS Temperature Measurements in a Subsonic Combustion Chamber

W. Clauß, R. Söntgen  
A. Rudolph, M. Böhm

DLR, D-7101 Lampoldshausen, Germany

## Experimental Setup of the $H_2$ Combustion Chamber

The CARS technique is used to determine temperatures in a  $H_2$ /air subsonic combustion chamber. The inlet conditions are tabulated in table 1. The teststand is a blowdown windchannel with preheated air produced by  $H_2/O_2$ -combustion. Pressurized air is taken from a  $10\text{ m}^3$  reservoir. The mass fluxes are metered by sonic nozzles with pressure and temperature probes.

Inlet conditions	Air	$H_2$
Total pressure [bar]	2 to 8	0 to 30
Total temperature [K]	280 to 1500	300
Mach number	0.1 to 0.5	$\leq 1$
Velocity [ $\text{m s}^{-1}$ ]	30 to 150	
Mass flow [ $\text{kg s}^{-1}$ ]	1 to 3	0.01 to 0.06

Table 1: Inlet conditions of the subsonic combustor

The subsonic combustion chamber consists of a cylindric channel. The chamber is .5 m long and .1 m in diameter. The CARS setup was situated about 6 m in the light pass away from the combustion chamber.

The combustion chamber described here is a model for future ramjet combustion chambers for hypersonic spaceflight transporters. In this case the combustor has a connected pipe inlet and a sonic nozzle to the environment. The gasflow in the chamber is totally subsonic at Mach numbers between 0.1 to 0.3 at the entrance and Mach 1 in the outlet nozzle.

The combustion zone is a region of a highly turbulent flowfield. Single shot USED-CARS spectra are required at a 10 Hz rate. Experiment runs are between 5 and 10 s. The air heater system allows a repetition rate of about 20 min. The CARS signals were guided to the spectrograph using a 20 m long 0.55 mm quartz fiber.

## The state of gas during and after combustion

The energy release in the combustion chamber is used to expand the gas to high velocity and therefore to produce high thrust.

At the throat the gas flow is sonic. To model the combustion process it is essential to know the temperature profile, pressure, and velocity. In turbulent diffusion flames, the extend of combustion is determined mainly by convective mixing of oxidator and fuel. Additionally to CARS,

LDA and split-film measurements have been done.

In the investigated experimental configuration,  $H_2$  was injected with high swirl ( $Sw = 1.6$ ). This swirl breaks down in the combustion chamber and forces a back-flow region on the chamber axis. Like a conventional flame holder, this back flow may be used to stabilize the turbulent diffusion flame. This phenomenon of swirl breakdown has been characterized theoretically by Navier-Stokes calculations. In experiments, the similarity between swirl number and Reynolds number for  $H_2$  injection has been realized.

## CARS Measurements

CARS measurements have been done in the combustion chamber near the injection point to describe the flame structure and the quality of mixing. Because of the turbulent combustion in the chamber, the temperature profiles are broad.

In an other series, the temperature have been measured directly behind the exit nozzle to characterize the process. The resulting temperature profiles have been compared to pressure measurements. Combining the total mass flow through the nozzle and the pressure in the combustion chamber it is possible to determine the total temperature  $T_t$  before the nozzle. Expanding to sonic condition one can conclude the average temperature at the nozzle exit. Because of the poor estimate of the gas condition and the assumption of an ideal one-dimensional expansion, this method is not very accurate. These temperatures are significantly lower than the CARS temperature.

Temperatures have been also calculated on the basis of an ideal one-dimensional combustion [1] assuming complete mixing of fuel and air at equilibrium conditions. At  $\Phi = 1$ . (Fig. (1)), these calculated temperatures are slightly higher than the measured CARS-temperatures. But at lower mixing ratios, the calculated temperatures are slightly lower. This is due to the incomplete fuel/air mixing.

## Conclusions

Temperatures in a subsonic combustion chamber have been determined using the CARS technique. The results have been compared to theoretical calculations on the basis of ideal one-dimensional combustion. The agreement is sufficient for calculations assuming complete mixing at equilibrium condition.

Inhomogenities in the dynamic mixing are described experimentally by LDA- and split-film measurements.

The phenomenon of swirl breakdown is described theoretically by Navier-Stokes calculations.

## References

- [1] S. Gordon, B.J. McBride  
Computer Program for Calculation of Complex Equilibrium Compositions, Rocket Performance, Incident and Reflected Shocks, and Chapman-Jouguet Detonations  
NASA-SP-273, NASA Lewis Research Center, 1971.



# Temperature Profile in the Nozzle Exit Plane of a Hydrogen-Air Subsonic Combustion Chamber

Test conditions		
$\dot{m}_L$	=	1.2 Kg/s
$\dot{m}_{H_2}$	=	40 g/s
$\Phi_{st}$	=	1.0
$p_t$	=	6.0 bar
$T_{in}$	=	870 K

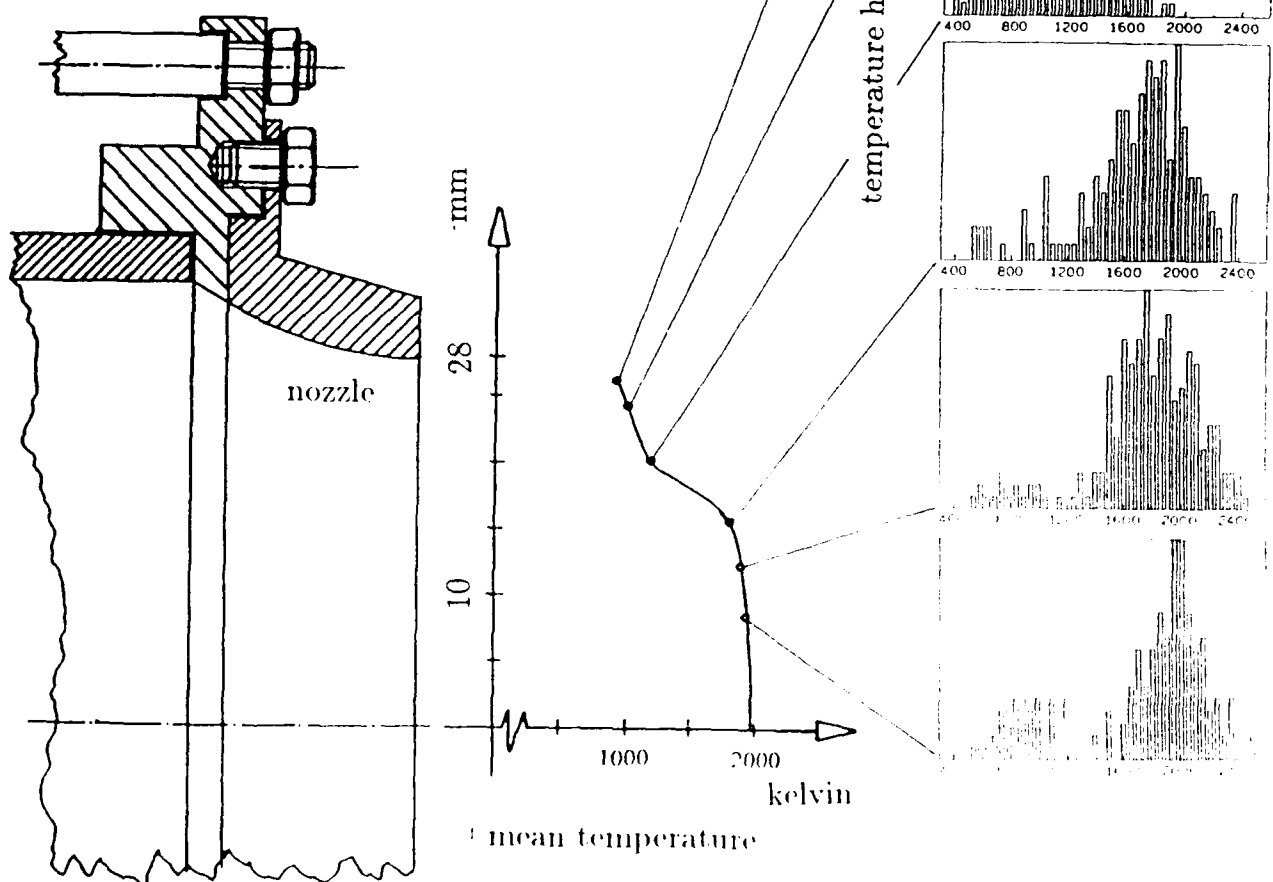


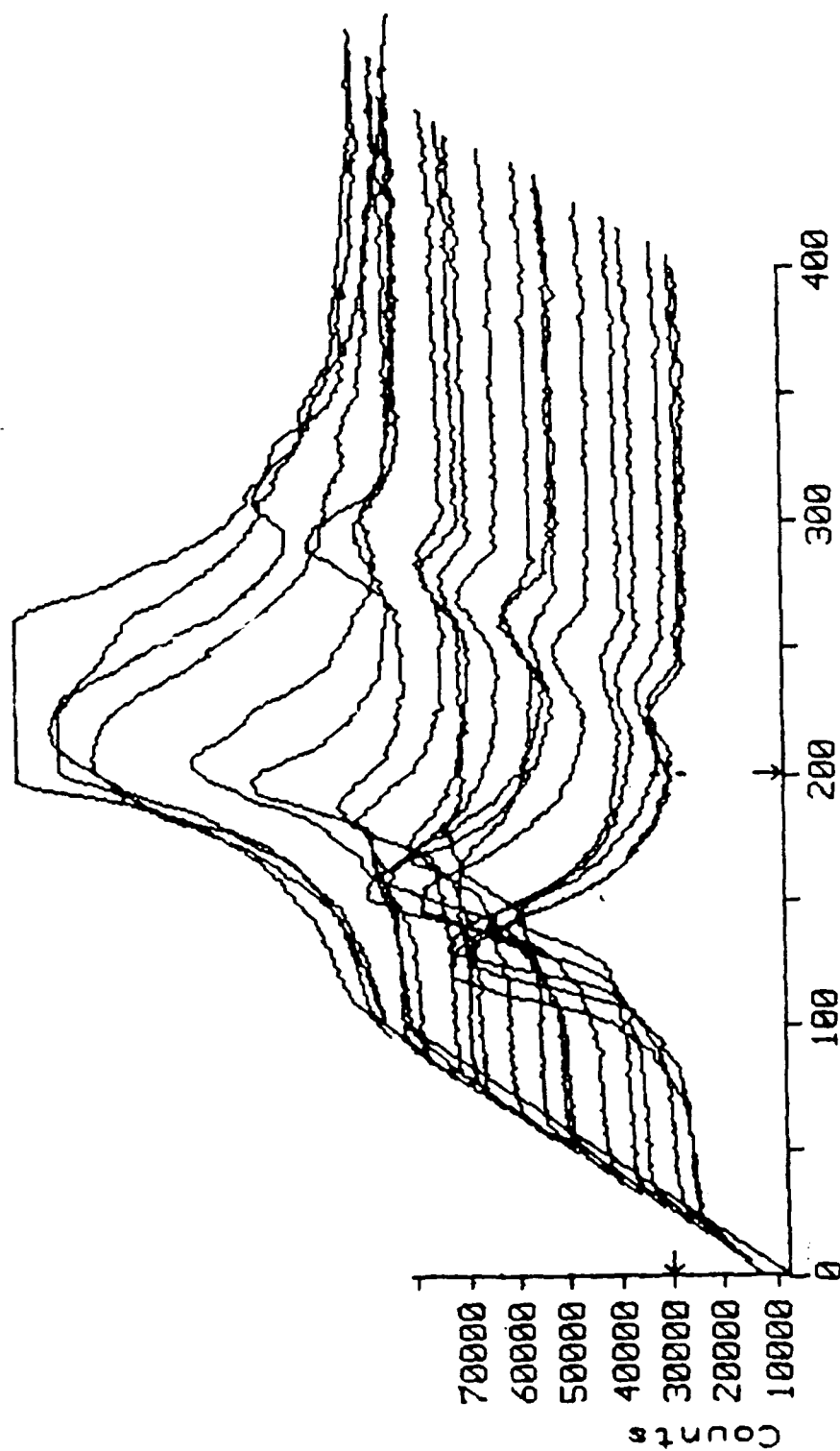
Fig. 1: Temperature Profile in the Nozzle Exit Plane at  $\Phi = 1$

## Measurements of the Flame Temperature of Solid Propellants Using the Single-Shot CARS Technique

*Dah-Ming Chen\* and Huey-Cherng Perng Hsueh-Chi Wang*  
Chemical System Research Division, Chung Shan Institute of Science and Technology,  
Taoyuan, Taiwan 32526, Republic of China

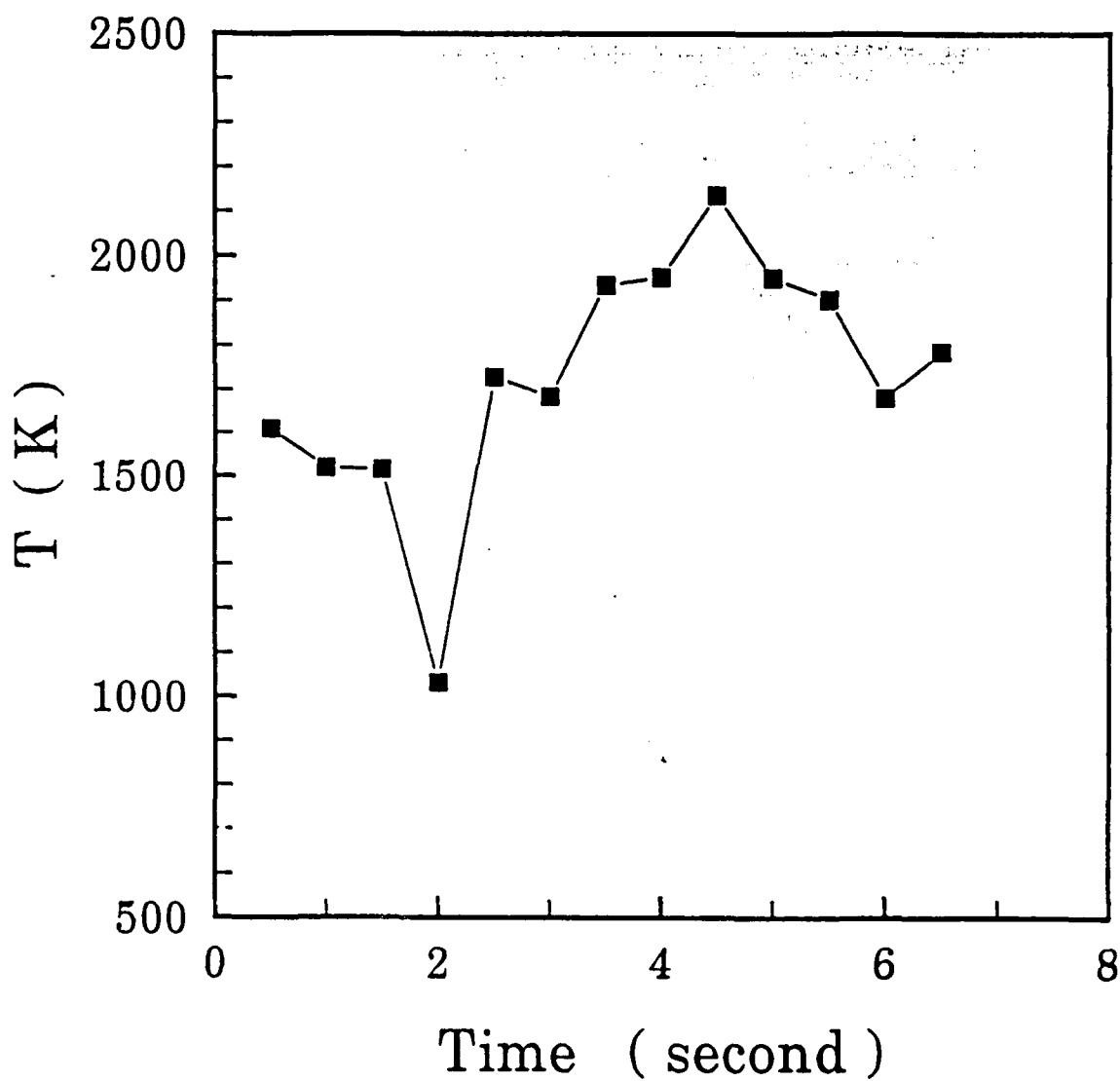
*Yen-Tsung Hsu and Yuan-Pern Lee*  
Department of Chemistry, National Tsing Hua University  
Hsinchu, Taiwan 30043, Republic of China

A single-shot, broad-band CARS system has been constructed for the measurements of flame temperature of solid propellants. A Nd-YAG laser system which produced 550 mJ/pulse energy of a near-Gaussian beam at 532 nm was employed. Approximately half of the energy was used to pump a R640 dye laser system with grating set at the zeroth-order so as to produce broad-band ( $\sim 20$  nm) output near 606 nm. The BOXCARS beam arrangement was used and the laser was operated at 10 Hz. The CARS signal was spatially filtered before it was passed through a double monochromator and detected by an optical multichannel analyzer. The combustion vessel was a high-pressure chamber with quartz view-ports and two arms for laser-beams; a purge system was employed to reduce the interference by the smoke generated from combustion of propellants. CARS spectra of  $N_2$  were recorded at 0.1 s intervals throughout the combustion process. These spectra were later transferred to a microcomputer and fitted with the spectra predicted by theory to yield the temperature of the flame. Typically a sample strand of propellant  $\sim 5$  cm in length lasts for  $\sim 10$  sec. A brief review of the development of this instrument in Taiwan will be presented, with comparison of beam arrangements: USED CARS, HYBRID CARS, and BOXCARS. Recent results on the measurements of the flame temperature of both the  $CH_4$  flame and solid propellants will be discussed.



Compilation of the  $N_2$  CARS Spectra from Combustion of  
Sample A. Time = 0 - 10 sec.

## D09U980413-04 Data



Temperature Variation of the Combustion of Sample A.

Table    Temperature Measurements of the Combustion of Sample A.

Time	Temperature
/sec.	/K
0.5	1609
1.0	1518
1.5	1514
2.0	1033
2.5	1727
3.0	1684
3.5	1934
4.0	1952
4.5	2134
5.0	1951
5.5	1902
6.0	1679
6.5	1785

# Quantitative Nitric Oxide CARS Spectroscopy in Propellant Flames

A. Kurtz<sup>1</sup>, D. Brüggemann<sup>2</sup>, U. Giesen<sup>1</sup>, S. Heshe<sup>2</sup>

<sup>1</sup> *Bundesinstitut für chemisch-technische Untersuchungen (BICT)  
Grosses Cent. D-5357 Swisttal 1, Germany*

<sup>2</sup> *Lehrstuhl für Technische Thermodynamik, RWTH Aachen (Univ. of Technologie)  
Schinkelstr. 8, D-5100 Aachen, Germany*

## Abstract

The merits of coherent anti-Stokes Raman spectroscopy (CARS) measurements in propellant flames has been reported in numerous papers. Some of these temperature measurements were performed under low pressure to resolve the reaction zone /1/. Qualitative concentration estimations for several species were deduced from CARS spectral signatures. Quantitative concentration measurements in propellant flames in an elevated pressure environment were first reported by Stufflebeam and Eckbreth /2/.

Due to the chemical composition of propellants with preformed NO<sub>2</sub> compounds the initial NO concentration during the combustion process is by orders of magnitudes above the equilibrium value and may exceed a mole fraction of 10%. Under elevated pressure NO decomposition processes are very fast. Therefore the NO concentration is within the range of the thermal equilibrium concentration value which is below the sensitivity of conventional CARS methods. Under ambient pressure however, the rate of NO decomposition strongly depends on temperature which may be influenced by the rate of additional airfeed.

Combustion of energetic material under normal pressure is currently discussed as a technique for disposing explosive waste. Therefore our measurements were performed under ambient pressure to investigate the reaction mechanism which influences the nitric oxide emission. Our measurements were performed using a cylindrical tube as combustion chamber to stabilize a quasi 1-D flame structure. The gaseous decomposition products of the propellant were mixed with an axially induced flow of air. The fuel/oxygen ratio was adjusted by different flow rates taking into account the linear burning velocity of the propellant.

CARS spectroscopy was applied to measure as a first step temperatures under different combustion conditions by analysing the signature of N<sub>2</sub>-Q-branch spectra. Then nitric oxide Q-branch spectral shapes were modelled depending on temperature and concentration using recommended molecular data /3/. Measured spectral shapes in propellant flames were fitted to these spectra to evaluate to the first time NO concentrations using the well-known interference between resonant and non-resonant susceptibilities.

The evaluation of NO CARS spectra exhibits an initially high NO concentration near the surface of the propellant strand which decreases more or less rapidly downstream depending on the flow rate of additional air. Correlated CARS temperature measurements show that NO decomposition processes start at the temperature level above 2500 K. This is the required temperature to reduce NO emission by combustion processes.

## References:

1. K. Aron, L.E. Harris, *Chem. Phys. Lett.*, **103** (1984) 413
2. J.H. Stufflebeam, A.C. Eckbreth, *Combust. Sci. and Tech.*, **66** (1989) 163
3. D. Brüggemann, A. Kurtz, U. Giesen, S. Heshe, in *Coherent Raman Spectroscopy: applications and new developments*, eds. F. Castellucci, R. Righini, P. Foggi (World Scientific Publishing Co Pte Ltd, Singapore 1992) in press

## **SESSION R-4: LIF and PLIF Diagnostics**

**Co-Chairs: Prof. E. Bar-Ziv and  
Dr. H. B. Levinsky**



## Measurements of Rotational Energy Transfer in OH A $v' = 0$ at Elevated Temperatures

M. P. Lee, R. Kienle and K. Kohse-Höinghaus

DLR-Institut für Physikalische Chemie der Verbrennung

Pfaffenwaldring 38-40, D-7000 Stuttgart 80, Germany

Laser-induced fluorescence (LIF) has been shown to be one of the most versatile and sensitive diagnostic techniques for combustion studies. The hydroxyl radical (OH) has been widely utilized for LIF studies because of its importance as an intermediate species in chemical reactions occurring in combustion. The development of quantitative OH LIF diagnostics requires data on energy transfer processes in order to accurately predict and evaluate fluorescence signals. Rotational energy transfer (RET) is particularly important, since this process is often the most rapid mechanism for energy transfer into and out of the laser-coupled levels.

RET of OH A  $v' = 0$  at room temperature has been extensively studied.<sup>1,2</sup> These measurements have shown significant variations in RET rates with colliding species and rotational level. In contrast, few measurements have been performed at elevated temperatures, the regime of interest for combustion processes. Stepowski and Cottureau<sup>3</sup> have determined total RET rates for a single rotational level ( $J' = 7.5$ ) for collisions with  $N_2$  and Ar. Lucht et al.<sup>4</sup> have measured data on OH RET from collisions with  $H_2O$  for four rotational levels. The accuracy of these results were insufficient to observe a systematic variation of the RET rate with rotational level. Thus, improved data on OH RET at elevated temperatures is required.

Energy transfer rates for several rotational levels of OH A  $v' = 0$  have been measured in low-pressure flames. Individual rotational states in  $v' = 0$  have been excited via the A-X (0,0) transition at 308 nm, and the temporal decay of the fluorescence originating from the entire  $v' = 0$  level and from the laser-excited state has been observed. The simultaneous observation of the broadband LIF and the state-specific LIF signal provides data on both the RET rate and the rotationally-averaged quenching rate. Results acquired in a stoichiometric 5 mbar  $CH_4/O_2$  flame indicate that the total RET rate tends to decrease with increasing rotational level. This data will be used to extend models for OH rotational energy transfer and to improve the accuracy of interpretation of OH fluorescence signals.

1. Lengel, R. and Crosley, D., J. Chem. Phys. **67**, 2085 (1977).
2. Jörg A., Meier, U., Kienle, R. and Kohse-Höinghaus, K., accepted for publication in Appl. Phys. B.
3. Stepowski, D. and Cottureau, M., J. Chem. Phys. **74**, 6674 (1981).
4. Lucht, R., Sweeney, D. and Laurendeau, N., Appl. Optics **25**, 4086 (1986).

**Collisional energy transfer in OH ( $A^2\Sigma^+$ ): investigations for  
quantitative LIF combustion diagnostics**

R. Kienle, M. P. Lee, U. Meier, K. Kohse-Höinghaus  
DLR-Institut für Physikalische Chemie der Verbrennung  
Pfaffenwaldring 38-40, D-7000 Stuttgart 80, Germany

Laser-induced fluorescence is a very attractive technique for the measurement of radical concentration and temperature in combustion. One of the key problems associated with the quantitative interpretation of LIF experiments is the competition of the fluorescence emission with collisional energy transfer processes. Detailed modelling is necessary in order to understand the influence of the different types of energy transfer (i.e., rotational energy transfer (RET), vibrational energy transfer (VET), electronic quenching) on the fluorescence signal. We have developed a multi-level model for simulation of the temporal evolution of the OH rovibronic populations following laser excitation. With this model, the sensitivity of the fluorescence signal to variations in transfer rates can be examined. In addition, the applicability of simple models (e.g. the balanced cross-rate model) can be tested. Finally, the model can be used for evaluation and optimization of experimental approaches.

The development of this model may be divided into three steps. In the first study, state-to-state rotational energy transfer coefficients for thermal collisions of OH ( $A^2\Sigma^+$ ,  $v'=0$ )<sup>1,2</sup> and OH ( $A^2\Sigma^+$ ,  $v'=1$ )<sup>3</sup> with several colliders (He, Ar, N<sub>2</sub>, H<sub>2</sub>O, C<sub>2</sub>O) were measured. We have observed that the magnitude and qualitative behaviour of the RET depends strongly on the collision partner, but is roughly independent of the vibrational level. In the next step, we have examined various scaling and fitting laws to describe and extrapolate our experimental data base. Our approach is based upon the IOS scaling law for  $^2\Sigma^+$  molecules<sup>4</sup>, combined with a energy-based fitting law for the basis coefficients. With this model we can accurately represent the measured RET of OH ( $A^2\Sigma^+$ ) in collisions with the most important colliders H<sub>2</sub>O and N<sub>2</sub>. In the last step we have adapted a numerical code, originally developed for the simulation of large chemical kinetic systems (LARKIN<sup>5</sup>), to model energy transfer in the OH A-X band system. This numerical model permits simulation of time-dependent level populations and

fluorescence spectra. The calculated transients and spectra are in good agreement with measurements acquired in a low-pressure flow reactor and in a low-pressure flame. The model has in a first application been used to study the complex influence of RET and quenching on the accuracy of two-line temperature measurements. The results of this study illustrate the sensitivity of two-line thermometry to the ratio of the total RET versus quenching and to the rotational level dependencies of the RET and quenching.

- 1 A. Jörg, U. Meier, K. Kohse-Höinghaus, J. Chem. Phys. **93**, 6453 (1990)
- 2 A. Jörg, U. Meier, R. Kienle and K. Kohse-Höinghaus, Appl. Phys. B (1992),  
accepted for publication
- 3 R. Kienle, A. Jörg, K. Kohse-Höinghaus, manuscript in preparation
- 4 M. Alexander, J. Chem. Phys. **76**, 3637 (1982)
- 5 P. Deuflhard, G. Bader, U. Nowak: LARKIN - a software package for the  
numerical simulation of large systems arising in chemical reaction kinetics.  
In: K. H. Ebert, P. Deuflhard, W. Jaeger (eds.): Modelling of Chemical Reaction  
systems.  
Springer Series Chem. Phys. 18 (1981)

TWO DEGENERATE FOUR-WAVE MIXING TECHNIQUES FOR MEASUREMENT OF  
OH IN FLAT FLAMES AT 1 TO 9 BAR COMPARED WITH LASER-INDUCED  
FLUORESCENCE AND ABSORPTION MEASUREMENTS

Eric Domingues and Marie-Joseph Cottureau

CORIA URA CNRS 230 B.P. 118

76134 Mont Saint Aignan, France

Douglas Feikema

The University of Alabama in Huntsville

UAH Propulsion Research Center. E-31 RI Building

Huntsville, AL 35899 USA

The OH radical number densities have been measured in laminar premixed methane-air flames up to 9 bar using four different non-intrusive optical techniques. Two of these techniques are well-established methods :

- Absorption
- Laser Induced Fluorescence (LIF)

The other two techniques are relatively new non-linear optical processes for measuring minor reactive species :

- Degenerate Four-Wave Mixing (DFWM)
- Double Phase-Conjugate Four-Wave Mixing (DPCFWM)

The major conclusions of the present effort are as follows :

1 ) Contrary to LIF, neither DFWM nor DPCFWM demonstrates drastic collisional quenching effects at 9 bar pressure. However, beam steering effects due to large fluctuating density gradients at the edge of the flame makes DFWM a low-biased technique at 9 bar. Histograms of DFWM and DPCFWM signals at 9 bar demonstrate this point.

2 ) DPCFWM enables OH number density measurements up to 9 bar in present experiments without correction for quenching or other effects (fig.1).

3 ) OH rotational temperature ( $1940 \text{ K} \pm 150 \text{ K}$ ) in a laminar laboratory,  $\Phi=0.85$  flame at 9 bar as well as in other flames have been successfully measured with DPCFWM, demonstrating the capabilities of this promising non-intrusive combustion diagnostic tool.

4 ) A series of experiments designed to evaluate the effects of saturation and pressure on DPCFWM and DFWM on FWHM spectral linewidth demonstrates that :

- a ) Saturating pump intensities increases both DFWM and DPCFWM FWHM linewidths.
- b ) Pressure broadening occurs and is nearly linear between 1 and 9 bar pressure

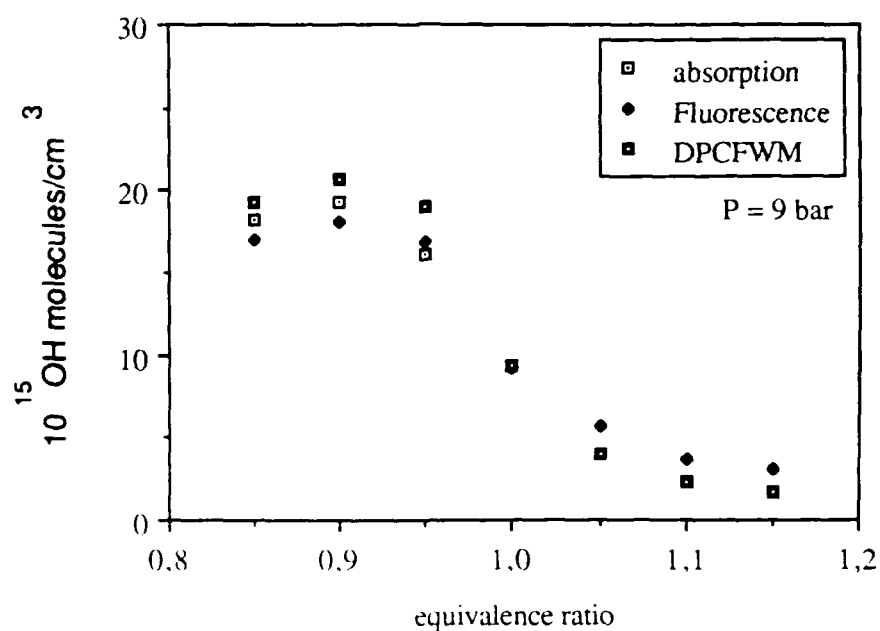


Figure 1 : OH number density in the postflame gases (i.e. 5 mm above the burner) as a function of equivalence ratio at 9 bar obtained by absorption, LIF, and DPCFWM. To take into account quenching effects the LIF intensities have been multiplied by 7.0

**SESSION R-5: Combustion Diagnostics of  
Solid Propellants**

**Co-Chairs: Dr. A. Davenas and Dr. R. S. Miller**

STUDY ON THE SUBATMOSPHERIC BURNING RATE CHARACTERISTICS  
OF COMPOSITE PROPELLANTS

Kazushige Kato and Motoyasu Kimura  
NOF Corporation, 61-1 Kitakomatsudani, Taketoyo-cho, Chita-gun,  
Aichi 470-23, Japan

Masahiro Kohno and Kiyokazu Kobayashi  
Institute of Space and Astronautical Science, 3-1-1 Yoshinodai  
Sagamihara, Kanagawa 229, Japan

ABSTRACT

Institute of Space and Astronautical Science (ISAS) is undertaking development work of its newest satellite launcher M-V. HTPB base highly aluminized composite propellants have been newly developed to be loaded to the motors. Subatmospheric burning rate characteristics of them were investigated to anticipate the thrust decay behavior well into the residual thrust region of every stage motor. A simple but unique method was employed in the measurements. The size of propellant specimen was quite small; 8 mm long and 8 mm in diameter. Ignition was detected by a photo-transistor and burnout by an ion probe or by a fine thermocouple.

## TRANSIENT BURNING BEHAVIOR OF A SOLID PROPELLANT\*

K.K. Kuo<sup>1</sup>, Y.C. Lu<sup>2</sup>, Y.J. Yim<sup>3</sup>

Department of Mechanical Engineering  
The Pennsylvania State University  
University Park, PA. 16802, U.S.A.

and

F.R. Schwam<sup>4</sup>

Olin-Rocket Research Company  
Redmond, WA 98073, U.S.A.

### ABSTRACT

The objective of this investigation is to study the transient burning behavior of a solid propellant using a real-time X-ray radiography system, a high-pressure test rig, and a high-speed video camera. The utilization of X-ray radiography system presents a method for direct measurement of propellant burning rate in a non-intrusive manner; the variation of burning rate with respect to time can be observed without interference with test condition.

The test sample was ignited by an igniter system which consisted of an electric match and a certain amount of black powder. The regression rates of the end-burning cylindrical propellant grains were deduced directly by analyzing the time variation of the displacement of burning surface from instantaneous X-ray radiographic images recorded by the camera. The pressure-time history of each test run was recorded using a high-frequency pressure transducer with a Nicolet oscilloscope. High pressurization rates were achieved and controlled by adjusting the size of the free volume in the test chamber and the amount of igniter charge. A set of deduced transient burning rates versus pressure is shown in Fig. 1 for different pressure-time histories given in Fig. 2. Based on these two figures, it is obvious that propellant burning rate can indeed be significantly influenced by the nature of the entire pressure-time history, not just by the magnitude of the instantaneous pressure.

The transient burning rates were compared to the steady-state data obtained from an optical strand burner. The strand burner tests were conducted for broad ranges of initial temperatures (-40 to 70° C) and chamber pressures (0.1 to 41.4 MPa). The steady-

---

\* This work was sponsored by Olin-Rocket Research Company. The authors would like to thank Drs. W. H. Hsieh and S. R. Wu of PSU for their participation in several experimental test runs.

<sup>1</sup> Distinguished Professor and Director of the High Pressure Combustion Laboratory

<sup>2</sup> Post-Doctoral Fellow

<sup>3</sup> Visiting Research Associate, presently at Agency for Defense Development of Korea

<sup>4</sup> Principal Analysis Engineer



state burning rate up to 41.4 MPa is also shown in Fig. 1 for the purpose of comparison. It is clear that the transient burning rate can be quite different from the measured and extrapolated steady-state burning rate. Therefore, the effect of pressure transient on propellant burning rate has to be accounted for prior to the actual usage of the propellant in propulsion systems.

Fine-wire micro-thermocouples were embedded in solid propellant strands for subsurface and surface temperature measurements. The steady-state burning rate and surface temperature data were used for the construction of a Zeldovich map, which was utilized for determining the amount of heat feedback for any given set of values of burning rate and chamber pressure. Based on the quasi-steady flame assumption adopted in the Zeldovich method, the amount of heat feedback is a function of pressure and instantaneous burning rate only, no matter the propellant is under a steady-state or transient burning condition. Therefore, Zeldovich map provides an important information for calculating transient burning rate. Figure 3 shows Zeldovich map in terms of dimensionless burning rate, heat feedback, pressure, and initial temperature for the propellant under investigation.

In order to determine the subsurface temperature profile prior to the burning of solid propellant sample, the heat flux from the gas phase to the sample surface created by the igniter charge was also measured. The heat flux versus time trace was deduced from the data obtained by a thin heat flux gauge placed on the sample surface location. A transient heat conduction equation was solved for the time variation of subsurface temperature profile using the heat flux-versus-time trace as one of the boundary conditions. Transient burning rate of a solid propellant was determined through an iteration procedure. Detailed comparison of calculated results with experimental data will be given in the paper.

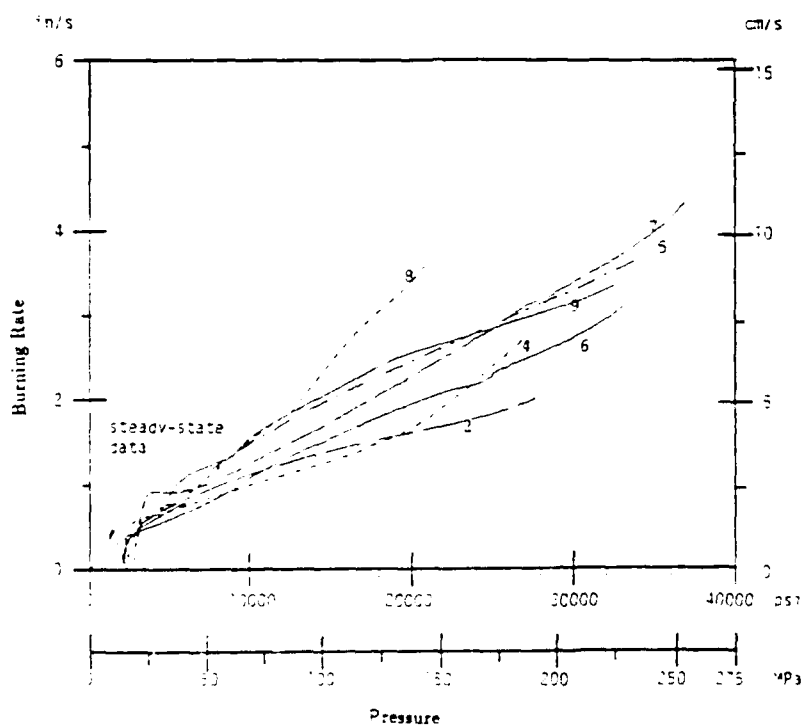


Fig. 1 Transient burning rate versus pressure

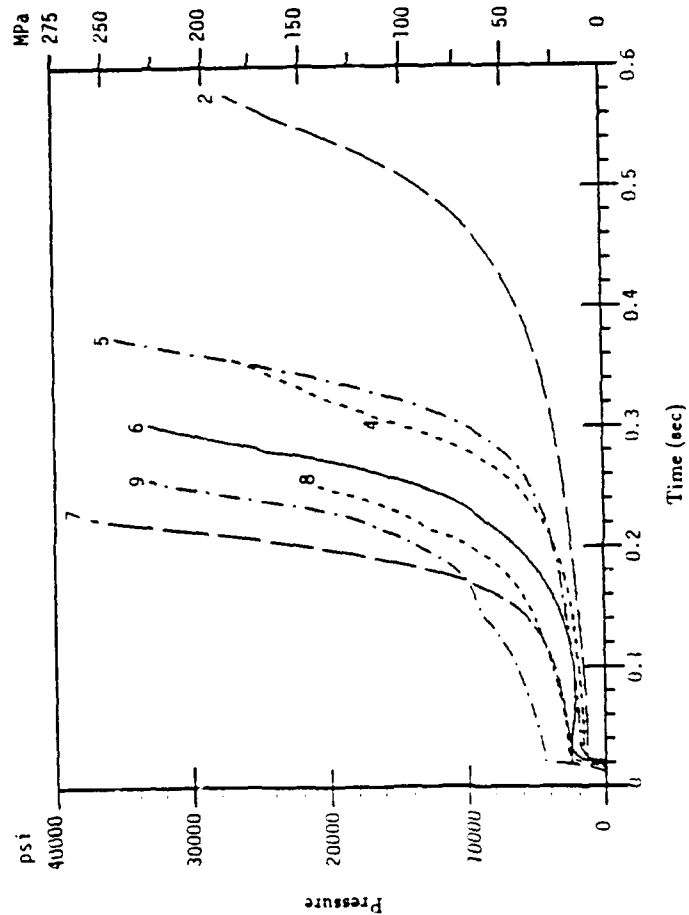


Fig. 2 Pressure-time traces of different test runs

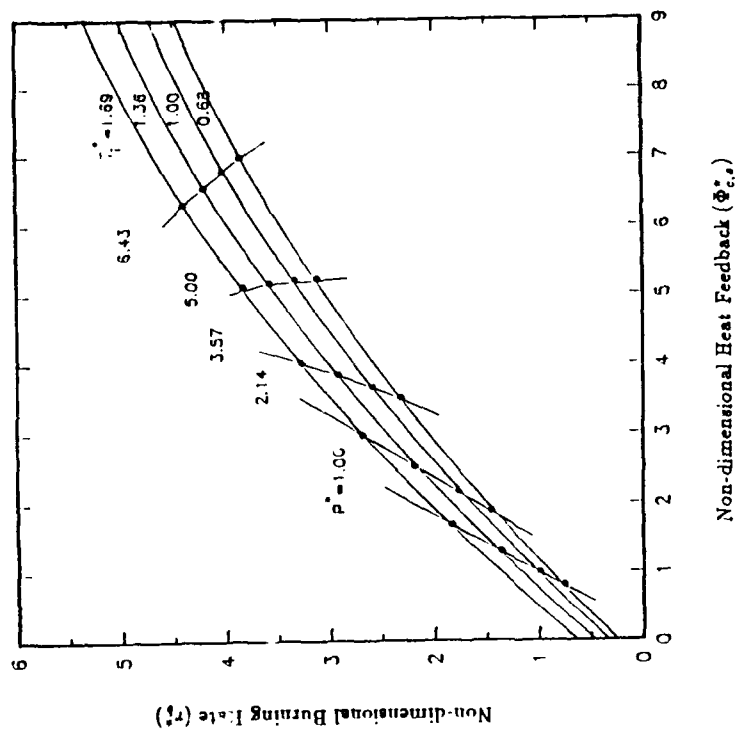


Fig. 3 Burning rate versus heat feedback

## **DIAGNOSTIC TOOLS FOR STUDIES ON BURN RATE BEHAVIOR OF ADVANCED SOLID PROPELLANTS**

**S.N. Asthana, A.N. Nazare, S.S. Dhar, P.G. Shrotri and Haridwar Singh**  
Explosives Research & Development Laboratory, Pune 411 008. INDIA.

Burning rate-pressure relationship is one of the major criteria in the selection of propellant for various applications. Regression rate of solid propellant is an important parameter pertaining to solid propellant performance. Various non-intrusive methods like Crawford Bomb (Strand Burner), Microwave Technique and Optical Surface Tracking Devices are recommended for the determination of propellant burn rates. During 70's the Ultrasonic Acoustic Technique has emerged as the direct method for determination of burn rates at constant pressure. This technique which is based on the principle of recording the acoustic waves in the ultrasonic range generated when a propellant strand burns, is increasingly being used as a research tool for evaluation of new propellant compositions and also as a quality control method for well established propellant formulations.

During the present study, exhaustive burn rate data at different pressures has been generated for double base, composite, nitramine based minimum signature compositions and GAP based propellants using this technique. An attempt has been made to correlate the burn rates obtained by Acoustic technique and Crawford Bomb method with rocket motor firings.

The results obtained indicate that double base propellants exhibit a close relationship between the Crawford Bomb burn rate and Static Firing test. For composite propellants, results obtained using Acoustic technique were found to be in close agreement with static firing results. An empirical relationship has been established between the acoustic burn rate data and static firing results for nitramine based minimum signature compositions and GAP based propellant systems. This paper analyses the static firing results obtained from 2-40 kg motor in case of AP-Al based composite and AP-Al based CMDB propellants.

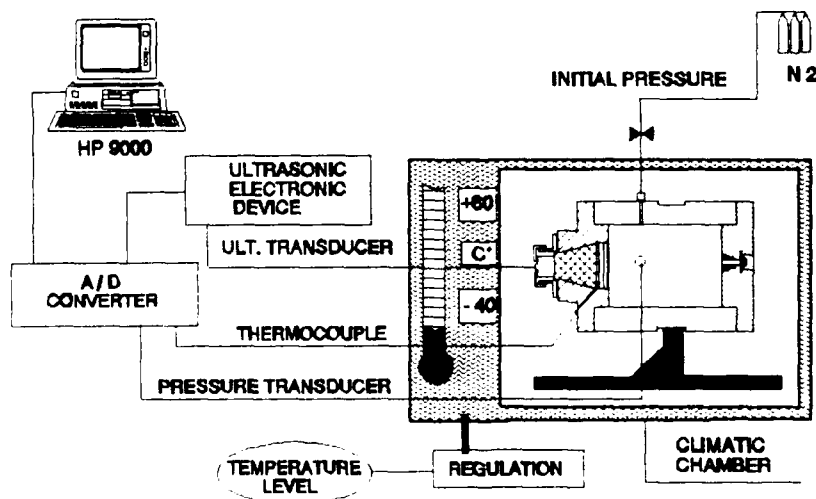
# DETERMINATION OF SOLID PROPELLANT BURNING RATE SENSITIVITY TO THE INITIAL TEMPERATURE BY THE ULTRASONIC METHOD.

F.Cauty, J.C Démarais and Ch. Eradès

Office National d'Etudes et de Recherches Aérospatiales  
29, avenue de la Division Leclerc  
92320 Chatillon (France)

The sensitivity to initial temperature of solid propellant burning rate is an important parameter for the propellant manufacturer and for the missile designer. The firing of solid propellant rocket motors with large grains at various initial temperatures is expensive and not easy to run. Usually only a limited number of tests are done. At ONERA, an ultrasonic method is used to determine solid propellant burning rates at room temperature. A program has been set up to develop this method at different initial temperature in the range  $-40^{\circ}\text{C}$ ,  $+60^{\circ}\text{C}$ .

The work started with the development of an ultrasonic transducer usable at low temperature, classical ones embedding burning surface echoes within multiple reflections of their internal backside damping material. A coupling material is used as a delay line between the transducer and the propellant sample. Its acoustic impedance must be closely matched to the propellant one to minimize interface echoes. This fact must be verified whatever the initial temperature is. So the ultrasonic wave velocities and dampings have been determined in a large temperature range for selected propellants and coupling materials which are castable resins. Finally, the ultrasonic method has been applied to burning tests in a closed vessel which is pressurised by combustion gases of the propellant sample itself. The set-up is thermally regulated.



The main difficulties concerned the castable resin choice related to each propellant, its behavior during heating or cooling (thermal dilatation coefficient), its mechanical properties and adhesive qualities. The pressure influence on the ultrasonic wave velocities by means of the stress distribution, is taken into account for each initial temperature. The web distance burned and the regression rate are then deduced from the ultrasonic wave propagation time variation measured during the propellant surface regression.

This method has been carried out successfully for three solid propellants, each of them belonging to different propellant type (homogeneous, AP/HTPB and HMX propellants) at three initial temperatures ( $-40^{\circ}\text{C}$ ,  $+20^{\circ}\text{C}$ ,  $+60^{\circ}\text{C}$ ). The results are represented by regression rate laws and initial temperature sensitivity coefficients. They are compared to results obtained by classical means (Strand-burner, rocket-motor tests). This ultrasonic method can increase the productivity by limiting the test number and the grain masses involved, the regression rate being obtained from only one test in a large pressure range. SNPE, French propellant manufacturer, is working on this subject in terms of an industrial procedure application (acceptance specification control).

This work has been supported by "Service Technique des Poudres et Explosifs, Direction Générale de l'Armement", France, and by "Société Nationale des Poudres et Explosifs", France.

INVESTIGATION ON SOLID ROCKET PROPELLANT COMBUSTION  
BY LASER DOPPLER ANEMOMETRY.

A. Volpi and C. Zanotti

CNPM- *National Research Council*  
viale F. Baracca 69  
20068 Peschiera Borromeo (Milan) ITALY

The experimental study of solid rocket propellant combustion has been improved by using Laser Doppler Anemometry (LDA) which is able to measure the velocity of the gases coming out from the burning propellant surface.

A He-Ne laser (25 mW,  $\lambda = 632.8$  nm) is used to form the probe volume. The scattered light generated signals, coming from the particles suspended in the gas flow and crossing the interference fringes in the probe volume, are processed by a Burst Spectrum Analyzer (BSA) and a dedicated personal computer stores data (up to 12000 velocity data for each run) and performs the frequency analysis.

The diagnostic technique has been used to test homogeneous propellants under steady state combustion conditions in the pressure range from 20 to 40 atm (Fig.1) and composite propellants from the pressure daflagration limit (PDL) up to 5 atm.

The results obtained under this configuration have given a good picture of the flame structure. For homogeneous propellant, it was possible to get data concerning the dark zone length and the residence time.

Self-sustained oscillatory burning occurring at low pressure for composite propellants was investigated (Fig.2) and their oscillatory frequencies were determined by FFT techniques. Different composite propellants were tested and the results have clearly shown the influence of the AP particle size on the oscillatory behavior.

The same methodology was used in the experimental study of the frequency response of solid burning propellant driven by modulated laser radiation flux for an AP/HTPB(86/14) propellant in the sub atmospheric pressure range (Fig 3).

The results show that the gas-phase response to the external stimulus depends on the forcing laser frequencies with a maximum for every working pressure. The comparison of the overall data set with results obtained using other experimental techniques confirm the validity and the reliability of the LDA in the solid rocket propellant combustion study.

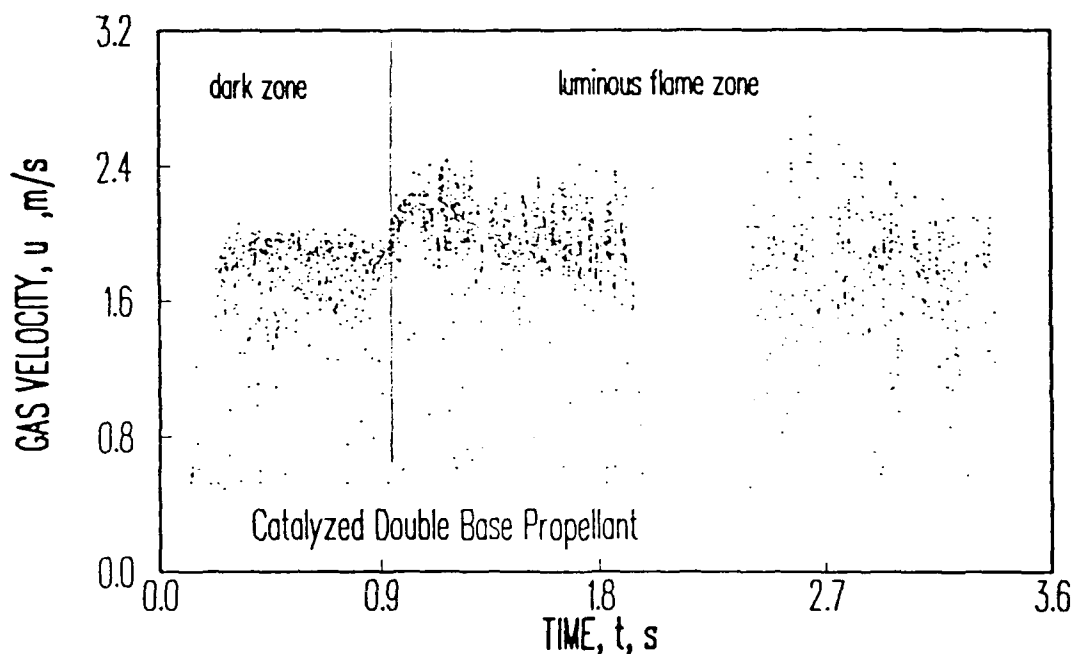


Fig.1 Double Base flame structure by LDA technique.

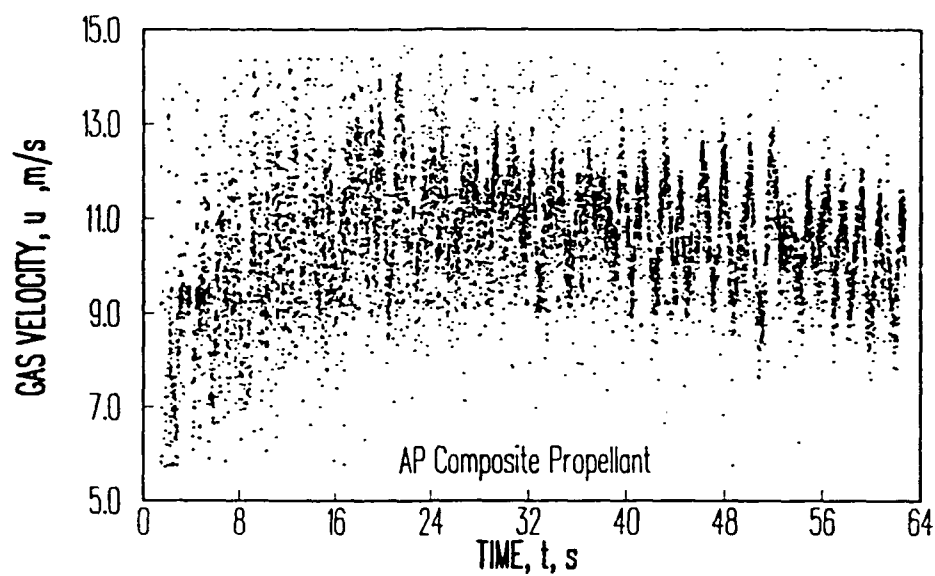


Fig.2 Typical gas velocity behavior in the self-sustained oscillatory combustion regime.

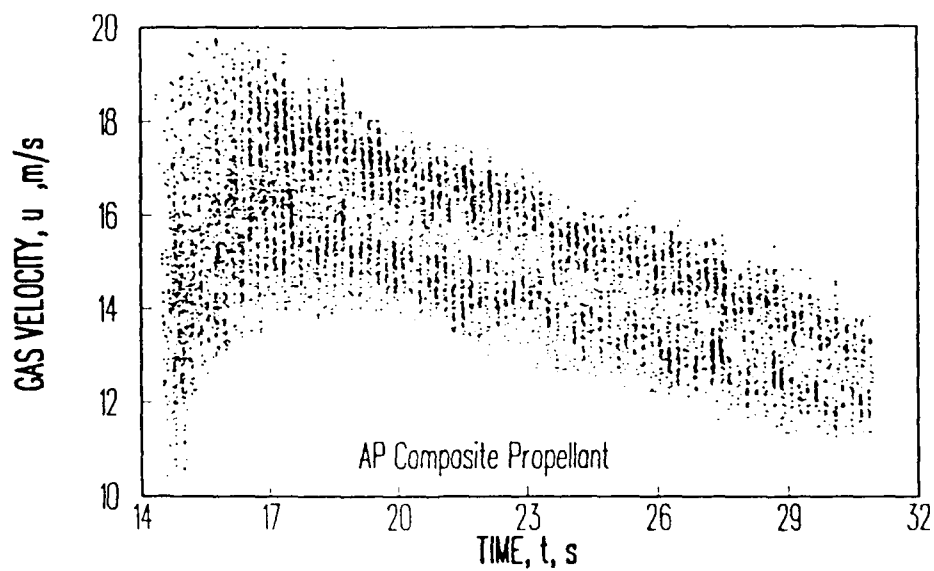


Fig.3 Data obtained by LDA technique with a forcing frequency  $f=5$  Hz in the frequency response.



**SESSION R-6: Quantitative Spectroscopic  
and Interferometer Measurements**

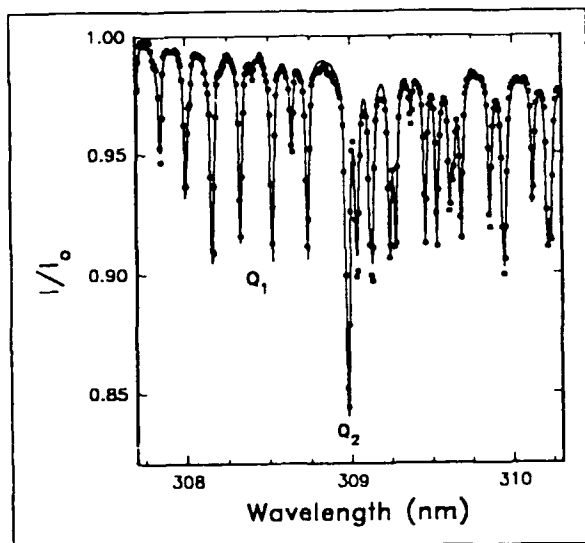
**Co-Chairs: Dr. R. Pein and Dr. T. Wijchers**

## TEMPERATURE MEASUREMENTS IN HOSTILE COMBUSTING FLOWS USING MULTICHANNEL ABSORPTION SPECTROSCOPY

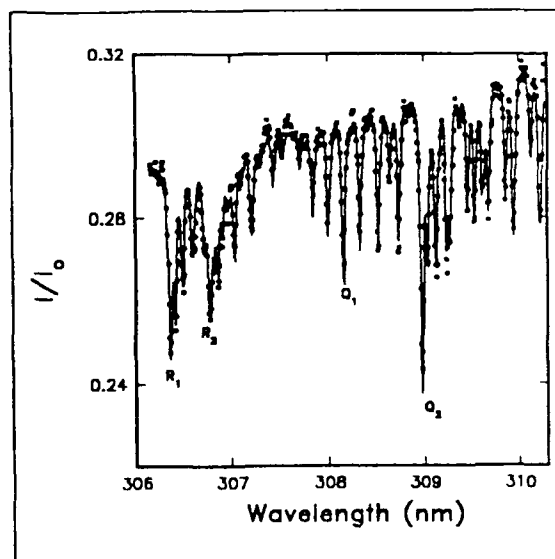
J. A. Vanderhoff, A. J. Kotlar, and R. A. Beyer  
US Army Research Laboratory  
Aberdeen Proving Ground, Maryland

Absorption spectra of diatomic molecules, NO, CN, NH and OH, which are present in a variety of combustion processes have been used to determine temperatures in both steady state and transient combustion. A high intensity xenon arc lamp light source and spectrograph coupled to an intensified photodiode array detector comprise the major components of the experiment. The combustion sources probed were an atmospheric pressure premixed  $\text{CH}_4/\text{N}_2\text{O}$  laminar flame and solid propellant flames burning at pressures ranging from 0.3 to 2.0 MPA. Both of these sources contained sufficient amounts of gas phase NO and OH for study; in fact, the solid propellant flames had enough NO to produce 100% absorption in the (0,0) gamma band. Rotationally resolved absorptions in the A - X (0,0) vibrational band system of OH around 307 nm were least squares fitted to obtain best values for temperature and OH concentration. Both rotationally resolved and vibrationally resolved absorptions in the A - X (0,0), (0,1), and (0,2) vibrational band systems of NO over the wavelength range from 220 to 240 nm have been fitted to obtain temperatures and NO concentrations. NO, CN, NH and OH spectra are sufficiently well characterized that parameters associated with the experimental setup, instrument response function and absorption baseline can be fitted under a variety of conditions. The multiparameter least squares fit of the spectra gives values and statistical uncertainties for these parameters; in particular, temperature and species concentration. For cases that can be approximated with one dimensional geometry the spatial resolution is governed by a 0.1 millimeter diameter pinhole aperture. Under the best conditions, it took less than 0.1 second to obtain an absorption spectrum from which a temperature could be determined. Temperature profiles for a solid propellant flame burning at elevated pressure have been obtained.

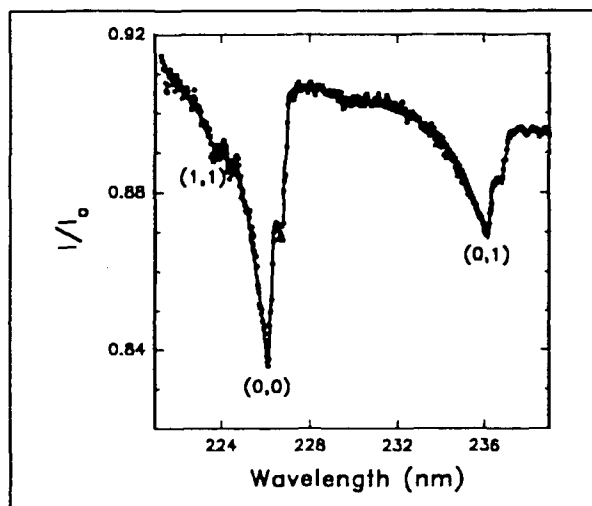
Shown in the Figures for comparison are data (points) and computer fits (lines) for OH and NO spectra from pre-mixed flames and propellant samples.



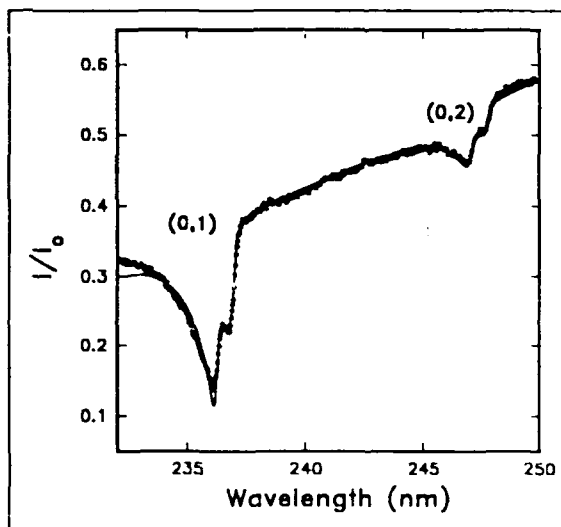
OH Absorption Spectrum Taken in a Lean  $\text{CH}_4/\text{N}_2\text{O}$  Flame.



OH Absorption Spectrum Taken in the Luminous Flame Region of JA2 burning in 1.6 MPa nitrogen.



NO Absorption from lean  $\text{CH}_4/\text{N}_2\text{O}$  Flame.



NO Absorption Spectrum Taken in the Dark Zone of JA2 Propellant Burning in 0.68 MPa nitrogen.

# Study of Relation Between Characteristic Length and Plasma Jet by Measuring the Electron Temperature

Koji Yoshida

Mechanical Engineering Course, Department of Industrial Technology,  
Junior College of Nihon University  
7-24-1, Narashino-dai, Funabashi-shi, Chiba 274, Japan

Atsushi Saima

Department of Mechanical Engineering,  
College of Science and Technology, Nihon University  
1-8, Kanda-surugadai, Chiyoda-ku, Tokyo 101, Japan

As to the combustion of a spark ignition engine, it is recognized that the operation with the lean mixture is effective to reduce the exhaust gas emission of pollutants and to enhance the thermal efficiency. However, the misfire and the burning velocity reduction make the thermal efficiency diminish, when the further lean mixture is used. Accordingly, it is necessary to ignite certainly and to increase the burning velocity.

Plasma jet ignition has been investigated as an effective method for ignition and enhancement of burning velocity. In a plasma jet ignition, it is recognized that the plasma jet igniter which enhances a combustion effectively has a large characteristic length  $L^*$  ( $L^* = \text{cavity volume} / \text{effective orifice area}$ ). The purpose of this study is to elucidate the issuing duration and advance of a hydrogen plasma jet, as a high temperature plasma. The experiment aimed at investigating the relation between the penetration of plasma jet and the characteristic length  $L^*$ . Electron temperatures were measured in local points on the central axis of the plasma jet. Their temporal changes were measured in an environment of hydrogen.

The plasma jet igniter consists of three parts: a cavity that is a cylindrical hole, an orifice plate that has a circular orifice in its center and a center electrode with diameter of 1 mm. The igniter is mounted on the end of a cylindrical combustion vessel. The vessel has two quartz observation windows in both sides and a pressure transducer. Two supplied electrical energies of 2.45 and 5 J were stored in capacitance of 0.1  $\mu\text{F}$ .

Figure 3 shows a schematic diagram of the apparatus. This system can measure intensities of two different wavelengths at a point simultaneously, to measure the local electron temperature by the two-line radiance ratio method. In the experiment, pure hydrogen was charged into the cavity and vessel at atmospheric pressure and room temperature. It was assumed that the plasma jet existed in a local thermodynamic equilibrium state, because experiments were at atmospheric pressure, and the discharge used in experiments was similar to a large current arc. The electron temperature was obtained by the two-line

radiance ratio method, and two wavelengths were selected from the Balmer series of the hydrogen spectrum.

We explored preliminary experiments. The experiment aimed at investigating the relation between the combustion enhancement and the characteristic length  $L^*$ . Air-propane pre-mixture was used as inflammable gas mixture (equivalence ratio  $\phi=1.1$ ). In figure 4, typical property of plasma jet ignition is shown; the combustion enhancement rate  $\phi$  increases with increasing of  $L^*$ . The effective combustion promotion is indicated in the case of the large supplied energy. However, the inclination of plots changes at  $L^*$  above 20 cm. The effect of supplied energy gradually disappears, and  $\phi$  is almost independent of energy at that range of  $L^*$ . The combustion enhancement seems depending on the effect of flame jet in cases of such igniters.

From these results, three different cavity dimensions were selected for the measurement of electron temperature. Orifice diameters of 1, 2 and 3 mm were used. Table 1 indicates each characteristic length  $L^*$  of plasma jet igniter.

Experimental results of electron temperature measurements and conclusions are:

(1) The discharge voltage is dampened with oscillation. The luminous intensity indicates several maximum values, when the discharged voltage peaks with plus and minus voltage. Luminous intensities decrease accordingly as the discharged voltage decays. Therefore, the generation of plasma depends on the discharge wave form. This is particularly apparent in the vicinity of the igniter. (See figure 5.)

(2) The electron temperature is higher than that of the other cavities in the whole region. As the cavity volume reduces, the plasma jet reaches to distance. (See figure 6.)

(3) With a large cavity volume, electron temperature increases in the vicinity of the igniter with an increase in the orifice diameter. With a small cavity, jet penetration increases with an increase in the orifice diameter. (See figure 6.)

(4) When supplied electrical energy is doubled, electron temperature merely rises up about 1000 K. However, the issuing duration and the penetration become about 1.5 times longer. The supplied electrical energy exerts an influence on the penetration of the plasma jet, rather than the electron temperature. (See figure 6.)

(5) A small characteristic length of the igniter seems favorable with regard to the penetration of the plasma jet and the generation of a high temperature plasma, compared with the case of an excessive  $L^*$  of the igniter. Therefore, it is considered that the plasma jet igniter configurations exert the different influences on the plasma jet penetration and the combustion enhancement. (See figure 4 and figure 7.)

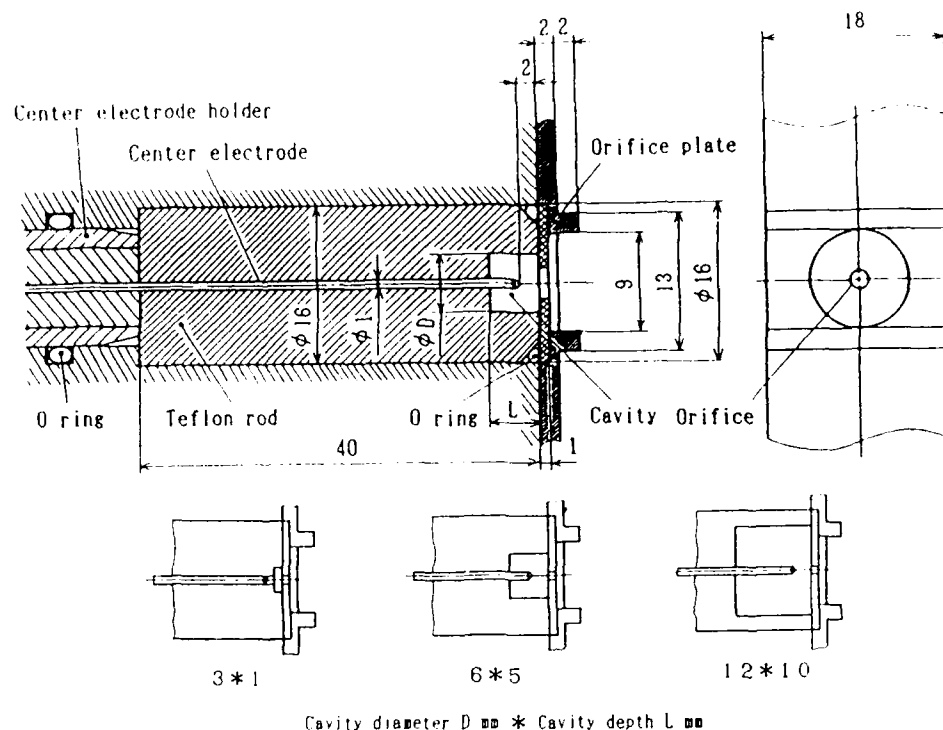


Fig.1 Cross section of plasma jet igniter and three kinds of cavity. Three different cavity are 3\*1, 6\*5 and 12\*10. Symbol of 3\*1 denotes the cavity diameter D of 3 mm and the cavity depth L of 1 mm. Each volume is about 7.1, 141.4 and 1131.0 mm<sup>3</sup>.

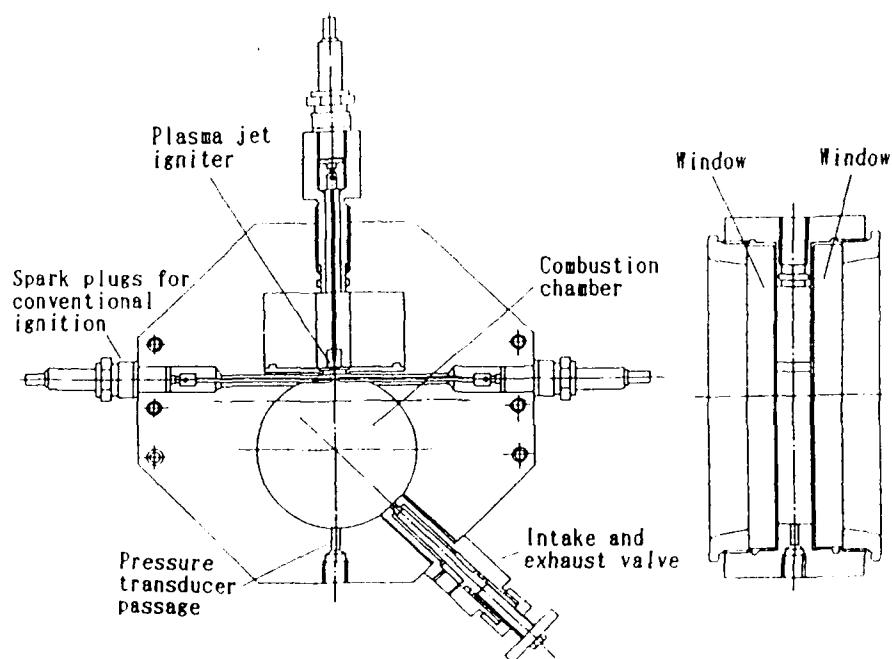


Fig.2 Figure of constant volume combustion vessel. The combustion chamber has a cylindrical shape; diameter of 80 mm, depth of 20 mm and volume of 100 c.c..

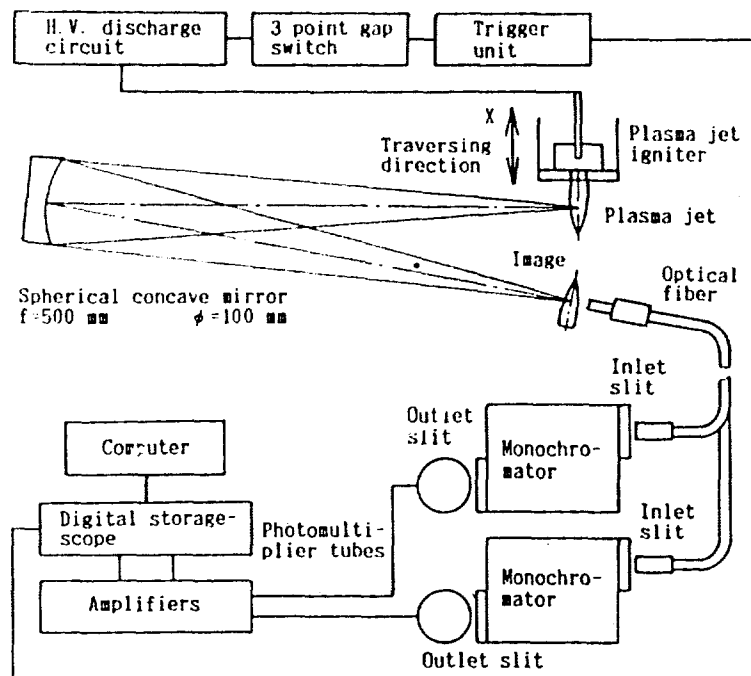


Fig.3 Schematic of local electron temperature measurement system by the two-line radiance ratio method. The apparatus can measure intensities of two different wavelength at a point simultaneously.

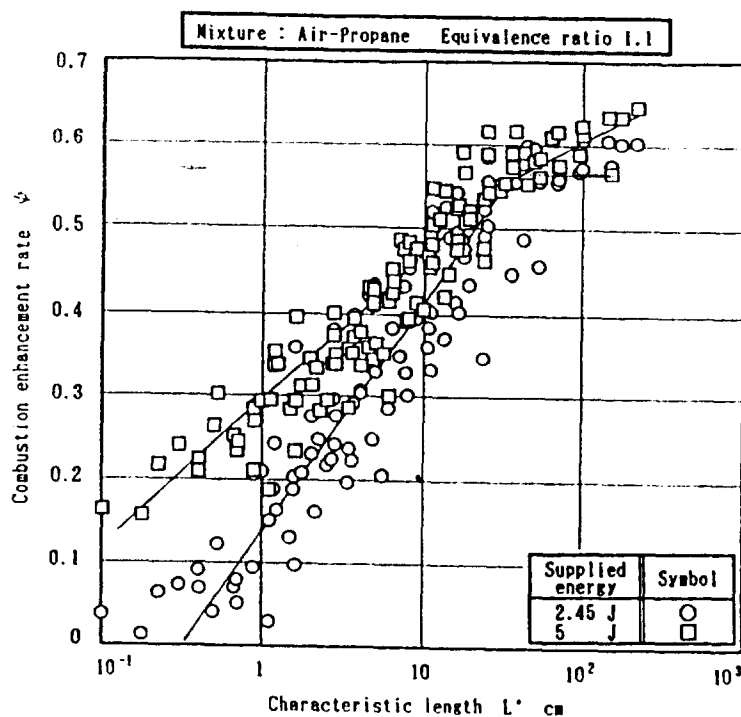


Fig.4 Combustion enhancement rate  $\phi$  as a function of characteristic length  $L^*$ . Air-propane mixture equivalent ratio:1.1. Here the combustion enhancement rate  $\phi$  is defined by the ratio of the burning time of the plasma jet ignition  $\tau_{pl}$  and that of the conventional ignition  $\tau_{con}$ .  $\phi$  is expressed by the equation:  $\phi = 1 - \tau_{pl} / \tau_{con}$ .

Table1 Characteristic length  $L^*$  of plasma jet igniters used in experiments of the local electron temperature measurement.

Characteristic-length $L^*$ cm			
Orifice diameter $d$ mm	Cavity configuration Cavity diameter $D$ mm * Cavity depth $L$ mm		
	3*1	6*5	12*10
1	0.90	18.0	144
2	0.23	4.50	36.0
3	0.10	2.00	16.0

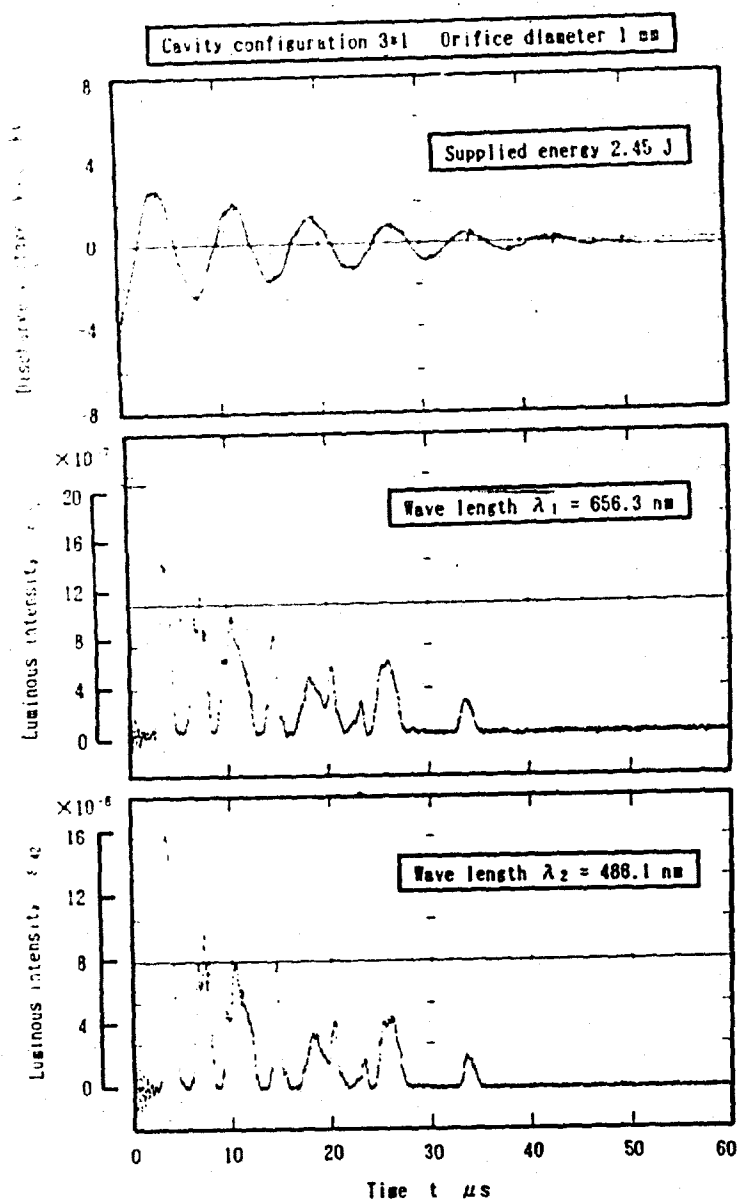


Fig.5 Typical wave forms of discharged voltage at supplied electric energy of 2.45 J and luminous intensities of wave length 486.1 nm and 656.3 nm measured at distance of 1.5 mm from plasma jet igniter. Cavity configuration:3\*1; orifice diameter:1 mm.



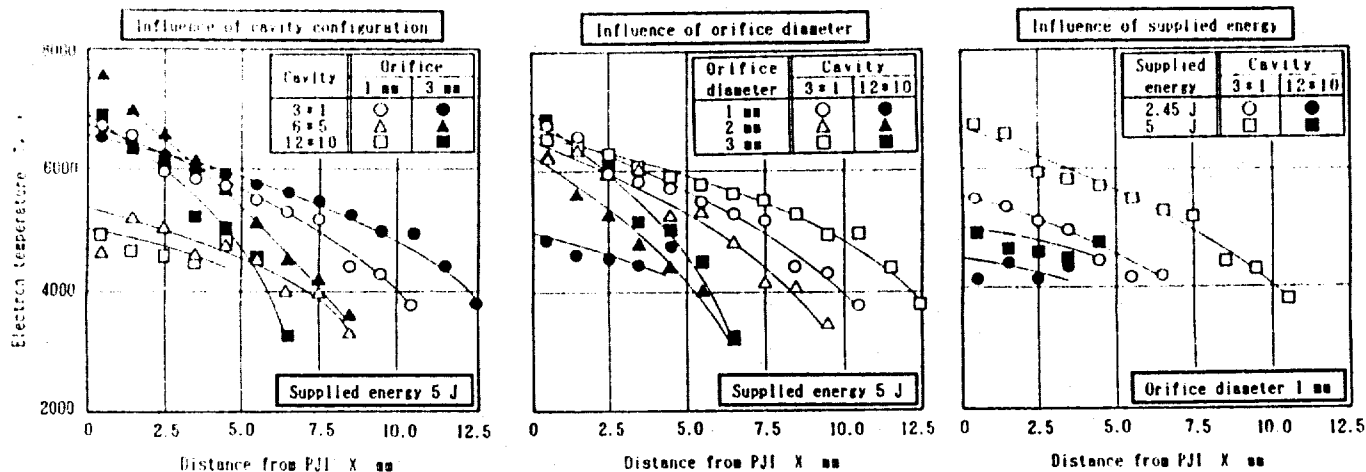


Fig.6 Local electron temperature  $T_e$  measured at the time when the most intense luminous intensity was measured as a function of distance  $X$  from plasma jet igniter for various conditions.

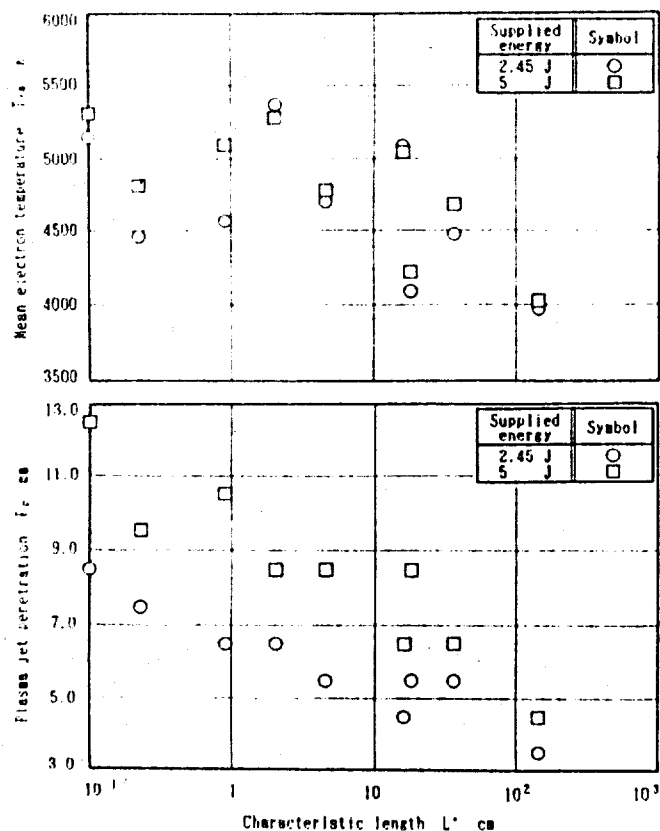


Fig.7 Mean electron temperature  $T_e$  and the penetration depth of plasma jet  $P_p$  as a function of characteristic length  $L^*$ .

# The Preflame Reaction in a Spark Ignition Engine

H. SHOJI, A. Saima and H. Watanabe

Department of Mechanical Engineering  
College of Science and Technology, Nihon University  
1-8, Surugadai, Kanda, Chiyoda-ku, Tokyo 101 Japan

There are strong demands today to improve the thermal efficiency of internal combustion engines in order to conserve energy and address environmental issues. However, a major obstacle to further improvement of the thermal efficiency of spark ignition engines is knock. With the aim of elucidating the mechanism generating knock, an examination was made of the preflame reaction behavior of unburned gas in the combustion chamber in the transition from normal combustion to abnormal combustion characterized by the occurrence of knock.

This study focused on light absorption and emission behavior at wavelengths corresponding to the spectra of the OH (characteristic spectrum of 306.4 nm), CH (431.5 nm) and  $C_2$  (516.5 nm) radicals, which play an important role in combustion reactions. The aim of this study was to gain a better understanding of the combustion reaction mechanism from the occurrence of preflame reactions in the end-gas region and the development of autoignition to the generation of knock pressure oscillations. In order to examine the behavior of these radicals by spectroscopic methods, the authors have developed a new polychromator (in Fig.1) that is capable of measuring spectral properties at four wavelengths simultaneously. In this work, the apparatus was set to detect the wavelengths of the OH, CH and  $C_2$  radicals and the wavelength of the Na-D line (characteristic spectrum of 589.3 nm), which was used in measuring the combustion gas temperature. The wavelength resolution used in this experiment was 1.8 nm, which was obtained by setting the width of the incidence slit of the polychromator at 0.4 mm.

Using this apparatus, measurements were made of the absorption and emission behavior of the three radicals under normal and abnormal combustion with many types of fuels having different octane numbers. The fuels used were n-heptane (0 RON), iso-octane (100 RON), a blend of n-heptane and iso-octane (60 RON), gasoline (91 RON), methanol (105 RON) and MTBE (methyl tertiary butyl ether: 118 RON).

The configuration of the test equipment A (case 1) used in this

work is shown in Fig.2. Measurements were made of the combustion gas temperature at the same time the behavior of the intermediates was examined by emission spectroscopy. The combustion gas temperature was measured with an optical system, indicated by ① and ② in the figure, which incorporated a Halogen lamp. This system provides a continuous indication of the combustion gas temperature. The brightness of the Halogen lamp, which serves as a comparative light source, is varied in relation to the output waveform of the energy radiated by the flame in the combustion chamber. The waveform can thus be calibrated in terms of temperature, and the combustion gas temperature is found by the spectral D-line reversal method.

Examples of the measured data obtained with one polychromator in the end gas region with cylinder head A (in Fig.3) are shown in Figs.4-8.

These figures show the light emission and absorption behavior of the three intermediates for two cycles, in which emission spectroscopy and absorption spectroscopy were employed for one cycle each.

The results obtained for normal combustion with n-heptane (0 RON) as the fuel are shown in Fig.4. Point B denoted in the absorption waveforms for the radicals indicates the occurrence of a cool flame, which has been observed in experiments conducted with rapid compression machines. It is assumed that chemical reactions are already under way at this point and that intermediate products are being produced.

When n-heptane was used as the fuel, CH and C<sub>2</sub> radicals appeared in the preflame reaction interval(B-A interval in Fig.4) under normal combustion. However, in abnormal combustion cycles that gave rise to knock, they did not appear prior to autoignition. This is thought to be due to differences in elementary reaction processes in the progression from low-temperature end-gas chemistry under normal combustion to high-temperature autoignition chemistry under abnormal combustion( in Fig.5). Compared with normal combustion, OH radicals began to be produced earlier on in abnormal combustion cycles giving rise to knock.

With the spectral D-line reversal method, which was used in this study to obtain combustion gas temperature measurements, it is virtually impossible to measure temperatures below approximately 1300 K using conventional equipment. For this reason, end-gas temperature measurements were not obtained prior to flame arrival.

In abnormal combustion cycles with the blended fuels (60 RON), OH radicals were produced earlier than under normal combustion and

increased up to the occurrence of autoignition. In contrast, the CH and  $C_2$  radicals showed no increase and remained virtually constant in some regions(F-G interval in Fig.11(c)). It is thought that those regions corresponded to the region of the Negative Temperature Coefficient (NTC) which has been observed in rapid compression machines, and this would therefore confirm that the NTC region also appears in the combustion chamber of ordinary engines.

Using two newly developed polychromators, the absorbance and emission intensity of three radicals were measured simultaneously as indices of their behavior in the unburned gas. The configuration of the test equipment B (case 2) used in the second research is shown in Fig.12. When absorption spectroscopy was employed, the absorbance behavior of the radicals was measured using the optical system denoted as A-A, which passed through the end zone of the combustion chamber. In this case, a xenon lamp was illuminated to a certain brightness and measurements were made with polychromator(1). With emission spectroscopy, emitted light passed through a quartz observation window(B), attached perpendicular to the A-A optical system, and was transmitted via an optical fiber cable to polychromator(2) to measure the light emission intensity. Figure 13 shows the configuration of the cylinder head B and the positions where measurements were made.

Figure 14 shows an example of the results obtained for normal combustion with a blended fuel(50 RON) consisting of n-heptane and iso-octane. An examination of the absorbance waveforms of the radicals in the preflame reaction interval between point C and A reveals that a cool flame occurred at points C(6°ATDC) and that an initial increase in absorbance occurred at point C'(9°ATDC). The CH and  $C_2$  radicals disappear immediately after point C' and the waveforms return to nearly the zero level. It is thought that this change corresponds to the degeneracy of the cool flame. Figure 15 shows a condition of trace knock with a blended fuel(50 RON). The absorbance waveforms of the CH and  $C_2$  radicals do not show any discontinuity corresponding to the C' point that was observed in the preflame reaction interval under normal combustion and attributed to the occurrence of a cool flame. However, in the B-A interval of these waveforms, an increase in absorbance is observed at point B'(20°ATDC) just prior to the occurrence of autoignition at point A(22°ATDC). This change is presumed to indicate behavior corresponding to the occurrence of a blue flame. Thus the behavior of the OH radical differed from that of the CH and  $C_2$  radicals.

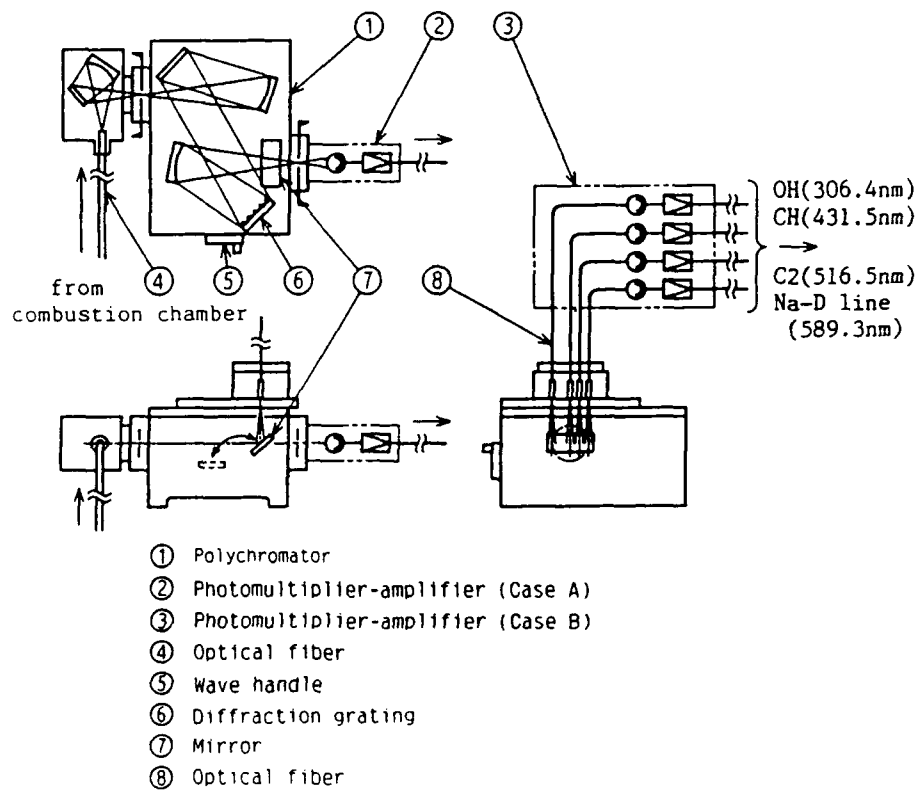


Fig.1 Polychromator for measuring emission and absorption behavior at four wavelengths simultaneously

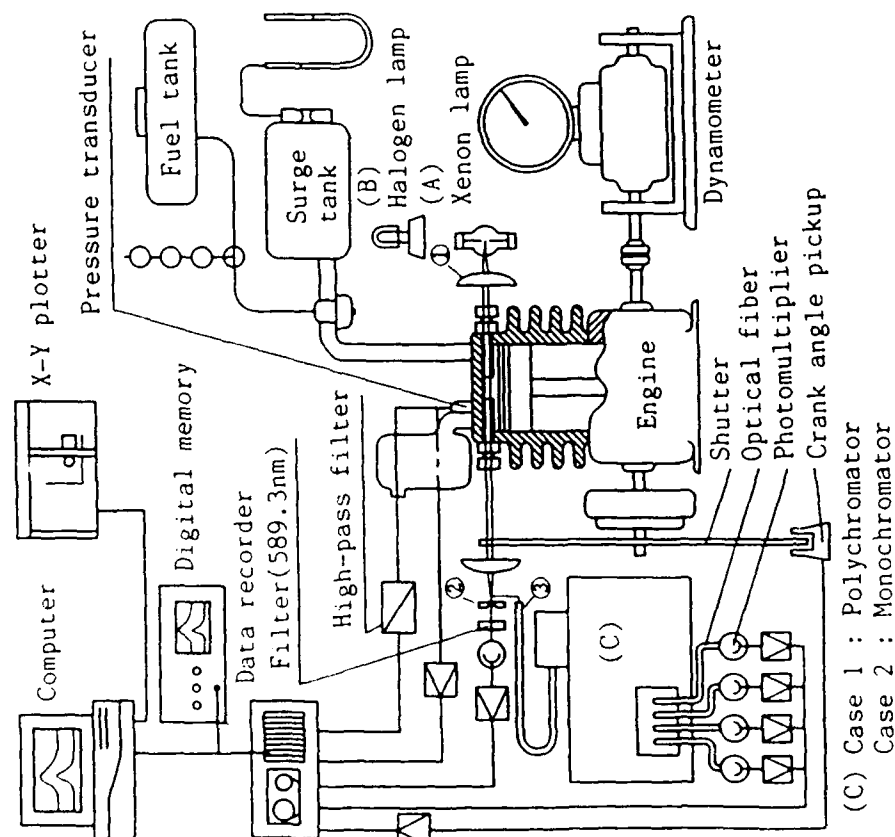


Fig.2 Configuration of test equipment A

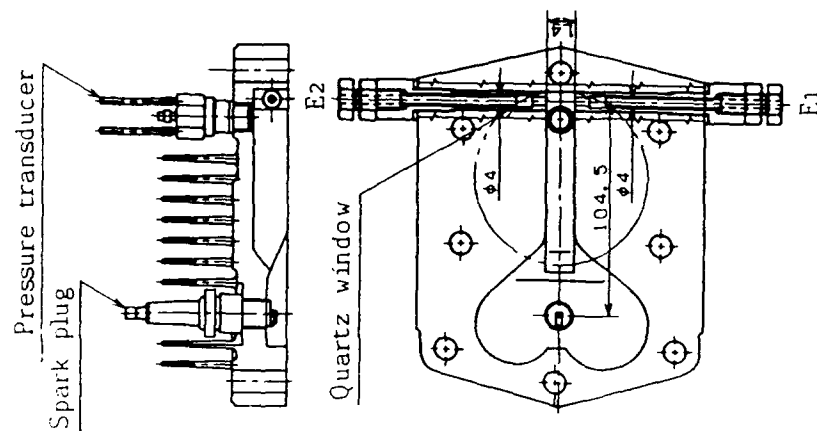


Fig.3 Cylinder head A and measurement positions.

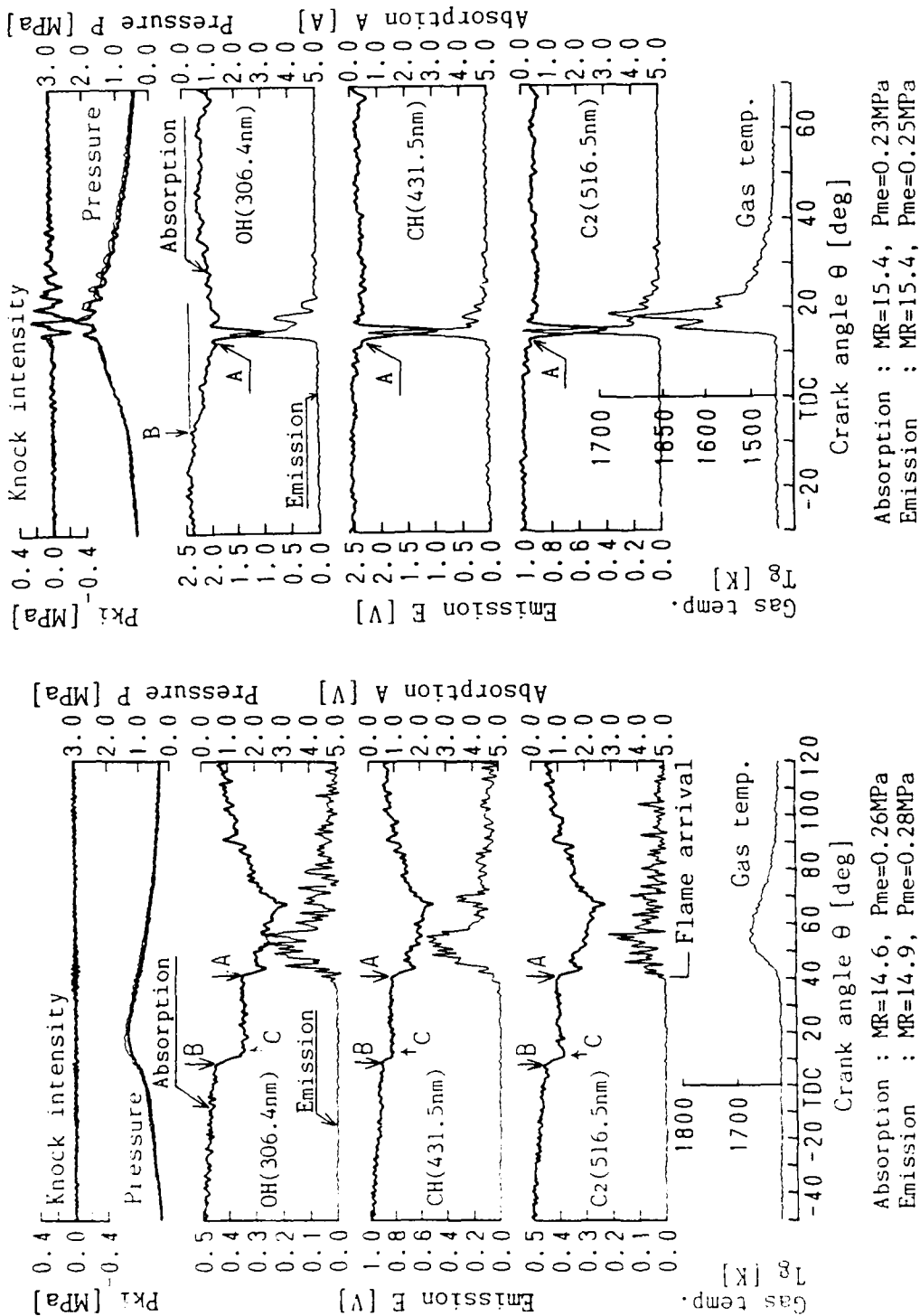


Fig.5 Abnormal combustion with n-heptane (0 RON)

Fig.4 Normal combustion with n-heptane (0 RON)

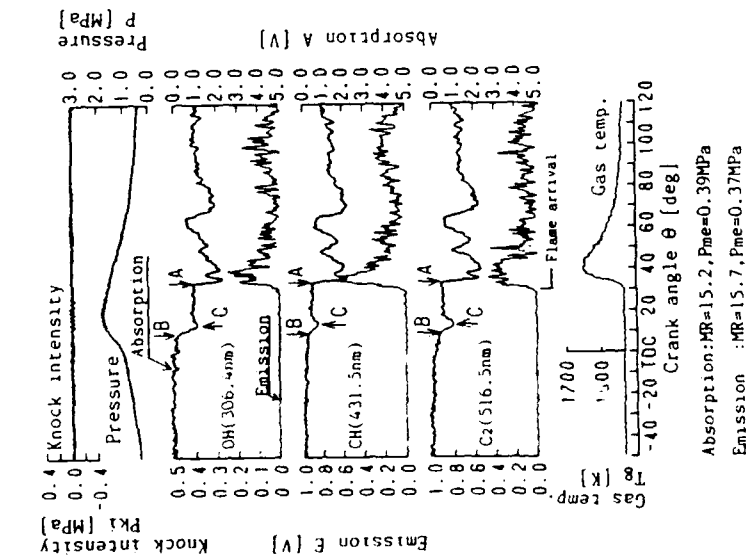


Fig.6 Normal combustion with blended fuel (50 RON)

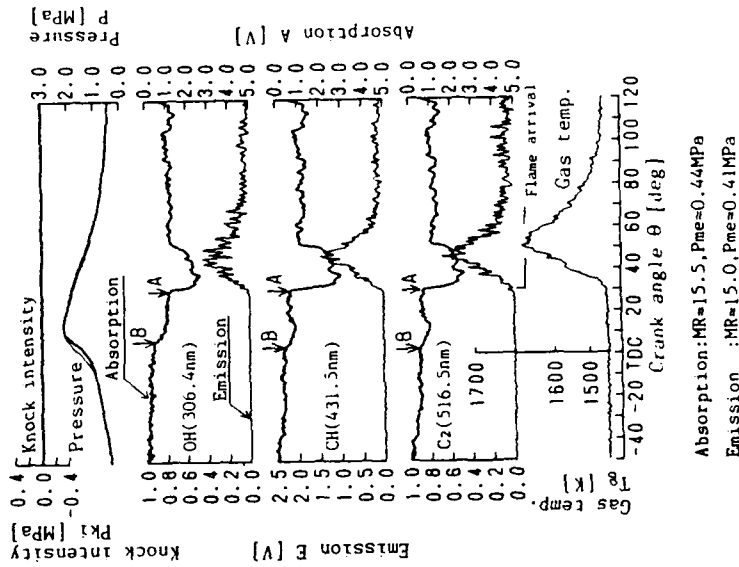


Fig.7 Normal combustion with gasoline (91 RON)

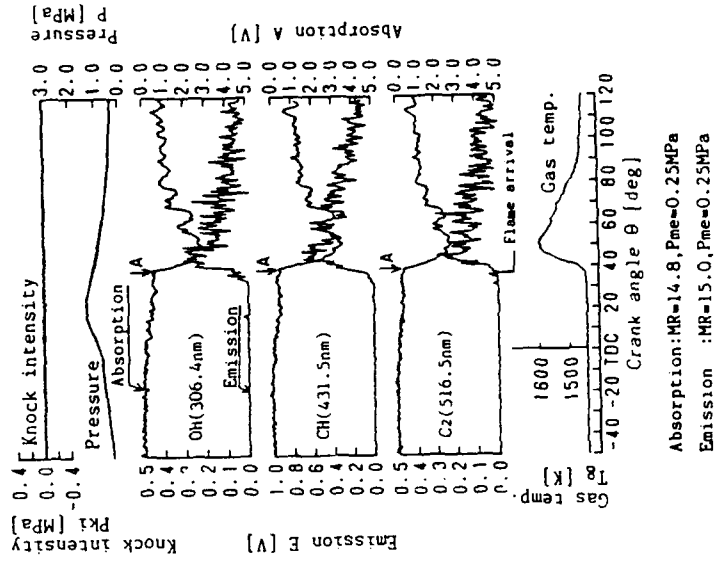
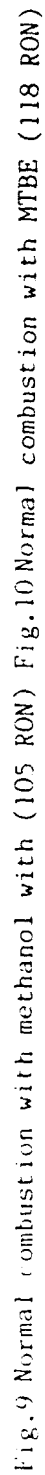


Fig.8 Normal combustion with iso-octane (100 RON)





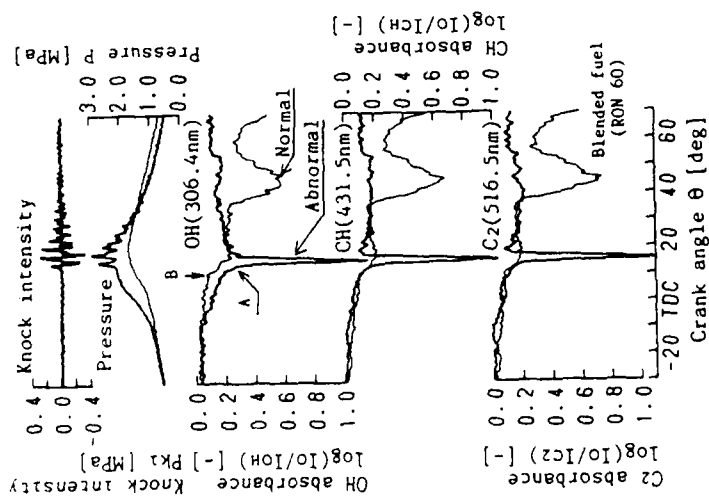


Fig.11(a) Radical absorbance behavior for normal and abnormal combustion with blended fuel (60 RON)

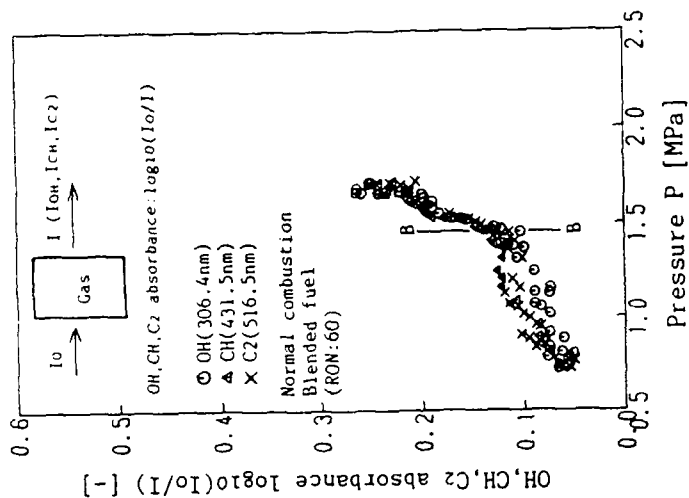


Fig.11(b) Radical absorbance vs. pressure for normal combustion with blended fuel (60 RON)

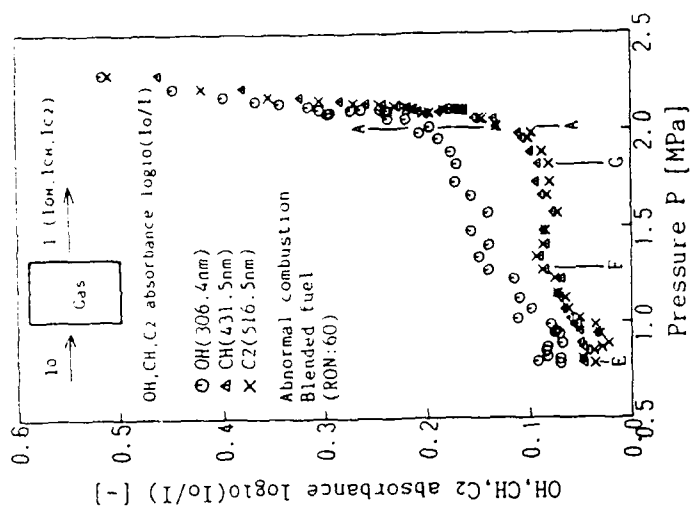


Fig.11(c) Radical absorbance vs. pressure for abnormal combustion with blended fuel (60 RON)

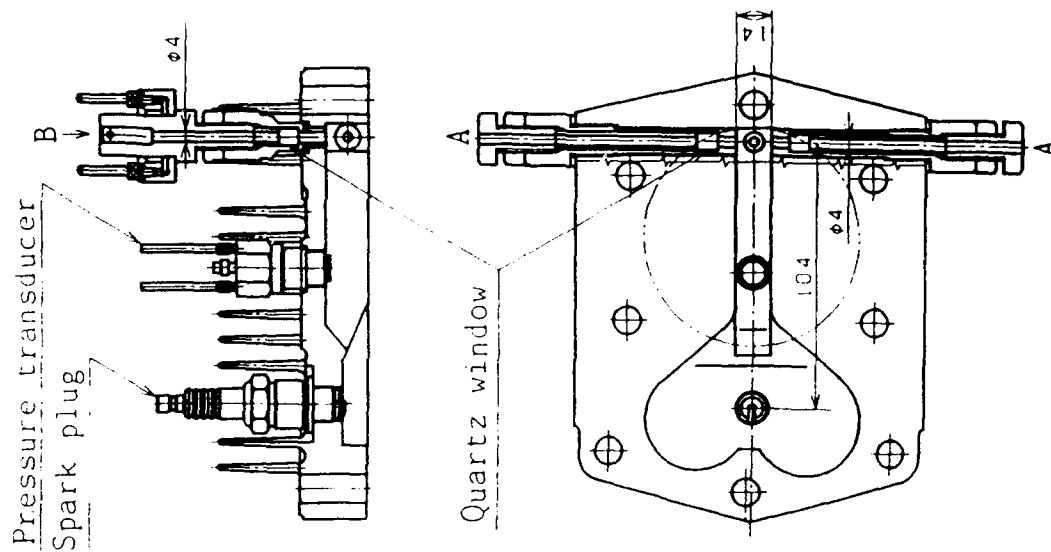


Fig.13 Cylinder head B and measurement positions

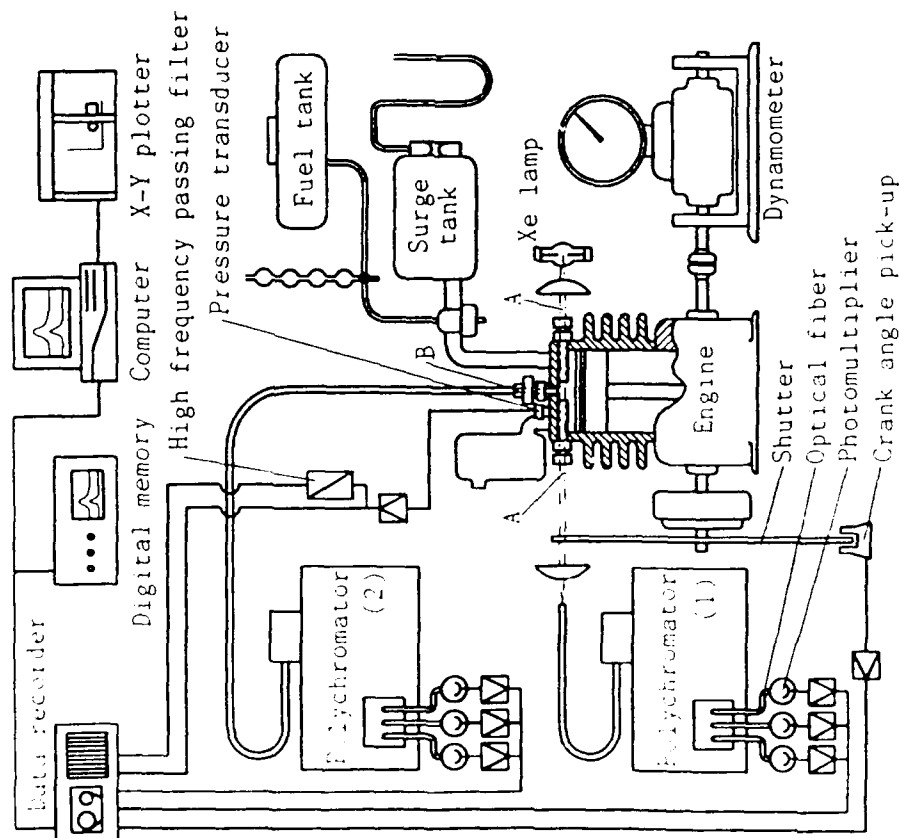
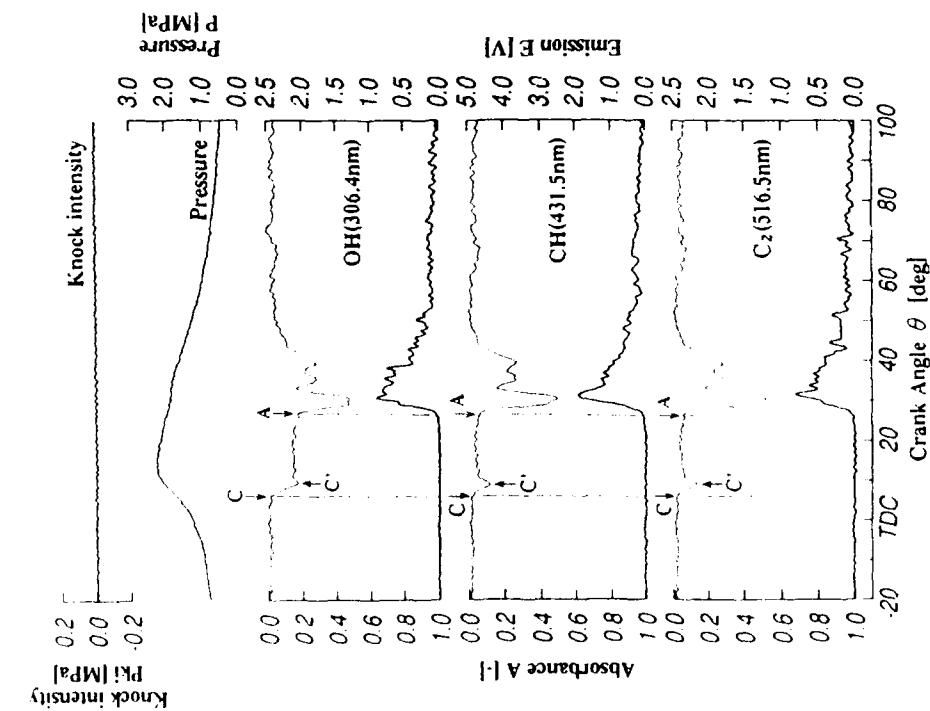
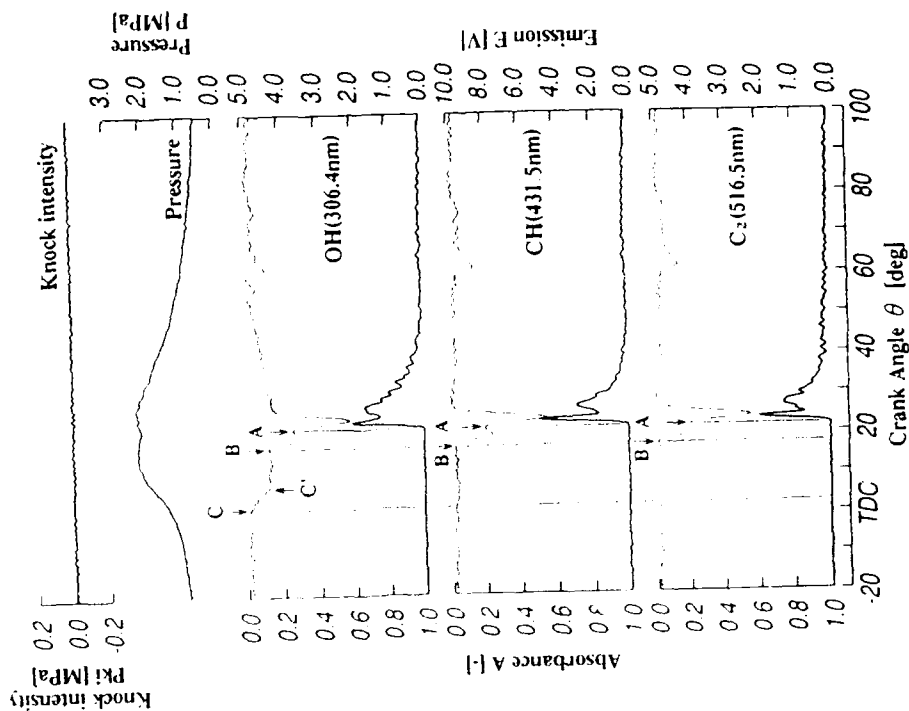


Fig.12 Configuration of test equipment B



BMEP=0.47 MPa, MR=15.9

Fig. 14 Normal combustion with a blended fuel (50 RON)



BMEP=0.47 MPa, MR=15.2

Fig. 15 Trace knock with a blended fuel (50 RON)

# Vacuum-UV cw-Resonance Fluorescence Studies on Laser Photodissociation of Hydrazine Fuels

Ghanshyam L. Vaghjiani

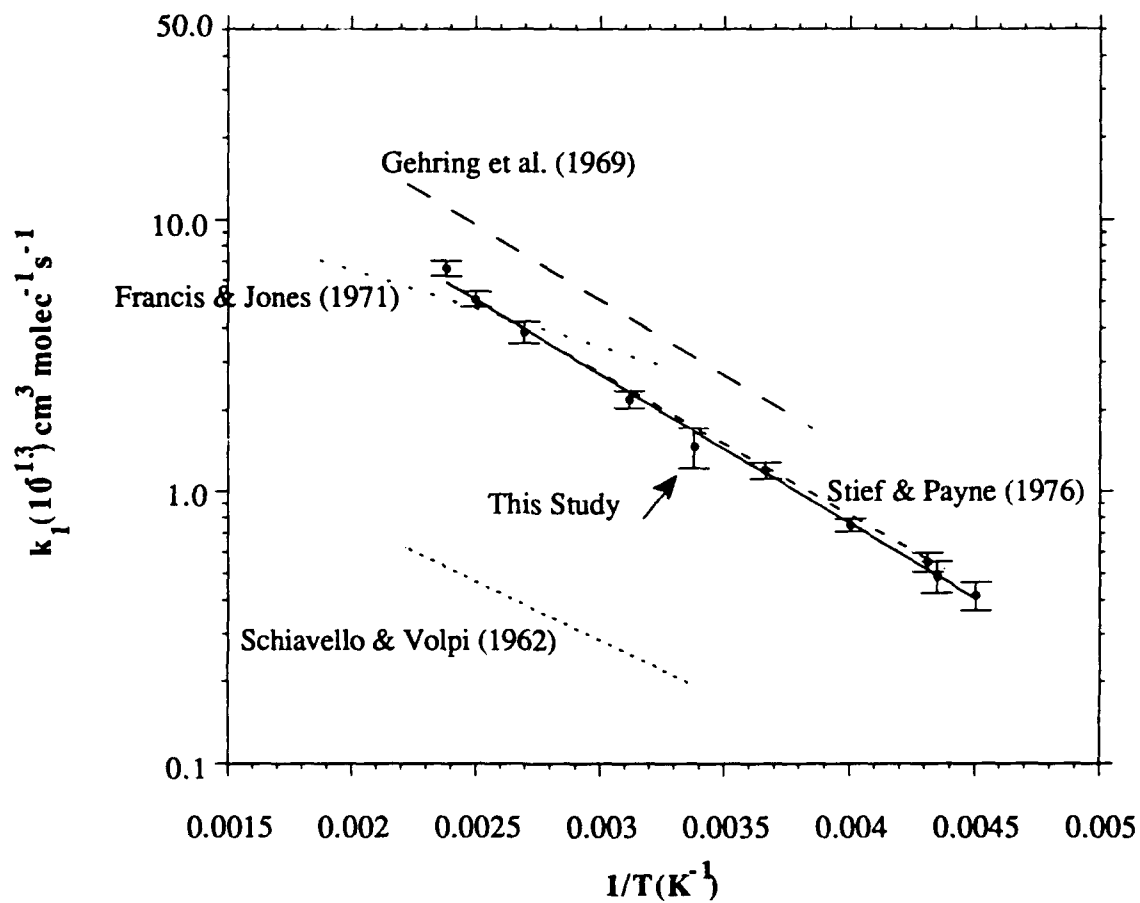
University of Dayton Research Institute  
Phillips Laboratory, PL/RKFA  
Edwards Air Force Base, CA 93523, U.S.A.

Decomposition of hydrazine ( $\text{N}_2\text{H}_4$ ), methylhydrazine ( $\text{CH}_3\text{NHNH}_2$ ) and dimethylhydrazine ( $(\text{CH}_3)_2\text{NNH}_2$ ) offer a wide variety of industrial applications including, amongs others, electrical power cells, fuels for thruster engines aboard the Space Shuttle and the Titan launch vehicles, as a mono-propellant, and in explosives. In order to model and understand the combustion and pyrolysis of these hydrazine fuels, detailed chemical kinetic information is required on the elementary reactions involved in these processes. The temperature (and where applicable pressure) dependence of the reaction rate coefficient of important individual chemical reactions and their products branching ratio are required.

In our laboratory we are currently studying the gas-phase photochemical decomposition of  $\text{N}_2\text{H}_4$ . The study is relevant to combustion and pyrolysis of  $\text{N}_2\text{H}_4$  because all three modes of decomposition can involve common reaction intermediates. The products and reactions initiated in the laser photolysis of  $\text{N}_2\text{H}_4$  are followed using non-intrusive optical methods. Time-resolved fluorescence detection techniques are used to probe the temporal profiles of reactants (and products) to measure reaction rate coefficients.

The major product in the 248.3-nm photodissociation of hydrazine is hydrogen atoms,  $\text{N}_2\text{H}_4 + h\nu \rightarrow \text{H} + \text{N}_2\text{H}_3$ . Here we report the quantum yield for  $\text{H}(^2\text{S})$  in the reaction. The elementary reaction,  $\text{H} + \text{N}_2\text{H}_4 \rightarrow \text{products}; (k_1)$ , that is initiated in the photolysis is also important in hydrazine pyrolysis. In this study we also report the the temperature dependence for this reaction. The Arrhenius activation energy and pre-exponential factor determined are presented and compared to previous studies.

# H+N<sub>2</sub>H<sub>4</sub> Reaction



# Development of a broadband microwave interferometer for diagnostic measurements of detonations

Julian J. Lee, T. J. F. Pavlasek, J. H. S. Lee, R. Knystautas  
McGill University, Montreal, Canada

## ABSTRACT

This paper describes the use of a novel coaxial waveguide configuration to perform detonation velocity measurements using the microwave Doppler interferometry technique. With this non-intrusive method, continuous velocity histories of detonation waves propagating in explosive gaseous mixtures can be obtained. Existing microwave diagnostic techniques are mostly based on the use of the detonation tube as a hollow waveguide. Consequently, the phase and group velocity of electromagnetic waves propagating in the waveguide have a strong frequency dependency, rendering swept frequency and other broadband techniques impractical. The principle advantage of using the coaxial configuration is the possibility of operating in the TEM (the transverse electric-magnetic) mode, where the phase and group velocities are frequency independent in a lossless medium, permitting the use of broadband remote sensing radar techniques.

In the present study, the feasibility of a TEM mode coaxial system is examined and demonstrated under single frequency conditions. The microwave interferogram is first digitized then analyzed using computer software developed to facilitate the extraction of velocity information from the microwave Doppler interference signals by applying digital signal processing techniques.

The detonation tube used in the present microwave interferometer consisted of a copper tube 38.4 mm in diameter, 3.5 m long, with a thin wire stretched along the center axis acting as a center conductor for the coaxial configuration. The system was tested at microwave frequencies of 6.70GHz and 9.21GHz by performing a number of detonation experiments in gaseous mixtures of  $\text{C}_2\text{H}_2+2.5\text{O}_2$  and  $\text{C}_3\text{H}_8+5\text{O}_2$  at low initial pressures (6torr to 80torr). Average velocity measurements obtained by the microwave method agreed with independent photodetector measurements to within 2%.

In this study, the present technique has been used to explore unstable detonations propagating in near-limit conditions. The results demonstrate that the improved microwave Doppler interferometer is particularly well suited for unstable detonations where the large scale velocity fluctuations must be monitored continuously over long distances. It may be concluded that the present coaxial microwave Doppler interferometry technique shows promise as a useful diagnostic tool for studying unstable detonations and may provide insight into characterizing near-limit behaviour.

**SESSION R-7: Diagnostics in Propellant  
Combustion**

**Co-Chairs: Prof. V. E. Zarko and  
Ir. P.A.O.G.Korting**



# TEMPERATURE SENSITIVITY STUDIES ON NITRAMINE BASED PROPELLANT

## Abstract

Lalitha Ramachandran, T.E. Krishnan, A.J. Kurian,

S. Someswara Rao & K.N. Ninan

Propellant and Special Chemicals Group

Vikram Sarabhai Space Centre

Trivandrum -695022

Rocket motors stored in ambient conditions experience variations in environmental temperature. This can result in the dispersion of burning rate and thrust level of the grain due to the temperature sensitivity characteristics of the propellant formulation and have thus a significant effect on the rocket performance. Motor designer has to minimise this effect in order to ensure repeatable motor performance under varying ambient conditions.

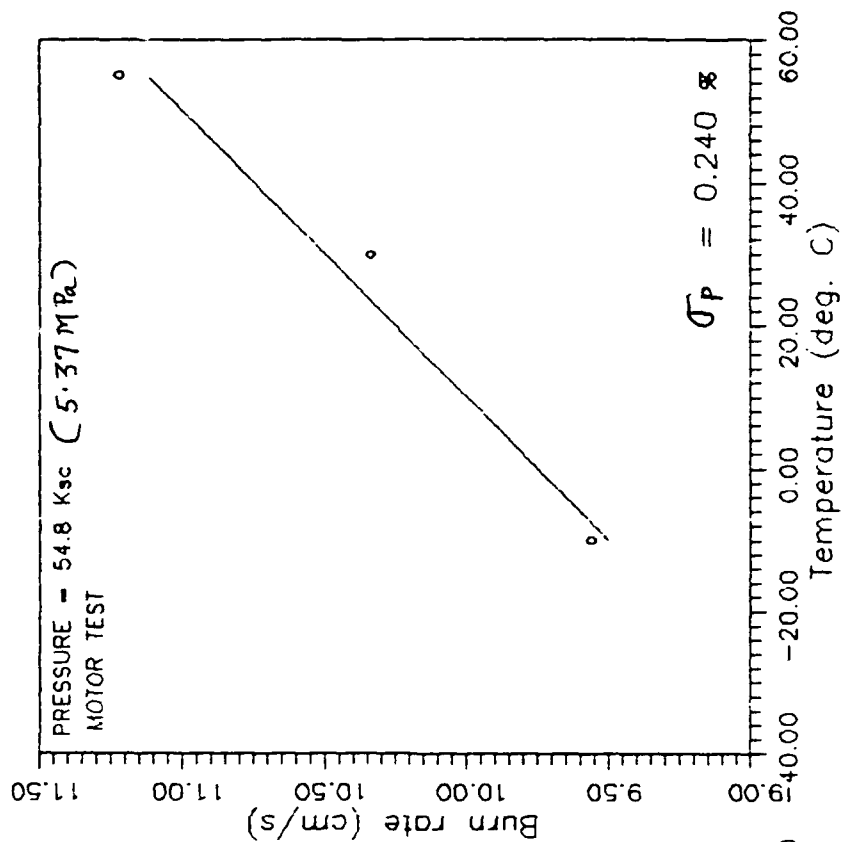
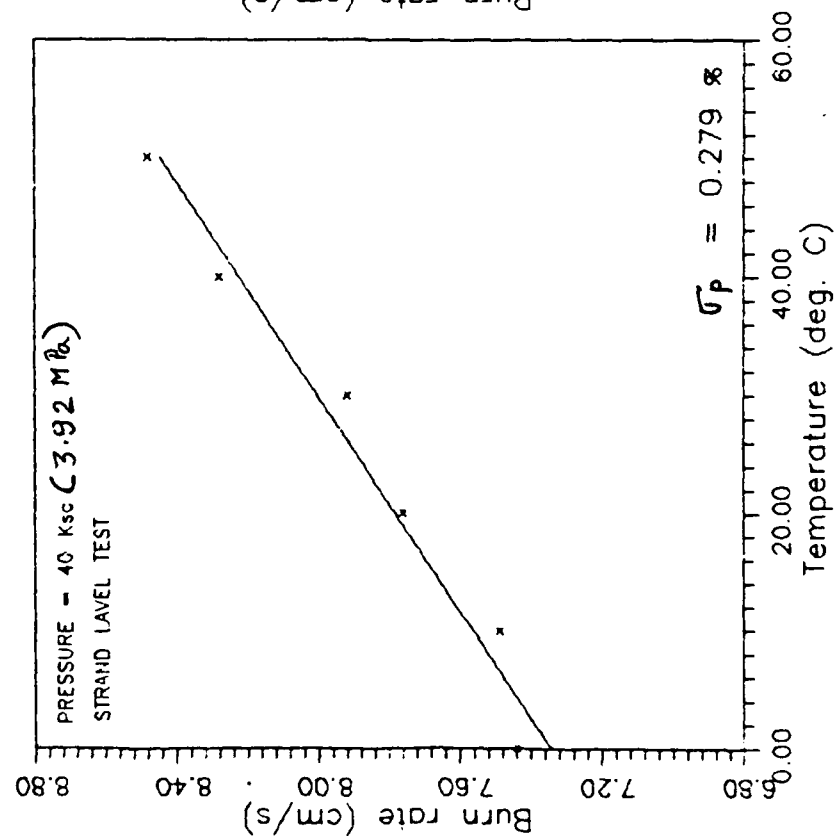
The objective of this study is to investigate the temperature sensitivity on burn rate of nitramine based solid propellant. The propellant consists of double base composition (nitroglycerine, nitrocellulose) incorporating cyclotetramethylene tetranitramine as a high energy additive. The experiments were carried out both at strand level and at motor level.

The temperature sensitivity coefficient on burning rate at the strand level was established using the acoustic emission detection system. 6mm X 6mm square, 80mm long propellant strands were prepared and tested inside the combustion chamber which was maintained at a particular pressure and temperature. The sound signals released during the deflagration were picked up by the acoustic emission sensor and the burn rate was calculated from the output. The experiment was repeated at various temperatures ranging from 0°C to 50°C while the pressure was maintained at 3.92 MPa in all the experiments. From the data obtained the temperature sensitivity coefficient of burn rate of the propellant worked out to be 0.28%/°C.

In order to study the temperature sensitivity of burn rate in the motor level, solid propellant grains were cast and assembled inside the motor, designed for the purpose. The grain assembly consists of an outer grain and an inner grain housed inside the chamber. The motors after assembly were conditioned at  $-10^{\circ}\text{C}$ ,  $30^{\circ}\text{C}$ ,  $50^{\circ}\text{C}$  and static tested. The temperature sensitivity coefficient for the motor tests was  $0.24\% / ^{\circ}\text{C}$  which is within the limit of the design value.

It is noteworthy that strand level investigation using the acoustic emission system gives the value which is close to that from the motor tests. The acoustic emission strand level investigation can thus serve as an effective quality control tool and can save a lot of efforts.

# TEMPERATURE SENSITIVITY STUDIES ON NITRAMINE PROPELLANT



# METHOD TO DERIVE SOLID PROPELLANT EROSION BURNING RATE USING REACTIVE MOTOR PRESSURE DIAGRAM

I. G. Assovskii

Institute of Chemical Physics RAS  
Kosigin St. 4, 117977 Moscow V-334, Russia

An experimental-calculating method is proposed in the present paper to derive the local erosive burning rate and other characteristics of solid propellant combustion by pressure diagram of semi-closed chamber.

The velocity of gas flowing along the combustion surface of condensed propellant is one of the main factors (together with gas pressure and initial temperature of the propellant) governing the combustion rate. Experimental determination of the burning rate needs constancy of the mentioned factors during a measurement. This requirement presents a severe problem for investigations of the gas flow influence on the combustion rate (the so-called *razduvaniye* (O. I. Leipunskii, 1942) or erosive burning effect).

The basic way of such investigations is the propellant burning in a small-scale rocket motor. The majority of these methods is based on the direct measurements of the average erosive burning rate during a rather prolonged time interval and a burnt part of propellant grain. Thus, it is impossible to determine exactly enough the local burning characteristics, especially for thin solid propellant elements or propellant grains with narrow channels. This obstacle is responsible for the wide scatter of the published data on erosive burning.

So, the purpose of the proposed paper is to show the approach resolving that difficulty using correlation between the varying combustion rate and the pressure diagram. It is possible to take exact data on the combustion and ignition by comparing the experimental and calculated pressure diagrams corresponding to special points of the reactive chamber. Also, this procedure allows one to correct the data taken from experiments on combustion in constant volume bombs.

The offered experimental-calculating method employs the physico-mathematical model [1] of the solid propellant combustion in the semi-closed vessel, taking into account lingering and unsimultaneous ignition of propellant grains as well as the unsteady erosive burning rate which depends on local values of pressure, gas flow velocity, and ignition conditions [2].

The use of this approach is demonstrated for example of a model propellant charge involving only the tubular elements. The one-dimensional quasi-steady approximation is used for calculation of the flow pattern in the channel with gas inject through the side surface. Unsteady combustion rate during the pressure rise is described by the asymptotic solution in analytical form [2]. It is assumed that the law of ignition

wave spread along the propellant surface is known.

The numerical analysis of relationship between the propellant combustion rate and the pressure diagram allows to make following conclusions.

The relative magnitude of the peak on the pressure diagram is an important indicator of combustion character. However the estimation of the erosive burning rate using this peak can lead to significant errors if the effect of accelerated combustion after ignition [2] and the ignition spread rate are not taken into account.

The erosive burning and accelerated combustion effects are similar in the influence on the pressure peak. Meanwhile the erosive burning action is very nonuniform along the propellant element. It causes appearance of wedge-shaped remains and their combustion delay ( long tail of the pressure diagram ).

The duration and other features of the pressure decay in the reactive chamber depend highly on the propellant combustion law. Such correlation provides a way for refinement of combustion rate data using the tail part of experimental pressure diagram.

1. Assovskii I.G. Method for calculation of characteristics of solid propellant combustion in semi-closed vessel. ICP RAS, Moscow, 1989, (in Russian) .
2. Assovskii I.G. Dokl. Phys. Chem., Proc. of AS USSR, 294, 1-3, 421, (1987).

## LASER ASSISTED HIGH-SPEED SHUTTER TV CAMERA FOR INVESTIGATIONS ON ALUMINIZED PROPELLANTS COMBUSTION.

R. Akiba\*, M. Kohno\*, A. Volpi<sup>+</sup>, T. Shibata<sup>§</sup>, S. Tokudome<sup>£</sup>

\* ISAS -Institute of Space and Astronautical Science (Sagamihara -Japan-)

+ At ISAS from CNPM- Consiglio Nazionale delle Ricerche (Milano -Italy) with the Grant STP5 issued by DG XII of the Commission of the European Communities

§ Postgraduate student, Tokai University, (Tokyo -Japan-)

£ Postgraduate student, Tokyo University, (Tokyo -Japan-)

Aluminum is frequently used in solid rocket propellants for two main purposes: to increase the specific impulse through a raising of the flame temperature and to enhance their burning stability. However, most of the Al, generally present in powder state in the propellant, does not vaporize onto the burning surface so tending later to agglomerate into large particles before their ignition. The ejected Al agglomerates burn, sometimes hardly, in the flame following the gas flow.

The diagnostic developed allows one to observe, despite the flame emission, the Al agglomerates on the burning surface and their ejection into the hot gas flow. As the emission of aluminized propellant flame is quite low in the UV region and becomes more intense monotonically from the visible to the infrared one, the experimental set-up consists of a Nd-YAG laser equipped with harmonics generators emitting in the visible and UV spectral region ( $\lambda = 532$  nm with  $E = 165$  mJ and  $\lambda = 355$  nm with  $E = 55$  mJ) whose pulses (repetition rate  $\nu = 5$  Hz) are synchronized, through a chain of pulse generators, with a high-speed shutter TV camera (gate time up to 100 ns) sensible in the spectral range 200 - 800 nm. Suitable narrow bandwidth filters (centered on the selected laser wavelength) protect the camera from the light emissions of the flame. Moreover in order to light up properly the flame with a homogeneous pattern, the laser beam is enlarged, collimated and only its central part adopted.

The combustion tests are carried out in a nitrogen pressurized chamber equipped with optical accesses and the measurements are performed in the pressure range 10-50 atm. The synchronization of the laser light, stray light filtering and high-speed shutter yield clear images of the agglomerates highly contrasted with the surrounding ambient. Quantitative results are later obtained from the recorded TV images by digital processing of the frames.

HTPB.12/AP.68/Al.20 propellants with different kinds of Al and AP particles size distribution are tested. The formation of Al "streams" and "bridges" between particles are clearly seen and studied. Dimensions, shape and local distribution of the agglomerates on the burning surface and in the gas flow are measured. The pressure dependence of the aggregation process is also studied. Results are compared with data obtained by other techniques and the reliability of this diagnostic in a wide range of experimental situations is demonstrated.

Although the resolution of the still pictures, raising the pressure, becomes rather limited due to the light diffusion, caused by the increased smoke, the images obtained are quite useful to understand both qualitatively and quantitatively the combustion processes of the Al particles loaded in the tested composite propellants.

## NON-INTRUSIVE TEMPERATURE MEASUREMENT OF PROPELLANT FLAMES AND ROCKET EXHAUSTS ANALYZING BAND PROFILES OF DIATOMIC MOLECULES

W. Eckl, N. Eisenreich

Fraunhofer-Institut für Chemische Technologie, ICT

D-7507 Pfinztal, FRG

Remote sensing of flames via analysis of emitted radiation in the UV/Vis-spectral region is mainly limited to diatomic species. The observed band profiles are formed with the temperature as a dominant parameter. Early analysis related single rotational lines to the energy levels to obtain temperatures /1/. The resulting rotational temperatures were often expected to be influenced by chemical reactions in which the investigated molecules are involved.

A concept more reliable and of better applicability to practical flames proceeds from a comparison of the experimental and calculated band profiles /2-4/ which is possible as most molecular constants of the important species are known /1,5/. In this way, the bands of molecules OH, NH, CN, CH, C<sub>2</sub>, CuH, MgO and AlO in the UV/Vis have been calculated for two wavelength resolutions of spectrometers and fitted to experimental spectra with the temperature and peak profile being the fit-parameters.

Gaussian, Lorentzian and experimental peak profiles were applied.

The method was tested using flames of stationary burners and comparison to CARS measurement in the past /6/.

Recent applications aimed at temperature measurement of propellant flames and rocket plumes. With respect to thermodynamic calculations and other experimental methods a good agreement could be found. Time resolutions up to the ms-range can be obtained using diode array spectrometers. In case of OH, self-absorption has to be considered.

1. G. Herzberg, 'Molecular Spectra and Molecular Structure I. Spectra of Diatomic Molecules', D. van Nostrand Co. Inc. Princeton, New Jersey, 1950
2. D.B. Vaidya, J.J. Horvath, A.E.S. Green, Appl. Optics, 21(1982)3357
3. D.H. Campbell, S. Hulsizer, T. Edwards, D.P. Weaver, J. Propulsion 2 (1986) 414
4. H. Schneider, N. Eisenreich, 19th Int. Annual Conference of ICT, Proceedings, 1988, pp 88-1
5. I. Kovacs, 'Rotational Structure in the Spectra of Diatomic Molecules' Adam Hilger Ltd., London, 1969
6. W. Clauß, R. Söntgen, W. Eckl, N. Eisenreich, H. Schneider, 22th Int. Annual Conference of ICT, Proceedings, 1991, pp 102-1



## **Experimental studies on rocket exhaust plumes : support for computed simulation**

*V. Bodart - J.C. Chastenot*

Exhaust plumes of solid propellant missiles are heterogeneous flowfields containing gases and liquids or solid particles. Exhaust species mix with the atmosphere and can produce an afterburning flame. Propellant combustion may produce chloric acid which contributes to atmospheric water vapor condensation.

Missile exhaust plumes have harmful operational consequences. It may disturb the missile guidance system and increase engine and launch platform detectability. Specific computer codes are used in order to simulate operational missile exhaust plume effects. These codes have to be verified by experiments. Therefore, experimental techniques have been developed in order to characterize static rocket exhaust plumes. Radiation structure, radiance and temperature are measured by video, infrared and UV cameras. Radiative chemical species are identified by spectroradiometry. Flowfield is studied by laser doppler anemometry and laser tomography. Collected smoke particles are analysed by electronic microscope and X-ray spectrometry. Meteorological thresholds for water vapor condensation are noticed for various propellant compositions.

Experimental set-up, instrument and tested propellant compositions are chosen in order to optimize comparisons between experimental results and numerical computations. Moreover, computer codes are modified to take experimental data into account.

Experimental and computed results allow to establish correlations between exhaust plume characteristics, motor parameters and propellant compositions.

**SESSION R-8: Flame Visualization and  
Measurements**

**Co-Chairs: Dr. K. Schadow and  
Prof. V. S. Abruikov**

## PLANAR MIE SCATTERING VISUALIZATION OF REACTING AND NONREACTING SUPERSONIC COAXIAL JETS

Ken H. Yu, Tim P. Parr, and Klaus C. Schadow

Research Department  
Naval Air Warfare Center  
China Lake, CA 93555

The proposed paper describes the planar Mie-scattering technique for visualizing high-speed reacting and non-reacting flows. The merits and limitations of the technique are discussed. The application of the technique is demonstrated in supersonic coaxial jet studies. The contents of the paper are summarized in the following paragraphs.

The present flow visualization system consists of a copper vapor laser (20 nsec pulses, 4 mJ/pulse), beam-focusing optics, and a standard CCD camera. Both reacting and nonreacting supersonic coaxial jets were visualized using the system (figures 1 and 2). Reacting flows were seeded with fine aluminum oxide particles while nonreacting flows were visualized by condensed ethanol droplets. An optical band-pass filter was used in reacting case to isolate the Mie-scattered signal from natural chemiluminescence.

Compared to other visualization techniques which are typically used in high-speed-flow studies, the present technique has certain advantages. Since the technique is planar, it provides spatially-resolved cross-sectional views of three-dimensional flows. Also, the technique can be easily implemented at substantially less cost than other laser-based techniques such as planar laser-induced fluorescence and Rayleigh scattering technique.

The Mie scattering visualization technique was used to study turbulent flow structures in compressible shear flows. The compressible shear flows with *convective Mach numbers* of 0.23, 0.46, and 1.1 were created between two supersonic coaxial jets with different Mach numbers. The two lower convective Mach numbers were obtained with nonreacting jets while the highest required a combination of reacting and nonreacting jets. The images revealed that the supersonic shear layers are dominated by large-scale coherent structures. Under certain conditions (figure 1a), the structures were remarkably coherent, similar to those found in low-speed turbulent shear layers. They remained generally coherent at the two lower convective Mach numbers. At the highest compressibility condition tested (figure 2), the coherent structures became smaller in size and occurred only in a sporadic fashion.

The visualization was also made for a different nozzle shape and varying lip thicknesses. For a nozzle with five swept ramps on the expansion side, a significant difference in the coherent-structure shape and size was detected (figure 1b). To investigate the dependence on nozzle-lip size, the center-nozzle-lip thickness was systematically varied from 1.3 mm to 9.9 mm. From digitized images of the flows, wavelength and angular orientation of the coherent structures were quantified using Fast Fourier transform (figure 3). It was found that while streamwise wavelength is a monotonic function of nozzle-lip thickness the degree of coherence is much higher with certain lip thicknesses. The results suggest that a coupling between parallel shear flow and lip-created wake flow is responsible for the high degree of coherence in the structures.

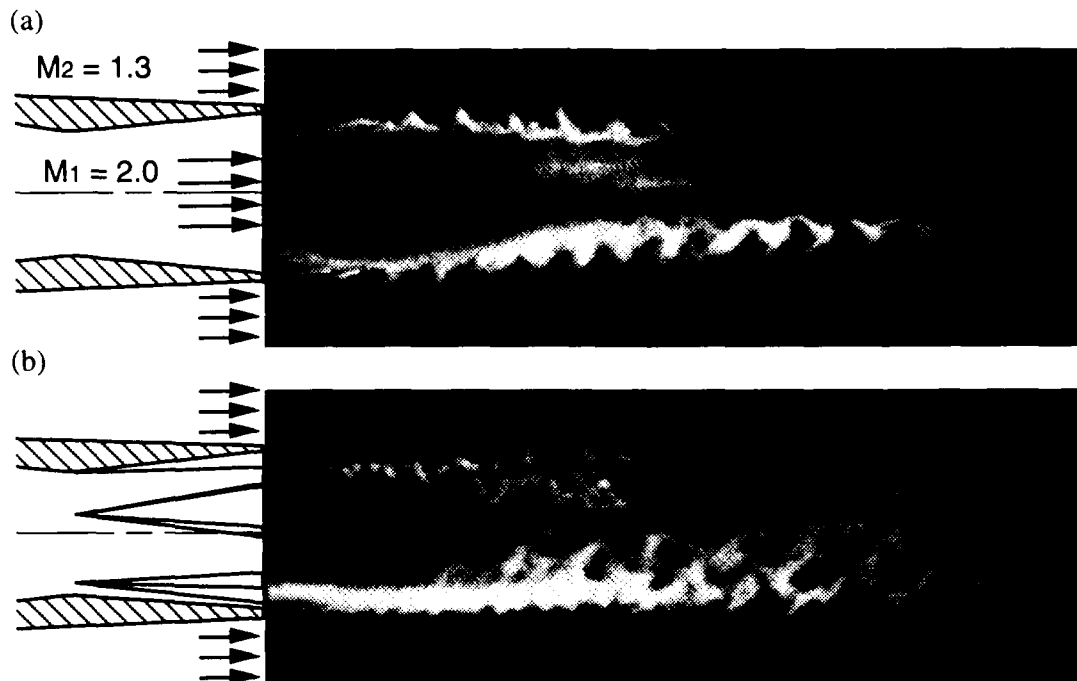


Figure 1. Planar Mie scattering images of supersonic coaxial air jets. The center jet is seeded with ethanol vapor and the outer jet is unseeded. (a) circular nozzle, (b) nozzle with five swept ramps on the expansion side.

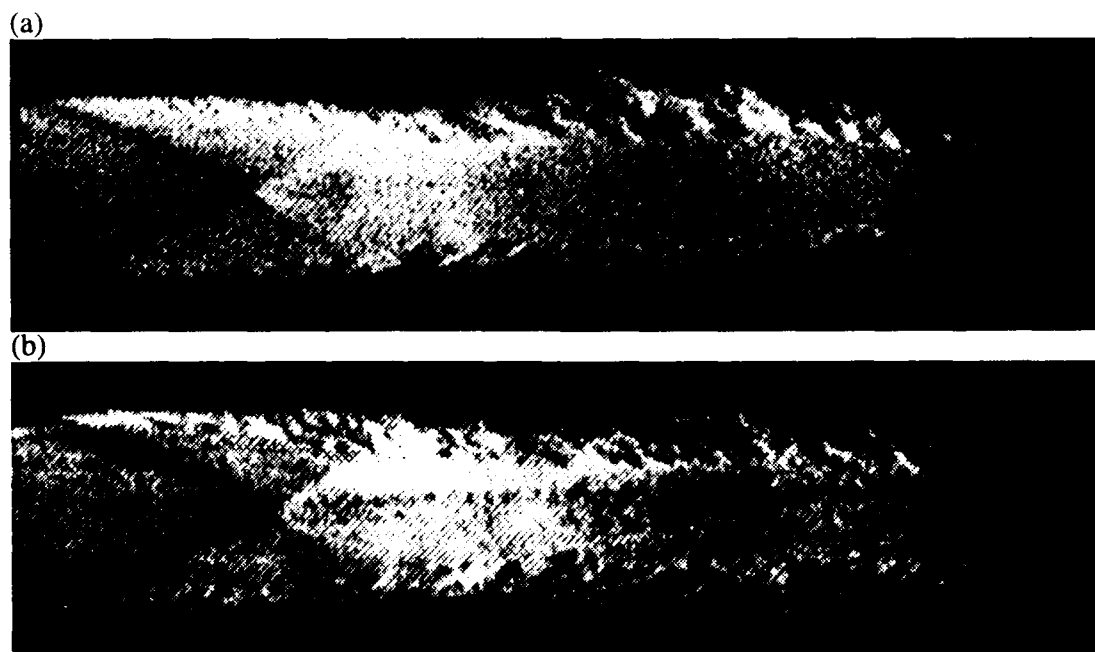
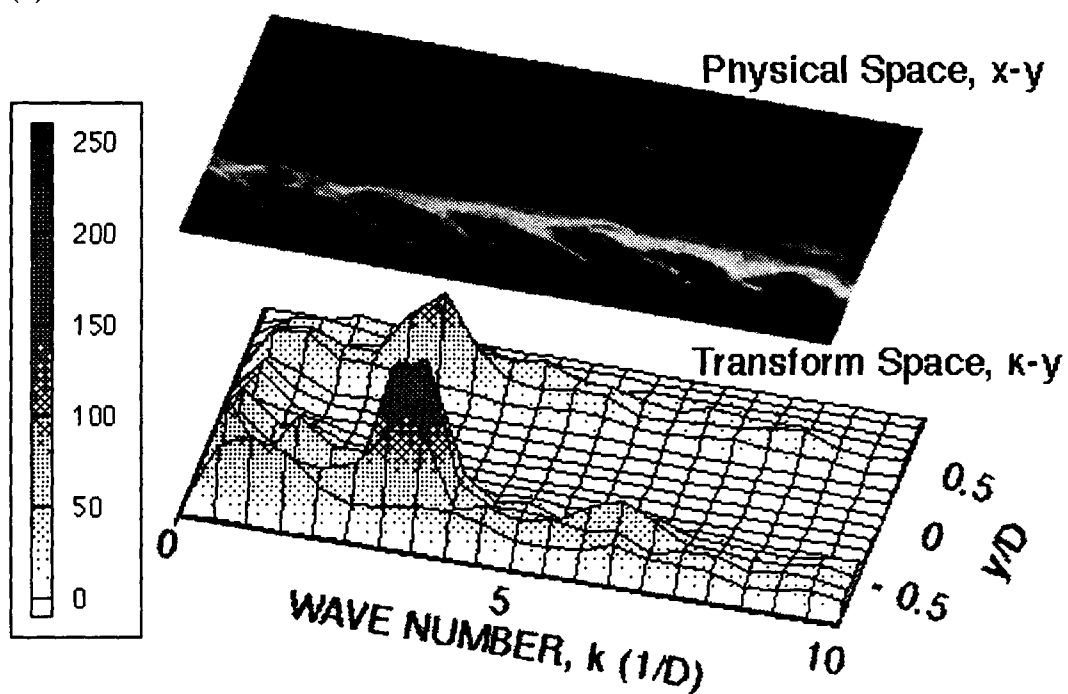


Figure 2. Reacting supersonic coaxial jets. High-temperature fuel-rich center jet is seeded with aluminum oxide particles. Cold oxygen-rich outer jet is unseeded. (a) circular nozzle with lip thickness  $t/D=0.09$ , (b)  $t/D=0.22$ .

(a)



(b)

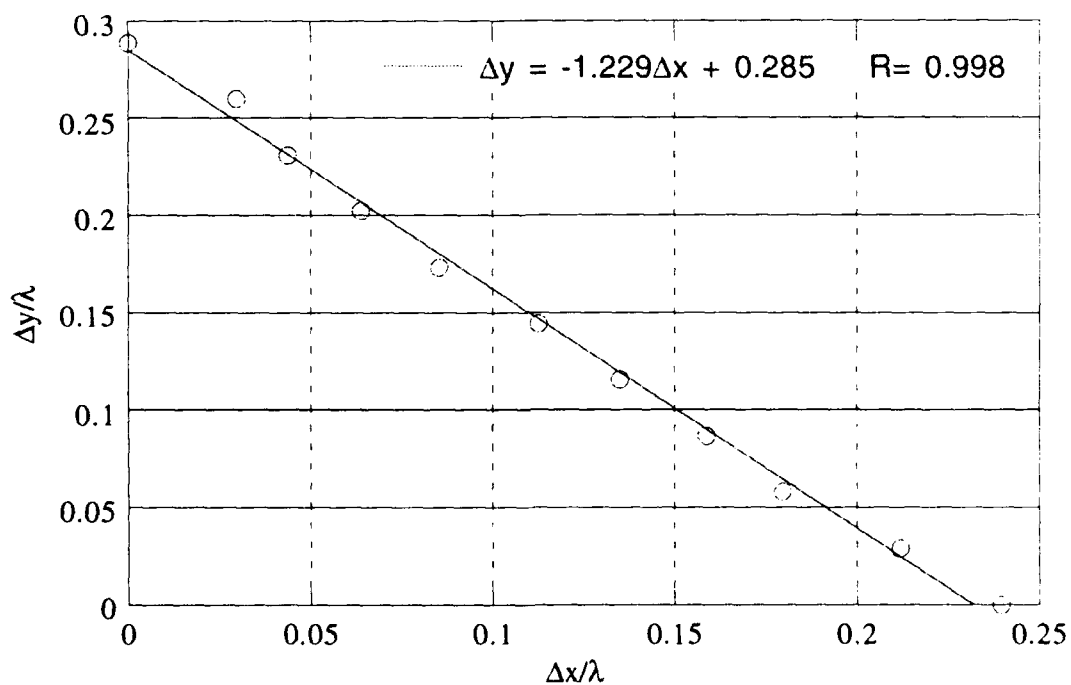


Figure 3. Quantitative reduction of digitized data. (a) Spectral intensity map of a digitized image. (b) Angular orientation of the large-scale structures based on spectral phase.

# IMAGING OF IMPINGING JET BREAKUP AND ATOMIZATION PROCESSES USING COPPER-VAPOR LASER SHEET ILLUMINATED PHOTOGRAPHY

By

M. C. Kline, R. D. Woodward, R. L. Burch, F. B. Cheung, and K. K. Kuo  
Propulsion Engineering Research Center  
Pennsylvania State University  
University Park, PA 16802

Liquid rocket engines over the years have employed a variety of impinging-jet injector designs to mix the fuel and oxidizer. Impinging injector elements may be classified under two categories, unlike- and like-impingement. Unlike elements cause the direct impingement of fuel and oxidizer jets. For like elements, impingement occurs with the same type propellant component to create a spray fan which then mixes with the spray fan of a neighboring element, thus achieving the mixing of fuel and oxidizer. Applications of impinging-element injectors are wide ranging within the liquid rocket field; including the Atlas, Titan III, F-1, LEM Ascent and many small reaction control engines.

Of particular interest to the design of liquid rocket engines is liquid jet breakup, atomization and mixing by means of multiple jet impingement. Critical to injector design and performance prediction is the determination of jet breakup and spray atomization characteristics as a function of impingement angle, propellant mass-flow rates, jet velocities, injector geometry and fluid properties. Combustion instabilities can arise due to improper injector design. The objective of this study is to investigate the dynamic interaction in the near-injector region of impinging jets using a non-intrusive diagnostic technique. The technique developed and used is copper-vapor-laser-sheet-illuminated photography which yields high-resolution photographs of the spray structure, spray boundary and droplet domain.

Observation of a like-on-like injector element in the near-injector region has been accomplished with laser-sheet illuminated photography to investigate the spray characteristics and geometry as a function of jet Reynolds number. The laser-sheet photographic method produced high-resolution photographs with 30 to 60 nanosecond laser pulses. A short-duration exposure of 30 to 60 ns from a single laser pulse produced a instantaneous picture of the injection and subsequent breakup processes (see Fig. 1a) while a multiple-exposure picture provided a time averaged representation of the spray (see Fig. 1b). Many injectors of various impingement angles were tested at Reynolds numbers ranging from 3000 to 107,000 (1.5 to 55 m/s). Instantaneous photographs of light scattered by the spray from two-dimensional cuts of the flow-field in the plane of the two impinging jets and perpendicular to this plane are obtained. In addition to the four previously documented spray regimes, the data suggest the inclusion of a higher Reynolds number regime in which the pre-impingement jets are fully turbulent and undergoing surface breakup. This spray regime is characterized by the presence of many fine droplets and the disappearance of the well-defined liquid breakup wave pattern in the post-impingement region.

An attempt to further examine the higher Reynolds number regime was made using Plexiglas injector pieces. The results revealed that a cavitating region was present within the orifice. Discharge coefficients were calculated and found to be relatively constant for each injector tested. Prior studies have shown either a decrease in discharge coefficient with the occurrence of cavitation or a decrease with hydraulic flip. The result of this study showing no decrease in  $C_d$  possibly confirms other works which associate  $C_d$  decreases with the occurrence of hydraulic flip. The angled orientation of the injector orifice created a stable cavitating region in which the phenomenon of hydraulic flip was not seen to occur, but increased turbulence led in turn to an atomization of the jets prior to impingement. After the inception of cavitation in the orifice, the location of the reattachment point was found to shift linearly downstream with increasing pressure drop.

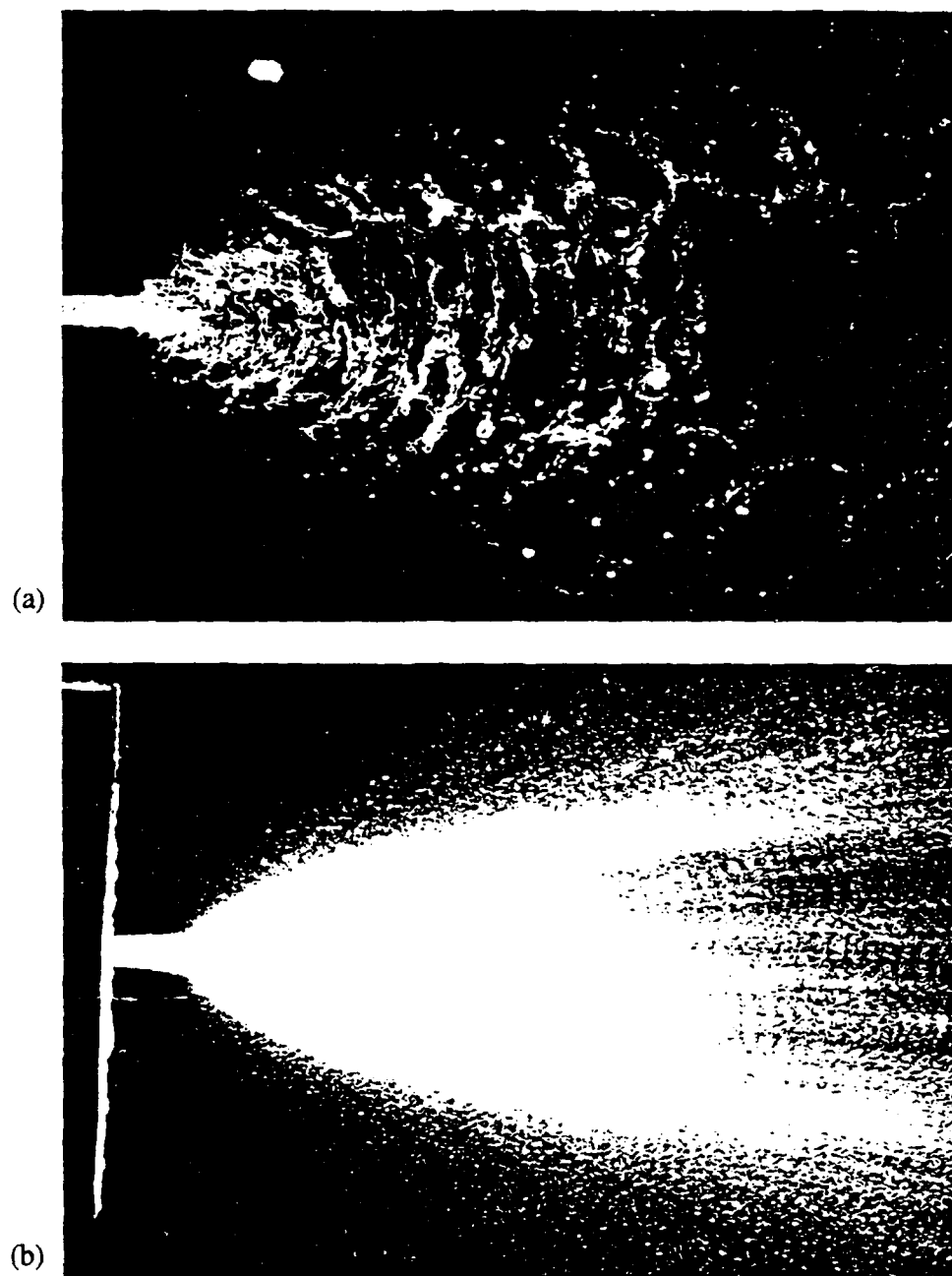


Figure 1. Copper-vapor-laser-sheet-illuminated images of like-on-like impinging jets.

(a) Instantaneous picture.

(b) Multiple-exposure picture.



## Soot diagnostics based on simultaneous measurements of soot particle size and of its temperature dependent optical constant in flames

B. Ineichen and B. Mandel

Swiss Federal Institute of Technology  
Internal Combustion Engines Laboratory  
CH-8092 Zurich  
Switzerland

To acquire a better understanding of soot particle origin and growth, it is necessary to measure and compare particle sizes in a flame with theoretical investigations. Laser light scatter transmission methods of G. Mie's theory have been used to study the behaviour of soot particles in flames. These methods have made it possible to measure with some accuracy the diameter, number and density of soot particles in steady, and non-steady flames. However the optical constant of soot particles is an uncertain element in determining accurately their diameters. It is very difficult to determine accurately the complex temperature dependent refractive index.

Two strategies, one using an opto-acoustic laser beam deflection technique to measure the soot temperature and a light scattering polarization ratio method to measure the refractive index, were examined.

The technique called *opto-acoustic laser-beam deflection* (Fig. 1) was introduced to measure the local temperature in a diffusion flame as basic data for the determination of the refractive index of soot particles. An acoustic wave, produced by a high energy Nd-YAG-laser pulse, spreads through the flame and deflects two parallel HeNe-laser beams, which are detected by position sensing diodes. By comparing the two similar signals delivered by the diodes it is possible to determine the acoustic velocity of the gas in the flame at the measurement point. To gain the local temperature belonging to the measured acoustic velocity it is necessary to compute the local composition of the flame considering the local equivalence ratio at the measurement point. A model for the local equivalence ratio was developed and examined.

The measurement of the acoustic wave velocity of a particle, produced by a high-energy pulse close to the HeNe-laser beams enables the determination of the surrounding particle temperature.

The change in optical properties and the underlying change in particle characteristics are determined by the scattering/polarization ratio method and the transmission/attenuation coefficient factor ratio method (Fig. 2). By scattering and transmission measurements, the refractive index and the particle diameter can be accurately determined.

The experimental verification of the scattering/transmission method for particle size measurements in flames will be presented, and the properties of this technique to combustion diagnostic will be discussed.

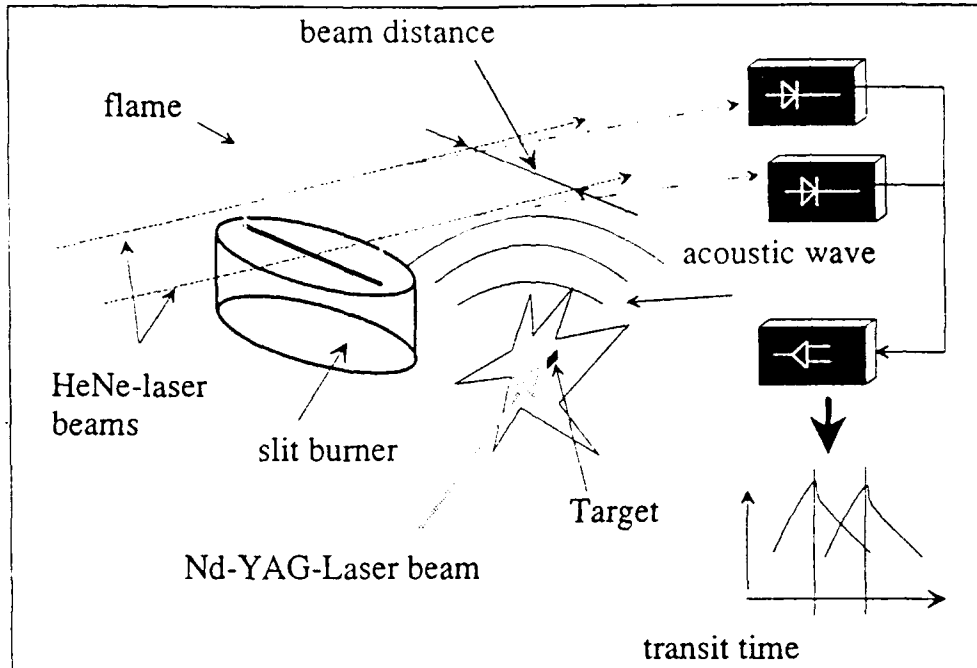


Fig.1 Temperature measurement by opto-acoustic laser beam deflection

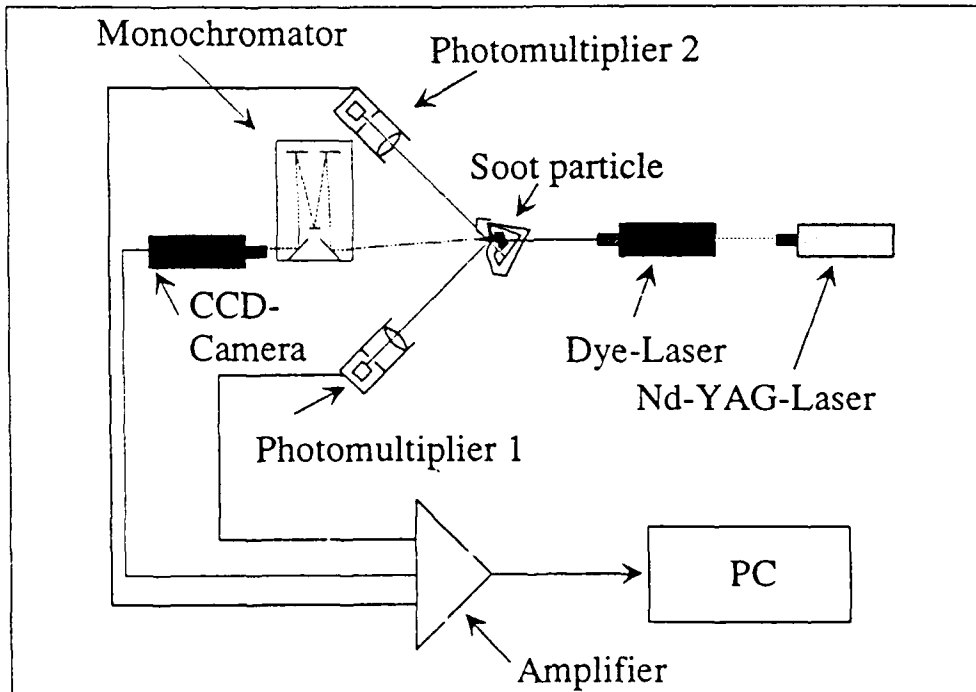


Fig. 2: Scattering light experiment for particle measurement

# FTIR SPECTROMETRY OF LAMINAR, PREMIXED HYDROCARBON/AIR FLAMES

I.T. Huang, S.T. Thynell and Kenneth K. Kuo  
Department of Mechanical Engineering  
Pennsylvania State University  
University Park, PA 16802

## I. Introduction

Liquid hydrocarbon fuels are employed in a variety of propulsive devices including, among others, airbreathing missiles, airplanes and automobiles. The products of combustion may contain pollutants, such as soot, unburnt fuel and nitrogen oxides. Since these products are a health hazard, governments all over the world have imposed stringent regulations on their emission. Furthermore, soot is a strong emitter of thermal radiation; if present in significant quantities, the result will be a reduced life time of gas turbines. Although being the subject of numerous studies, the combustion and sooting behaviors of most liquid hydrocarbon fuels are poorly understood. In order to obtain an improved understanding of the combustion processes of such fuels, it is necessary to examine in detail the flame zone using a wide variety of diagnostic tools. The overall objective of this work is to describe the application of FTIR spectrometry for the characterization of the combustion behavior of liquid hydrocarbon fuels in laminar, premixed flames. The sections below summarize the following: (1) a brief discussion of the experimental facility developed; (2) the novel approach and new data analysis procedure for determining absolute species concentrations and temperature profiles within the flame zone; and (3) typical results obtained from fuel-rich premixed flames.

## II. Method of Approach

*Experimental Facility:* A flat-flame burner has been employed to obtain a highly one-dimensional premixed flame. An evaporator was designed and constructed in order to vaporize various types of liquid hydrocarbon fuels. The burner was enclosed in a transparent chamber which allowed optical access to the flame zone through two ZnSe windows. The chamber was purged with nitrogen to eliminate effects from ambient oxygen on the flame zone.

*Diagnostic Approach:* In most fuel-rich, hydrocarbon flames, there are significant amounts of CO formed. By carefully using selected lines within the *P*-branch of the CO fundamental band centered at  $2150\text{ cm}^{-1}$ , both temperature and CO absolute concentration are determined from an iterative, least-square based approach. In the course of its development, two significant advancements have been made. First, a new analytical approach has been developed for evaluating a complex integral required in correcting for the FTIR instrumental effects.<sup>1</sup> The use of this analytical approach significantly reduces the time required for processing the data (from an hour to a few seconds). Second, the line broadening effects due to an IR source of a finite area have been incorporated into the data analysis. To our knowledge, this broadening effect has not been quantified by other researchers utilizing FTIR spectrometry at low spectral resolution. In addition to the analysis of CO fundamental band, the *R*-branch of the fundamental band of  $\text{CO}_2$  centered at  $2350\text{ cm}^{-1}$  has been employed as a second nonintrusive approach to determine the temperature, as well as the  $\text{CO}_2$  absolute mole fraction. Based upon the development of this analytical approach, the absolute concentration of  $\text{H}_2\text{O}$  was determined from the use of line-strength and line-width data.<sup>2</sup> In the field of FTIR spectrometry utilizing low spectral resolution ( $0.3\text{--}1\text{ cm}^{-1}$ ), the water vapor concentration is rarely quantified. Finally, the absolute concentration of the fuel and the integrated soot volume fraction (integrated across the

6-cm diameter flame) are also determined as a function of distance above the burner surface. The temperature profiles deduced from absorption data obtained by the FTIR spectrometer have been compared with intrusive measurements using 100  $\mu\text{m}$ ,  $\text{SiO}_2$  coated thermocouples.

### III. Discussion of Results

Figure 1 shows the measured profiles of temperature, absolute species mole fractions, and integrated soot volume fraction in a fuel-rich  $\text{CH}_4/\text{O}_2/\text{N}_2$  flame as well as the calibration relationship between the integrated absorbance and the partial pressure of  $\text{CH}_4$ . Examination of the temperature profiles shown in Fig. 1a reveals an excellent agreement between those obtained from absorption data and thermocouple. The thermocouple measurements are uncorrected. The numerical values of the measured temperatures using different methods and standard deviations of the deduced temperatures from absorption spectra of CO and  $\text{CO}_2$  are approximately 100 K. The adiabatic flame temperature calculated from the NASA/Lewis CEC86 equilibrium code is also included as a reference value in Fig. 1a. However, the code does not consider the kinetics of soot formation, as well as radiative heat losses. Thus, some difference between the experimental data and calculated flame temperature is expected.

Figure 1b shows the deduced absolute concentration profiles of CO,  $\text{CO}_2$ ,  $\text{H}_2\text{O}$ , and  $\text{CH}_4$  as well as the integrated soot volume fraction. A comparison of the experimentally determined absolute mole fractions with those calculated from the equilibrium code reveals a reasonable agreement for CO and  $\text{CO}_2$ . However, the measured water vapor concentration is somewhat higher than the calculated one, which is included here for reference only.

The results of the integrated soot volume fraction indicate that most of the soot is formed in the low-temperature region near the burner surface. As the soot travels further above the burner surface, it agglomerates and forms larger chains of particles; therefore a decrease in the integrated soot volume fraction with respect to axial distance was observed in the line-of-sight measurements. The relatively constant levels of CO and  $\text{CO}_2$  mole fractions beyond 3 mm (shown in Fig. 1b) further support this interpretation that the decrease in integrated soot volume fraction is not caused by oxidation but by agglomeration.

Figure 2 shows the measured temperature, absolute species mole fractions and integrated soot volume fraction profiles in a fuel-rich  $\text{C}_6\text{H}_6/\text{air}$  flame as well as the calibration relationship between the integrated absorbance and the partial pressure of  $\text{C}_6\text{H}_6$ . Again, the agreement between temperature profile obtained from absorption measurements to those obtained from micro-thermocouple is excellent. The gaseous benzene enters the burner at approximately 390K and very rapidly reaches temperatures above 1000 K. Regarding absolute mole fractions, the measured values are below those calculated by the NASA/Lewis CEC86 code. The conversion of fuel to soot is quite slow in the region close to the burner surface and soot formation continues to about 5 mm above the burner surface. Afterwards, it remains nearly constant.

### IV. References

1. Thynell, S.T., I.T. Huang and K.K. Kuo, "Analytical Evaluation of the Convolution Integral Involving the  $\text{Sinc}^2$  x Function," submitted to *Applied Spectroscopy*, 7/92.
2. Dana, V., et al., "Measurements of Collisional Linewidths in the  $\nu_2$  Band of  $\text{H}_2\text{O}$  from Fourier-transformed Flame Spectra," *Applied Optics*, Vol. 31, pp. 1928-1936, 1992.

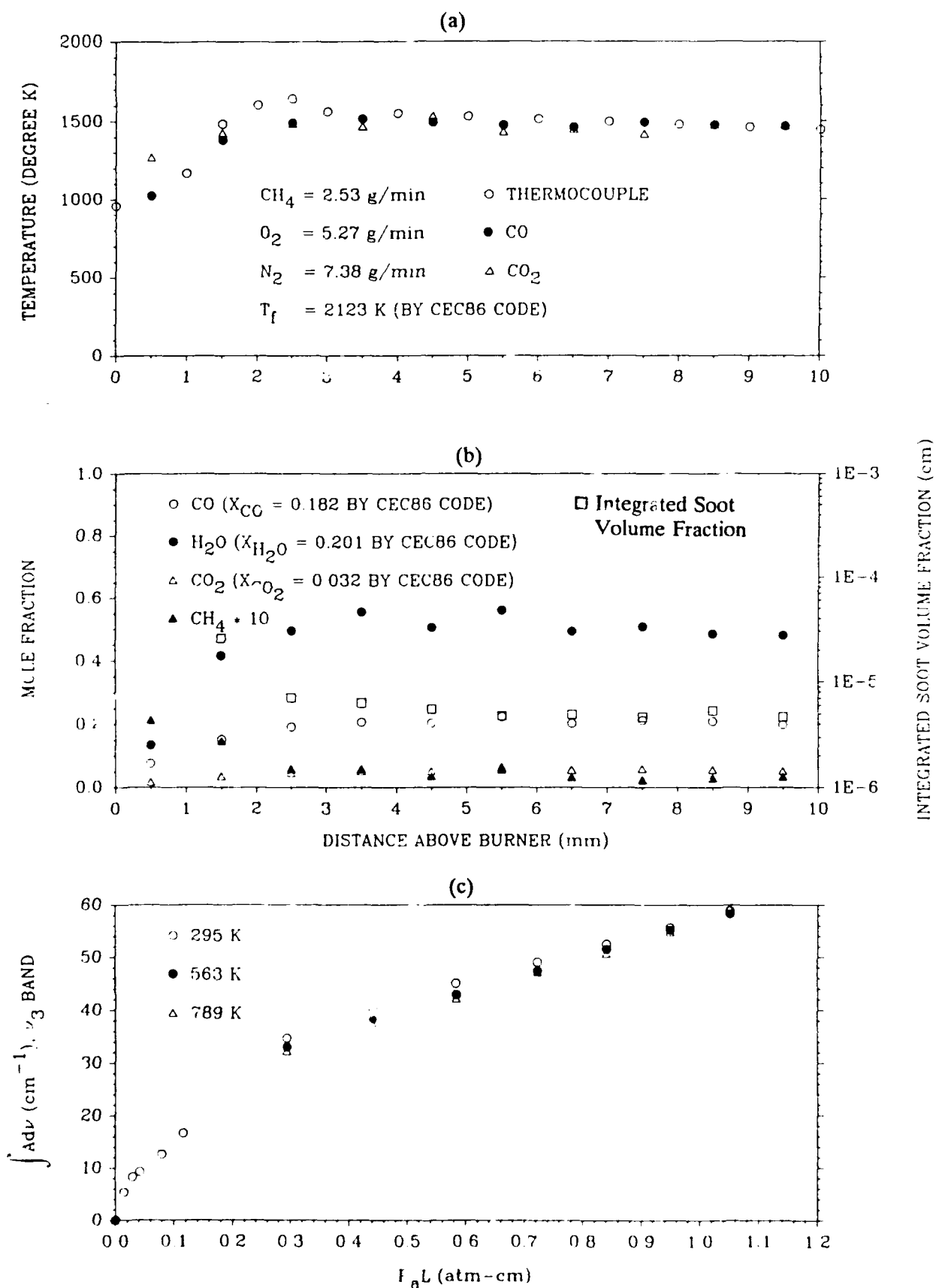


Fig. 1 Measured profiles of temperature, absolute species mole fractions, and integrated soot volume fraction in a premixed CH<sub>4</sub>/air flame with an equivalence ratio  $\phi = 1.94$ , as well as calibration data between integrated absorbance and partial pressure of CH<sub>4</sub>.

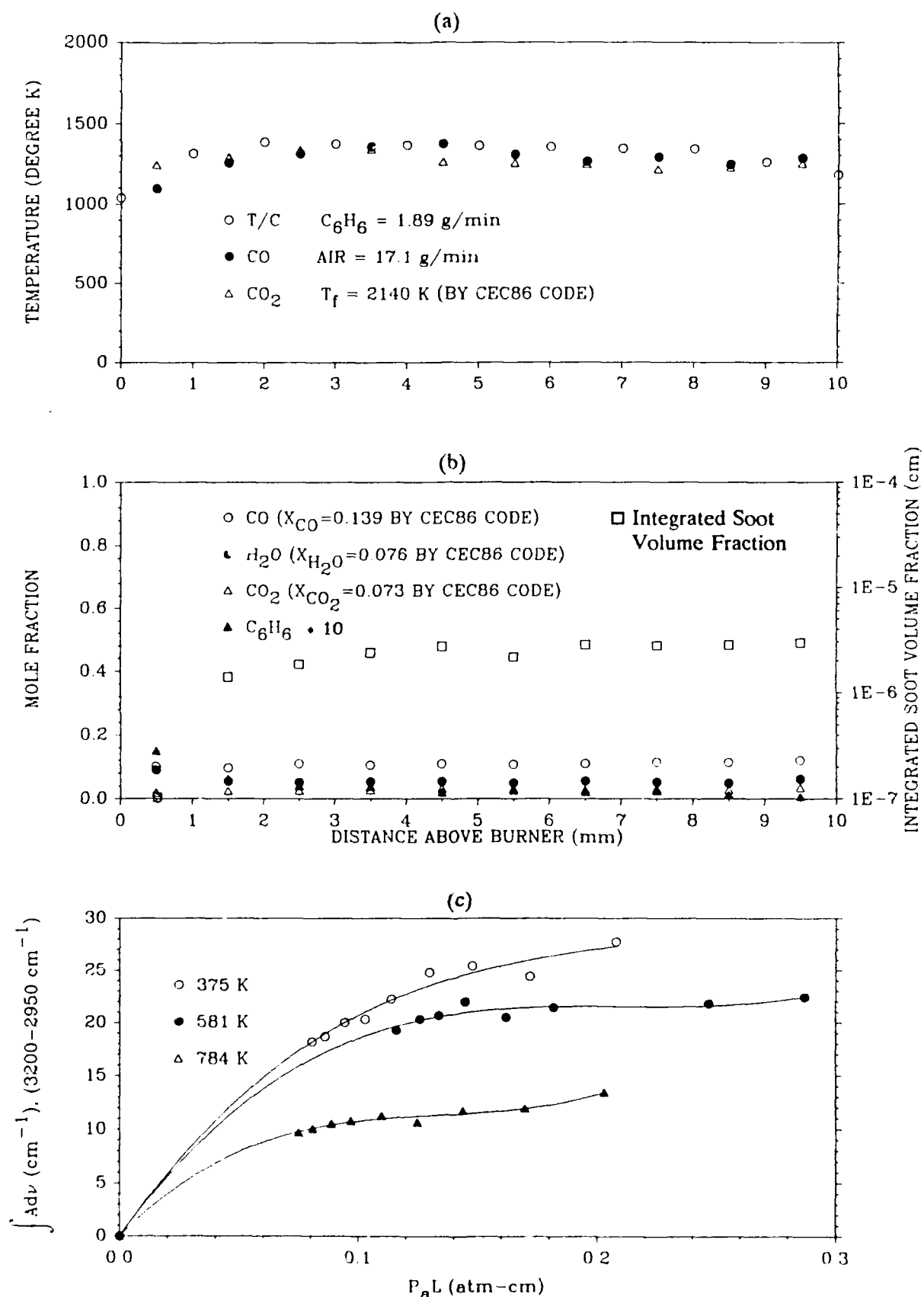


Fig. 2 Measured profiles of temperature, absolute species mole fractions, and integrated soot volume fraction in a premixed  $C_6H_6$ /air flame with an equivalence ratio  $\phi=1.47$ , as well as calibration data between integrated absorbance and partial pressure of  $C_6H_6$ .

OPTICAL METHODS FOR THE DETERMINATION OF RELATIVE RADICAL  
CONCENTRATION, AND SOOT TEMPERATURE.

T. Wijchers

TNO Prins Maurits Laboratory

P O box 45, 2280 AA Rijswijk, The Netherlands.

The spectrum of the flame inside a solid fuel ramjet combustor made of (transparent) acrylic, is dominated in the visible by the continuous spectrum of radiating soot at pressures above about 0.5 MPa, but the spectrum of electronically excited radicals OH, CH, and C<sub>2</sub> is clearly present below that pressure.

Knowledge of (relative) concentrations of these radicals, as well as knowledge of temperatures is important for validating computer codes which intend to model, among others, the chemical processes in this ramjet combustor.

The scheme of the general optical layout of the spectrographic setup which acquired the spectra of radicals and soot, is depicted in fig.1.

To obtain the relative projected concentrations of excited CH and C<sub>2</sub>, the setup of fig.1 was modified into that of fig.2. In this setup, the transparent ramjet combustor is imaged by L<sub>2</sub>' through fieldlens L<sub>4</sub> onto the length of the slit of the spectrograph. The detector-array is vertical now to measure the relative spectral intensity of the image of the combustor, and hence of the combustor itself as a function of the wavelength setting on the spectrograph. The contribution of soot is subtracted. A typical result of this measurement is given in fig.3.

The temperature of the radiating soot is measured with the aid of two-colour pyrometry of which the setup is schematically depicted in fig.4. The effective beam from the source is geometrically well defined by the optical train L<sub>1</sub>, A<sub>1</sub> .. L<sub>3</sub>, A<sub>3</sub>, and next divided into a green part and a red part by filters GF and RF respectively.

The ratio  $E_p$  of the green signal and the red signal is a measure of the two-colour temperature, while the red signal alone is a measure of the intensity of the radiation.  $E_p$  and  $E_m$  have been calibrated against a tungsten-ribbon lamp of which the temperature  $T(I)$  is precisely known as a function of electric current  $I$ . A data-processing program, which contains the calibration-data, converses  $E_p$  into the two-colour temperature  $T_c$ , and converses  $E_m$  together with  $T_c$  into the emissivity of the cloud. A typical example is given in fig. 5, showing the temperature and the emissivity.

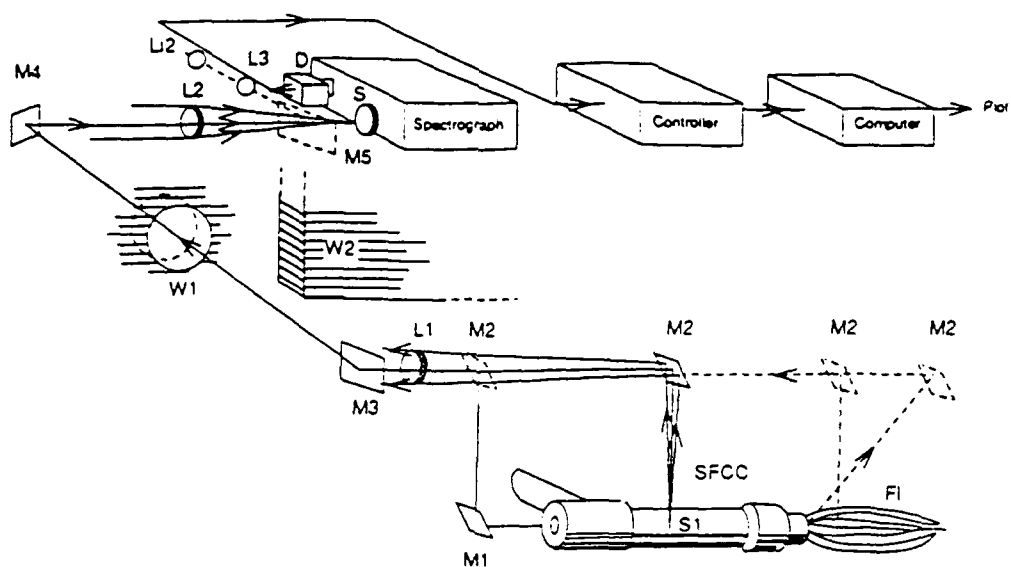


Figure 1 Optical equipment for spectrographic measurements

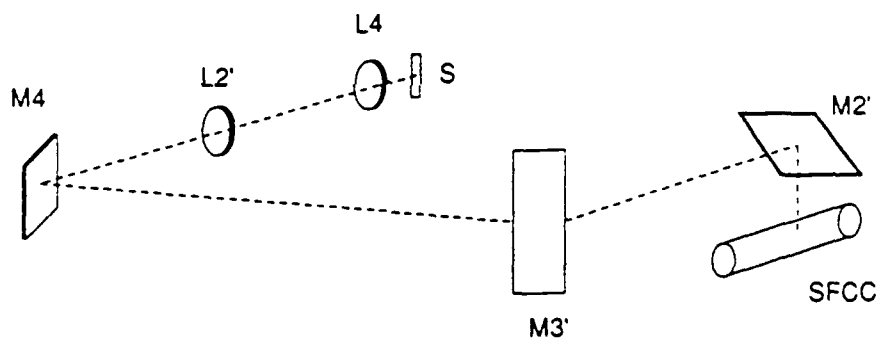


Figure 2 Modified optical set-up

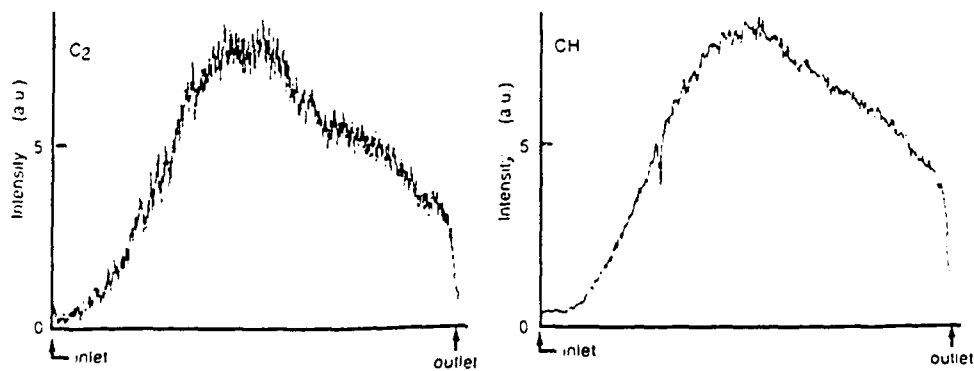


Figure 3 Typical projected concentration profiles of CH and C<sub>2</sub>



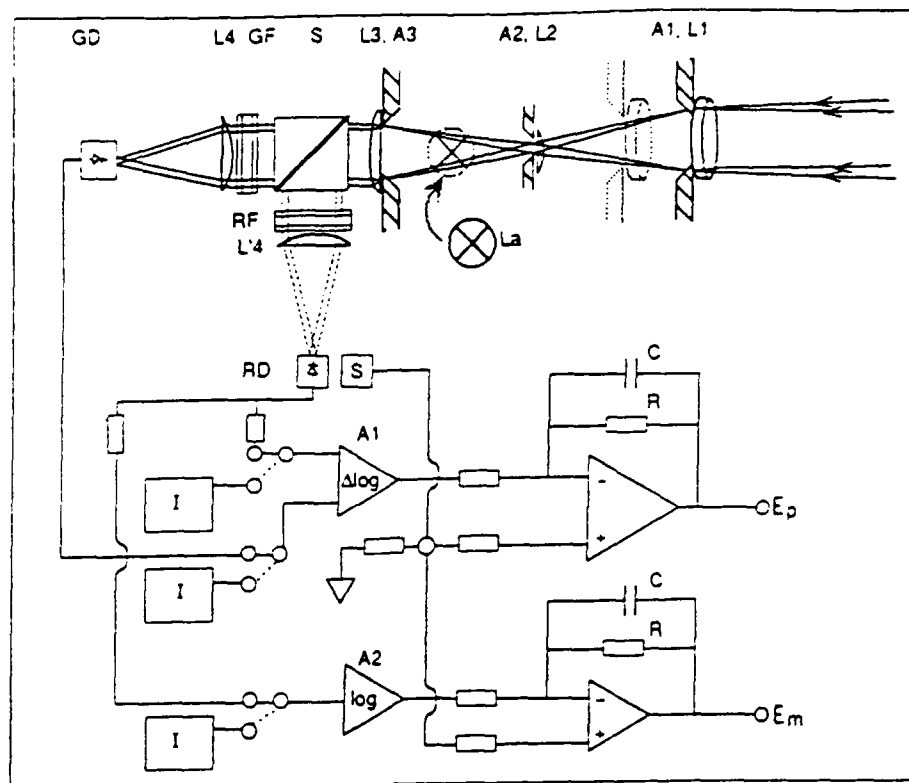


Figure 4 Layout of the two-colour pyrometer

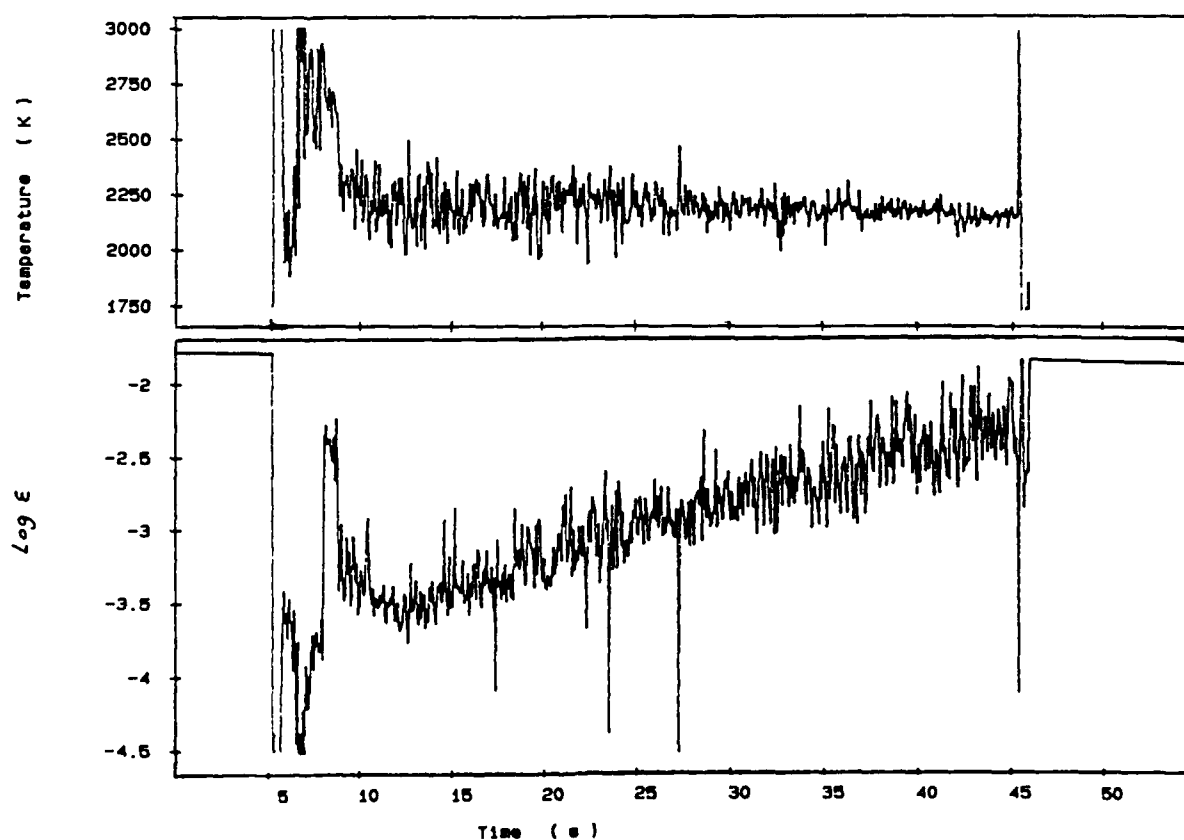


Figure 5 Two-colour temperature (top) and emissivity (bottom)

## The Use of Non-Intrusive Combustion Diagnostics to Investigate the Intrusiveness of Probing Measurements in Flames

O. P. Korobeinichev, E. Yu. Fedorov, K. P. Kutsenogii, P. A. Mavliev

Institute of Chemical Kinetics and Combustion S.D. Russia Ac. Sc.,  
Russia, Novosibirsk, 630090

### ABSTRACT

The most important advantage of non-intrusive combustion diagnostics compared to the probing technique is the absence of flame perturbations. However, the probing methods (for example, probing mass-spectrometry) are often more universal and informative, particularly in studying flame structure with narrow combustion zones. Important tasks of flame structure studies are the simultaneous use of probing and non-intrusive methods and the application of the latter to estimate flame perturbations by the probe. One of the tasks of the present work was experimental determination of a probe-perturbed field of velocities in a flowing one-dimensional gaseous stream at the distance of several orifice diameters from the probe. Another task is to utilize the obtained data for the estimation of errors of the probe measurements of concentration profiles in flames with narrow combustion zones. To perform these tasks, we employed the equipment and the method of visualizing submicron particles using a pulsed laser with a short pulse duration and a tv registration technique. Experimental results have shown good agreement with the calculations of the velocity field of an ideal gas flow near a probe. The data obtained allowed us to suggest a semi-empirical formula for estimating hydrodynamic perturbations of flame by the probe. The shift of the sampling site relative to unperturbed flow is denoted as  $z$ . Another task of this work was the determination of the concentration profile of methane in a methane-air flame by non-intrusive and mass-spectrometric probing techniques. The premixed methane (8%) - air (80%) - argon (12%) flame was stabilized on a flat flame burner at 1 atm. Analysis of obtained data showed that the profiles of methane concentration measured by both methods coincided within 15% if one makes a shift of the distorted profile towards the burner by a value close to  $z$ . The simultaneous use of non-intrusive and probe measurements is recommended for future investigations of flame structure.

**SESSION R-9: Flow Field Measurements and  
Observation**

**Co-Chairs: Prof. F. Durst and  
Prof. M. V. Heitor**

## APPLICATION OF NON-INTRUSIVE DIAGNOSTIC METHODS TO SUB- AND SUPERSONIC H<sub>2</sub>-AIR-FLAMES

M. Haibel, F. Mayinger, G. Strube

Institute A for Thermodynamics  
Technische Universität München  
Arcisstr. 21; D-8000 München 2; FRG

The design of hydrogen fired, supersonic combustion chambers for future hypersonic propulsion systems requires basic knowledge on the physics and the controlling mechanisms of high speed H<sub>2</sub>-air flames extracted from experiments. The goal of the present experimental investigation is an improved understanding of the behaviour of sub- and supersonic H<sub>2</sub>-air flames as regard to the mixing process of hydrogen and air, the stabilization and the structure of the flames. Non-intrusive diagnostic methods like holographic interferometry, self-fluorescence and Raman scattering are utilized.

Holographic interferometry is used to determine the three dimensional concentration profile of the H<sub>2</sub>-air mixing jet after the injection of gaseous hydrogen into the high speed air flow and the temperature distribution in and around the flame. Self-fluorescence, resulting from chemical reactions and thermal excitation, gives good qualitative information on the location and the behaviour of the stabilization spot of the flame as well as on the structure of the whole flame. The temperature and the quantitative distribution of the H<sub>2</sub>-, O<sub>2</sub>-, N<sub>2</sub>- and the H<sub>2</sub>O-molecules inside the flame are determined by means of Raman scattering.

The experiments were performed in a blow down windtunnel with a two dimensional combustion chamber. The Mach number of the main air flow inside the combustion chamber was varied between  $Ma = 0.2$  and  $Ma = 1.3$ . Hydrogen was injected at different angles and geometries upstream from a rearward facing step, which induced a turbulent recirculation zone. The concentration profile of the H<sub>2</sub>-air mixing jet was determined in two perpendicular directions by means of holographic interferometry. The use of a CCD-camera allowed very short exposure times of only 100 ns. The stabilization spots and the structure of the flames were determined by recording the OH-fluorescence of the reaction zone around 306 nm using an intensified CCD-camera operated with exposure times of 1 to 1000  $\mu$ s and an interference filter of  $\lambda = 308 \text{ nm} \pm 5 \text{ nm}$ . The main components of the Raman system used for the simultaneous determination of local species concentrations and temperatures are a tunable, pulsed excimer laser for molecular excitation and an intensified diode-array detector coupled to a polychromator for signal detection.

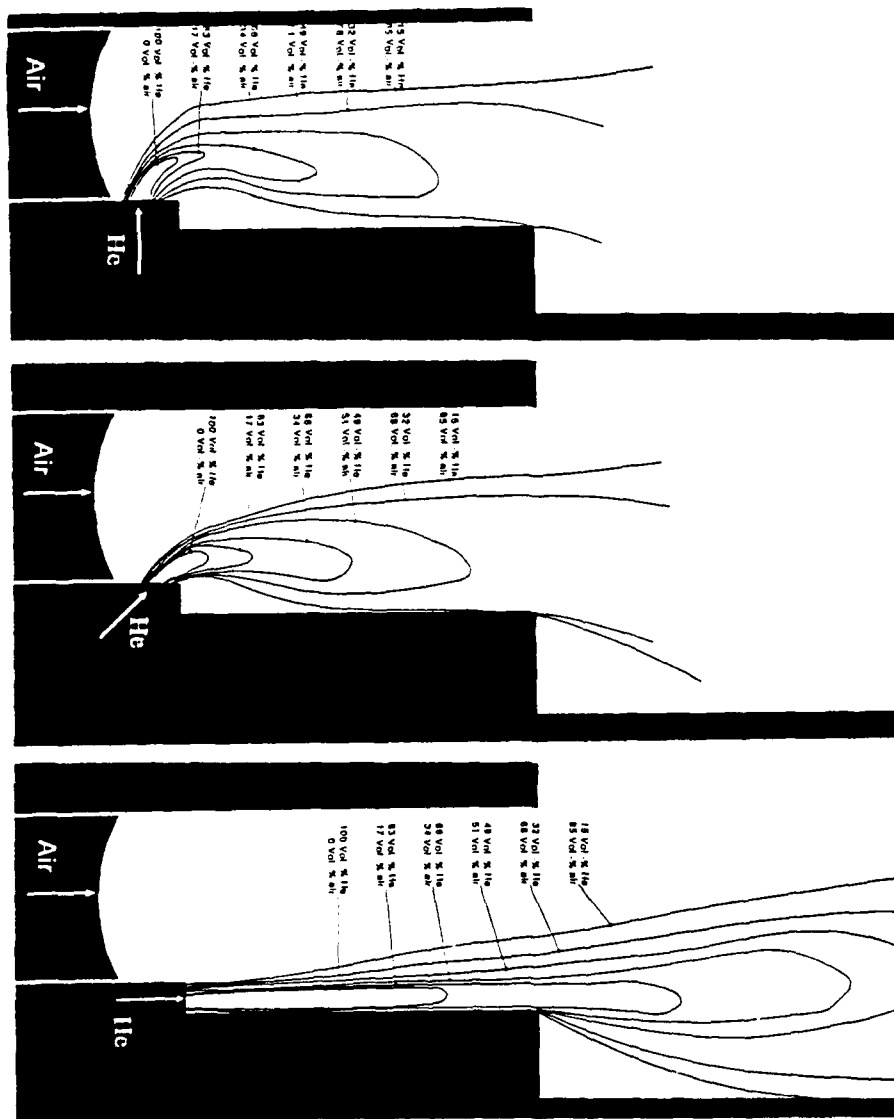
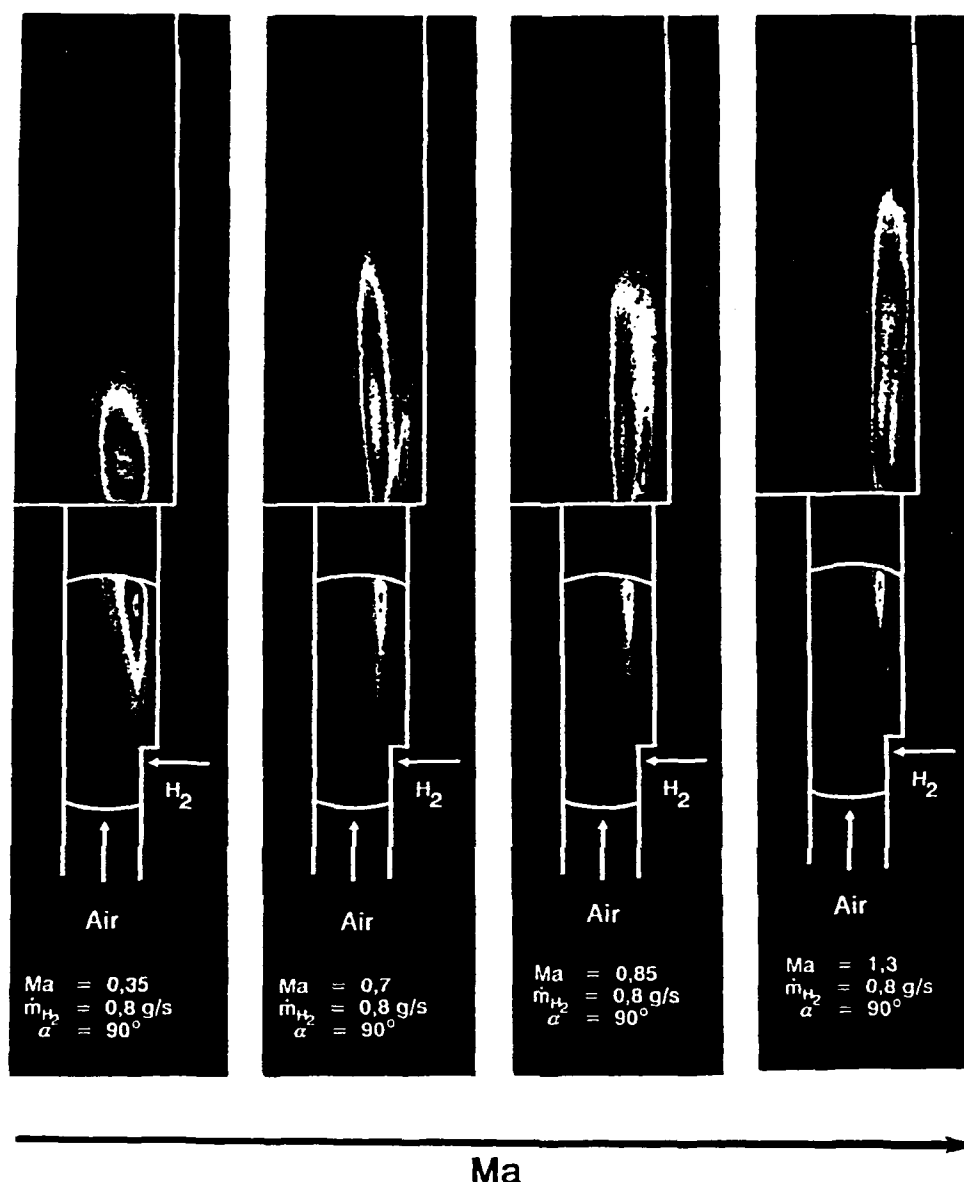


Fig. 1: Determination of the concentration profile of the mixing jet by means of 2-direction holographic interferometry with an air Mach number of  $Ma = 0.6$  under different injection angles  $\alpha$ : (no combustion)  
top:  $\alpha = 90^\circ$ ; middle:  $\alpha = 45^\circ$ ; bottom:  $\alpha = 0^\circ$

COPY AVAILABLE TO DTIC DOES NOT PERMIT FULLY LEGIBLE REPRODUCTION



It is shown that the mixing process of  $H_2$  and air is completely controlled by large scale turbulent structures induced by the injection of the hydrogen jet into the main air flow and the recirculation zone downstream of the rearward facing step. The mixing length and the penetration depth of the mixing jet could be obtained under various flow conditions (Fig. 1). The OH-fluorescence technique showed that the stabilization spots of sub- and supersonic  $H_2$ -air flames are located within the free turbulent shear layer between the mixing jet and the induced recirculation zone (Fig. 2). The experiments showed that the highly turbulent structure of the flames downstream of the stabilization spot could be recorded with an exposure time of the CCD-camera of  $100 \mu s$ . Longer exposure times caused significant averaging of the obtained signal, leading to a disclosure of the turbulent structure. Raman scattering measurements yielded the quantitative, simultaneous determination of the molecular concentration of  $H_2$ ,  $O_2$ ,  $N_2$  and  $H_2O$  which are related to the degree of combustion as well as the local flame temperature (Fig. 3).

In general it can be said that the combination of the three non-intrusive measurement techniques mentioned above gave new information about the structure and the behaviour of sub- and supersonic  $H_2$ -air flames.

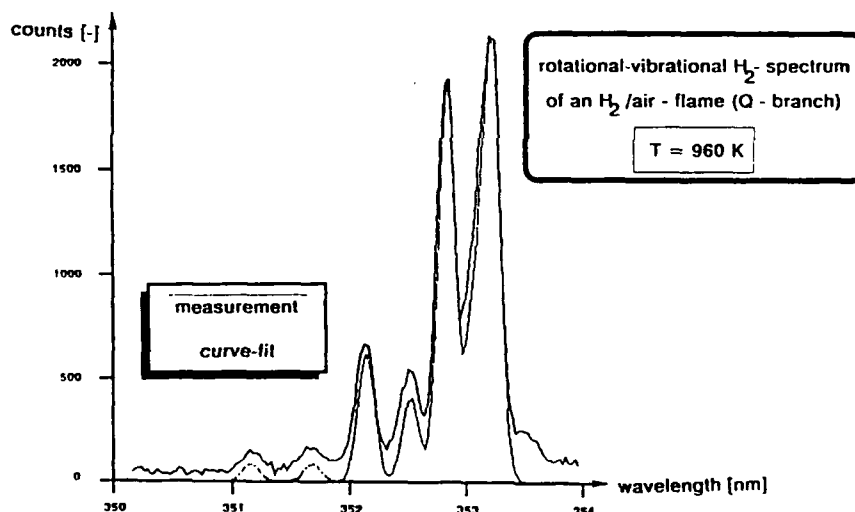


Fig. 3: Temperature determination by means of Raman scattering using the computer-fit-method applied to the rotational-vibrational  $H_2$ -spectrum

# Investigation of the Flowfield of a Scramjet Combustor with Parallel H<sub>2</sub>-Injection through a Strut by Particle Image Displacement Velocimetry

M.Oschwald, R.Guerra, W.Waidmann

German Aerospace Research Establishment, Lampoldshausen

A supersonic combustor with parallel fuel injection through a strut is investigated for a combustor entrance Mach number of 2 and the hydrogen fuel injected sonically. The velocity of H<sub>2</sub> is 1200m/s while the velocity of the free stream, depending on the stagnation temperature, varies between 500m/s and 1100m/s. Typical mass flows are 1kg/s for air and 2g/s for hydrogen. The test chamber (see Fig. 1) is designed to exhibit a two dimensional flowfield. This flowfield is characterised by the shock trains, which originate at the strut leading edge (a recompression shock occurs downstream of the base of the strut in most cases), an expansion originating at the strut base, and by the interaction of the fuel and air flows (see the Schlieren photo in Fig.2). Since this interaction is important for the efficiency of the mixing of the reacting components and since shock and expansion waves interact with the flame zone producing local gradients which can enhance or suppress combustion, the quantitative visualization of the flowfield is being investigated.

The instantaneous flowfield is measured with the PIV method with and without combustion. Two sequentially fired ND:YAG-Lasers are used as a light source for the photographic recording of the supersonic flow. The two lasers allow the choice of short time delays that are necessary for these high velocities. The flow is seeded with glycerol droplets due to their small specific mass for the investigation of cold flows and with metal-oxide particles for combustion. The double exposures are analysed by the Young's fringes method.

The performance of the PIV technique under the conditions of the scramjet test facility which corresponds to high noise and vibration levels is presented. Also the problems of the seeding under conditions of the supersonic flow with combustion, i.e. the influence of the limited ability of the particles to follow large velocity gradients and the stability of the metal-oxide particles in hot environments, are discussed.



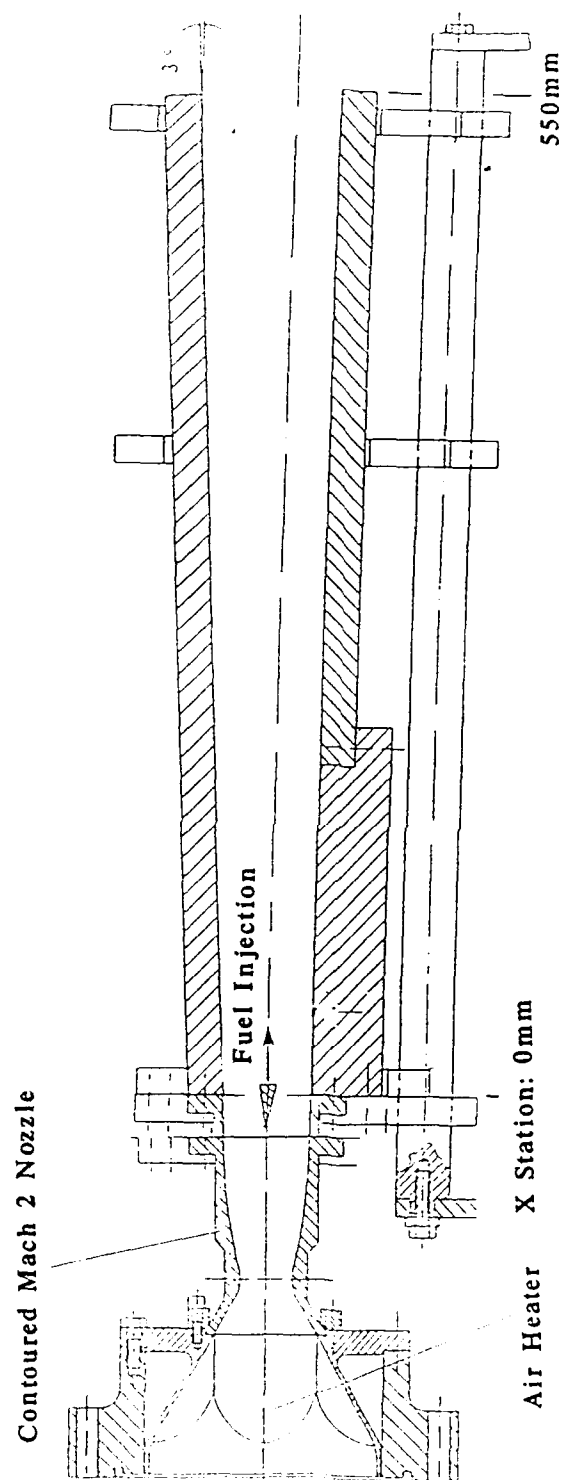
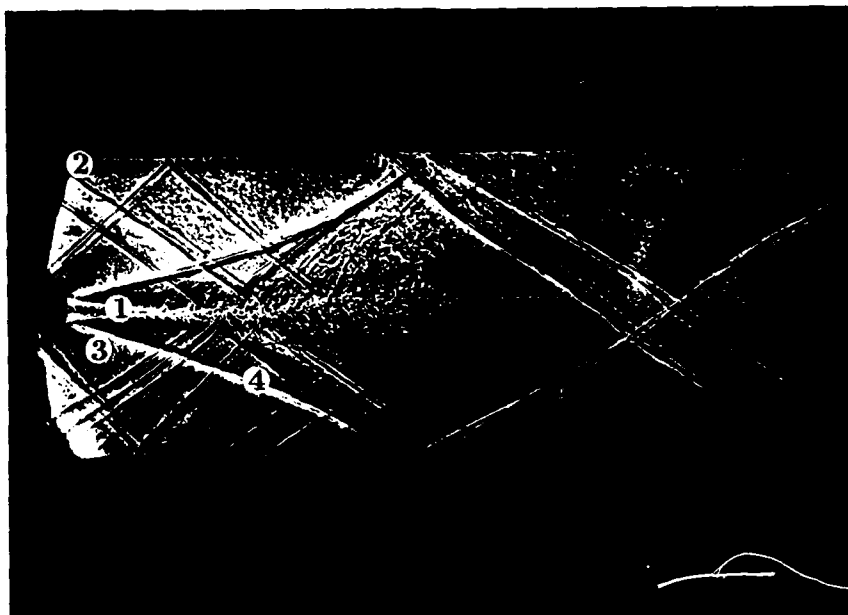


Figure 1: Sketch of the supersonic test chamber

a.)



b.)



**Figure 2:** Schatten photograph of the supersonic flow behind the strut, a.) without combustion, b.) with combustion. The flow direction is from left to right.

- (1) fuel injection behind strut base
- (2) leading edge shock
- (3) base expansion
- (4) recompression shock

# OPTICAL ANALYSIS OF TURBULENT HEAT TRANSFER IN DISC-STABILIZED FLAMES FOR COMBUSTION REGIMES

by

P. Ferrão and M.V. Heitor

Instituto Superior Técnico  
Department of Mechanical Engineering  
Av. Rovisco Pais  
1096 Lisboa, Codex  
PORTUGAL

Phone: (351 1) 847 34 53/4; Fax: (351 1) 84 61 56

## ABSTRACT

Improved understanding of the processes of turbulence mixing in laboratory type of flames has been achieved in recent years with the use of advanced diagnostic techniques for making spatially- and temporally-resolved measurements in combustion systems<sup>1-3</sup>. The difficulties inherent to the implementation of simultaneous measurements of velocity and scalar characteristics<sup>4</sup> have however limited the extent of the analysis of practical combusting flows, and are the main motivation of the present paper.

A laser-Doppler velocimeter, LDV, has been extended to the analysis of turbulent heat transfer in a strongly sheared disc-stabilized propane air-flame through its combination with laser Rayleigh scattering, Figure 1.

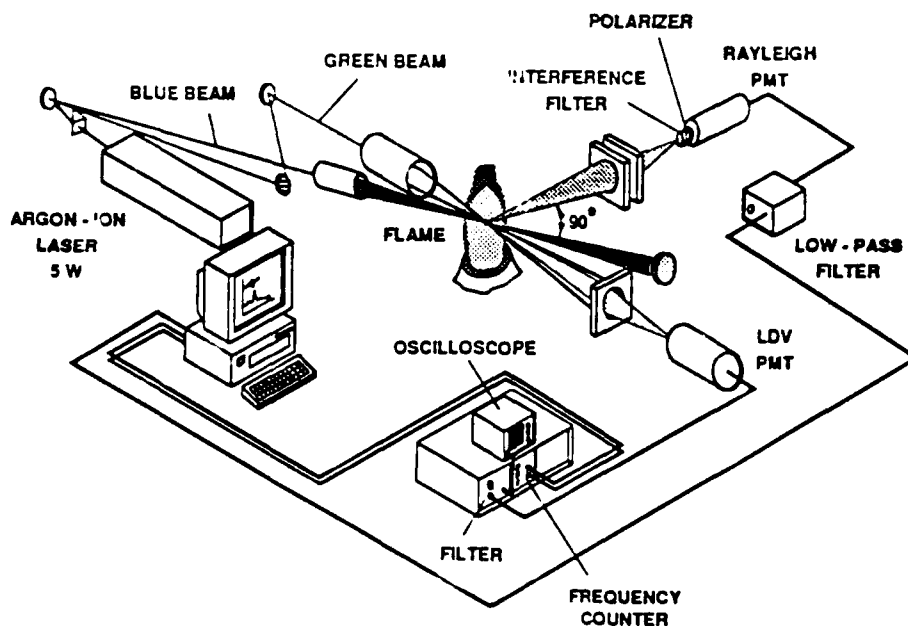


Figure 1. Experimental apparatus developed for the LDV-Rayleigh simultaneous measurements

Rayleigh scattering has been used in a number of turbulent premixed and non-premixed flames, although the Rayleigh scattered power depends on both the total number density

and the chemical composition. For example, for heavy hydrocarbon flames (e.g. propane) the variation of the Rayleigh cross section with the transition from the reactants to the products can be higher than 10%<sup>5</sup> and, as a consequence, compensation of the signal were performed based on the evolution of the Rayleigh cross-section as a function of temperature.

A major limitation of the technique derives from its sensitivity to the presence of small particles such as soot, but relatively low concentrations of larger seeding particles may be allowed if discrimination between the Mie and the Rayleigh signals is considered. This precludes temporarily simultaneous velocity-scalar measurements and requires the implementation of dedicated data reduction strategies in order to associate each velocity measurement with a Rayleigh signal which was obtained at a time interval  $\Delta t$  before or after the valid Doppler signal, with  $\Delta t$  small compared to the integral time scale of the flow. As a result, considerably low data rates, with values lower than 25Hz, have been reported in the literature<sup>4</sup>.

The work reported here was used for the combined LDV-Rayleigh measurements, Ferrão and Heitor<sup>6</sup>. The Rayleigh signal was continuously sampled and stored in a circular buffer, which was triggered by each valid Doppler signal and, then, analysed to select the last Rayleigh signal free of Mie contamination. In general, the time interval between the valid velocity and Rayleigh signals was between 33 and 99  $\mu\text{sec}$ , as depicted in Figure 2, although the maximum combined data rate obtained was around 130 Hz. This value represents a considerable improvement relative to other systems described in the literature and should be considered as the optimum compromise between the data rate of valid Doppler signals and the fraction of validated LDV-Rayleigh pairs of data, as clearly shown in Figure 3.

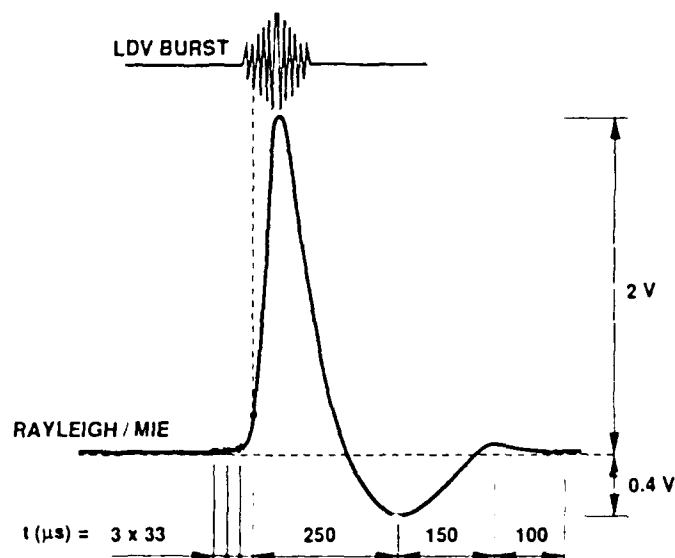


Figure 2. Schematic diagram of the simultaneous measurement of LDV and Rayleigh scattering, giving rise to the Mie contamination on the Rayleigh signal

The results are used to discuss the extent up to which the "thin flame" model of burning represents the aerothermochemistry of premixed flames with practical interest and quantify the processes of non-gradient diffusion in a strongly recirculating premixed flame.

The flames are open to the atmosphere and are only partially premixed, but offer the advantage of easy processes. The annular bulk velocities at the trailing edge of the disc were varied between 18m/s and 40m/s, resulting in Reynolds numbers based on the disc diameter up to  $1.43 \times 10^5$ ; for the experiments reported here the equivalence ratio was

varied between 0.55 and 0.80 to allow analysis of the structure of disc-stabilized flames for different combustion regimes.

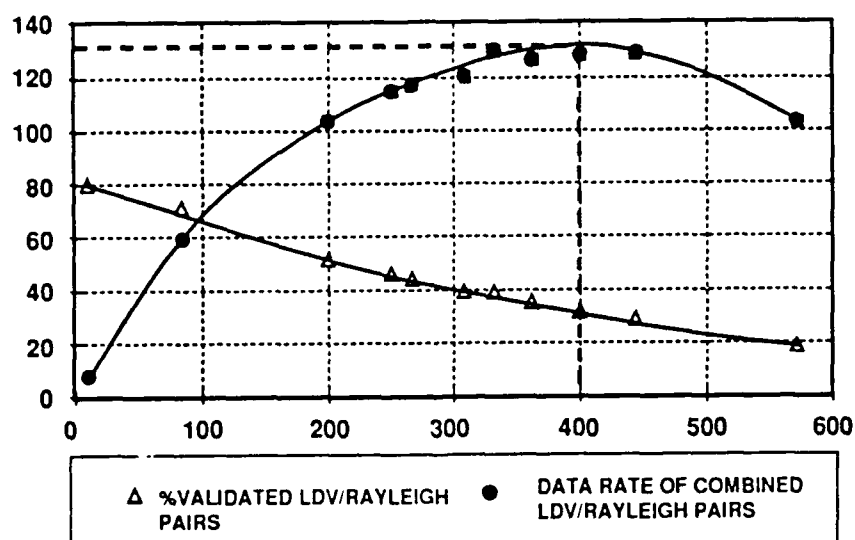


Figure 3. Data rate of combined LDV/Rayleigh simultaneous measurements

The results show that the isotherms are highly curved and reveal a non-planar flame oblique to the oncoming reactants with near-Gaussian temperature distributions across the reacting shear layer for the highest Reynolds numbers. For these conditions, the reaction region occurs outside the locus of the mean separation and is curved along its length. This curvature imposes mean velocity effects on the turbulence field and the result is a strongly sheared flame.

The results also quantify the magnitude of the velocity-temperature correlations and have allowed to estimate the axial and radial turbulent heat fluxes across the reacting shear layer, Figure 4. These quantities represent heat transfer rate (or, equivalently, the exchange rate of reactants), which is responsible for the phenomenon of flame stabilization around the recirculation zone and for flame propagation downstream of this zone. It should be noted that it is the spatial gradients of the heat flux components, and not the components themselves, that give rise to heat transport. The axial gradients of  $u''c''$  are substantially smaller than the radial gradients of  $v''c''$  and hence the turbulent transport of heat is principally in the radial and not in the axial direction. In general, the results show that the net turbulent scalar flux calculations using conventional gradient transport hypothesis would be inaccurate for any system of co-ordinates. If the present results are transformed into streamline co-ordinates, the net turbulent scalar transport occurs mainly along the streamlines as a consequence of the highly oblique flame.

The results of Figure 4 correspond to the highest Reynolds number considered under the scope of this work, and the results have shown that the magnitude of the scalar-velocity correlation decreases when  $Re$  is decreased: the scalar-viscosities are, however, kept constant. A notable remark is the alteration of the combustion regime when  $Re$  decreases up to  $0.7 \times 10^5$ . The reacting shear layer is then characterized by near bimodal temperature distributions, which have been fully characterized by the Rayleigh system. For these conditions, analysis has also shown that the mean axial velocity of the combustion products is smaller than that of the reactants, although the radial velocity of the products is slightly larger than that of the reactants. This is because the low-density hot products exist mainly in zones dominated by adverse pressure gradients and, consequently, are preferentially decelerated relative to high-density cold reactants, as

discussed by Heitor et al.<sup>7</sup>. However, the effect of the radial positive mean pressure gradient does not prevail in the momentum balance, since it has not preferentially deflected the light products towards the centre of the flame. The analysis suggests that gradients of mean pressure can affect the transport of turbulent heat flux in premixed flames and this implies the use of modeled transport equations, rather than the turbulent viscosity hypothesis, if the values of  $\overline{u_i c''}$  are to be calculated.

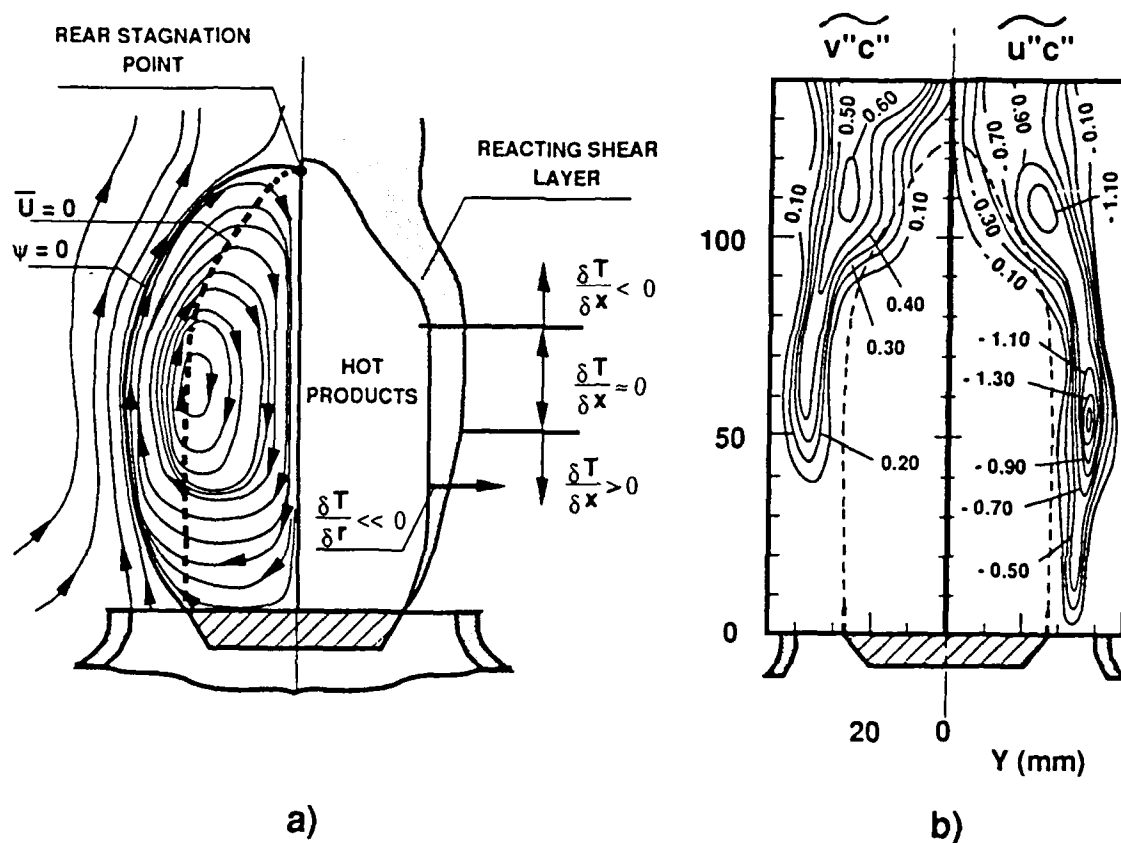


Figure 4. Bluff-body stabilized flame characteristics:  
a) Flow configuration and reacting shear layer characterization;  
b) Heat flux measurements

## REFERENCES

1. Eckbreth, A.C.: Laser Diagnostics for Combustion Temperature and Species, Abacus Press, 1988.
2. Durão, D.F.G., Heitor, M.V., Whitelaw, J.H. and Witze, P.O.: Combusting Flow Diagnostics, Kluwer Academic Publ., 1991.
3. Taylor, A.M.K.P.: Experimental Methods for Flows with Combustion, Academic Press, London 1991.
4. Ferrão, P. and Heitor, M.V.: Combusting Flow Diagnostics (Eds. D.F.G. Durão et al.) Kluwer Academic Publ. Nato/ASI series, p. 169, 1991.
5. Namer, I. and Schefer, R.W.: Exp. in Fluids, 3, p. 1 (1985).
6. Ferrão, P. and Heitor, M.V.: Proc. 6th Intl. Symp. on Appl. of Laser Tech. to Fluid Mechanics, Lisbon, 20-23 July 1992.
7. Heitor, M.V., Taylor, A.M.K.P. and Whitelaw, J.H.: J. Fluid Mechanics, 181, p. 387 (1987).

# UV RAMAN MEASUREMENTS OF TEMPERATURE AND CONCENTRATIONS WITH 308 nm IN TURBULENT DIFFUSION FLAMES

F. Lipp, E.P. Hassel, J. Janicka  
Technische Hochschule Darmstadt,  
Fachgebiet Energie- und Kraftwerkstechnik  
Petersenstr.30  
W-6100 Darmstadt, Germany  
Phone : Germany-6151-162157  
Fax : Germany-6151-166555

Most practical combustion devices are turbulent, nonpremixed flames. The development of appropriate computer models is very important. Empirical constants used in the models depend on comparison with experiments. Therefore simultaneous space and time resolved measurements have been made using spontaneous Raman scattering in turbulent  $H_2/N_2$  and  $CH_4/N_2$  diffusion flames.

This paper presents new experimental results of a  $H_2/N_2$  diffusion flame containing concentrations, temperatures, mixture fractions  $f$ ,  $f$ -plots and *rms* of fluctuations of  $f$  in comparison to numerical predicted results obtained with a Reynolds stress combustion model.

In [1,2] the experimental setup, the data reduction scheme based on linear Raman theory [3] and the signal interferences of soot and PAH are described. Figure 1 shows an isometric projection of the experimental setup. A narrowband  $XeCl$  excimer laser, a spectrometer with high resolution and an intensified multichannel array camera are used to give full information about all major species and spectral background simultaneously.

Fuel stream exit parameters are: mass fraction  $H_2 = 0.0168$ , nozzle diameter  $D = 6.0mm$ , Re-number = 14500. For stabilization the flame was piloted. At each flame location 100 spectra are taken. For comparison of the Raman results with predictions density weighted statistical moments are calculated from the single shot data applying Favre formalism.

The UV Raman results exist in comparison with predictions in the following form: spreading rate as normalized  $r_{0.5}/D = radius(\tilde{f}_c/2)/D$  and axial decay of centerline mixture fraction  $\tilde{f}_c$  versus  $x/D$ ,  $f$ -plots of temperatures and mass fractions  $X_i$  determined from the  $O$ ,  $H$  and  $N$  atom ratio versus  $f$  for the

entire flame and specific regions, mixture fraction as normalized  $\tilde{f}/\tilde{f}_c$ , *rms* of fluctuations of the mixture fraction  $(\tilde{f}''^2)^{1/2}/\tilde{f}_c$ , favre averaged temperature and mass-fractions  $\tilde{X}_i$  versus normalized radius  $\eta = r/r(\tilde{f}_c/2)$  and three dimensional surface plots of mixture fraction, *rms* of fluctuations of the mixture fraction, temperature and mass fractions for global flame structures.

Examples of the results are shown in Figure 2 to Figure 4. In Figure 2 the overall correspondence of  $\tilde{f}_c$  decay is good. The maximum temperature is 1100 K in both cases and at the same  $x/D$  level. Figure 3 shows the  $f$ -plot of mass fractions for the entire flame. The agreement is very good. The absolute scattering at poor and rich mixture fractions for  $N_2$  and  $O_2$  is less than  $\pm 1.5\%$ .

As a demonstration of the important informations obtained with this measurement technique a temperature surface plot of the entire flame is shown in Figure 4. In this plot all temperature informations are depicted in comprehensive form. For example at  $x/D = 0$  and  $\eta = 2.5$  the influence of the pilot flames is to be seen as a small temperature increase, which disappears at higher levels.

The informations obtained with this work are important for a deeper physical understanding of turbulence phenomena in turbulent diffusion flames and suitable for improving turbulence models.

**Acknowledgement:** This work was supported by Deutsche Forschungsgemeinschaft, contract number JA 544/1-1

## References:

- [1] E.P. Hassel, Applied Optics, (accepted October 1992)
- [2] F. Lipp, J. Hartick, E.P. Hassel, J. Janicka, Twenty-fourth Symposium (international) on Combustion, The Combustion Institute, 1992
- [3] D.A. Long, Raman Spectroscopy, McGraw Hill (1977)



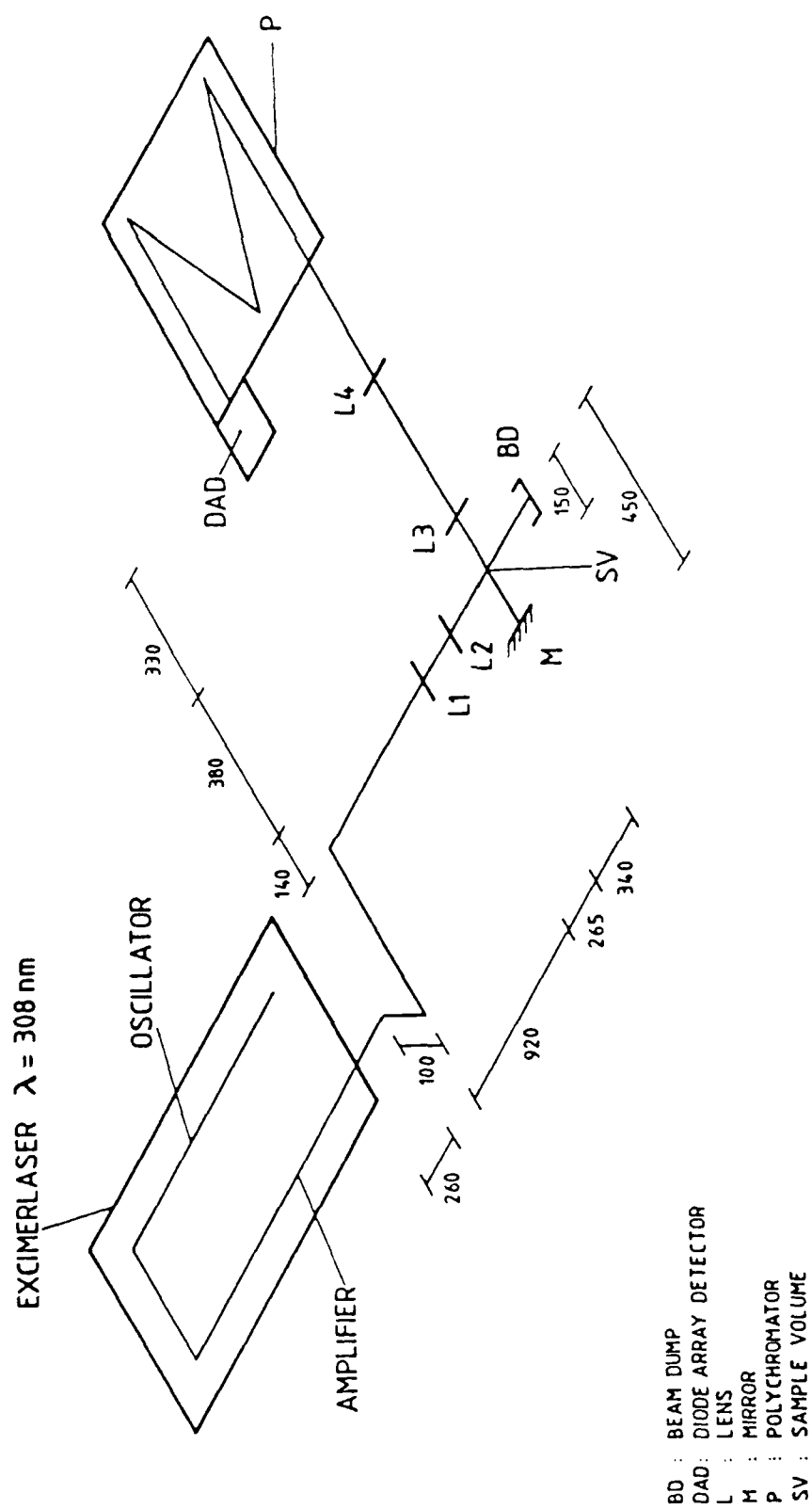


Figure 1: Raman optical setup in an isometric projection.

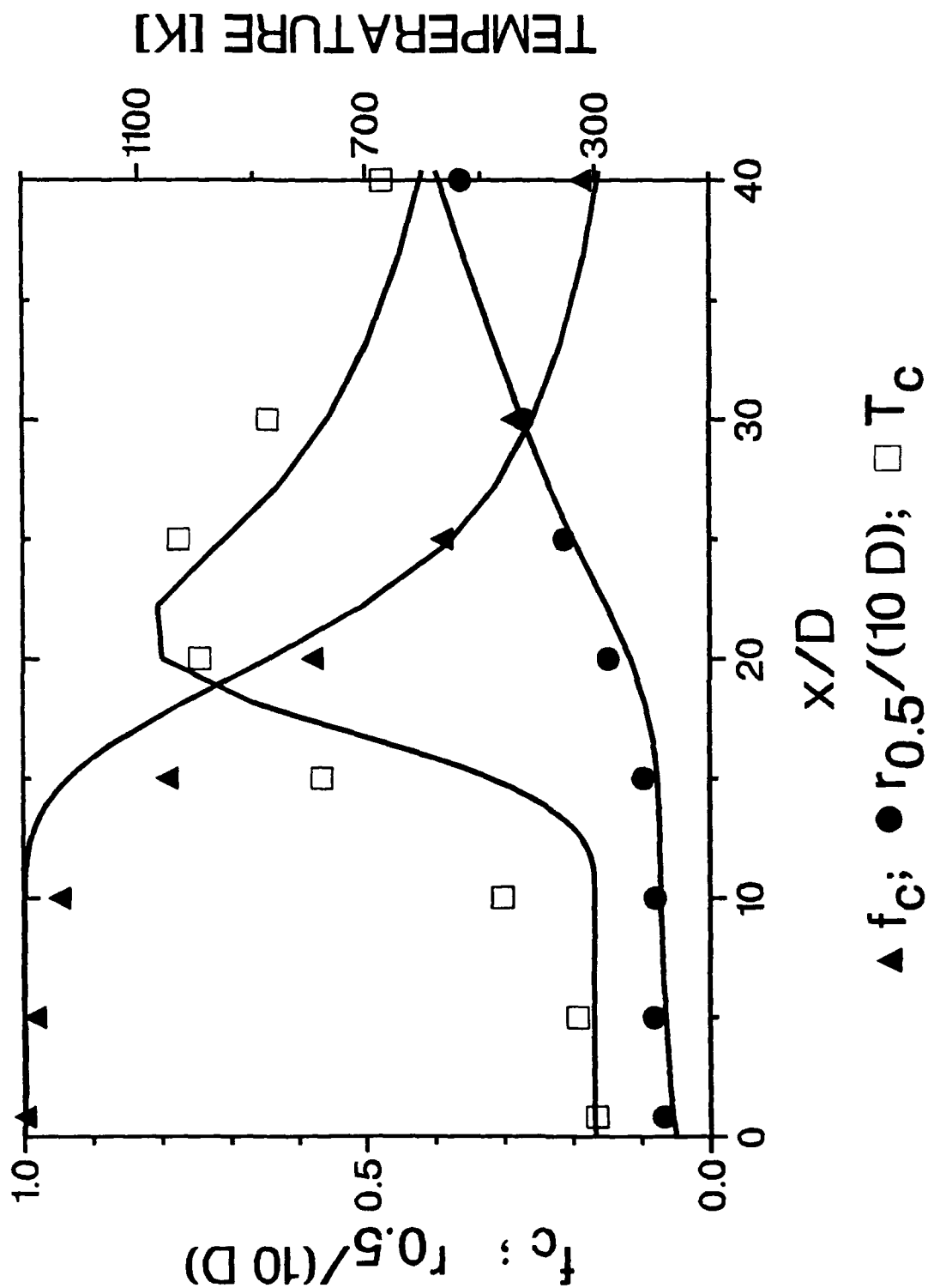


Figure 2: Comparison of experimental and theoretical axial decay of centerline mixture fraction  $\tilde{f}_c$ , jet spreading rate as  $r_{0.5}/(10D) = \text{radius}(\tilde{f}_c/2)/(10D)$ , centerline temperature  $T_c$  and fraction of evaluated spectra  $\epsilon$  versus normalized flame axis  $x/D$ .

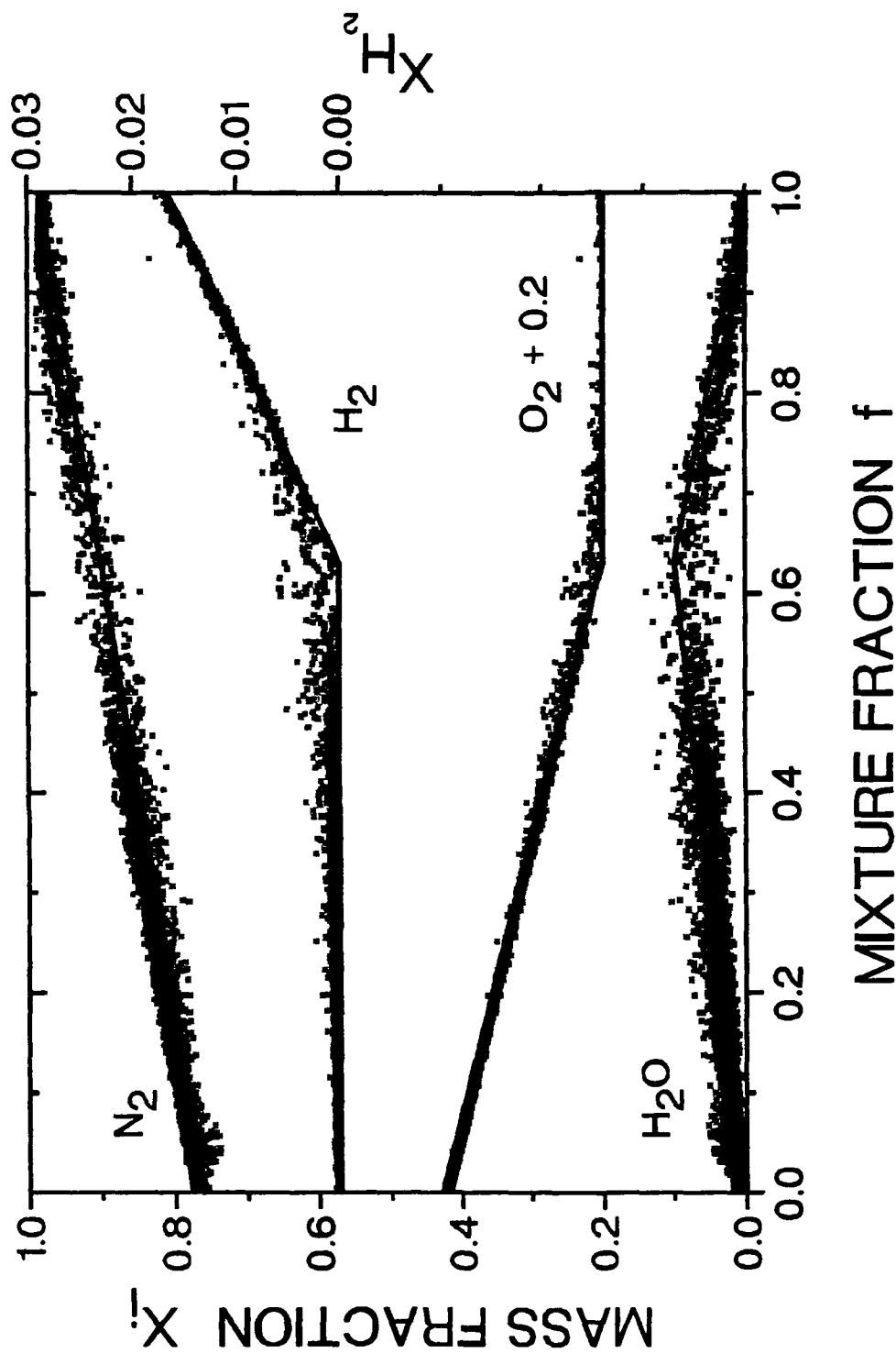


Figure 3:  $f$ -plots of concentrations in form of mass fractions  $X_i$  of the species versus mixture fraction  $f$  determined from the  $O$ ,  $H$  and  $N$  atom ratio. The concentrations of  $O_2$  are added to a constant to get all curves in one figure. A single shot Raman spectrum gives four concentrations and thus four dots but for clarity of the picture the values of only every tenth spectra out of all spectra from the entire flame ( $x/D = 0$  to 40) are plotted. Lines: prediction.

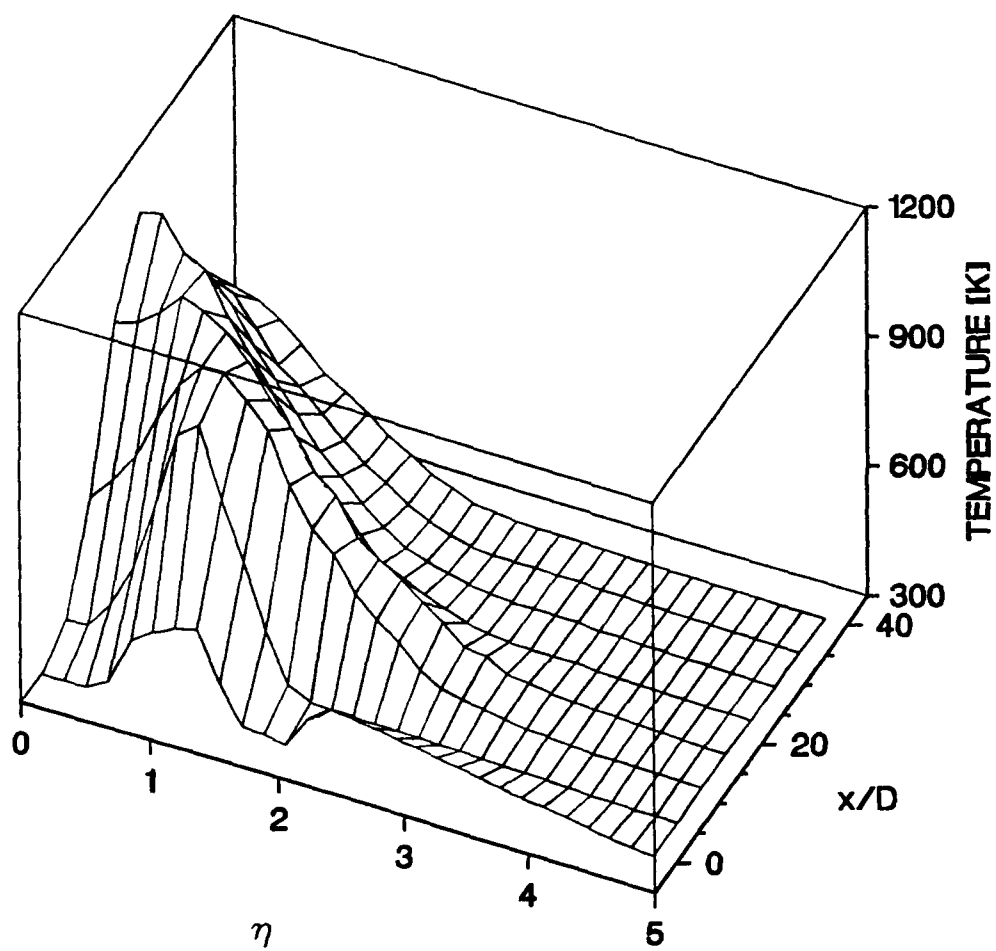


Figure 4: Favre averaged temperatures versus  $\eta$  and versus  $x/D$  in a three dimensional plot.

# DOPPLER VELOCITY MEASUREMENTS USING A PHASE STABILIZED MICHELSON SPECTROMETER.

G. Smeets

French-German Res. Inst. of Saint Louis  
F-68301 Saaaint-Louis Cedex, B.P. 34

## Abstract

A laser Doppler system is described that enables real time velocity recording with  $\mu\text{s}$  time resolution being specially well adapted to highly instationary gas flows including combustion phenomena.

The basic arrangement is illustrated in Fig. 1. Monochromatic laser light is transmitted by a light fiber and is concentrated in a small measuring volume within the flow field. A bundle of Doppler shifted light scattered by small tracer particles passing through this volume is collected and transmitted to the spectrometer using a second light fiber. The Doppler shift  $d\lambda$  depends on the velocity component  $u$  of the particles in the direction of the bisector between illumination and observation directions and the angle  $\beta$  between these directions:

$$d\lambda/\lambda = 2 \cdot u/c \cdot \cos[\beta/2].$$

The principle of the interference spectrometer used for detecting the extremely small relative wavelength changes is explained in Fig. 2. In a Michelson interferometer having a large optical path difference, small wavelength changes lead to detectable phase changes of the interference (fringe shifts). When a Pockels cell is arranged in series with the interferometer, the phase can be stabilized by means of a suitable feedback system. A distinct phase can be automatically sustained by applying at any instant the exact voltage to the Pockels cell to compensate for the wavelength change. As the feedback system reacts faster than within a  $\mu\text{s}$ , the Pockels cell voltage follows with high time resolution proportionally to the wavelength changes.

The basic idea of this velocimeter goes back to 1975. It has been applied for numerous experiments in gasdynamics and ballistics. The full paper will concentrate especially on its applications and applicability to combustion phenomena and the following experiments will be described in some detail.

In interior ballistics, the vector field of the flow velocity in the muzzle region could be determined for different times after projectile passage. Laser light was scattered by small soot particles being formed at high number density in the gun tube flow.

Velocity profiles as well as velocity fluctuation profiles could be recorded at ISL in a supersonic jet issuing from a kerosene burner. The upstream flow was seeded with polydisperse submicron  $\text{TiO}_2$  particles resulting in a sufficiently intense continuous scattered light stream to enable low noise velocity signals of 10 kHz bandwidth.

Similar experiments were recently made at ONERA on a hydrogen burner. Adding sufficient concentrations of 80 nm in diameter graphite particles, together with profiles of the mean velocities, different components of the turbulent fluctuations in the shear layer could be recorded up to about 100 kHz. As an example, measured mean velocities along the axis of the hot supersonic jet issuing from a nozzle having 26 mm exit diameter are shown in Fig. 3. The estimated flow parameters at the exit plane were:  $T = 1500 \text{ K}$ ,  $p = 1 \text{ bar}$ , and  $\text{Ma} = 2.4$ . The measured velocity decay was much faster than predicted by a simple code.

2 shock tube experiments have been begun at ISL to study combustng supersonic flows. In one experiment hydrogen injection and combustion in a configuration simulating a scramjet burner is studied. A suitable way was found to seed the the air in the driven tube with a high number density of submicron  $\text{TiO}_2$  particles. The other experiment concerns ignition of a combustible mixture at superdetonative speeds. Scattering particles can be formed during combustion. In both experiments, velocity recordings are expected to give both, insight into details of the combustion processes as well as quantitative data on its efficiency.

The technique can equally well be applied to many other combustion phenomena like in burners, piston motors and turbines also including such cases when flow velocities are of only a few m/s. By using optical path differences up to 7 m together with an auxiliary sytem for laser noise suppression, a dectibility limit of  $d\lambda/\lambda = 10^{-10}$  could be obtained enabling velocity resolution to a few cm/s.

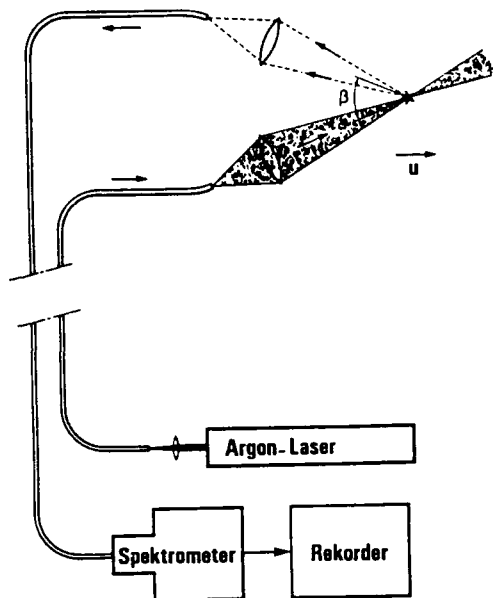


Fig. 1 Optical arrangement for flow velocity measurements

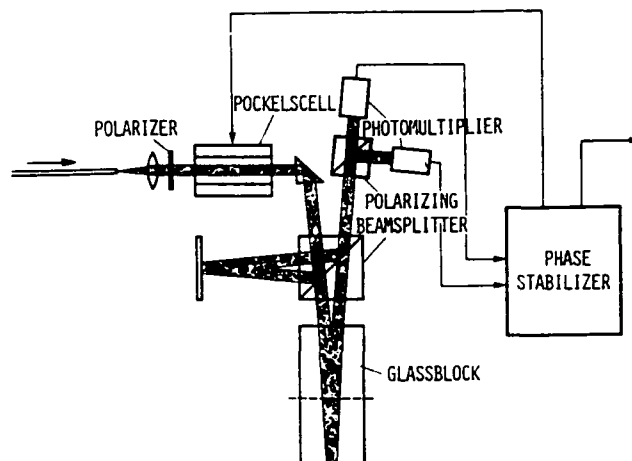


Fig. 2 Autostabilized Michelson spectrometer

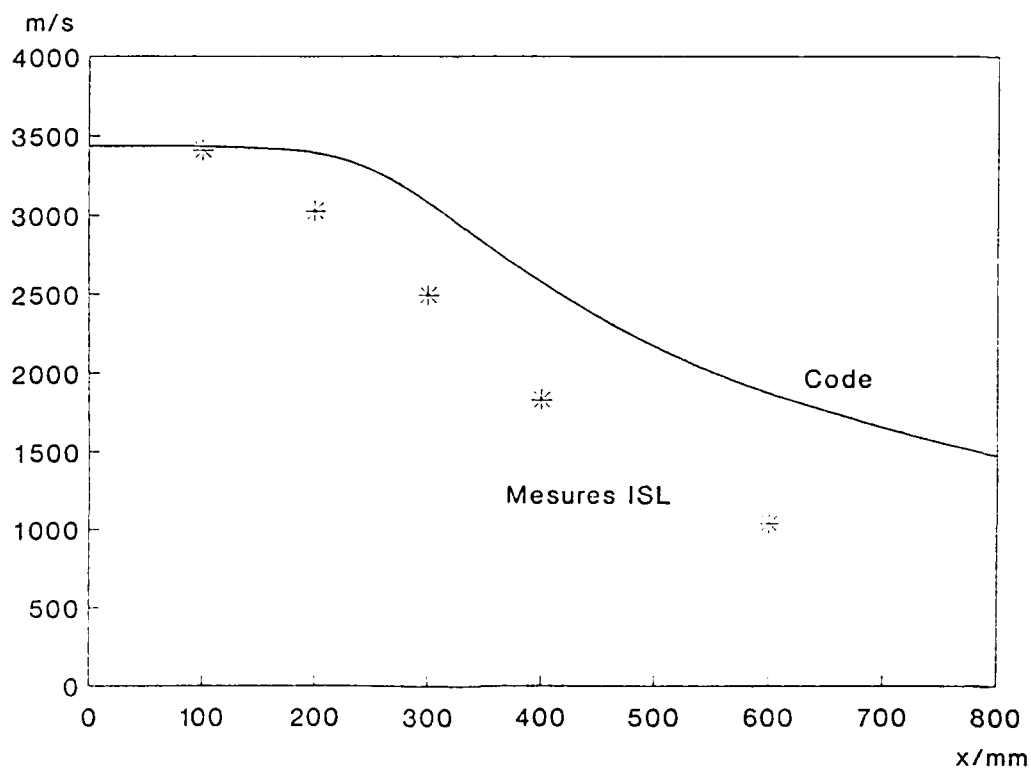


Fig. 3 Mean velocities at the axis of hydrogen combustor jet

## Development of laser diagnostic techniques for full-field velocity measurements

B. Ineichen and R. Müller

Swiss Federal Institute of Technology  
Internal Combustion Engines Laboratory  
CH-8092 Zurich  
Switzerland

The use and analysis of the signatures of light reflected by scattering of moving particles have been actively pursued for the determination of flow velocities, in particular to determine velocity magnitude and direction. Here we address the problem of image processing associated with data reduction, data filtering and data evaluation.

To cope with the increasing demand on full flow field velocity measurements, it is necessary to utilize measurement and evaluation techniques to determine simultaneously the direction and velocity magnitude for a considerable large flow field. This kind of particle image velocimetry is of considerable interest, especially in those cases where there is only limited transverse motion. In many situations of interest these conditions are met.

Going beyond current practice of recording the data on photographic film followed by manual data reduction and data evaluation, we address the case of imaging processing available from a video camera after A/D conversion.

A frame grabber board digitizes and stores the particle images. The frame grabber board allows to store up to sixteen images  $512 \times 512 \times 8$  bit (256 gray level). The board processes any particle images stored in real time, as well as processing images actively being digitized. Multiple particle images captured and stored in separate buffers can be processed.

The image data base, representing a two-dimensional intensity trace of a moving particle, contains also a number of disturbances and distortions. These influences have to be taken into account during image processing. The main issues are:

- Terms of a bright background, most a Gaussian intensity distribution caused by the illumination of the test regime
- Multiplicative noise, i.e. out of the laser speckles or additive noise resulting from the electronic recording and digitization of the optical signal
- Diminished image contrast caused by background illumination and noise
- Destructive interference patterns mainly from optical components in the experimental setup

In general, the main digital image processing steps required to reduce those disturbing influences, are:

- *Image enhancement*: Arithmetic corrections to the intensity of the entire image and filter operations which serve to smooth the data



- *Image restoration*: Specific components of the data set have to be treated, i.e. to sharpen the contours or optimize interpolation values growing out of zoom operations
- *Data segmentation*: The initial amount of data gets reduced and the gray level distribution has to be set in order to get a high gradient
- *Image data analysis*: The final objective is the determination of particle trace lengths out of the preprocessed image including the interesting length data and their first derivative. The resulting flow field can be represented in a 2-D velocity vector plot

Assuming that preprocessing steps and the foregoing identifications of each particle trace are made, the search and determination of the projected particle displacement which is equivalent to the particle trace is performed. This processing step allows determination of the total displacement distance over the whole particle trace. The acquired data ratio of the particle trace lengths, in the combination with the exposure time, determines a two-dimensional velocity vector field plot.

The described technique and the application of a jet velocity field on a two-dimensional slit burner will be presented.

## TEMPERATURE MEASUREMENT IN FLAT LAMINAR PREMIXED GAS/AIR FLAMES BY LASER DOPPLER VELOCIMETRY

A. van Maaren   L.P.H. de Goey   R. van de Velde

Eindhoven University of Technology  
Faculty of Mechanical Engineering (WH-3.116)  
P.O.Box 513, 5600 MB Eindhoven, the Netherlands

A new method is presented which can be used to measure temperature in premixed laminar gas/air flames, stabilized on a flat flame burner. In perfect one-dimensional flames, a linear relationship exists between the density of the gas and the velocity. Consequently, the temperature profile could be determined from measurement of the velocity profile, when the ideal gas law is used to relate the density with the gas temperature. In a practical flat flame however, besides the velocity component in axial direction ( $x$ ), also the velocity component in radial direction ( $r$ ) is of importance. This is caused by expansion and buoyancy of the hot combustion gases in the cold environment. Therefore, both the axial and the radial velocity profiles must be measured and taken into account in the method, to be able to determine the temperature profile.

In this paper we apply the method to a mixture of methane with air with equivalence ratio  $\phi = 0.8$ . Then to a good approximation the number of moles of the mixture will not change due to the chemical reaction, so that the ideal gas law can be used with constant average molar mass. The application of the method to other gas mixtures will be investigated in the near future.

The velocity field is measured using a one-component Laser Doppler Velocimetry system, consisting of a 35 mW He-Ne laser, a Counter with Frequency Shifter and photomultiplier, and  $1\text{ }\mu\text{m}$   $\text{Al}_2\text{O}_3$  particles as seeding. The seeding is supplied to the unburnt gas flow by means of a fluidized bed. Micrometer translation stages are used to translate the burner with respect to the measuring volume, which is 0.1 mm wide. This yields a good spatial resolution, which is necessary due to the steep velocity gradients in the flow. A new flat flame burner is used, designed to make LDV-measurements in the flame possible (see figure 1). The overall error in the temperature due to errors in the measured velocity is about 1 to 3%, depending on the LDV signal quality.

In figures 2 to 5 some results are presented. The unburnt gas speed is 9.1 cm/s, at an initial temperature of 298 K.

The performance of the flat flame burner is demonstrated in figure 2, showing that the unburnt gas velocity is constant within 3%. In figure 3 the effect of buoyancy is clearly shown. It appears that in this case the velocity increases about 25% over a distance of 6 mm.

The measured profile of the radial velocity component (see figure 4) is used to determine the area where environmental effects like heat loss and air entrainment

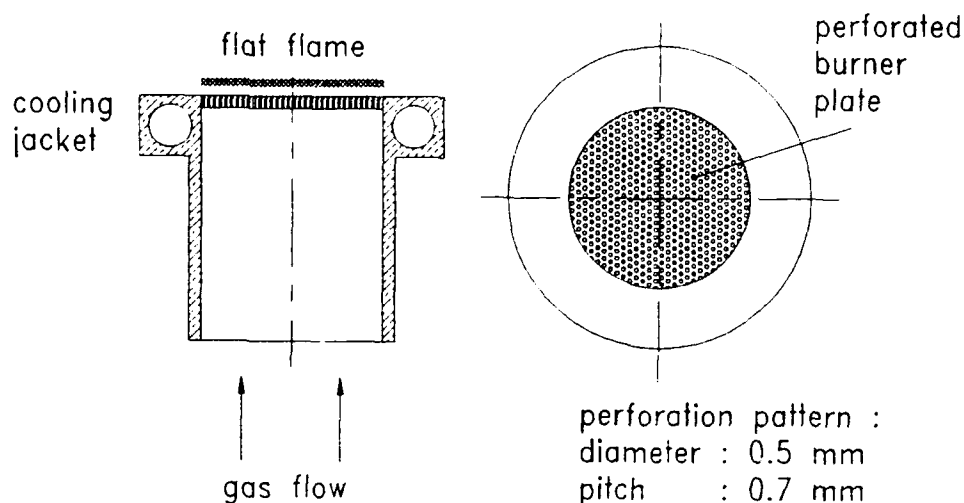


Figure 1: flat flame burner

are negligible. When the density and the axial velocity are independent of radius (i.e. the velocity and the temperature distribution are flat) from conservation of mass it can be derived that the radial velocity component must be linearly dependent on  $r$ , throughout the entire flow. From figure 4 it can be seen that this area is about 20 mm wide.

The results of the temperature calculations presented in figure 5 are compared with one-dimensional flame calculations using the detailed chemistry software package provided by *Kee et al* (1985)<sup>1</sup>, and close agreement is found. The temperature decrease at large axial distance from the burner is caused by air entrainment and conductive heat loss to the environment.

The method is, although restricted to flat flames, particularly useful in studies concerning the velocity and temperature field of laminar premixed flames, since it is non-intrusive and accurate. Since the results are obtained using a one-component LDV system, improvement of the measurement procedure is possible by using a two-component LDV system or a two-dimensional velocity imaging technique, allowing to measure both velocity components simultaneously, and thereby reducing the total measurement time.

This work is supported by Gastec (Apeldoorn) and Novem (Utrecht), the Netherlands.

<sup>1</sup>Kee, R.J. *et al* (1985). Sandia Report SAND85-8240 · UC-401. A Fortran program for modeling steady laminar one-dimensional premixed flames. Sandia National Laboratories, Livermore, California 94551, U.S.A.

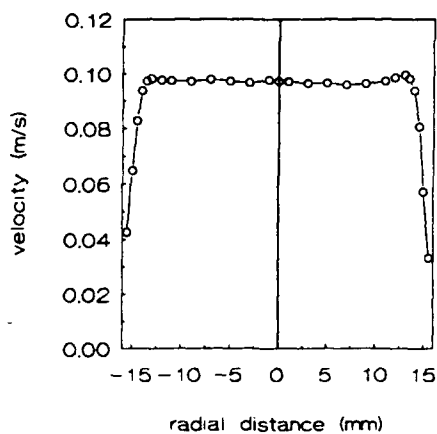


Figure 2: axial unburnt gas velocity as function of  $r$ ;  $x = 3$  mm

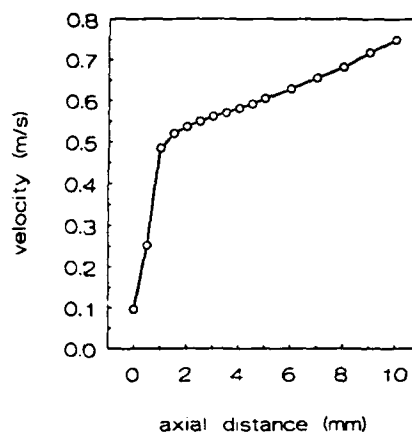


Figure 3: axial burnt gas velocity as function of  $x$ ;  $r = 0$  mm

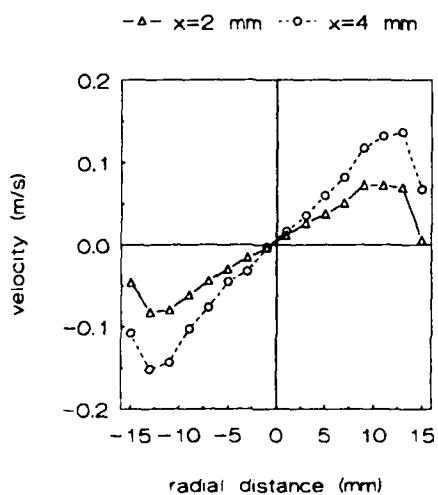


Figure 4: radial burnt gas velocity as function of  $r$ ;  $x = 2$  and  $4$  mm

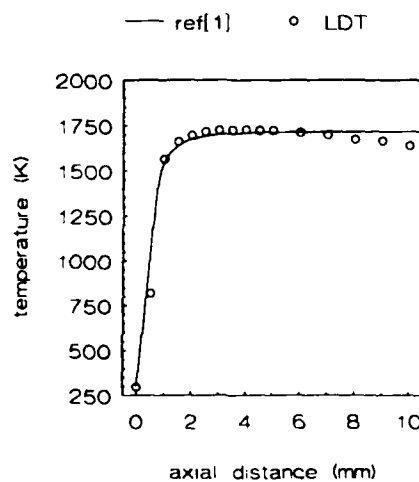


Figure 5: gas temperature as function of  $x$ ;  $r = 0$  mm

## INTERFEROMETRY TECHNIQUES IN COMBUSTION RESEARCH

Victor S. Abrukov, Stanislav V. Ilyin, Vladimir M. Maltzev

All-Union Polytechnical Institute  
and Institute of Structural Macrokinetics  
of the USSR Academy of Sciences

The most essential advantages of interferometry are a wide spatial and temporal range of measurements and a wide variety of characteristics to be determined.

The present report deals with the methodological guidelines developed by the authors. They show the potentialities of interferometry techniques in determining the basic thermodynamic and gas dynamic characteristics of combustion processes. Based on these characteristics, many other properties of the combustion wave, in a wide variety of tasks, can be studied.

1) Calculation of density,  $\rho$ , and temperature,  $T$ , fields as a function of refractive index,  $n$ , fields. The use of the equations derived by the authors is justified by the rule stating that the magnitude of the variation of the Gladstone-Dale constant,  $k$ , and of the molecular refraction,  $M$ , in a chemical reaction is small (within 10 per cent in most cases). This magnitude has been derived from calculations made for a fairly large number of reactants (of the order of 100). For specific cases, a formula to calculate  $T$  that takes the character of the  $M$  variation into account is recommended.

2) Calculation of the basic thermodynamic integral characteristics of the gaseous phase in the burning wave using directly a function of the interferogram phase difference distribution  $S(x, y)$ :

$$m = [(n_0 - 1)V - \lambda \iint S(x, y) dx dy] / k; \quad H = mc_p(T - T_0); \quad H_m = H/m; \quad H_v = H/V;$$

where  $m$  is mass,  $H$  is enthalpy (isobaric thermal effect),  $H_m$  is

average specific enthalpy,  $H_v$  is average enthalpy divided by volume  $V$ ,  $n_0$  is refractive index of an undisturbed medium,  $\lambda$  is the interferometer light source wave length,  $k$  is the average Gladstone-Dale constant,  $c_p = a + bT$  is average specific heat capacity,  $a$  and  $b$  are constants,  $T = T_0 \rho_0 V / m$  is average temperature,  $T_0$  and  $\rho_0$  are temperature and density, respectively, of the object medium (generally taken at NTR) which are related to each other.

3) Calculation of the time-variable integral characteristics  $m(t)$  and  $H(t)$ , calculation of the non-stationary burning mass rate  $\dot{m}(t)$  and heat release power  $\dot{H}(t)$  at ignition, their use being based on the heat balance equation as well as on a certain assumption (e.g., a pseudo-one-dimensional approximation of a stream in the burning wave) for the purpose of determining:

- the resulting thermal effect of chemical reactions

$$Q = \dot{H}(t) / \dot{m}(t);$$

- the power of the non-stationary convective heat flow in the burning wave

$$q(y_i, t) = \dot{m}(t) H(y_i, t),$$

$y_i$  is the coordinate;

- the profile of  $q$  in the stationary burning wave

$$q(y) = \dot{m} H_m(y);$$

- the profile of the average (with respect to the stream section) heat release rate in a stationary burning wave

$$\Phi(y) = [dH_v(y)/dy] v(y),$$

where  $v(y) = m / \rho(y) s_1(y)$  and  $\rho(y)$  is average density,  $s_1(y)$  is the flow section area;

- the profile of the conductive heat flow (using the heat balance equation and the values of  $q(y)$  and  $\Phi(y)$  as determined above).

4) Calculation of the gasification work  $F_0(t) = p_0 V(t)$ , the condensed system force (force of powder)  $F = \max[F_0(t) / m(t)]$  and the specific volume at ignition of the condensed system.

5) In addition to the above characteristics, in a number of cases, the following parameters can be determined:

- response of  $\dot{m}(t)$  and  $\dot{H}(t)$  to changes in the ambient condi-

tions,

- thickness of the various burning wave zones of condensed systems.

The most representative application conditions for the methods developed are:

- ambient pressure: (0.01 ...1) MPa,
- spatial measurement range: ( $10^{-4}$  ... $10^{-1}$ ) m,
- temporal measurement range: ( $10^{-8}$  ... $10^2$ ) sec.

The most adequate application conditions are:

- non-stationary objects,
- objects in an open volume,
- investigation into the combustion gaseous phase,
- availability of a computerized system of interference pattern processing.

All the methodologies are illustrated.

An approach to determining the total mechanical impulse,  $P$ , of a non-stationary gaseous stream section using interference cine films has been developed as well. According to this,  $P \sim ds/dt$  during the ignition of condensed and gaseous systems. This approach allows the reconstruction of velocity and pressure fields of a non-stationary gaseous stream to be implemented based on the reconstructive tomographic concept. To determine them an integral equation (1D Radon transform) must be solved (Radon inversion).

The authors wish to thank Prof. Sergei A. Abrukov for helpful discussion, and Mr. Alexander Ponomaryov for assistance.

**SESSION R-10: X-Ray Diagnostic and Image  
Analysis of Combustion of Liquids and Solids**

**Co-Chairs: Mr. J. P. Reynaud and  
Dr. Th. H. Van der Meer**



## **THE APPLICATION OF COLOR IMAGE ANALYSIS IN STUDIES OF DENSE MONOPROPELLANT SPRAY COMBUSTION**

**Avi Birk and Michael J. McQuaid  
US Army Research Laboratory  
Weapons Technology Directorate  
Aberdeen Proving Ground, MD 21005-5066 USA**

### **ABSTRACT**

Propulsion systems based on a regenerative injection principle are currently being developed to facilitate the use of hydroxylammonium nitrate (HAN) based liquid monopropellants in large caliber gun applications. The regenerative injection cycle produces a propellant spray which combusts at very high pressures. We have conducted experiments which visualize the dynamics and structures of combusting HAN-based liquid propellant (LGPs) sprays at low gun pressures. The experiments involved the injection of LGP1845 or LGP1898 at 150 m/s through a circular orifice into 33 MPa, 500°C nitrogen. The visually clear nitrogen was obtained by the use of a unique particle bed heater which provided test times of up to 3 sec. Images of the sprays generated in these experiments were obtained using high speed cinematography. Good visualization was achieved by illuminating the spray with a pulsed copper vapor laser sheet and seeding the propellants with lithium or sodium nitrate to enhance flame emission.

This paper concentrates on the use of color image analysis and processing as a tool for extracting information on particle dynamics in a dense combusting spray. It was observed spectroscopically that (visible) radiation associated with combustion was essentially restricted to sodium and lithium transitions at 589 nm and 671 nm, respectively. Coupled with the color sensitivity data for the high speed film, the spectroscopic data and laser specifications provided a basis for identifying and separating spray processes and structures in an image based on color. The correlations facilitated noise reduction and image enhancement through image processing. In particular, the technique enables the visualization of the liquid spray patterns underlying the flame. Application of sequential intensity histograms of laser light scattering from the liquid provided information regarding temporal particle size fluctuations. The results demonstrate that image analysis and processing have the potential to be a powerful tools in studying spray combustion phenomena.

**REAL-TIME X-RAY RADIOGRAPHY  
STUDY OF LIQUID JET BREAKUP  
FROM ROCKET ENGINE COAXIAL INJECTORS**  
Roger Woodward, Robert Burch, Kenneth Kuo, and Fan-Bill Cheung  
Propulsion Engineering Research Center  
and  
Department of Mechanical Engineering  
The Pennsylvania State University  
University Park, PA 16802

**ABSTRACT**

The investigation of liquid jet breakup and spray development is critical to the understanding of combustion phenomena in liquid-propellant rocket engines. Much work has been done to characterize low-speed liquid jet breakup and dilute sprays, but atomizing jets and dense sprays have yielded few quantitative measurements due to their high liquid load fractions and hence their optical opacity. Real-time X-ray radiography, capable of imaging through the dense two-phase region surrounding the liquid core, is used to make measurements of intact-liquid-core length and void-fraction distribution. The specific application considered is that of shear-coaxial-type rocket engine injectors.

In this study, propellant simulants are injected downward into a pressurized chamber through a single coaxial element. Two injector sizes are used, having liquid exit diameters and annular-gas-flow exit areas of 1) 4.8 mm (3/16 in) and 45 mm<sup>2</sup> (0.069 in<sup>2</sup>) and 2) 2.4 mm (3/32 in) and 11 mm<sup>2</sup> (0.017 in<sup>2</sup>). The larger injector is similar in dimensions to a SSME injector element. Solutions of potassium iodide (KI) in water are used as an X-ray absorbing LOX simulant, and gaseous nitrogen is typically used as the annular-flowing gas.

A 160 kV constant potential industrial X-ray system generates a continuous stream of X-rays, which passes through the test chamber window to penetrate the liquid jet. X-rays are attenuated by the iodine in the injected KI solution. The attenuated X-ray stream passes through a second window to reach the X-ray image intensifier in which the X-ray signal is converted to visible light. An intensified/gated CCD camera is used to record the output in RS-170 video format on S-VHS video tape.

A Macintosh-based image processing system is used to reduce and quantify the video data. A typical radiographic injection image is shown in Fig. 1. A background is divided from each injection image to compensate for the spatial nonuniformity inherent in the imaging system. Assuming that the X-ray attenuation by the KI solution follows Beer's law, the natural log of the divided image is taken to linearize the measured intensity as a function of absorber thickness. A series of calibration cells containing known thicknesses of the same solution as injected are present in each jet image to give a real-time calibration for obtaining the integrated liquid thickness at each point in the jet. A processed jet image is depicted in Fig. 2. The core length is measured directly from the processed images.

Axisymmetric (r-z) void-fraction-distribution measurements are obtained from time-averaged injection

images for which the statistically steady assumption holds. The aforementioned image processing provides a jet image in which the indicated pixel radiance level is linear with the integrated liquid thickness. The void-fraction distribution is deconvolved from the line-of-sight image data based on an axisymmetric jet.

Figure 3 is a plot of dimensionless intact-core length ( $L_b/D$ ) versus dimensionless chamber pressure with curve #1 corresponding to a set of coaxial injection tests from the small injector with approximately constant annular gas exit velocity ( $V_g \sim 260$  m/s) and the same mean liquid exit velocity ( $V_l \sim 30$  m/s). Curve #2 is obtained from a set of single jet (no annular gas flow) tests also from the small injector with the same liquid exit velocity as in curve #1. The large difference in the trend of these two curves is a result of the internal flow conditions within the liquid injector post. Since the annular gas velocity is constant along curve #1, while the gas density increases with chamber pressure, the momentum ratio of gas to liquid is increasing with pressure. Hence, one obtains the expected result that the core length decreases with increasing inertial force applied by the gas flow to the surface of the liquid jet.

In contrast, curve #2 indicates a steady rise in intact-liquid-core length with increasing chamber pressure. Also note that the measured intact-core length for the single jet at one atmosphere is nearly the same as that for the high-relative-velocity coaxial jet. It is believed that this is due to strong cavitation caused by flow separation at the injector inlet. The increase in breakup length with increased chamber pressure along curve #2 would then be caused by suppression of the injector inlet separation, and hence a weakening of the breakup mechanism responsible for the low  $L_b/D$  at 1 atm. In comparing curves #1 and #2, one sees how effective the high-velocity annular-gas flow can be in disintegrating the liquid jet. Note that even though the cavitation/turbulence breakup mechanism (which should be equivalent in both curves at the same pressure) is reduced with increased chamber pressure, the measured intact-core length for the coaxial jet continues to be significantly reduced.

X-ray radiography has been shown to be an effective technique for visualizing the dense, two-phase near-injector region of atomizing liquid jets to provide quantitative information on intact-liquid-core length and void-fraction distribution. Present findings clearly demonstrate the relative importance of two competing liquid-jet-breakup mechanisms, i.e. cavitation/turbulence breakup and aerodynamic shear.

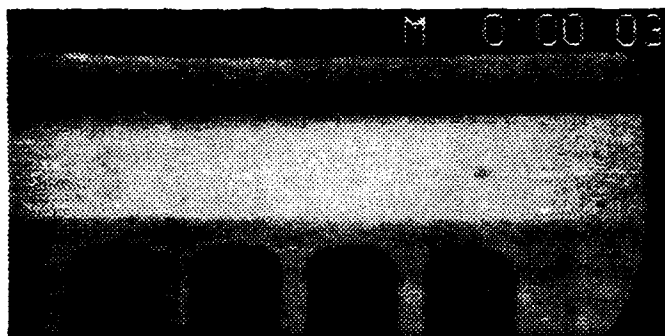


Figure 1. Typical radiographic image of a coaxial jet.  
Flow is pictured right to left.

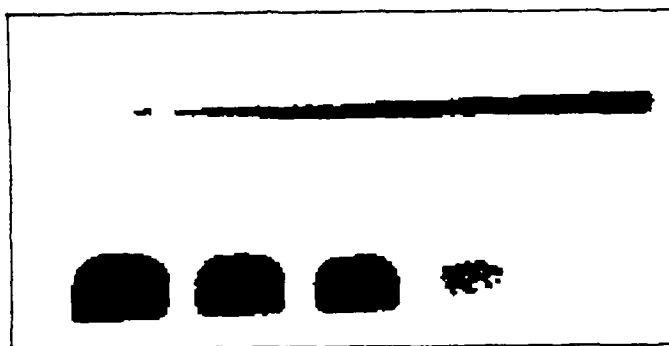


Figure 2. Processed binary image of a coaxial jet  
(same as in Fig. 1) for directly measuring  
intact-liquid-core length

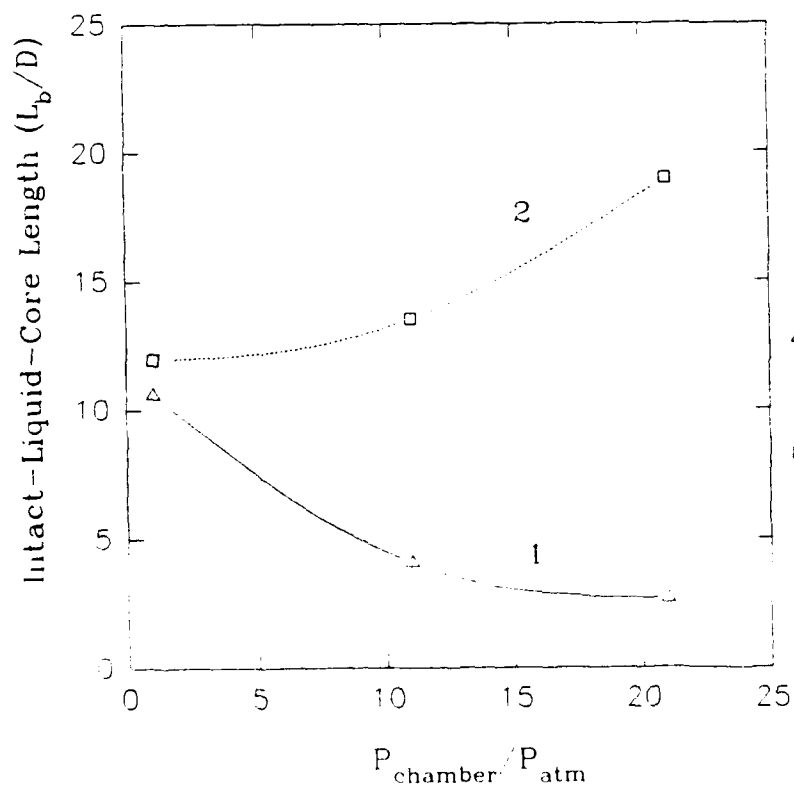


Figure 3. Effect of chamber pressure on intact-liquid-  
core length.

- $\Delta$  Coaxial Jet, Small Injector  
( $V_{l,\text{exit}}$ ) = 30 m/s  
( $V_{g,\text{exit}}$ ) = 260 m/s
- $\square$  Single Jet, Small Injector  
( $V_{l,\text{exit}}$ ) = 30 m/s

## **X-RAY DIAGNOSTICS METHODS FOR CLOSED LIQUID METAL COMBUSTION: REAL-TIME RADIOGRAPHIC EXPERIMENTS AND SIMULATIONS**

**L. A. Parnell, R. S. Nelson, K. A. Kodimer and T. R. Ogden**  
Naval Command, Control and Ocean Surveillance Center  
Research, Development, Test and Evaluation Division  
San Diego, CA, USA 92152-5000

### **Abstract**

Results are presented of real-time x-ray radiographic studies of the closed combustion of a jet of a gaseous halogenated oxidizer ( $\text{SF}_6$ ) in a liquid alkaline metal (Li) fuel bath. This type of confined combustion is a feature in the U.S. Navy's development of energy sources for propulsion of undersea vehicles. Diagnostics systems and techniques adapted from state of the art methods and equipment used for radiological imaging in medicine are employed in a combustion laboratory. These experimental methods permit detailed study of flames and of the jet-driven recirculating flow characteristic of closed liquid metal combustion (CLMC). Medical radiological techniques and equipment are found to be optimal for studying characteristics of the dynamic internal processes in CLMC, and thus superior to industrial methods and systems in this case. Ray tracing and Monte Carlo techniques (based on the the widely-used radiation transport code, MCNP) are used in the simulations. Both simulations include a complex focal spot, monochromatic or polychromatic emission spectra, a 2-dimensional detector array with characteristics of an x-ray phosphor screen and energy-dependent material attenuation coefficients. The results of the two simulations of the imaging system are compared with each other and with selected video frames from radiographic records of operating closed liquid metal combustors. Simulations of imaging of flow-tracing particles in the combustion bath are performed to assess the potential to derive three dimensional localizations from two dimensional projections. Representative results are presented and the methods of producing both the radiographs and simulations are discussed.

ANALYSIS OF SOLID PROPELLANT BEHAVIOR DURING FIRING TEST USING  
X-RAY RADIOSCOPY

**P. LAMARQUE - Y. DENIGES - S N P E**  
DEFENSE ESPACE - 33160 ST MEDARD - FRANCE

**M. GIMBRE - CELERG - DTD/EM**  
33160 ST MEDARD - FRANCE

This paper describes the use of real-time X-ray radioscropy for studing solid propellant rocket motor behaviour during test firing.

The main purpose is to visualize various combustion phenomena, *including*

- . Motor ignition phase
- . Burning front propagation and possible disturbance
- . Motor possible failure

The highly transitory nature of these events, in some cases it lasts only a few milliseconds, requires the use of high speed data acquisition systems.

The connection of a high-speed video camera (up to 1000 pictures/second) with an X-Ray intensifier allows high-speed data acquisition during test firing. Pictures restitution and analysis can be done at a low speed.

The set up must satisfy X-Ray and pyrotechnic safety rules and equipment must be protected from damage due to vibration, heat or fragment impact.

Main items of the device are :

- . 420 kv X-Ray tube
- . X-Ray image intensifier : 300 mm diameter
- . high-speed video camera with image intensifier
- . image processing

Items are held by a travelling device which allows end burning front survey and emergency return in case of firing incident.

Results obtained in term of spatial resolution are depending of signal-to-noise ratio witch result of video camera rate. A defect of few millimeters could be seen at 500 Frames/secondes in a 200 mm large sample.

The device has been used for burning visualisation of end burning grain, wires embedded grain, star grain, finocyl grain.

Survey of ignition phase is particularly interesting in order to reveal grain deformation or propellant profile during pressure rise. Failure coming at the end of burning has been shown by propellant ignition damage in wires embedded grain. Crushing of small voids during ignition creates micro-cracks, and the motor burst when the burning front arrives in void area.

A disturbance in burning front propagation in finocyl grain could be viewed and explained by profile deformation during ignition phase.

In small gas generator, burning pellets and motion filters could be seen.

The device is used as a substitute for firing test with extinction, and it has been helpful in developing an understanding combustion phenomena. The technic provides an efficiency tool for rocket development programs, it saves time and money.

However, some improvements are asked by users : 1000 pictures/second are not enough for transitory phenomena like failure. Limitation comes from video camera speed and available light on X-Ray intensifier, new improvements have to encrease signal-to-noise ratio.

LASER MIE SCATTERING FOR THE CHARACTERIZATION  
OF DIESEL INJECTION PROCESSES

Dipl -Ing. K. U. Münch and Prof. Dr.-Ing. A. Leipertz

Lehrstuhl für Technische Thermodynamik  
Universität Erlangen-Nürnberg  
Am Weichselgarten 9, D-8520 Erlangen, Germany

So far combustion in Diesel engines is not fully understood. Its performance strongly depends on the quality of the injection and mixing process. Therefore much investigation has been performed relative to the jet tip penetration, the spray cone angle and the fluid dynamic conditions inside the Diesel engine. Most equations which numerically describe these effects were empirically derived from injection chamber experiments under simplified conditions. These equations are not very useful for the understanding of the real Diesel engine process. Therefore new measurement techniques are required for real engine experiments taking into account appropriately the complex transient real engine conditions.

Irradiating a two-dimensional laser light sheet into the piston bowl of a four-cylinder VOLKSWAGEN 1.9 l Diesel engine with optical access, Mie scattering could be detected which was generated by the Diesel droplets inside the light sheet and outside the sheet as well. A new evaluation procedure was developed which allows additional information on the spray penetration in direction of the piston axis. Quantitative results have been obtained on the jet tip penetration and the spray cone angles of the jets. From liquid fuel distributions inside a laser sheet an appearance frequency distribution (ADF) has been calculated, which gives a quantitative statistical information on the liquid fuel distribution inside the light sheet plane with high local and temporal resolution. By means of the AFD the jet penetration in direction of the jet axes can be reconstructed in good approximation. The information provided by the AFD is also very suitable for the validation of results obtained by computer codes.

Figure 1 displays a typical measurement signal detected by the intensified CCD camera. The two-dimensional camera images contain the information of two different scattering processes resulting in two different signals on the 2d pictures. One is caused by a three-dimensional integral scattering signal from



droplets of the whole jets inside the piston bowl (bright regions in Figure 1) and the other is the scattering signal generated by droplets staying inside the light sheet plane during the shutter time of camera (dark regions inside the jets).

The integral scattering signal is generated by droplets outside the light sheet plane. The droplets inside the whole piston bowl are illuminated by the stray light caused by reflections at the windows and engine components. Droplets far away from the light sheet plane are also detectable. Thus, this signal displays the integral contour of all five different jets in the observation direction. When the jets have passed the light sheet the whole piston bowl was additionally illuminated by multiple scattering enhancing the integral jet signals.

The part of the scattering signal which is generated by droplets inside the light sheet plane is much more intense than the signals from droplets outside the plane. Therefore a steep gradient in the signal intensity can be found at those local positions in the 2d image, where inside the laser sheet the liquid fuel phase distribution appears.

According to the two different simultaneously detected Mie scattering signals from the droplets inside the piston bowl and from those inside the laser light sheet plane alone, both signals can give different information on the Diesel injection process with high temporal resolution. The first signal is integrated in direction of the cylinder axis when detecting its intensity through the window at the piston crown. It provides information on the contour of the five individual jets. From it the cone angle and the tip penetration of the single jets can be evaluated.

The second signal from droplets inside the laser sheet provides an information on the liquid fuel distribution at the position of the plane with high local and temporal resolution. From it a binary liquid fuel distribution can be calculated. This distribution contains the information, that liquid fuel is present inside the light sheet and at which local position the liquid appears. For several different injection cycles investigated by this information an appearance frequency distribution (AFD) of the liquid fuel can be calculated which provides useful statistical information on the injection process.

The measurement technique developed may also be used successfully for the investigation of other spray or injection processes of interest.

The work has been supported by the commission of the European Communities within the frame work of the JOULE Program, by the Swedish National Bord for Technical Developement, and by the Joint Research Committee of European automobile manufactures (Fiat, Peugeot SA, Renault, Volkswagen and Volvo) within the IDEA program.

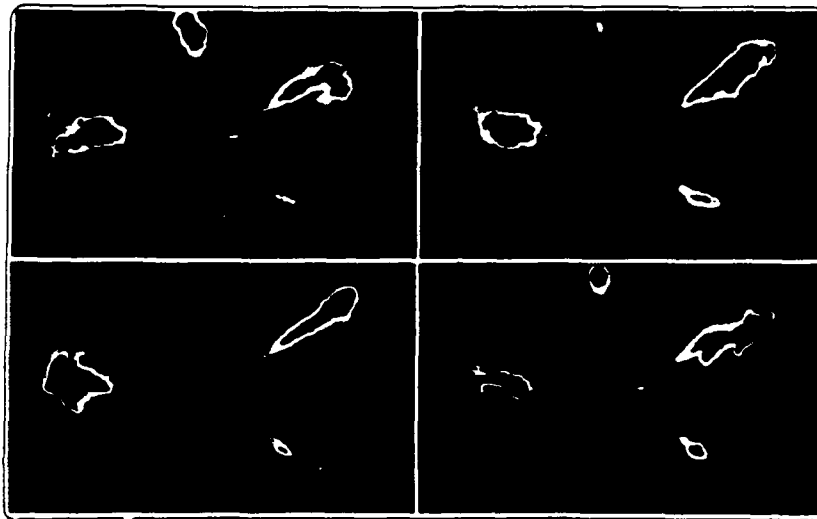


Figure 1:  
Typical measurement signal taken at the same engine crankangle  
in different motor cycles

# **POSTER SESSION PAPERS:**

**Presented at Two Time Periods**

**WEDNESDAY, 12 May 1993 from 4:00 to 6:30 PM**

**Co-Chairs: Dr. H. J. Pasman and  
Dr. T. Wijchers**

**and**

**THURSDAY, 13 May 1993 from 4:30 to 6:45 PM**

**Co-Chairs: Dr. H. J. Reitsma and  
Ir. P.A.O.G. Korting**

**AREA 1: Non-Intrusive Temperature Measurements**

**AREA 2: Diagnostics in Gaseous Flames**

**AREA 3: Diagnostics of Combustion Processes of  
Condensed Phase Systems**

**AREA 4: Diagnostics in Practical Combustion Systems**

**POSTER SESSION AREA 1:  
Non-Intrusive Temperature Measurements**

# COMPARISON OF TURBULENT DIFFUSION FLAME TEMPERATURE MEASUREMENTS AND RE-STRESS MODEL PREDICTION

A.A. Neuber\*, E.P. Hassel, J. Janicka  
Technische Hochschule Darmstadt,  
Fachgebiet Energie- und Kraftwerkstechnik, Petersenstr.30,  
W-6100 Darmstadt, Germany

In this paper the results of  $N_2$  Q branch broadband CARS temperature measurements in a turbulent natural gas diffusion flame are presented. The experimental set-up and the object of measurement are shortly discussed. The experimental single shot results were shown in the form of mean temperature and standard deviation of temperature versus normalized flame radius and compared to values obtained from numerical simulation.

Because of the nonlinearity of the CARS process it has to be assured for local measurements that the spatial resolution is of the same order as the spatial variations [1]. A beam arrangement for measurements with high spatial resolution in objects with strong fluctuations of refraction index, USED CARS, recommended by [2] is used for our measurements. A frequency doubled Nd-YAG laser and a laser pumped broadband dye laser are used as pump and Stokes laser (fig. 1). The inner part of the output beam is blocked to avoid deterioration of the spatial resolution caused by the appearance of collinear CARS despite of the strong spatial separation of the two laser beams at the focusing lens [3]. The burner of the free turbulent natural gas diffusion flame consists of a tube with diameter  $D = 4.0\text{mm}$  and a co-flowing air stream with  $0.4\text{m/s}$ . The flame with a Reynolds-number of 7000 was stabilized by pilot flames and thus was not lifted. We measured from  $x/D = 5$  to 110 eight downstream levels and at each flame location one hundred spectra were taken for statistics. Temperature is obtained from a CARS spectrum by analyzing its overall shape. A model spectrum is least square fitted to an experimental spectrum with temperature as the principal variable. The computer code [4] includes the full G-matrix inversion using the modified exp-gap-law [5]. The numerical combustion simulation is described in detail in [6] and is based on an equilibrium model describing the combustion, a Reynolds-stress-model for the turbulent flow and a coupling model. During our measurements we have not seen any mixed CARS-Spectra. means no overlap between cold and hot zones has occurred. The spatial resolution was better than  $1.5\text{mm}$  as can be seen at the steep gradients of the measured mean temperature and as was measured by nonresonant CARS-Signal of a  $0.3\text{mm}$  thick quartzplate. Examples of the measurement results are to be seen in the form mean temperature and standard deviation of mean temperature versus the normalized flame radius in

fig. 2. The normalization of the radius is done with the help of the theoretical mixture fraction half value radii. Points represent experimental values, lines numerical simulation. At both axial levels at  $x/D = 20$  and  $x/D = 90$  the experimental and theoretical curves are in good agreement concerning the peak values and the gradients. Also the temperature fluctuations are in good accordance. The flame spreading is faster in the theory than in the experiments. The temperature fluctuations are maximum at that locations where the gradient of the mean values are maximum.

In the poster the experimental set-up and the data analysis is described in detail, and the results are critically compared with the numerical simulations.

## References

- [1] A.C. Eckbreth; "Laser Diagnostics for Combustion Temperature and Species", Abacus Press, Cambridge, MA, (1988)
- [2] Klick, D.; Marko, K. A.; Rimai, L.; Broadband single-puls CARS spectra in a fired internal combustion engine, Appl. Opt. 20, 1178, 1981
- [3] Davis, L. C.; Marko, K. A.; Rimai, L.; Angular distribution of coherent Raman emission in degenerate four-wave mixing with pumping by a single diffraction coupled laser beam: configurations for high spatial resolution, Appl. Opt. 20 , 1685, 1981
- [4] Brueggemann, D.; Entwicklung der CARS-Spektroskopie zur Untersuchung der Verbrennung im Otto-Motor, Dissertation RWTH Aachen, (1985)
- [5] Koszykowski, M. L.; Farrow, R. L.; Palmer, R. E.; On the Calculation of Collisionally Narrowed CARS Spectra, Opt. Lett., 10 (5), 1985
- [6] Janicka, J.; A Reynolds-stress model for the prediction of diffusion flames. 21st Symposium on Combustion, 1988, S. 1409 - 1418

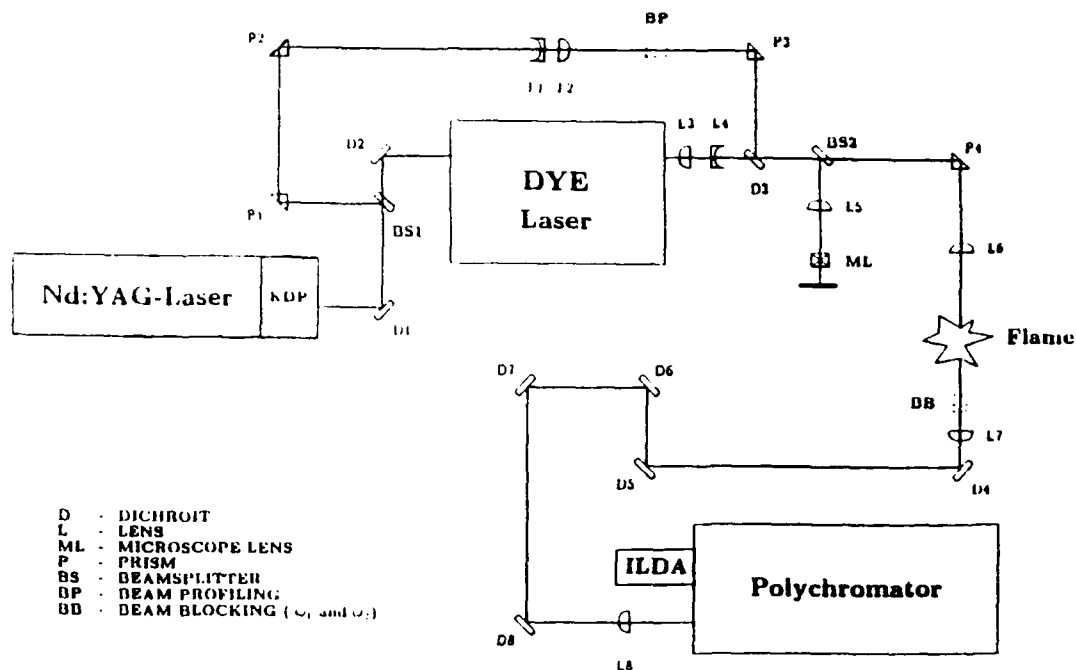


FIG. 1: CARS experimental set-up

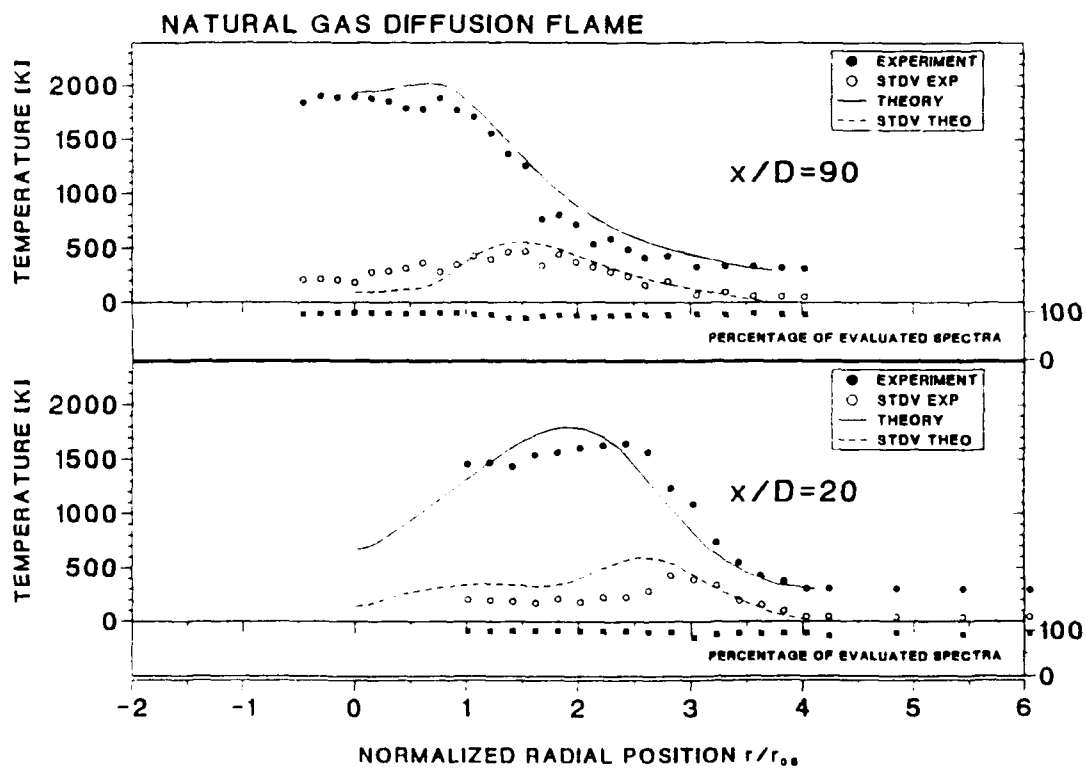


FIG. 2: Experimental and numerical simulation values of mean temperature and standard deviation of mean temperature versus the normalized flame radius at the downstream levels  $x/D = 20$  and  $90$ . Nozzle diameter  $D = 4.0\text{mm}$ .

# CARS Temperature Measurements in a Lean, Turbulent, 120 kW Natural Gas Flame

R. Bombach, B. Hemmerling, and W. Kreutner

*Laboratory of Energy and Process Technology, Paul Scherrer Institute  
CH - 5232 Villigen PSI, Switzerland*

A mobile CARS system was used for temperature measurements in a turbulent flame. The apparatus was hardened to meet the requirements dictated by the conditions at an industrial site. Therefore lasers and optics required for CARS signal generation are contained in one compact frame. The signal is transferred to a spectrograph by means of a quartz fibre bundle. The measurement location may be translated under remote control, and the data acquisition procedure is largely automatized.

Measurements were performed at a test site for industrial burner development. The burner employed in this work was operated at atmospheric pressure. The lean, highly turbulent flame ( $\lambda = 2,0 - 2,2$ ) was stabilized at a flow vortex. Natural gas was used as fuel, and the thermal power achieved was approximately 120 kW. The air was pre-heated to 670 K in order to simulate the effect of a compressor stage. The burner was attached to a combustion chamber with a 200 mm diameter. Radial temperature profiles were determined at several distances downstream from the burner exit.

Temperature probability density functions were extracted from single-pulse  $N_2$  CARS spectra recorded with a 20 Hertz repetition rate. Typically 1000 spectra were used at each point for a statistical analysis.



CARS AT TEMPERATURES UP TO 3200 K, DATA EVALUATION OF  
SINGLE-SHOT BROADBAND NITROGEN SPECTRA

M. FISCHER, E. MAGENS, A. WINANDY  
Institut für Antriebstechnik, DLR,  
Linder Höhe, D-5000 Köln 90, Germany

ABSTRACT

At hypersonic speed hybrid turbojet/ramjet engines, under theoretical and experimental study at the DLR-Cologne, are operated in ramjet mode: the ambient air is compressed in the supersonic inlet, hydrogen is injected into the hot air and the combustion products expand into the exhaust nozzle. The rapid change of the flow field can lead to nonequilibrium effects, reducing the combustion efficiency. Modelling of the combustion process and nozzle flow requires measurements of the temperature PDF under strongly varying conditions from the combustion chamber downstream to the nozzle exit.

We expect that some of the remaining answers at present can best be given by CARS thermometry because of its insensitivity to quenching effects and its good suppression of background radiation. However, very few quantitative CARS-measurements under these extreme conditions are known and a reliable interpretation of the expensive experiments requires a certain knowledge of CARS inherent noise sources. Additionally, line width data have to be extrapolated for the simulation of  $N_2$  Q-branch spectra under the combustion conditions, i.e. 3000 K, 10 bar and 50%  $H_2O$  content. The influence of different actual relaxation rate models leads to a temperature uncertainty which is subject of our actual investigations.

In the present study we report CARS measurements obtained in an electrically heated graphite tube furnace (Perkin-Elmer HGA 500). The temperature profile has already been studied in more detail<sup>1</sup>, and can be expected to be stationary for our spatial resolution and is therefore useful for calibration measurements. The obtained single shot spectra are used to specify the amount of temperature rms which can be attributed to the CARS statistics for temperatures up to 3200 K.

The CARS system is based on an injection seeded single mode pump laser which is advantageous for maximum CARS efficiency and good spectral resolution. The experimental results for the temperature rms are compared to results based on CARS intensity noise simulations.

References

1. B. Welz, M. Sperling, G. Schlemmer, N. Wenzel, G. Marowsky, *Spectrochimica Acta*, Vol.43B (1988) 1187

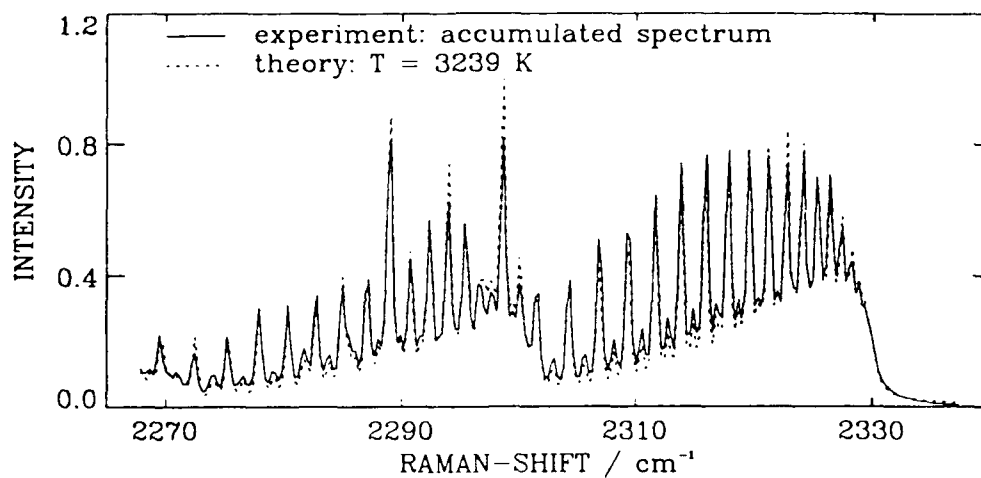


Fig.1: Temperature fit to an experimental nitrogen spectrum consisting of 45 accumulated single shots.

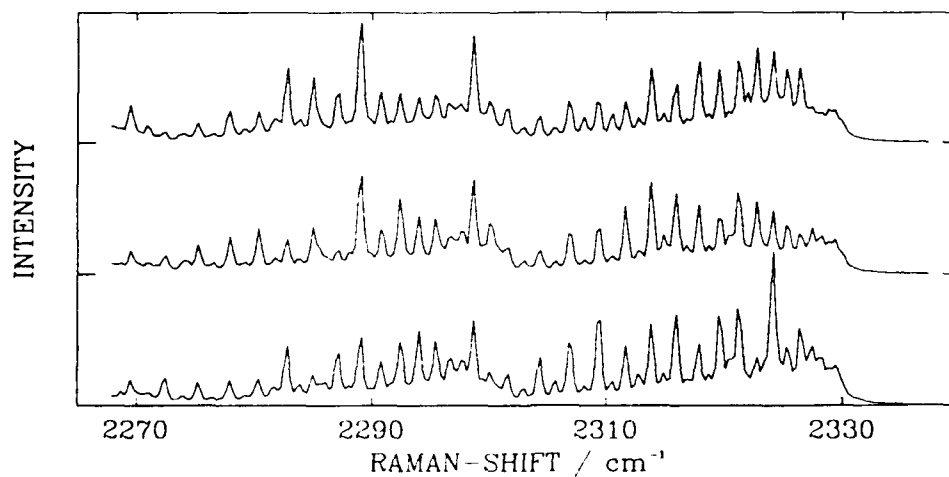


Fig.2: The first three single shots of the ensemble corresponding to Fig.1.

## Measurement of three-dimensional temperature fields by heterodyne holographic interferometry

B. Ineichen and R. Müller

Swiss Federal Institute of Technology  
Internal Combustion Engines Laboratory  
CH-8092 Zurich  
Switzerland

The general objectives have been experimental and theoretical investigations of methods for the quantitative determination of temperature profiles in boundary layers from holographic interferometry.

In earlier studies the temperature profile in the boundary layer of a hot gas near any cooled plate was found to be a function of the physical properties and surface temperature of the plate itself. Considering the calculation of the physically correct heat transfer to the combustion chamber wall this temperature fields have to be found by determination of only experimental and no modeling data. The experimental difficulties are illustrated by the fact that for the reconstruction of the temperature field in 27 space points as much as 934 fringe positions at 27 different angles of observation over a range of  $46^\circ$  had to be measured manually. The uncertainty in the reconstructed temperature was found to be  $\pm 10\%$  with respect to the maximum temperature difference of about 10 K.

Holographic interferometry is a powerful tool to measure the deviation between two wavefields within a fraction of the wavelength of the coherent monochromatic light source. In the reconstruction of the double exposure hologram the phase difference of the wavefronts due to a different spatial refractive index distribution of the two object states shows up as an intensity modulation, the resulting interference fringe pattern. Starting at a point of the field where the temperature remained constant, the temperature at any point in the field can be obtained by detecting the total phase difference at this position.

However, with classical holographic interferometry quantitative information on the interference phase is only reliable in the minima and maxima of the fringes, corresponding to multiples of  $180^\circ$  or  $\pi$ . The interpolation between the fringes is difficult and not very accurate. Furthermore, in regimes of higher fringe concentration as expected near the wall the image noise due to the laser speckles reduces the fringe contrast.

With heterodyne holographic interferometry these difficulties are nearly eliminated. Fig. 1 shows the concept of the optical set up that is being built at our laboratory. The basic idea of heterodyne holographic interferometry is to introduce a small frequency shift between the optical frequencies of the two interfering light fields. This results in an intensity modulation at the beat frequency of approx. 100 kHz of the two light fields for any given point in the interference pattern.

The phase difference between multiple detectors is measured with a zero crossing phasemeter, which interpolates the phase angle to  $0.1^\circ$ , so the resolution in the order of  $1/1000$  of a fringe can be realized.

The experimental verification of heterodyne interferometry for heat transfer measurements will be presented, and the properties of this technique will be discussed.

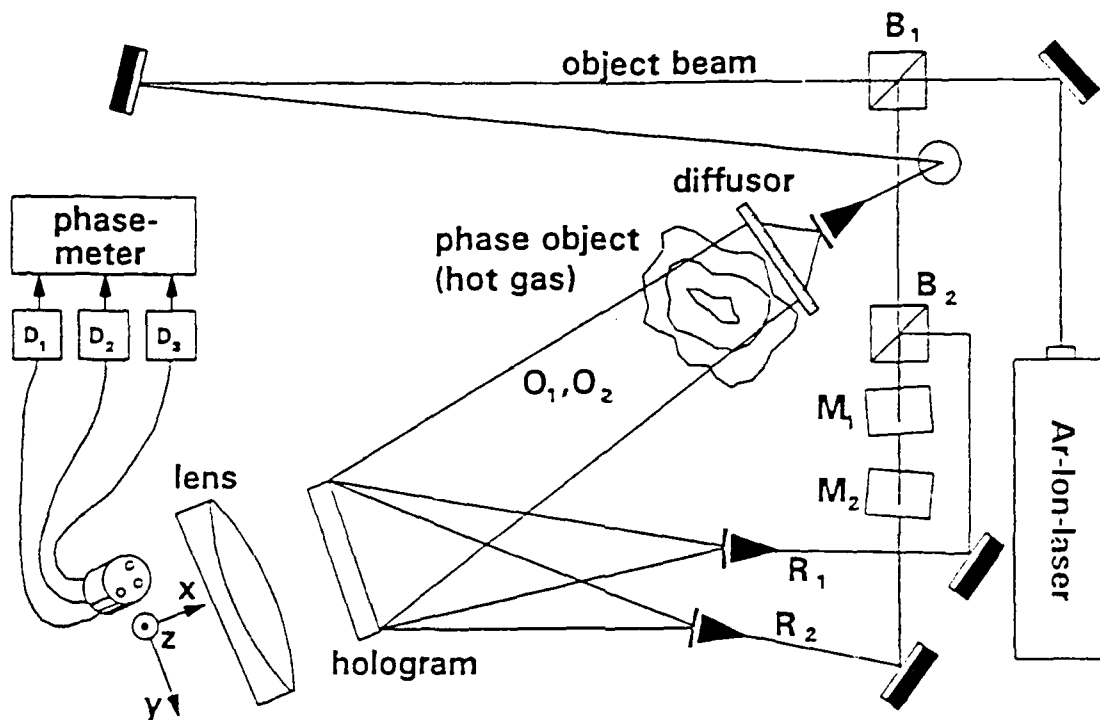


Fig. 1: Concept of the optical set up for heterodyne holographic interferometry

HOLOGRAPHIC TEMPERATURE  
MEASUREMENT ON AXISYMMETRIC  
PROPANE-AIR, FUEL-LEAN FLAME

Sheng Mao, Tieng\*

Wen Zen, Lai†

Institute of Aeronautics and Astronautics  
National Cheng Kung University  
Tainan, Taiwan 70101, R.O.C.

Toshi Fujiwara ‡

*Department of Aeronautical Engineering*  
Nagoya University  
Japan.

---

\* Associate Professor, corresponding author

† Graduate Student,

‡ Professor, Department of Aeronautical Engineering, Nagoya University, Japan

## ABSTRACT

Instead of using the conventional interferometry, the whole field temperature distribution of a laminar, axisymmetric, propane-air, fuel-lean flame is measured by using an advanced digital interferometric technique — digital phase shifting holographic interferometry. The measurement technique effectively improves the accuracy of conventional interferometric measurement as it circumvents the limitation of fringe counting interpolation. The results obtained by this technique are compared with that measured by conventional holographic interferometry (using interpolation) in order to evaluate the effect of interpolation on measurement accuracy. A modified dual reference beam holographic recording system is set up for this experiment and the fast Fourier transformation is used for Abel inversion. The structure of the test flame is analysed by holographic visualization and measured temperature distribution. In addition, the interferometric temperature distributions are compared with thermocouple measurements. Errors introduced in the measurement are analyzed and discussed.

Keywords: 1. temperature measurement  
2. holographic interferometry  
3. axisymmetric flame  
4. digital phase shifting technique

## TEMPERATURE MEASUREMENTS BY CARS: STATE OF THE ART, LIMITATIONS AND OBJECTIVES.

P. Bouchardy, G. Collin, F. Grisch, P. Magre  
and M. Péalat

*Office National d'Etudes et de Recherches Aéronautiques  
BP 72 F-92322 Châtillon Cedex - France*

In the area of time-resolved and spatially-resolved temperature measurements, coherent anti-Stokes Raman scattering (CARS) has the advantage of providing data even in situations of industrial interest.

Temperature measurements are often deduced from the spectral signature of  $N_2$ , which is generally the majority species of the gas mixture. In turbulent burners, broadband BOXCARS is required in order to get instantaneous and spatially-resolved measurements. The nonresonant background must also be cancelled. If this precaution is not taken, the CARS spectral shape depends both on the temperature and the chemical composition, especially when the burner is fueled with kerosene.

Using an optical arrangement where all these features had been implemented, the temperature has been mapped in a 10 cm-wide, 30 cm-high, 1 atmosphere-pressure, kerosene-fueled burner. Average temperatures and temperature probability density functions have been obtained from batches of several hundred repeated measurements at each point in space [1].

No difficulties are encountered when studying this burner operating at atmospheric pressure. We have also studied an 8 cm-diameter, axially-symmetric burner constructed for soot formation studies; similar results were found at atmospheric pressure. However, we noted that the CARS data reduction code fails to process many of the experimental CARS spectra at higher pressure. The phenomenon aggravates when pressure is increased. Thus, at 4 bars, only 20% of the spectra can be processed; this may produce uncontrolled temperature bias. Particles are likely to be the main problem because they facilitate laser-induced breakdowns which distort the  $N_2$  spectra.

Reducing the laser energies would probably solve the difficulty. The dual-line CARS technique, which we proposed for the study of low-density flows [2], is certainly the most promising solution. The temperature is no longer deduced from the shape of the Q-branch but from the intensity ratio of two isolated Q-lines. Because the Stokes energy is now used efficiently, the required energies are smaller. Further, breakdowns are less frequent. The dual-line CARS technique presents other advantages: the lasers being less powerful, the pulse repetition rate can be increased for the same average power; the data processing is simpler and consequently faster [3]. Preliminary results obtained during a demonstrative experiment are presented.

### References

- 1- P. Magre, G. Collin, D. Ansart, C. Baudoin and Y. Bouchié, 3<sup>ème</sup> Forum Européen sur la Propulsion Aéronautique, Paris, 13-15 Nov. 1991.
- 2- M. Péalat and M. Lerebvre, Appl. Phys., B53, 23-29, 1991.
- 3- M. Alden, K. Fredriksson and S. Wallin, Appl. Opt., 23, 2053-2055, 1984.

**POSTER SESSION AREA 2:  
Diagnostics in Gaseous Flames**



# A Study on the Emissivity Prediction of Open Propane Flame with Infrared Image

Jir-Ming Char  
Aeronautical Engineering Department  
The Chinese Air Force Academy

Jun-Hsien Yeh  
Institute of Aeronautics and Astronautics  
National Cheng Kung University  
Tainan, Taiwan, R.O.C.

In this paper, the flame emissivity prediction and flame temperature measurement for open propane flame are investigated by using an infrared (IR) measurement system. Based on this investigation, the scheme in non-intrusive flame temperature measurement and fuel combustion performance analysis may be further improved.

Many species created in the propane flame products, in which  $\text{CO}_2$  and  $\text{H}_2\text{O}$  are the main interested species for infrared emission measurement. Most portion of flame radiation lies in the infrared wavelength range. In this range, the wavelength of  $4.3\ \mu\text{m}$  band for  $\text{CO}_2$  has the strongest intensity, which is due to the asymmetric stretching vibration of carbon dioxide molecules. Therefore, a special filter for the scanner in the near-infrared range ( $\lambda \sim 4.3\ \mu\text{m}$ ) is adopted which indicates that only the  $\text{CO}_2$  emission at  $4.3\ \mu\text{m}$  wavelength can pass the filter and be measured. Based on these recorded emission intensity variation, the propane flame emissivity and the flame temperature can be obtained.

The capability of IR scanning frequency is 2500 Hz for line mode and 25 Hz for plane mode. Currently, plane mode is used to measure a cross-sectional plane flame temperature, and the measurement time is four seconds in each test. There are three types of flame combustion during the experiment: diffusion flame, premixed lean flame and partial premixed flame.

In flame emissivity determination, a theoretical analysis and iteration scheme are used coupling with the test data to predict the band emissivity at  $4.3\ \mu\text{m}$  wavelength. Two major parameters are selected in the iteration scheme, which are the distance between the flame and scanner, and the  $\text{CO}_2$  partial pressure in the flame.

products. Also, the wide-band theory is selected as the mathematical model in calculation. Using the results of emissivity calculation into a special software of the IR measurement system, the flame temperature can be obtained. Typical results for a premixed lean flame test are given in Figures(1) and (2).

The results of the propane flame temperature measurement with IR system are in good agreement with the thermocouple measurement, which proves the IR method is feasible in the flame temperature measurement. Also, by using a statistical analysis, the empirical correlations for the propane flame emissivity prediction can be obtained. They are

$$\epsilon = 0.0800850 \cdot (T / T_0)^{-0.0180363} \cdot e^P \quad \text{for optically thick case}$$

$$\text{and } \epsilon = 0.0780139 \cdot (T / T_0)^{-0.0201561} \cdot e^P \quad \text{for optically thin case}$$

$$\text{Where } P = 0.05 \cdot ((X^2 + Y^2)^{0.5} / R)$$

and  $T_0 = 300$  degree K ,  $R = 5\text{mm}$  (the burner radius) ,  $X$  and  $Y$  are position coordinates from burner exit center. The reasonable predictions from these empirical correlations are shown in Figures (3) and (4).

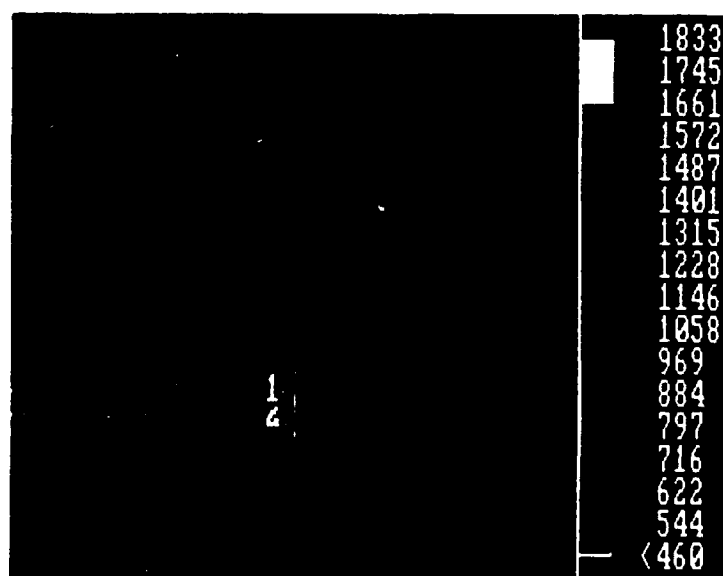


Fig.1 The thermal image of premixed lean flame

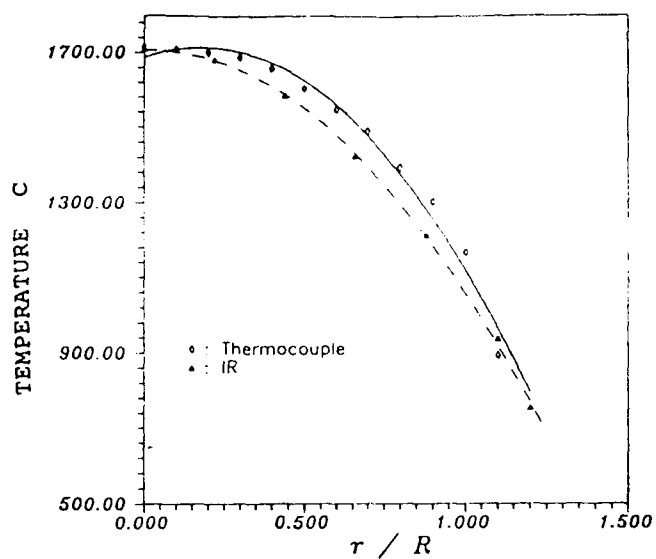


Fig.2 The IR temperature compared with thermocouple temperature of premixed lean flame above burner exit 17 mm.

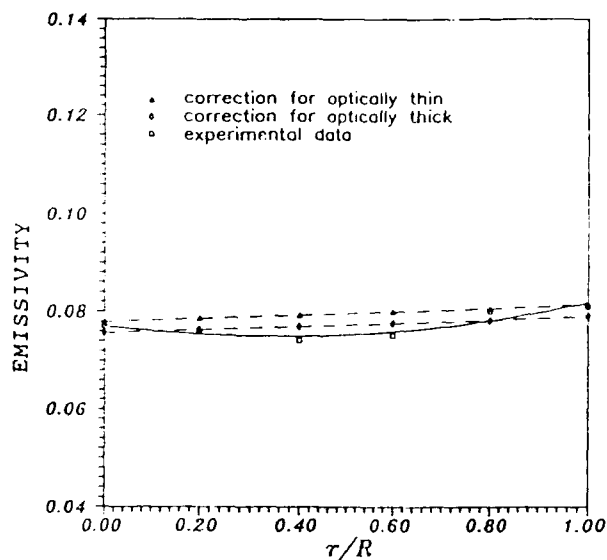


Fig.3 Empirical value of emissivity compared with standard value.

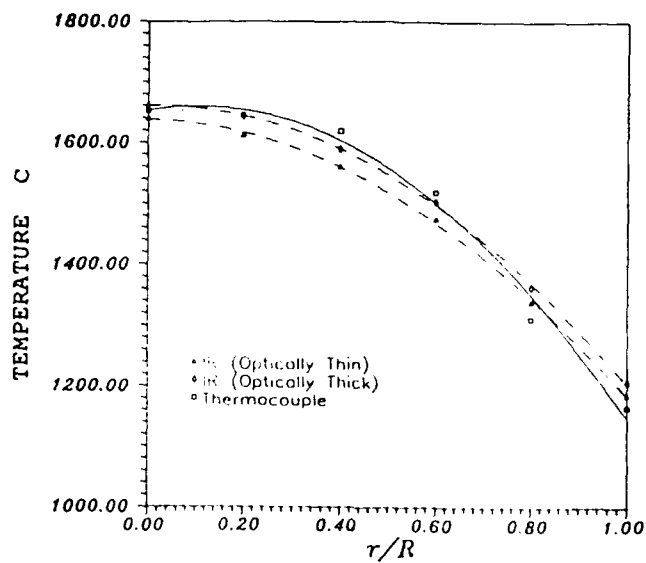


Fig.4 The IR temperature which is deduced by empirical correlation equation compared with thermocouple temperature.

# DETERMINATION OF RADIATION PROPERTIES OF THE GAS FLAME

Dr Jan NADZIAKIEWICZ

Institute of Heat Technology  
Silesian Technical University  
POLAND

## Abstract.

A method for the determination of radiation properties of the gas in the flame volume is presented. The determined properties are absorption coefficient  $\alpha$ , emissive power of flame gas  $e_v$  and their spatial distribution.

Equations of radiation transport in a gas layer are evaluated as a theoretical basis for the method. Main assumptions are non dissipating gas, and axial symmetry of the flame.

Increase of intensity of radiation  $i$  of a wavelength  $\lambda$  in the gas layer of a thickness  $dl$  is described by equation:

$$\frac{di_\lambda}{dl} = \alpha_\lambda(l) [i_b(l) - i_\lambda(l)]$$

where  $l$  is a coordinate in the gas layer,  $\alpha(l)$  is absorption coefficient of the gas and  $i_b(l)$  is a black-body emissive power in the point determined by coordinate  $l$ .

Solutions of this equation for two boundary conditions: "cold background" (for  $l=0$ ,  $i_\lambda(0)=i_{\lambda 0}$ ) and "hot background" (for  $l=0$ ,  $i_\lambda(0)=i_v$ ) gives, after some operations two equations:

$$\Phi(L) = \ln \frac{i_v}{i_h(L) - i_c(L)} = \int_0^L \alpha(l) dl$$

and

$$\Psi(L) = i_c \frac{i_v}{i_h(L) - i_c(L)} = \int_0^L i_v(l) \exp \left[ \int_0^l \alpha(x) dx \right] dl$$

where  $i_h(L)$  and  $i_c(L)$  are intensities of radiation coming out of a gas layer of a thickness  $L$  with hot and cold background respectively.  $\Phi(L)$  and  $\Psi(L)$  are new defined functions dependent on the gas layer thickness  $L$  - these functions can be determined from measurement results.

For axisymmetric gas layers (flame), one can obtain integral equations for determining radial distribution of  $\alpha(r)$  and  $i_v(r)$ :

$$\alpha(r) = -\frac{1}{\pi} \int_{x=r}^{x=R} \frac{\frac{d\Phi}{dx}}{(x^2 - r^2)^{1/2}} dx + \alpha_0$$

$$i_v(r) = -\frac{1}{\pi} \exp \left[ -\int_0^L \alpha(r) dr \right] \int_{x=r}^{x=R} \frac{\frac{d\Psi}{dx}}{(x^2 - r^2)^{1/2}} dx + i_{v0}$$

where  $\alpha_0$  and  $i_{v0}$  are values for the gas surrounding the flame.

To illustrate the method presented above for the determination of radiation properties of flames, a series of experiments have been made in an experimental combustion chamber.

The measurements of intensity of radiation of a flame were made with a narrow angle pyrometer with cold- and hot- background in different directions towards the flame. Results of experiments are approximated by a smooth curve and then numerically integrated over the flame volume.

It is possible to use this method for determining the radiation properties of a gas for particular wavelength  $\lambda$ . It needs measurements to be done in their spectral distribution. In the example presented here, a total radiation pyrometer has been used. As a result total values of absorption coefficient and emissive power for whole radiation spectrum are determined.

Some results of measurements are presented in tables and in figures. Results of calculations are presented in their spatial distribution as functions of flame radius and distance from the burner. The geometry of the gas volume, measured values of radiation intensity and distribution of  $\alpha$  are attached.

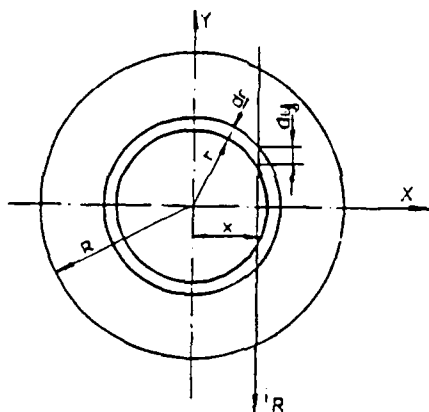
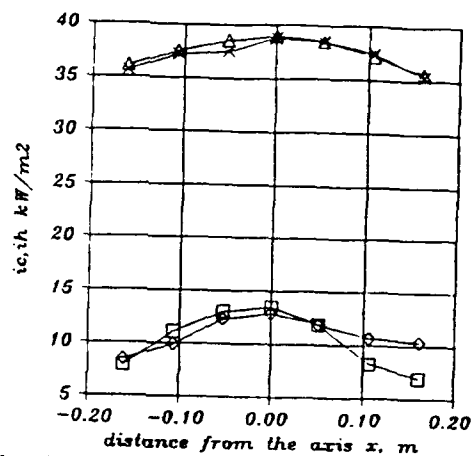


Fig. 1. Gas volume in cylindrical geometry.



□  $-i_c, L=0.2m$     Δ  $-i_h, L=0.2m$     ◇  $-i_c, L=0.4m$     ×  $-i_h, L=0.4m$

Fig. 2. Measured values of radiation intensity with cold- and hot background.

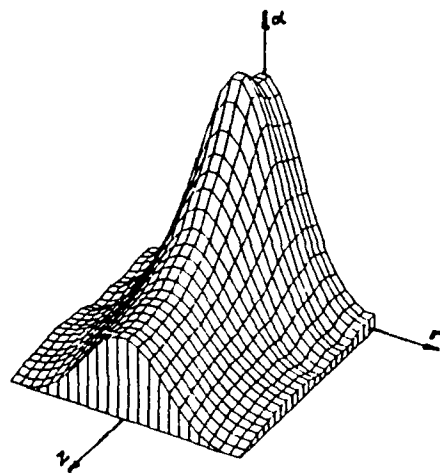


Fig. 3. Absorption coefficient  $\alpha$  vs. radius  $r$  and distance from the burner  $z$ .

# OBSERVATION OF FLOW INSTABILITY IN THE CONE OF BUNSEN FLAMES BY LIF.

A. A. Konnov, I. V. Dyakov, E. V. Belozeroва

Combustion Problems Institute,  
172, Kirov st., Alma-Ata, 480012,  
Kazakhstan, CIS.

The OH concentration profiles in the cone section of atmospheric pressure methane-air and propane-air flames stabilized over a Bunsen burner have been obtained with a laser induced fluorescence arrangement (Fig. 1.). The probing source was a frequency-doubled computer-controlled home-built tunable dye laser pumped by a frequency-doubled Nd:YAG laser. The output parameters of the probe laser were as follows: the spectral tuning range from 295 to 330 nm, bandwidth of 0.01 nm, pulse energy < 0.3 mJ, pulse duration 10 ns, and repetition frequency 12.5 Hz. The probing wavelength could be checked by a grating spectrograph with an OMA detector with an accuracy of 0.01 nm in the red. The relative intensity of each laser pulse in the red and uv was measured by vacuum photoelements and digitized by ADC. Laser radiation is focused by a lens which makes a 100-micron diameter spot in the burner flame. OH fluorescence was

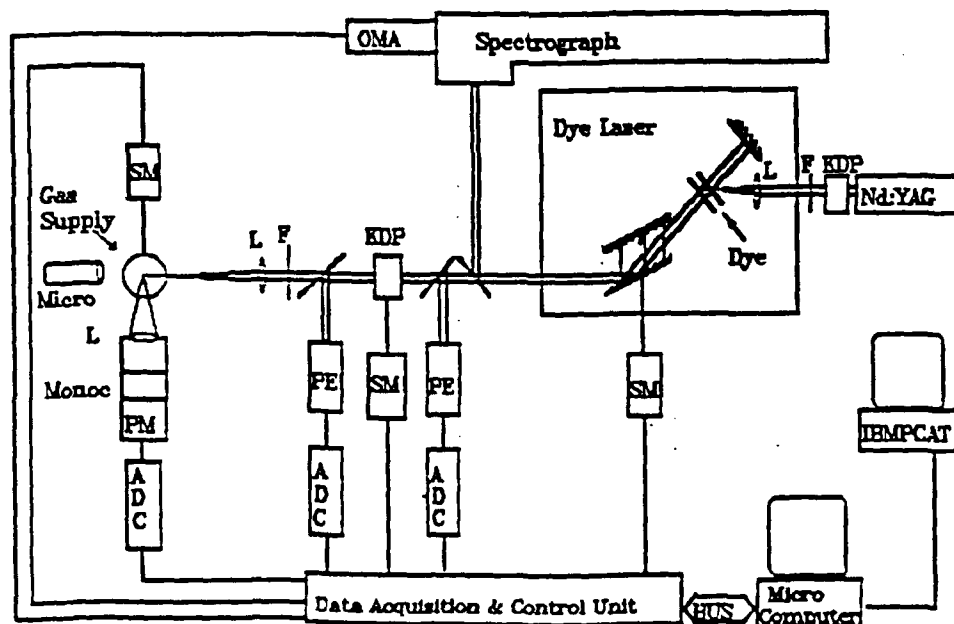


Fig.1. The schematic of the experimental rig.

collected at a right angle to the exciting beam by a quartz lens and focused onto a slit of monochromator outfitted with an photomultiplier (PM). The PM output was sampled by stroboscopic integrator and digitized by ADC. All three measured data were stored in a Schneider EURO PC computer after each laser shot. Besides, the flame luminescence proper was measured with a 2 ms delay after the laser pulse. The fluorescence signal was estimated as a difference between these two measurements normalized to the intensity of the laser pulse. Thus, the apparatus makes it possible to measure the excitation spectra of OH radicals and scan the flames along the cross section in different directions.

It has been established that the profile of the OH radical concentration in the pre-flame cool zone has a flattened section. Similar flattened sections are observed for Bunsen flames with different front curvature and this allows us to rule out the possibility of the signal registration from the neighboring flame zone. The OH rotational temperatures in the pre-flame zone were also measured. These temperatures agree with thermocouple measurements within the limits of estimated error.

Figure 2 shows the profile of the fluorescence signal obtained with a vertical Bunsen burner (right curve). The drop of the OH radical concentration in the cold pre-flame zone clearly deviated from the calculated dependence expectable on the assumption of purely diffusion process. The same results were obtained for Bunsen propane-air flames. Chemical reactions in the pre-flame zone can not explain of the observed effects due to their essential difference for methane and propane.

A number of experiments on the measurement of the OH radical profiles at horizontal position of the flame were carried out in order to study the potential hydrodynamic features of Bunsen flames and the influence of gravity on the flame structure. In addition, the flame was placed in a co-flow of nitrogen to investigate the effect of surrounding air. The profile of the OH radical concentration in the pre-flame zone practically does not change in this case. On the other hand, if a methane or propane flame has the horizontal luminous front, the profile of the OH concentration has a purely diffusional character (left curve in Fig.2) and agrees with literature data [1].

These structural differences between conical flames and flames of other shapes and numerical calculations enable us to make a conclusion about the effect of a stabilization mode



on the flame's aerodynamics. In particular, in [1] the front of a methane flame is arranged horizontally in a gravity field and differs from Bunsen flames. An analysis of the two-dimensional Navier-Stokes equation yields the result that in the field of gravity for a vertical or inclined flame front the horizontal pressure gradient leading to an added convection arises in the region of significant mixture density gradient. Thus, such a pressure gradient together with the buoyancy of the hot layers can cause an oscillating flow instability [2] and therefore some mixing in the cold region near the flame front. The analytical model for flow instability in the pre-flame zone is discussed.

1. Bechtel J.H., Teets R.E.: Appl. Opt. 18, 4138 (1979).
2. Durox, D., Baillot, F., Scouflaire, P., Prud'homme, R.: Combust. Flame 82, 66 (1990).

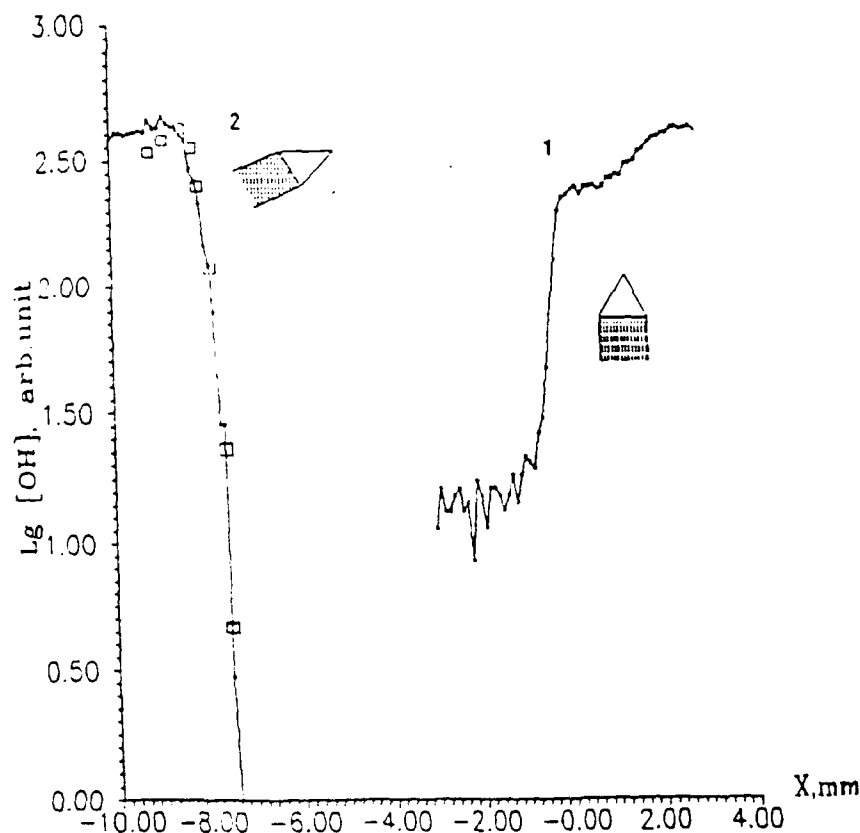


Fig.2. Profiles of the fluorescence signal for methane -air flames ( $\phi=1.3$ ). 1. Vertical position of Bunsen burner. 2. Horizontal position of luminous front. Points - OH concentration for flame with  $\phi = 1.25$  [1].

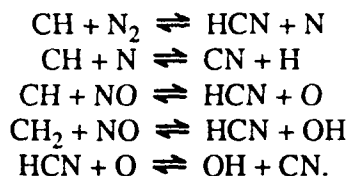
## Planar Laser Imaging of Species in a Novel Pulsating Burner

Berenice A Mann, Ian G Pearson and David Proctor

CSIRO

Division of Building, Construction and Engineering,  
PO Box 56, Highett, Vic 3190, Australia.

Planar Laser Induced Fluorescence (PLIF) has become increasingly important for imaging of species distribution in combustion environments. A thin sheet of laser light is used to excite a transition in the required species and the resulting fluorescence is imaged at 90° to the incident sheet onto a ccd camera, or other suitable two-dimensional detector. Here we have applied the technique to image CH, CN and OH in a novel pulsating burner. The images show the distribution of the species in the flame. CH and OH are generally used to indicate regions where chemical reactions are taking place in combustion and so we can expect minor species such as CN to be present, where the prompt mechanism is the major root to NO<sub>x</sub> species. The CH, OH and CN will be occurring essentially at the same position in the flame according to the following equations:



Further experiments are being performed using the relatively novel technique of Degenerate Four-Wave Mixing (DFWM). This technique requires three input beams at the same wavelength, usually derived from the same laser. Two beams, the pump and probe, are crossed at a small angle in the sample and a third beam is arranged to be counter-propagating to the pump beam. Although optically more complicated to set up, DFWM has the advantage of not requiring a 90° detection geometry. It has a signal in the form of a coherent beam, enabling detection remote from the hostile environment. This technique has also been extended to an imaging format, by expanding the pump beams into a thin collimated sheet and the probe into a circle of suitable area and uniform intensity. Comparison between the two techniques in terms of advantages, disadvantages, sensitivity, and applicability to combustion diagnostics are discussed.

Schlieren Method of Optical Registration  
of Combustion-to-Detonation Transition  
in Gaseous Mixtures

Nickolay N. Smirnov, Michael V. Tyurnikov

Department of Mechanics and Mathematics, Moscow State University  
Moscow, 119899, Russia

**ABSTRACT**

This paper presents the experimental method of non-intrusive diagnostics of the process of combustion-to-detonation transition in gas mixture with exothermic chemical reactions. Using an impulse laser as a source of light, Schlieren photography was taken through optical sections at different locations of the tube.

Experimental results of the visualization of the transition process in hydrocarbon-air gas mixtures show several different flow patterns: 1. The detonation wave originates in the flame zone, 2. The detonation wave originates between the flame zone and primary shock wave, 3. The secondary combustion zone originates between primary shock and the flame and causes the detonation, and 4. The occurrence of a spontaneous flame leads to the combustion-to-detonation transition. The influence of the flame zone on the development of a strong detonation wave will be discussed in the full paper.

Laser Doppler Velocimetry Measurements in a Laminar Counter Flow Premixed Double Flame : Comparison With Numerical Calculations

M.H. SENNOUN, E. DJAVDAN, N. DARABIHA and J.C. ROLON

Laboratoire EM2C, CNRS, Ecole Centrale Paris, 92295  
Chateauf-Malabry cedex, France

The scope of this study is to obtain realistic comparisons between numerical calculations and laser Doppler velocimetry measurements of the axial velocity profiles for a large number of strained laminar premixed propane-air double flames. Stationary conservation equations for strained flames have been derived including one-parameter (strain rate) and two-parameter (radial pressure gradient and flow divergence) formulations. The experimental study consists in measuring the axial velocity across the flame by means of LDV system for stoichiometric, lean, rich and near extinction limit flames. Experimental and numerical studies of strained laminar flames provide important informations for understanding turbulent combustion models based on the flamelet concept, in which, the turbulent flame is described as a collection of strained laminar elements embedded within the turbulent flow. In these models the local instantaneous structure of the reaction zone is depicted as an ensemble of quasi-steady state strained laminar flame elements. These flamelets are stretched and convected by the turbulent flow. In this context a standard problem considered by many authors is the stagnation point configuration featuring two laminar flames. In this configuration (Figure 1), two symmetrical reaction fronts are formed near the stagnation point by two identical reactive mixtures. In the theoretical calculations, the governing equations were solved by employing Newton iterations, adaptive continuation techniques, and using detailed transport and chemical kinetics (CHEMKIN and TRANSPORT) with a mechanism involving 31 species and 123 chemical reactions. The experimental study consists in measuring the velocity across the flame by means of a LDA system. The measurements were obtained for different equivalence ratio and inlet velocity (nozzle exit). We have also used a laser sheet to visualize the flow field. The experimental apparatus and LDA system are described in Figure 2. Numerical axial velocity and temperature profiles are shown in Figure 3, for stoichiometric propane-air flame. LDA measurements shows that increasing the inlet velocity decreases the double flame distance and the gas expansion velocity. This is essentially due to the decrease in flame temperature (Figure 5). For a fixed inlet velocity, increasing the equivalence ratio reduces considerably the double flame distance, the flame front speed and the maximum gas expansion velocity until the extinction limit is reached (Figure 4 and 5). In Figure 5, the rich flame (equivalence ratio = 2) is very important to understand the extinction mechanism.

The present work describes a numerical and experimental study of laminar strained premixed double propane-air flames. Laser Doppler anemometry is well adapted to investigate such flames and it can provide flow details. As shown in the paper, available numerical calculations and experimental measurements of the axial velocity component allowed us to confirm that the numerical calculations are in good agreement with LDA measurements in strained premixed flame.

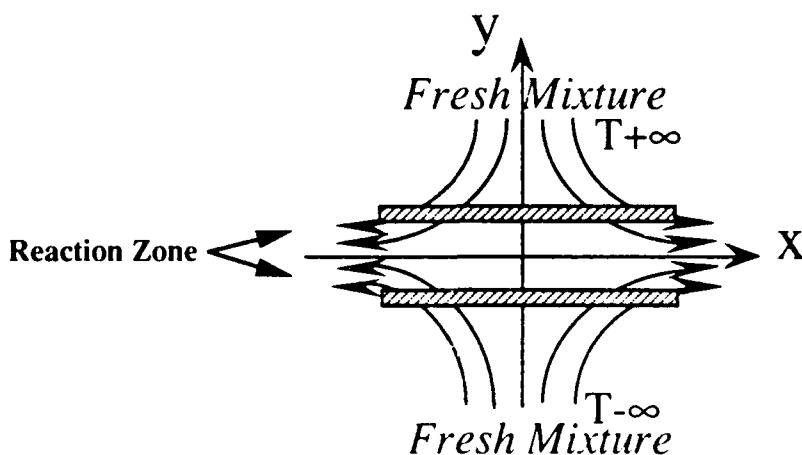


Fig.1. Strained premixed flames formed by counterflow mixtures.

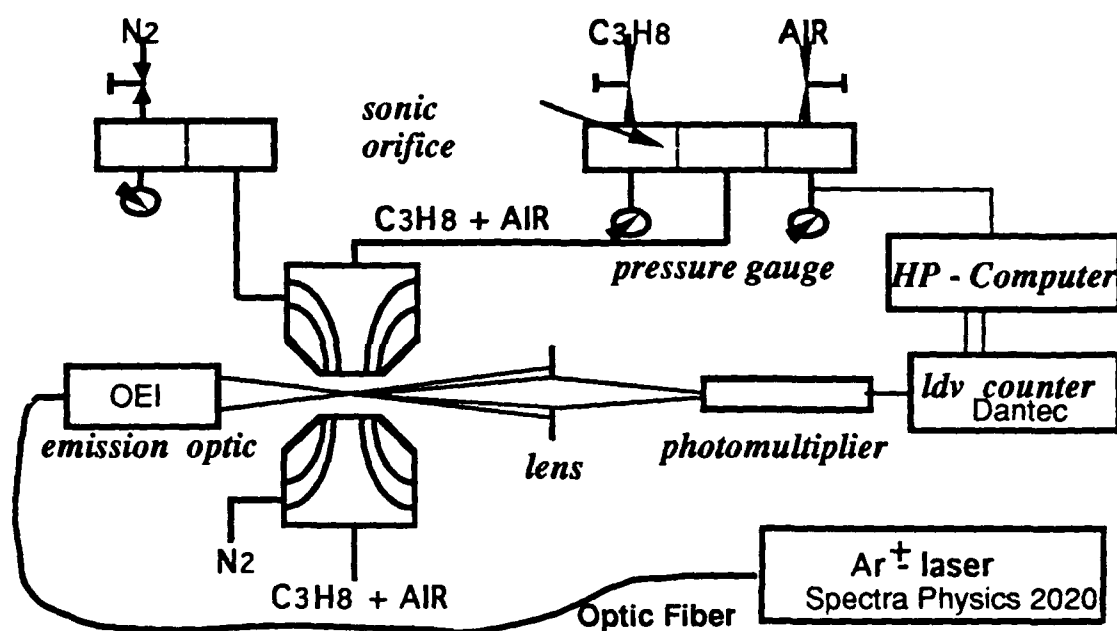


Fig.2. Sketch of the experimental set-up including the LDA system, burners and electronic equipment.

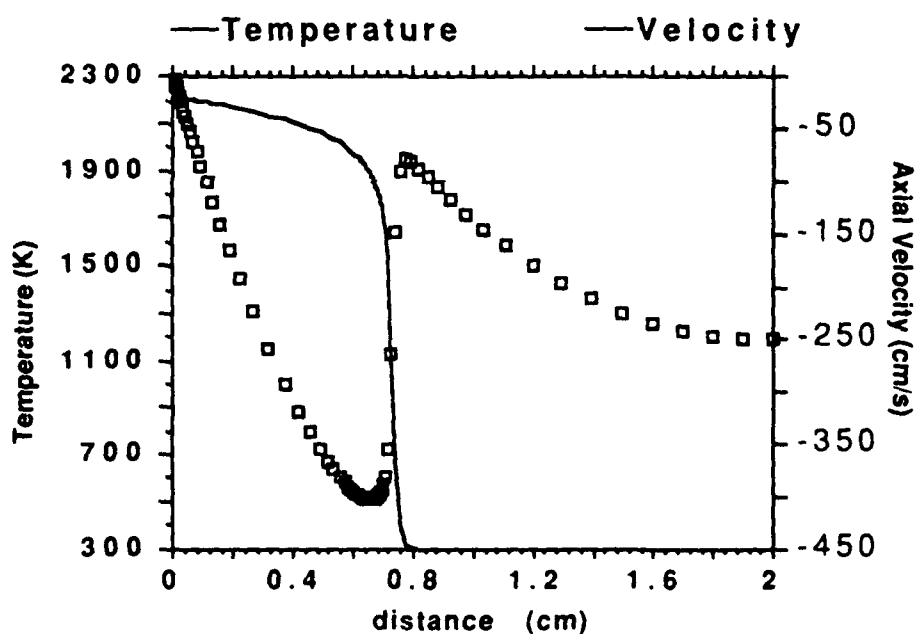


Fig.3. Numerical temperature and axial velocity profiles,  $\phi = 1$ ,  $V_0 = 2.5$  m/s.

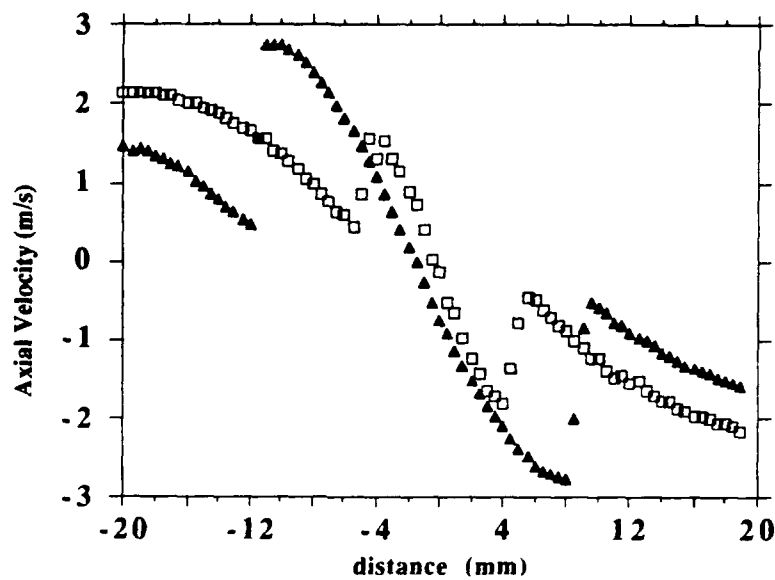


Fig.4. LDA axial velocity profiles for a stoichiometric flames and various inlet velocity (1.5 and 2 m/s).

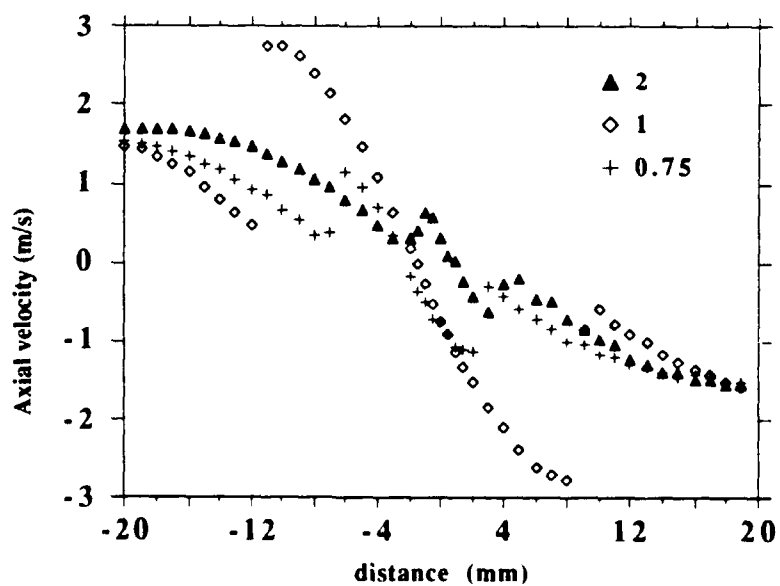


Fig.5. LDA axial velocity profiles for lean, stoichiometric and rich flames, inlet velocity = 1.5 m/s.

## NEW APPLICATIONS OF SHOCK TUBES FOR STUDIES OF COMBUSTION AND EXPLOSION PROCESSES

B.E. Gelfand, S.P. Medvedev, S.M. Frolov, A.N. Polenov

Institute of Chemical Physics, Russian Academy of Sciences

Kosigin Str., 4, Moscow 117977, RUSSIA

New applications of shock tube facilities for studying combustion and explosion processes are suggested and discussed. A detailed analysis of flows in a shock tube with various combinations of geometrical parameters of tube sections and thermophysical parameters of driver and test gases revealed a whole number of specific features which may be used for the new applications. Shock tubes with super short high pressure sections allow to simulate blast waves generated by high explosives in an unconfined atmosphere. It is found that in such tubes there exists a possibility to vary a temperature profile behind a shock wave: from decaying profiles at low shock Mach numbers to profiles with a local maximum at shock Mach numbers larger than a certain critical value. This allows to investigate ignition behaviour at variable pressure and temperature. For verifying theoretical findings experimental studies were undertaken in shock tubes with high pressure section 10-100 mm long. Of particular interest is a possibility of generating rarefaction waves for simulating operation of bursting diaphragms in vented explosions. A number of examples of applying unconventional shock tubes for studying self-ignition dynamics in blast waves, fuel droplet desintegration in compression and rarefaction waves are discussed.

# **TOMOGRAPHIC RECONSTRUCTION OF VELOCITY AND PRESSURE FIELDS OF IGNITION AND EXPLOSION GAS FLOWS BASED ON INTERFEROMETRY MEASUREMENTS**

Sergei A. Abrukov, Victor S. Abrukov, Stanislav V. Ilyin

The technique for determining the total mechanical impulse and the reactive force of an incipient non-stationary gas flow, on evidence derived from interference cine films (the technique has been developed by the present authors; see, e.g., [1]), allows a reconstructive tomography problem of reconstructing velocity and pressure fields in such objects to be formulated.

A problem of this type is readily formulated directly for the DENSITY field of the mechanical impulse rather than for the gas flow velocity. The potential constituent of the field is directly related to the data from interference cine film measurements using the one-dimensional Radon transform [2]. Regarding the vortex constituent, there are similar integral equations that relate it to interference measurements and the potential component of the field.

The pressure distribution in the flow is also determined by the Radon inversion of the data obtained from processing the interference films and from particular flow density and velocity values.

The tomographic concept developed allows the distribution of velocity and pressure fields in incipient non-stationary gas flows to be determined, but its feasibility is limited to the condition that all of the non-stationary portion of the flow should fall within the interferometer's view.

The potentialities of this concept have been taken advantage of in estimating velocity and pressure fields arising from laser irradiation ignited condensed systems.

## **REFERENCES**

1. Ilyin S.V., Abrukov V.S., Abrukov S.A. - In: Flame Structure. - Novosibirsk: Nauka, 1991, Vol. 1, PP. 156-159.
2. Pikalov V.V., Preobrazhensky N.G. Reconstructive tomography in gas dynamic and plasma physics. - Novosibirsk: Nauka, 1987. - 231 p.



**POSTER SESSION AREA 3:  
Diagnostics of Combustion Processes  
of Condensed Phase Systems**

THE AGGLOMERATION OF ALUMINIUM AND COMBUSTION  
OF AGGLOMERATES IN LASER RADIATION FIELD

V. A. Bezprozvannykh, V. A. Yermakov, A. A. Razdobreev.

Scientific Research Institute of Applied  
Mathematics and Mechanics  
Tomsk - 50, GSP-14, 634050, Russia

Experimental technique for observing micro-objects (such as metal particles, oxidizers, fuel, etc.) using IR laser radiation was adopted in this study for recording detailed processes by a high-speed cinemacamera. Measurement of temperatures by means of an optical technique and a thermocouple method was conducted at the same time.

Data on investigation of agglomeration of aluminium particles with diameter of  $200-600\text{ }\mu\text{m}$  when heating by laser radiation with intensity of  $400-10^4\text{ W/cm}^2$  are reported in the paper.

Typical agglomeration pattern is described in Fig.1. Growth kinetics of contact necking in dependence on particle size is shown in Fig.2. The effect of radiation energy, medium atmosphere, oxidation level of particles are determined. Temperatures of characteristic stages of agglomeration are measured. On the basis of experimental data physical model of aluminium agglomeration is proposed.

In the framework of agglomeration the combustion of aluminium agglomerates  $200-400\text{ }\mu\text{m}$  in size with metal content of 16-40 % when heating by radiation of  $300-3000\text{ W/cm}^2$  in intensity had been investigated. Based on composed droplet and equilibrium calculation the data of the relative amount of aluminium and aluminium oxide, coefficients of surface tension was estimated. Possible influence of substrate material on the accuracy of calculations was considered. Rates of change of aluminium and alumina oxide amounts during combustion were determined.

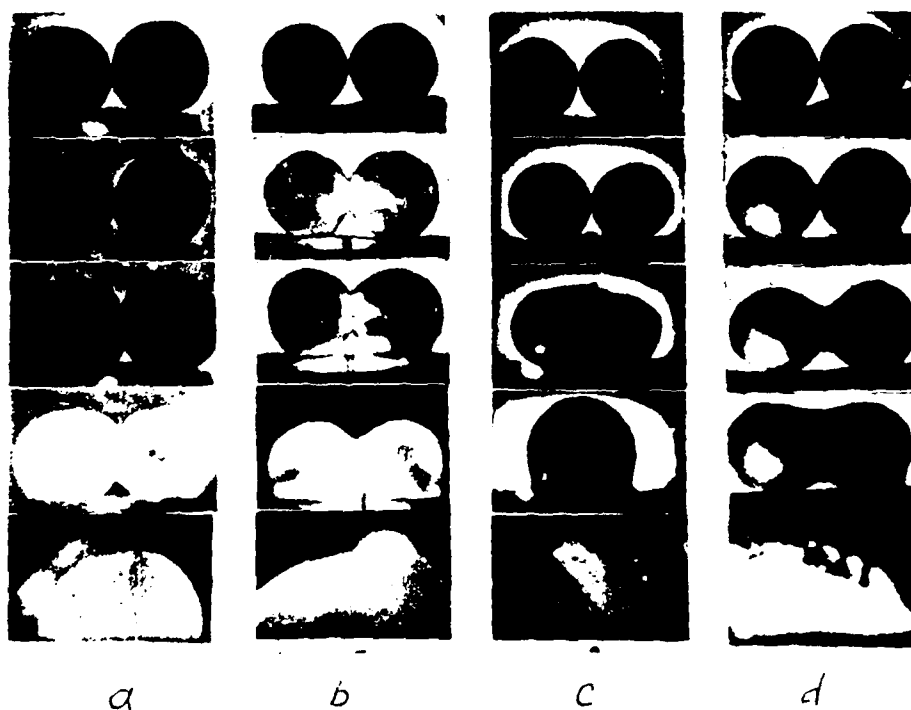


Fig.1. Typical agglomeration pattern of aluminium particles.

a,c - in air;

b,d - in helium;

c,d-after oxidizing in air ( $T=900$  K).

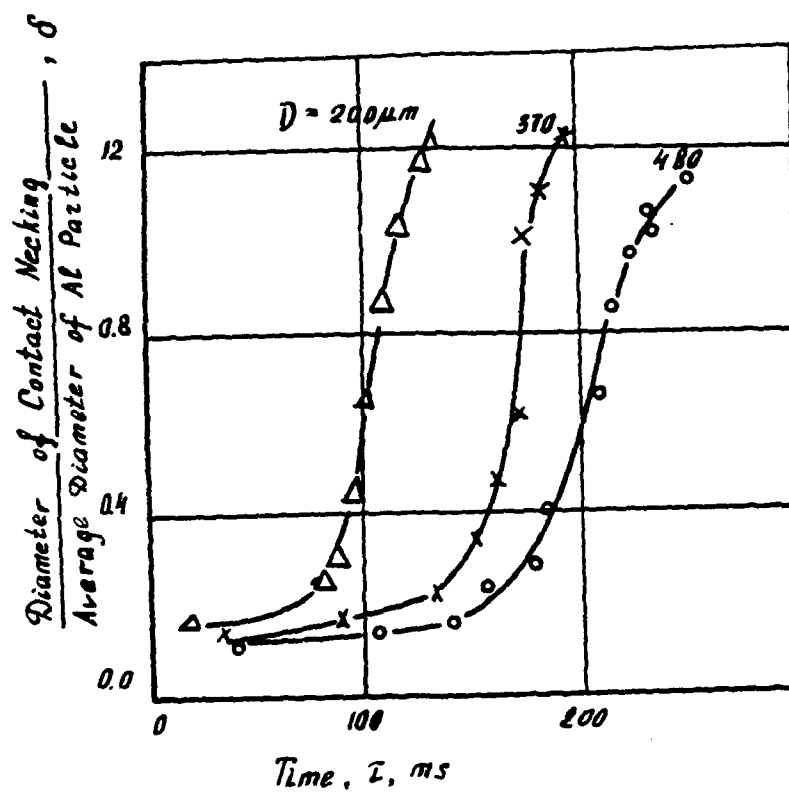


Fig. 2. The dependence of contact necking growth from particle size.

## EMISSION SPECTROSCOPY AND PYROMETRY OF PROPELLANT FLAMES AND ROCKET PLUMES

W. Eckl, N. Eisenreich, V. Gröbel, W. Liehmann, H. Schneider  
Fraunhofer-Institut für Chemische Technologie, ICT  
D-7507 Pfinztal, FRG

In propellant flames and rocket plumes, intermediates and final products emit radiation in the entire wavelength range. This radiation contains information on the concentration, temperature and reactions of the species and the particles being present. Various methods of pyrometry and spectroscopy have been applied to analyze flame and plume radiation:

- Particle temperatures

Temperatures of single particles were measured using a fast two colour pyrometer based on a Si/Ge-sandwich detector when the particles passed the area of view. The method was applied to boron particles emitted from a solid propellant surface highly filled with this fuel and to particles in the exhaust of a ram burner.

- UV/Vis-radiation

With an intensified diode array spectrometer the CO afterburning reaction has been identified. In addition the temperature measurement by fitting the overlapping continuous radiations. Emission/absorption temperature measurements were applied to transparent solid propellant flames at various pressures.

- NIR-radiation

Acusto optic tunable filters allow the realization of fast scanning spectrometers to record the radiation from 1000 to 2500 nm in ms time resolution and nm wavelength resolution. In the near infrared region mainly water emits band spectra beneath continuous grey body radiation as observed from the flame profile of a nitramine solid propellant combustion.

- IR-radiation

Fast rotating filter wheels with continuous changing wavelength transparency can acquire emission spectra in the infrared spectral region. The wavelength resolution is reduced but a robust spectrometer is obtained. The emission from flames and rocket plumes is due to water, carbon dioxide and carbon monoxide. In addition, metal oxides and partially oxidized hydrocarbons can be identified.

# THE COMPARATIVE ANALYSIS OF METHODS OF MEASURING THE NON-STATIONARY SOLID PROPELLANT BURNING RATE

V. A. Arkhipov , V. N. Vilyunov

Scientific Research Institute of Applied Mathematics  
and Mechanics, Tomsk-50, GSP-14, 634050 RUSSIA

For the development of condensed systems combustion theory, it is necessary to obtain the reliable experimental information on unsteady solid propellant burning rates. It is also of great applied importance to predict the transient processes in controlled solid propellant propulsive systems. Unlike a stationary regime, non-stationary burning rate measurements are possible only with the use of non-intrusive methods.

In this paper, a short survey of modern methods for measuring non-stationary solid propellant burning rates which are widely adopted in the works of Russian researchers will be presented. The advantages and restrictions of these methods will be discussed.

The semiempirical method of determining the non-stationary burning rate of solid propellants based on solving the inverse problem of internal ballistics (IPIB-method) has been proposed. As distinguished from a known variant of this method, published in B. T. Erokhin and O. Ya. Romanov's works, the dynamics of determining the quasi-stationary regime of outflow in opening the additional nozzle have been taken into account. An account of the last effect has been carried out on the basis of analytical, numerical and experimental analysis of generally accepted (at present time) hypothesis of quasi-stationary outflow.

The analysis of non-stationary solid propellant burning rate measurement results for a special run of experiments on the pressure drop in combustion chamber has been carried out. The measurements were carried out

by two independent methods : high-speed filming and the semiempirical method based on the inverse problem solution of internal ballistics for a semiclosed volume. The direct measurements of a pressure and the combustion products temperature in the transient process have been used while realizing the IPIB-method.

End burning charges were used in these experiments. The pressure drop was realized by opening a secondary nozzle. In the course of experiments, the quantity of a free combustion chamber volume, the diameters of main and secondary nozzle and the combustion surface area were varied.

The burning rate test data have been analyzed together with computational results on the different models of non-stationary combustion - Ya. B. Zeldovich's phenomenological theory of non-stationary combustion, B. V. Novozhilov's model with a constant and variable temperature of combustion surface as well as some models, developed by western researchers (e.g. Denison-Baum's model).

The analysis showed that the two methods of non-stationary burning rate measurement were complementary. The high-speed filming method allows the local linear burning rate to be measured, which can be substantially different from that of neighbouring combustion surface sections, thus confirming V. N. Marshakov's seat-pulsating combustion hypothesis; the IPIB-method provides the measurement of the average mass burning rate on a propellant surface.

It is necessary to take into account these parameters when analyzing the test data obtained by each of these methods. The estimation of errors and applicability boundaries of the methods considered shows the possibility of their use not only for laboratory specimens but also under firing test conditions of small-sized motors.

# CRITICAL PHENOMENA BY INTERACTION OF LASER IRRADIATION WITH REACTIVE SUBSTANCES

I.G. Assovskii

Institute of Chemical Physics, The Russian Academy of Sciences  
Kosigin St. 4, 117977 Moscow V-334, Russia

The use of laser-based diagnostic techniques to study the mechanism of fuel ignition and combustion demands the appropriate understanding of effects caused by specific properties of the laser - matter interaction, i.e. high concentration of heat flux in a small volume during finite time interval.

The purpose of this work is the theoretical analysis of heat regimes of laser beam interaction with a semi-transparent medium reacting in bulk and on the surface of contact with the environment.

Emphasis is placed on determining the temperature disturbance in medium, caused by the laser, and the critical conditions of interaction, their dependencies on chemical and optical properties of substances and on parameters of the heat flux.

The performed asymptotic analysis of the problem shows the possibility of a quasi-steady heat regim of the laser-reactive matter interaction, if the power of irradiation is smaller than critical one. This maximum power is proportional to the depth of radiation absorption and to the heat-conductivity of the irradiated substance.

The role of soot particles or other absorbing micro-inclusions is investigated. It is shown that, in the case of continuous irradiation, sufficiently large microinclusions may cause local heat explosion due to exothermic reaction.

During the pulse irradiation the largest disturbance of temperature is caused by the particles of medium size which increases with an increase of the substance heat-conductivity and the laser pulse duration.



INSTANTANEOUS BURNING RATE MEASUREMENT OF SOLID PROPELLANT  
STRAND IN 2-D MOTOR BY MEANS OF LASER SCANNING DEVICE

CHEN SHUXIANG \* ,HUANG JUN\*\*

Shaanxi Power Mechanical Research Institute  
P.O.Box 169,Xian,Postal Code 710000  
Shaanxi,People's Republic of China

The objective of this research work is to develop a technique for continuously attaining deflagration rate of solid propellant strand in a 2-D motor. Such a device, called laser scanning detector is designed, analyzed and tested.

In this device, a special made, 1.8x2mm rotating mirror is used. It is located at the focal point of a collimating lens. Laser light beam is reflected by the rotating mirror, and the collimating lens makes the beam parallel to the axis of the lens. When the rotating mirror rotates at constant angular velocity, the parallel beam scans the window of the motor at approximate constant speed. The scanning beam passes through the gas tunnel above the propellant surface, and it is stopped by the propellant strand. A penetrated light pulse is received while a scanning process. During the motor test, the propellant regresses, the gas tunnel height increases, so the penetrated light pulse becomes wider. Receiving unit of this device translate light pulse into electric pulse, then the electric pulse width is measured with the clock pulse of a singleboard-computer, and becomes a 16bits datum. data are stored in the computer RAM from PIO interface in interrupt mode of the computer. The value of single clock pulse representing gas tunnel height is demarcated before the motor test. The final results, gas tunnel heights as an intermittent function of time, are printed by a microprinter after the motor firing.

Thin metal film was used in the solid propellant motor in order that the propellant strand near the window burns faster and this device can determine the real gas tunnel heights. Window contamination of the motor is discussed in the paper.

Test results of non-aluminized AP propellant burning rates at pressure of 3.93- 4.17MPa are presented which give precision of 0.05mm.

**Influence of internal refractive index gradients on size measurements of spherically-symmetric particles by phase Doppler anemometry**

by

M. Schneider and E. D. Hirleman

*Mechanical and Aerospace Engineering Department*

*Arizona State University*

*Tempe AZ 85287-6106*

**ABSTRACT**

A model, based on geometric optics, for predicting the response of interferometric (phase-Doppler) instruments for size measurements of particles with radially-symmetric but inhomogeneous internal refractive index profiles is developed. The model and results are important for applications wherein heat and/or mass transfer from the particles or droplets is significant, for example in liquid fuel combustion. To quantify the magnitude of potential bias errors introduced by the classical assumption of uniform internal properties on phase-Doppler measurements, we have computed calibration curves for a sequence of times during the evaporation of a Decane droplet immersed in an environment of  $T = 2000\text{K}$  and  $p = 10$  bar. The results reveal considerable effects on the relation between phase difference and droplet diameter caused by the refractive index gradients present. The model provides an important tool to assess sizing uncertainties that can be expected when applying conventional (based on uniform properties) phase-Doppler calibration curves in spray combustion and similar processes.

# DETERMINATION OF EXPLOSIVE TRANSFORMATION ENERGY UNDER TRANSITION FROM COMBUSTION TO EXPLOSION OF HIGH-ENERGY MATERIALS

I.V.Kondakov, B.G.Loboiko, V.A.Rygalov

All-Russian Research Institute  
of Technical Physics,  
P.O.Box 245 Chelyabinsk-70  
454070 Russia

## ABSTRACT

While high-energy materials have been used in various propulsion systems, accident conditions can occur under which combustion of these materials leads to explosion. Determination of explosion energy for transient processes is necessary to estimate resulting effects and to take it into account during systems design, constructions and so on.

The given work presents the experimental investigations into the explosive transformation power of charges made of materials of the Type LX-07-02, located in a steel shell and having densities equal to 98% of the theoretical maximum density. The velocity of a flying plate was registered by the non-intrusive method, namely, by means of electrocontact gauges, and the relative throwing power of explosion was calculated in comparison with the detonation process.

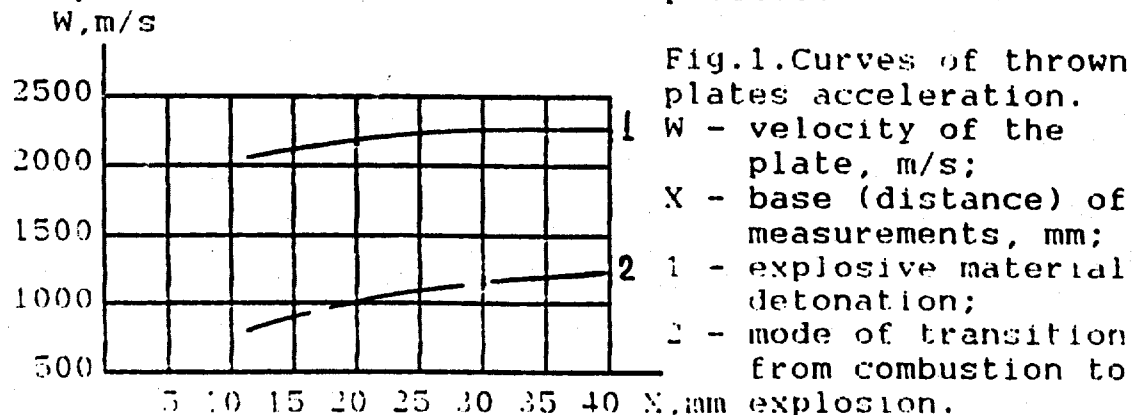


Fig.1. Curves of thrown plates acceleration.  
W - velocity of the plate, m/s;  
X - base (distance) of measurements, mm;  
1 - explosive material detonation;  
2 - mode of transition from combustion to explosion.

Fig. 1 presents the curves of the thrown plates acceleration in W-X coordinates for the case of detonation (1) and explosive transformation during the combustion process of the explosive material sample with sizes: 60 mm in diameter and 50 mm height. These curves have an identical increase in velocity ( $dW/dX$ ) on the bases (distances) equal to 25...40 mm.

While comparing them it is possible to calculate the throwing power of explosive transformation under transition from combustion to explosion, this power is approximately equal to 50% of the normal detonation case.

**COPY AVAILABLE TO DTIC DOES NOT PERMIT FULLY LEGIBLE REPRODUCTION**

EXPERIMENTAL INVESTIGATION  
OF TRANSITION FROM COMBUSTION  
TO EXPLOSION OF HIGH-ENERGY  
EXPLOSIVE MATERIALS IN A SHELL

I.V.Kondakov, B.G.Loboiko, B.V.Litvinov,  
V.A.Pestrichin

All-Russian Research Institute  
of Technical Physics,  
P.O.Box 245 Chelyabinsk-70  
454070 Russia

ABSTRACT

On the basis of the non-intrusive diagnostics of high-energy explosive materials combustion in a shell, such processes as the layer-by-layer burn-out of an explosive material charge, loss of the shell sealing with the subsequent termination of combustion and transition from combustion to explosion were investigated.

Experiments have been performed on the model explosive material charges of the type LX-07-02 being pressed to the density equal to 98% of the theoretical maximum density and located in a steel shell with holes for gases withdrawal from the combustion zone.

In the shell a membrane was mounted with its variable thickness ensuring the required calculated strength. In the experiments the clearances between the shell and the explosive material charge as well as the holes diameter and the membrane thickness have been varied. Conditions for realizing each of three processes mentioned above were achieved due to the proper combination of the variable parameters.

The layer-by-layer burn-out of explosive materials was realized while conserving the shell as well as non-spreading of combustion into clearances and possibility for exceeding the gas withdrawal over their arrival into the combustion zone. This

**COPY AVAILABLE TO DTIC DOES NOT PERMIT FULLY LEGIBLE REPRODUCTION**

phenomenon was revealed by visual inspection of the experimental arrangement after the experiment.

Under gas pressure increase in the zone of the explosive materials combustion the mode of layer-by-layer burn-out was disturbed that led to the loss of sealing of the shell due to the membrane cut and the shell break along the cylindrical generatrix. Under pressures less than the strength of the explosive material charge, the latter remained undestructed, but at higher pressures the explosive material charge was crushed (dispersed) into small pieces and dust. Combustion of explosive materials terminated and the rest of the charge scattered from the shell. This was substantiated by comparing the calculated pressure in the shell with the material strength as well as by the identification of explosive materials fragments.

The mode of transition from combustion to explosion takes place under intermediate conditions when the pressure increase rate was such that the explosive materials charge was crushed earlier than the shell and the shell scatter inertia was such that the crushed charge remained in the shell and convective combustion was developed in it with the subsequent transition into explosion.

The work points out some additional effects preventing the transition from combustion to explosion or contributing to its origin, namely, temperature effect, gluing of the explosive material charge surface, etc.

On the basis of experimental investigations and available literature data the authors show that the mechanism of transition from combustion to explosion in condensed systems of high density, including convective combustion, must involve the destruction (dispersion) of a high-density charge. However for realizing the mode of transition from combustion to explosion, such conditions are required under which the dispersed charge part scatter is limited just by the shell.

**COPY AVAILABLE TO DTIC DOES NOT PERMIT FULLY LEGIBLE REPRODUCTION**

USE OF ACOUSTIC EMISSION  
FOR INVESTIGATION INTO IGNITION AND  
COMBUSTION OF HIGH-ENERGY MATERIALS

I.V.Kondakov, B.V.Litvinov, B.G.Loborko,  
V.V.Shaposhnikov

All-Russian Research Institute  
of Technical Physics,  
P.O.Box 245 Chelyabinsk-70  
454070 Russia

ABSTRACT

During heating of high-energy explosive materials the signal of acoustic emission (AE) have been detected at the stages prior to ignition of these materials as well as in the process of their combustion in a shell.

The registered parameters, such as amplitude and intensity of AE signals, are time-dependent of processes of heating, ignition and on the character of the material combustion in a shell. AE signals are converted in a gauge based on piezoelectric ceramics, and the applied method relates to the non-intrusive diagnostics of the combustion process.

Investigations have been performed on the samples of high-energy material based on octogen of the type LX-07-02 and being pressed to the density equal to 98% of the theoretical maximum density.

Fig.1 is an example of the joint registration of temperature and AE signals under heating of an explosive material sample.

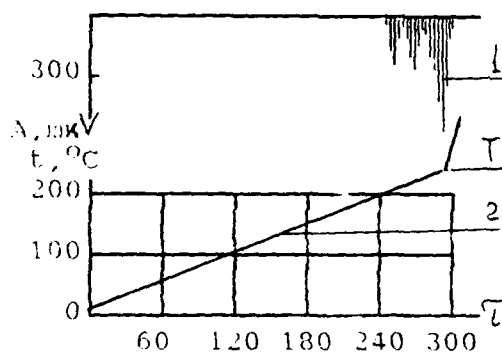


Fig. 1. Plot of registration of temperature and AE signals under heating of explosive material.  
1 - temperature registration;  
2 - AE registration;  
T - moment of ignition;  
A - AE amplitude, mV;  
t - temperature, °C;  
τ - time, s.

AE signals are generated at temperatures close to the ignition temperature (T) of the explosive material and their amplitudes reach the maximum value under explosive material ignition. It may be supposed that AE signals are generated at the processes of explosive material decomposition and microfractures which began to develop.

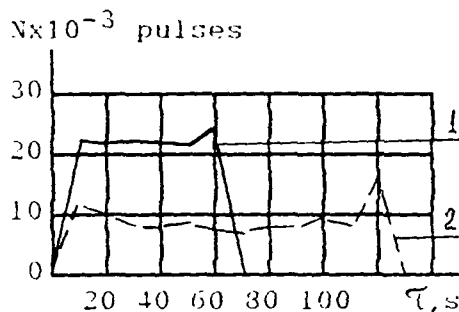


Fig. 2. Plot of registrations of AE signal intensity under explosive material combustion in a chamber with holes: 1 - 3 mm  $\phi$ , 2 - 4 mm  $\phi$ ;  
N - AE intensity, pulses;  
τ - time, s.

Fig. 2 shows the example of AE signals intensity registration during the time of high energy material burn-out in the undestructed chamber with different holes for gas withdrawal. In this case intensity of AE signals depends on the character of gas outflow through the hole determined by the character of the latter

Thus the AE method may be used for investigating the processes of thermal decomposition and high-energy materials dispersion prior to their ignition as well as the combustion processes of such materials in different constructions.



## **Sizing tolerance of non-spherical particles using a scattered light instrument compared with measurements of aerodynamic diameter**

Y Hardalupas, N G Orfanoudakis, A M K P Taylor, J H Whitelaw

*Thermofluids Section, Department of Mechanical Engineering, Imperial College, London SW7 2BX*

Pulverised solid fuelled flames are used to raise of steam in boilers and the motion of the fuel particles through the near burner recirculation zone is important to, for example, flame stability and the generation of fuel-rich regions to reduce the emissions of NO<sub>x</sub>. The motion is, in turn, dependent on the size of the particles and a number of light-scattering instruments can, in principle, provide local measurements of the optically-determined size of the particles and the corresponding velocity by combination with laser Doppler anemometry.

The sensitivity of sizing to the magnitude of the absorptive component of the refractive index, and its variation with temperature, of the particles has been quantified by calculations based on Mie theory (e.g. Holve, 1979), hence implicitly assuming that the particles are spherical. The results show that, provided predominantly diffractively scattered light is detected, then the expected inaccuracies are of the order of less than 15% (e.g. Holve and Annen, 1984). Less attention (e.g. Jones, 1993) has been paid to the effects of the non-spherical shape of the particles although Orfanoudakis and Taylor (1993) have presented calibration curves based on mechanical mounting of stationary coal particles within an instrument test volume. Their results showed that the expected tolerance was of the order of 5µm or about 10%. The result is encouraging but their experimental technique can be criticized on at least four counts. First, they could measure only a few tens of particles and, second, the generation of the signal from a stationary particle was different from the method to be used *in situ*, where the particle may pass on a number of trajectories through the sizing and pointer test volumes. Third, the method of mounting - electrostatic attraction to a glass flat - might have resulted in bias towards particle shapes amenable to this approach. Finally, the density of coal particles is known to vary from particle to particle and hence the extent to which the optically measured diameter corresponds to the aerodynamic - i.e. inertia-based - diameter is unknown.

This work address these four deficiencies. Its purpose is to quantify the accuracy and precision of the optical diameter of coal particles by comparison with independent measurements of the aerodynamic diameter. The principle of the latter (Marple & Rubow, 1976, Wilson & Liu, 1980) involved introducing a small number particles to be sized on the centreline at the upstream end of a nozzle which rapidly accelerated the air and particles. The velocity of the particles was less than that of the air at the exit by an amount which depended on the aerodynamic diameter of the particle: hence measurement of particle velocity, by a laser Doppler anemometer, together with calculation of the equation of motion of the particles as a function of diameter, provided the aerodynamic particle size. Similar work has been described by Hardalupas, Taylor & Whitelaw (1987) in the context of establishing the accuracy of a phase Doppler anemometer.

The optical system is shown in figure 1a,b and involves sizing of particles as these pass through a beam, shown in greater detail in figure 2. The amplitude of the scattered light was collected by a receiving optics and the maximum amplitude of the signal was measured by a processing system as described in detail by Orfanoudakis and Taylor (1993). The corresponding velocity was measured by a laser Doppler anemometer with the test volume placed at the centre of the sizing beam, thereby also

acting as a pointer volume to avoid trajectory ambiguity effects (e.g. Yeoman et al., 1982; Gouesbet et al., 1986) from the larger beam. The *optical-diameter* calibration curve, i.e. between the measured amplitude of scattered light and the size of the scatterer, was established using a range of precision pinholes which provided a good approximation to purely diffractive scatterers.

Figure 3 shows a typical scatter plot of measurements of maximum amplitude, in mV, and particle velocity, in m/s, at the exit of the nozzle for a pulverised coal particle mass fraction (mass flow rates of particles/air) of  $4.1 \cdot 10^{-5}$ . To make quantitative statements about the accuracy and precision of the sizing measurement, the velocity axis was divided into ten equally spaced windows. In figure 4, the measured mean values of amplitude in each of these windows are plotted: the corresponding rms values of amplitude are presented as error bars. In interpreting the statistical reliability of the measurements, the number of particles in each window is given in table 1 drawn from an artificially generated particle size distribution, using coal and seeding particles. Additionally, the calculated nozzle exit velocities for five particle diameters, found from the equation of motion of particles of density  $1000 \text{ kg/m}^3$ , given standard drag laws and knowledge of the centreline air velocity distribution within the nozzle, are also plotted. The amplitude corresponding to each size was found from the *optical-diameter* calibration curve and it should be noted that the abscissa, linear in mV, is strongly non-linear in terms of particle diameter, as the values on the right hand axis indicate. The resulting curve represents the *aerodynamic-diameter* calibration curve. Comparison between the measured and calculated curves shows that the inaccuracy varies over the size range and, at selected values of 15, 30 and  $60 \mu\text{m}$ , is about  $+2\mu\text{m}$ ,  $+7\mu\text{m}$  and  $-20 \mu\text{m}$  respectively. The corresponding values for precision are  $\pm 2\mu\text{m}$ ,  $\pm 7\mu\text{m}$  and  $\pm 10 \mu\text{m}$ . The poorer accuracy and precision associated with the  $60 \mu\text{m}$  window is at least partly associated with the low sample count of particles. An important result is that similar results, taken at the increased particle mass fraction of  $6 \cdot 10^{-4}$  resulted in values of accuracy and precision which were worse by 10% and 100%, presumably because of effects of multiple occupancy of the measuring volume and which therefore indicate the importance of introducing adequate software validation schemes to detect and reject these signals. The multiple occupancy is likely to be due to the large number of sub- $10 \mu\text{m}$  particles present in the batch of tested coal powder and, in measurements of combusting systems, these small particles will burn rapidly and hence permit reliable measurements at larger mass fractions than suggested here.

## References

- Gréhan, G, Gouesbet, G, Kleine, R, Renz, V and Wilhelmi, I, 1986. Corrected-laser beam techniques for simultaneous velocimetry and sizing of particles in flows and applications. Third International Symposium of applications of laser Doppler anemometry to fluid mechanics, Lisbon, paper 20.5
- Hardalupas, Y, Taylor, A M K P and Whitelaw, J H, 1987. Measurements in heavily-laden dusty jets with Phase-Doppler Anemometry. Second International Symposium on transport phenomena in turbulent flows, October 25-29. The University of Tokyo, Hongo, Bunkyo-ku, Tokyo 113 Japan.
- Holve, D J and Self, S.A., 1979. Optical particle counting, sizing, and velocimetry using intensity deconvolution.. Parts 1 and 2 *Applied Optics*, 18, 1632-1652.
- Holve, D J and Annen, K.D, 1984. Optical particle counting, sizing, and velocimetry using intensity deconvolution. *Optical Engineering*, 23 No.5, 591 - 603.

Jones, A R, 1993. 1993. Light scattering for particle characterization. In Instrumentation for flows with combustion (Ed. Taylor, A M K P), Academic Press, London.

Marple, V A and Rubow, K L, 1976. Aerodynamic particle size calibration of optical particle counters. *J Aerosol Sci*, 7, 425 - 433

Orfanoudakis, N G and Taylor, A M K P, 1993. The Effect of Particle Shape on the Amplitude of Scattered Light for a Sizing Instrument. *Particle and Particle System Characterisation*. In the press.

Wilson, J C and Liu, B Y H, 1980. Aerodynamic particle measurement by laser-Doppler Velocimetry. *J Aerosol Sci*, 11, 139 - 150.

Yeoman, M L, Azzopardi, B J, White, H J, Bates, C J and Roberts, P J, 1982. Optical development and application of a two colour LDA system for the simultaneous measurement of particle size and particle velocity. In Engineering Applications of laser velocimetry, Winter Annual Meeting ASME, Phoenix, Arizona.

TABLE 1.

window for measured velocity (m/s)	Total No of measurements
5.4-9.7	0
9.7-13.9	16
13.9-18.2	19
18.2-22.5	193
22.5-26.7	119
26.7-30.9	80
30.9-35.2	82
35.2-39.5	74
39.5-43.7	90
43.7-48.0	227

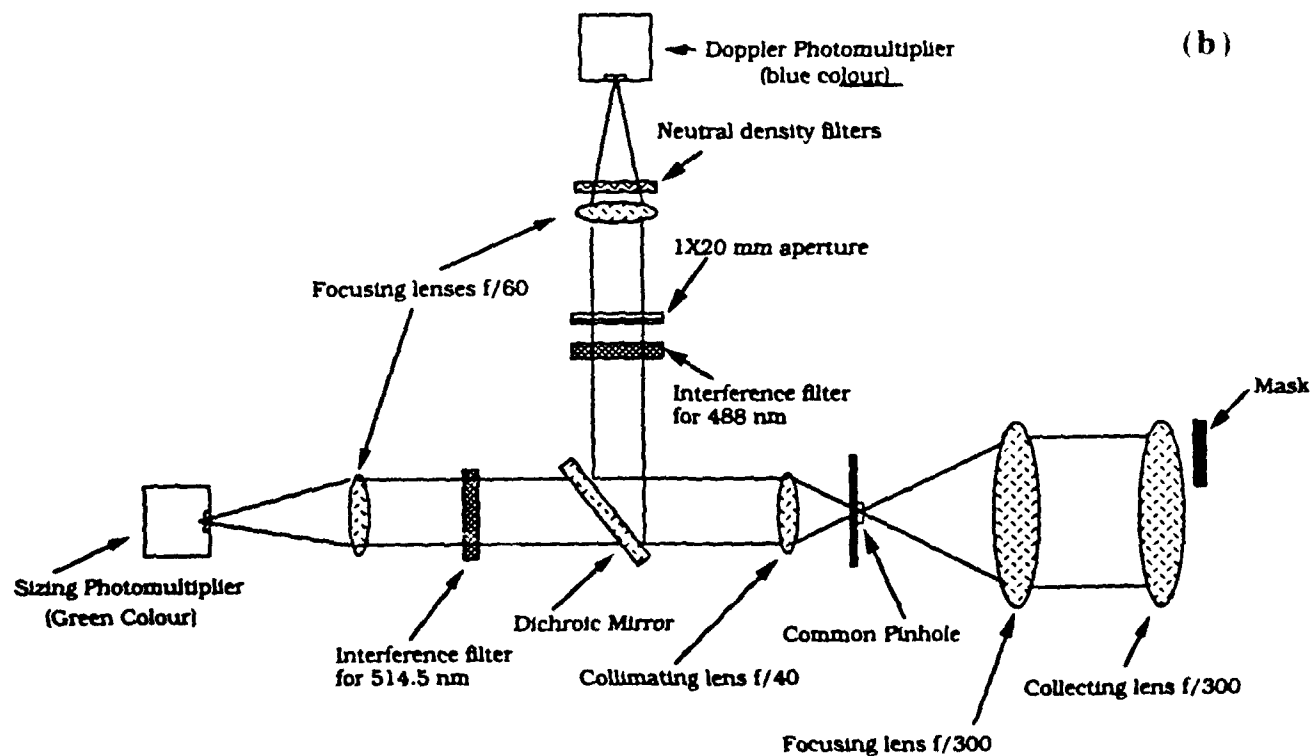
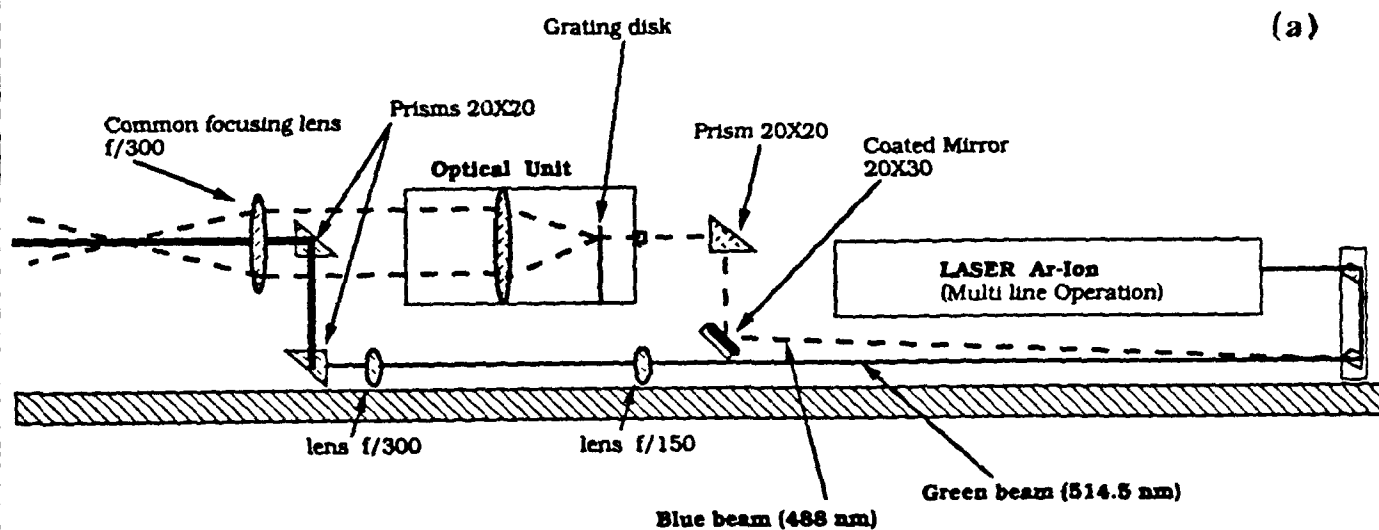


**Figure 1.**

Layout of the optical system; (a) transmitting and (b) receiving optics.

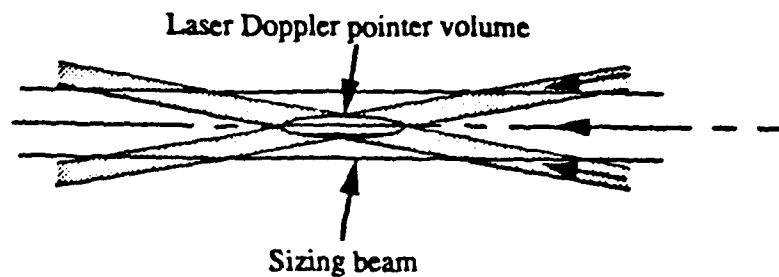


**Figure 2.**

Tested pointer volume arrangement used to eliminate trajectory ambiguity

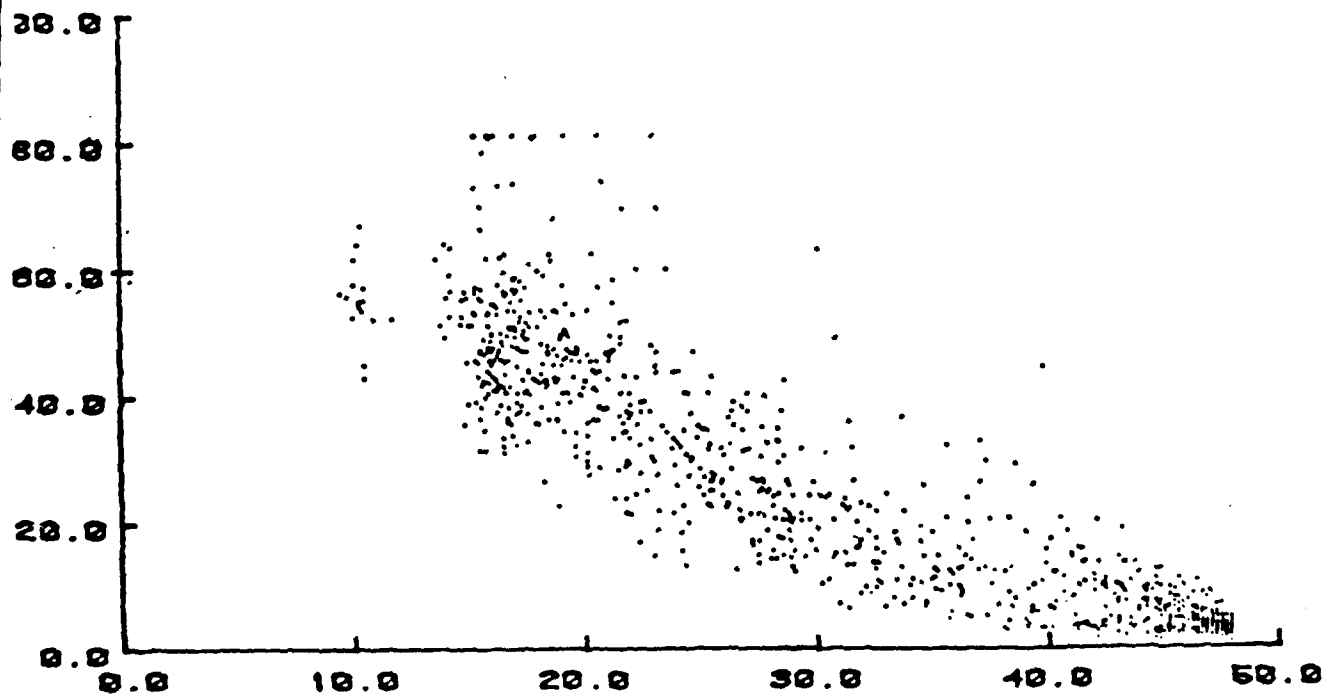


**Figure 3.**

Typical scatter plot of measured amplitude and particle velocity at the exit of the nozzle. Measurements of coal and seeding particles are shown.

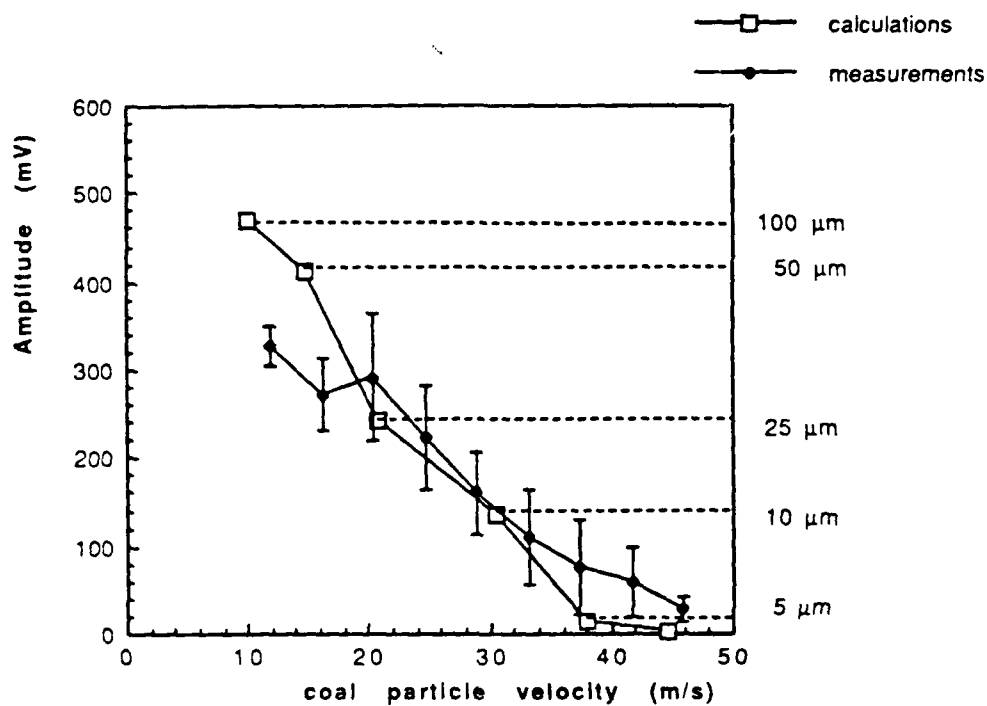


**Figure 4.**

Measured optical and aerodynamic diameters; comparison between measured and calculated particle diameters.

# ELECTRICAL DIAGNOSTICS OF CONDENSED FUELS COMBUSTION

A.N.ZOLOTKO, I.S.AL'TMAN, A.V.FLORKO, V.G.SHEVCHUK

Combustion Laboratory, Dept. of Physics, Odessa State  
University, Petra Velikogo 2, Odessa, 270100, Ukraine

The burning dispersion systems can be considered as plasma with condensed dispersion phase of combustion products.

1. The pulse method for measuring of electrophysical characteristics of condensed combustion products has been developed. This method permits to determine the net charge  $Z$  of C-phase particles, the rate of its generation and its mobilities. The typical dependence  $Z$  of  $MgO$  particles on external pressure for burning magnesium particle is shown on fig.1. This dependence has been explained, using theoretical conception given by [1]. The same results were obtained for  $Al_2O_3$ .

2. The essential difference between mobilities of condensed particles and electrons leads to the formation of the internal electric field due to ambipolar diffusion (fig.2). The role of the electrical transport in particle burning caused by this field is estimated.

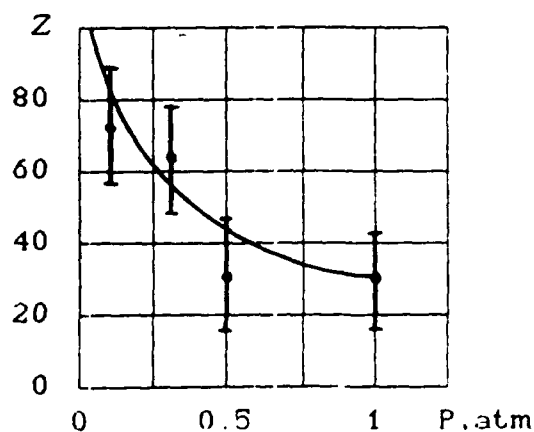


Fig.1 The dependence of  $MgO$  particles net charge on external pressure:

• - experiment,  
— - calculation

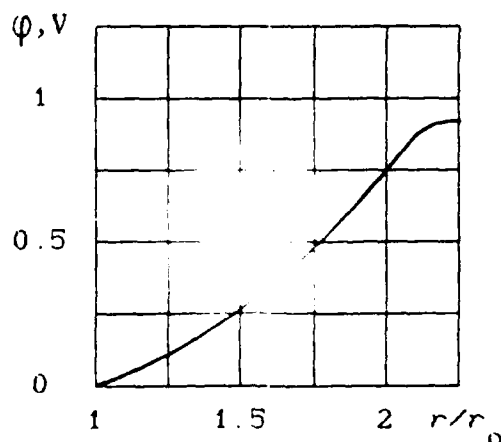


Fig.2 Distribution of the electrical potential near the burning  $Mg$  particle, ( $r_0$  - particle radius)

3. The electrical interaction between the C-phase particles causes the existence of the system natural electrical oscillation. The spectrum of such oscillation has been experimentally observed and theoretically explained. The effect of sound generation by burning particle in applied periodic electrical field had been revealed and studied. It has been shown that acoustic oscillation are conditioned by electroacoustical instability of stream tube in applied field. This stream tube is formed by charged C-phase particles frozen into gas.

4. The action of applied electric fields on burning object leads to the changing of dispersability of the end products of co-combustion, depending on the field frequency. It is caused by change of residence time of the growing condensed particle in combustion zone. It is shown in table:

$\nu$ , kHz	0	3.3	8
$\langle d \rangle$ , $\mu\text{m}$	0.11	0.075	0.05

Here  $\nu$  - the frequency of the applied field  
 $\langle d \rangle$  - the average size of MgO particles

5. The influence of uniform and nonuniform electrical fields on mass burning rate and flame structure of liquid hydrocarbon drops has been studied. It depends on soot particles content in flame. The revealed effects of field influence are caused by mechanism of ion wind.

#### REFERENCES

1. D.I.Zhuhovitskii, A.G.Hrapak, I.T.Yakubov//Chemistry of Plasma, Moscow,1984,N 11,p.130-170.



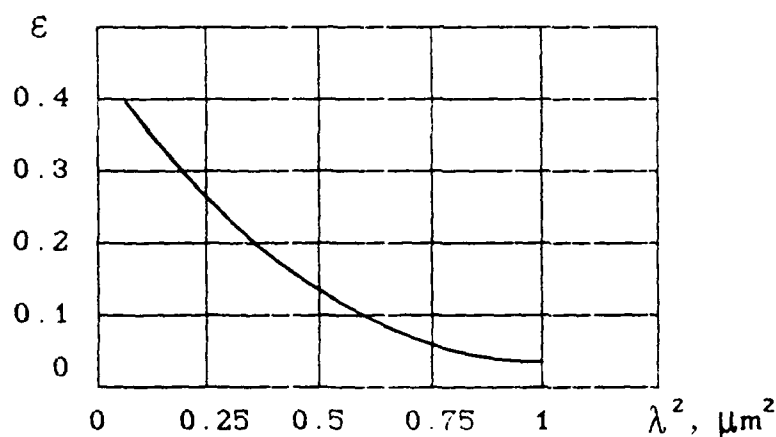
# THE METHOD OF THE END PRODUCTS OF Al AND Mg COMBUSTION DISPERSABILITY DETERMINATION BY RADIATION SPECTRUM

A.V.FLORKO,I.S.AL'TMAN,A.N.ZOLOTKO

Combustion Laboratory,Dept.of Physics,Odessa State  
University,Petra Velikogo 2,Odessa,270100,Ukraine

It is known, that spectral radiance of small particles essentially depends on its size. That leads to the dependence of particle spectral emissivity coefficient on wavelength. The kind of such dependence is defined by particle size.

The spectral radiance of condensed particles, created by Mg and Al combustion in oxygen containig media, had been measured. From obtained results the spectral emissivity coefficients of MgO and  $Al_2O_3$  particles were calculated. The typical dependence of spectral emissivity coefficient on wavelength is shown on figure:



The dependence of spectral emissivity coefficient  $\epsilon$  on  $\lambda^2$  for MgO particles

From this dependence the effective particle size had be determined (see table).On theory,this size is  $D_{eff}=(\langle D^3 \rangle / \langle D \rangle)^{1/2}$ . Moments of distribution of products of Mg and Al combustion, obtained by electron microscope, are given too. The products had spherical and cubical form, accordingly.

products	$\mu\text{m}$				
	$\langle D \rangle$	$\sqrt{\langle D^2 \rangle}$	$\sqrt[3]{\langle D^3 \rangle}$	$\sqrt{\frac{\langle D^3 \rangle}{\langle D \rangle^3}}$	$D_{\text{eff}}$
$\text{Al}_2\text{O}_3$	0,09	0,1	0,11	0,12	$0,1 \pm 0,02$
MgO	0,11	0,127	0,143	0,16	$0,18 \pm 0,03$

As it is seen, the results of different methods of  $D_{\text{eff}}$  determination are in satisfactory agreement.

Thus, the proposed method permits to determine the effective size of ultrafine particles by the G-phase radiation spectrum.

**POSTER SESSION AREA 4:**  
**Diagnostics in Practical Combustion Systems**

# Effect of the Ambient Pressure on Droplet Heating in Diesel Sprays

M. Haug and M. Megahed

Institute of Technical Thermodynamics

RWTH Aachen

(Aachen University of Technology)

Germany

## Abstract

The increase of the combustion chamber ambient pressure, which also means an increase of the ambient density, was shown to decrease the spray penetration length and increase the spray cone angle [1, 3]. The average sauter mean diameter (SMD) is also influenced by the ambient pressure. The average SMD decreases within the first 40 mm beneath the nozzle and increases further downstream by elevating the ambient pressure [1, 2]. The ignition delay is inversely proportional to the pressure in the combustion chamber. The probable ignition on set zone was found to be 20 mm to 40 mm beneath the nozzle; the higher the pressure the closer to the nozzle [4]. The effect of the ambient pressure on the heating processes of the liquid phase in diesel engines is however not known.

The heating processes of the liquid phase in a diesel spray has been recently made visible using a novel fluorescence thermometer, whose accuracy is within  $\pm 10$  K [5, 6, 7].

The present work investigates the heating processes of the first 40 mm of the spray. The results does not indicate an increase in the spray cone angle with the ambient pressure for the liquid phase. It is assumed to be significant for the vapour phase only. Further, the evaporation rate is enhanced by elevating the pressure. This is assumably due to the increase of the heat transfer surface area by decreasing the average SMD. The sensible heating phase of the liquid phase is shorter for higher ambient pressures. The higher the pressure the faster the heating process which explains the the movement of the probable ignition on set zone towards the injector when elevating the ambient pressure.

## References

- [1] R.D. Reitz and R. Diwakar, "Structure of High-Pressure Fuel Sprays," SAE Paper 870598.
- [2] H. Hiroyasu and T. Kadota, "Fuel Droplet Size Distribution in Diesel Combustion Chamber," SAE Paper 740715
- [3] A.J. Yule, S.-L. Mo, S.Y. Tham and S.M. Aval, "Diesel Spray Structure," ICCLASS-85.
- [4] F. Pischinger, U. Reuter, E. Scheid, "Self ignition of Diesel Sprays and its Dependence on Fuel Properties and injection Parameters," ASME, 88-ICE-14
- [5] H.E. Gossage, L.A. Melton, "Fluorescence Thermometers using Intramolecular Exciplexes," Applied Optics, Vol. 26, No. 11, June 1987.
- [6] R. Küfmeier and M. Megahed, "Introduction of a 2-D Temperature Measurement Technique for diesel Sprays," 24<sup>th</sup> International Symposium on Combustion, Poster Session, University of Sydney, Australia, July 5-10, 1992.
- [7] M. Megahed, "Entwicklung und Erprobung der Fluoreszenzthermometrie zur Dieselstrahldiagnostik," Ph.D. Thesis, RWTH Aachen. To be concluded end of 1992.

## 2D-LIF measurements of NO in a running Diesel engine

Th. Brugman\*, R. Klein-Douwel and J.J. ter Meulen  
Dept. of Molecular and Laser Physics, University of Nijmegen  
Toernooiveld, 6525 ED Nijmegen, The Netherlands

G. Huigen and E. van Walwijk  
Laboratory for Automotive Engineering, Technical University of Eindhoven  
P.O. Box 513, 5600 MB Eindhoven, The Netherlands

Two-dimensional distributions of NO in the combustion in a Diesel-engine are measured by LIF using a tunable Excimer laser. The cylinder is made optically accessible by mounting three quartz windows as high as possible in the cylinder wall. The pulsed laser beam is focussed into a laser sheet by means of two cylindrical lenses. Whenever the laser is tuned in resonance with a molecular transition, it causes fluorescence from a plane in the cylinder, which is recorded by a CCD-camera facing the third window in a perpendicular direction. On-line image-processing software enables an evaluation of the (live or recorded) 2D-LIF-signals.

At present the distribution of NO in the combustion is being studied at various motoring conditions and at different crank angles. The LIF from NO as it is formed just outside the edge of the flame-front of an oxy-acetylene welding torch is used for an on-line calibration of the wavelength of the laser beam. This wavelength is adjustable within a range of about 1 nm around 193 nm, employing ArF as the lasing medium. In this wavelength region NO can effectively be excited through many rotational channels of the electronic-vibronic transition:  $D^2\Sigma^+(v'=0) \rightarrow X^2\Pi(v''=1)$ . Due to quenching, however, the slightly lower level  $C^2\Pi(v=0)$  will be populated as well and the resulting fluorescence displays two sequences:  $D^2\Sigma^+(v'=0) \rightarrow X^2\Pi(v''=2,3,4,5,6)$  and  $C^2\Pi(v'=0) \rightarrow X^2\Pi(v''=1,2,3,4,5,6)$ , the strongest originating from the primary excited level. The 2D-LIF-signal is filtered by an adjustable band-pass filter (bandwidth 14 nm and centered around 216 nm) for an enhancement of the (S/N)-ratio.

The test-engine is a 4-stroke air-cooled one-cylinder indirectly injected Diesel engine (HATZ-Samofa) with a swept volume of 567 cc (bore 85 mm, stroke 100 mm). The synchronisation of the laser pulses to the running engine is performed by an opto-electronic device which continuously monitors the rotations of the cam-shaft. The resolution is about  $0.6^\circ$  and since in a 4-stroke engine the crank rotates at twice the speed of the cam-shaft, the error made in the crank angle is found to be  $1.2^\circ$ . In spite of the fact that the main constituents of Diesel fuel are not transparent to UV-radiation, both n-heptane and Diesel fuel are used in these measurements. The engine is lubricated by an unconventional UV-transparent, non-flammable and chemically inert lubricant, thereby extending the measurements themselves to an almost unlimited period of time. A miniature pressure transducer mounted in the wall of the swirl chamber permits the on-line monitoring of the pressure as well as the temperature, thus allowing the motoring conditions to be recorded simultaneously with the above-mentioned signals.

# A COMPARISON OF SOME OPTICAL AND SPECTROSCOPIC NON-INTRUSIVE DIAGNOSTICS METHODS IN COMBUSTION SYSTEMS

Y.M. Timnat  
Department of Aerospace Engineering  
Technion I.I.T.  
Technion City, Haifa 32000, Israel

Non-intrusive techniques for combustion diagnostics include optical and spectroscopic measurements of temperature, velocity, density and composition of the combustion products, as well as particle size and concentrations measurements; microwave measurements of burning rate and detonation velocity fall also in this category. Microwave and infrared radiation are of course included in the term spectroscopy. I shall emphasize particularly those methods in which I took an active part.

In chemical rockets remote sensing methods for the measurements of temperature are preferred, because of the high levels (over 3000 K) that may be reached. One of the early techniques employed is the line reversal method, described in detail by Gaydon and Woltwardt<sup>1</sup>. They estimate that for temperatures below 1800 K an overall accuracy within 10 K can be achieved, which becomes lower at higher temperatures. Helman and Timnat<sup>2</sup> applied the line-reversal technique to high temperature measurements in a two-dimensional hybrid rocket motor using three wavelengths (433, 533 and 590 nm); they obtained temperature traverses in the range 1800-3500 K with an estimated accuracy between 1 and 2% (see Fig. 1). By employing appropriate focusing they obtained good spatial resolution, while the classical method gives only an average value of the temperature. They showed that this technique can also be used to evaluate gas velocity.

Other non-intrusive methods for temperature measurements are spontaneous Raman scattering (see Eckbreth<sup>3</sup> and Johnston et al.<sup>4</sup>), which is an inelastic process; Rayleigh thermometry, based on the elastic photon-molecule interaction (Rayleigh scattering), which was used successfully by Dibble and Hollenbach<sup>5</sup> for a range between 700 and 2500 K. Coherent anti-Stokes Raman scattering (CARS) allows to determine temperature by analyzing the slope of the CARS spectrum. This can be performed, also for non-stationary combustion, see Eckbreth et al.<sup>6</sup>. CARS also allows to determine major species concentrations in a flame as shown by Eckbreth<sup>3,6</sup>, Dibble<sup>4,5</sup> and Taran and coworkers<sup>7,8</sup>.

Neer and Drewry<sup>9</sup> developed a technique for studying supersonic combustion flow fields by means of a rapid scanning spectrometer, which uses the hydroxyl radicals present in the combustion products of hydrogen-air flames they investigated. By exploiting an original graphical inversion technique, they inferred from the OH spectra temperatures and number densities. Logan and coworkers<sup>10,11</sup> employed laser induced fluorescence (LIF) to measure simultaneously temperature and density. The groups of Cattolica<sup>12,13</sup> and Hanson<sup>14,15</sup> exploited this technique for measuring temperature and species concentration obtaining high space and time resolution.

Ray and Semerjian<sup>16</sup> used laser tomography, based on multiangular absorption spectroscopy, for the simultaneous measurement of temperature and species concentration in reacting flows. They achieved an accuracy of  $\pm 3\%$  without filtering the noise and  $\pm 1.8\%$  with filtering. Their temporal resolution was 10 microseconds. Zoltani and White<sup>17</sup> developed flash x-ray tomography for diagnostics of microsecond phenomena and applied it to the interior ballistics of a gun.

Velocity and particle size measurements can be obtained by various laser methods. The one most widely used for measuring velocity is still laser Doppler anemometry (LDA), described in great detail by Durst and coworkers<sup>18</sup>. Greenberg and Timnat<sup>19</sup> applied it already in 1980 to the mean flow velocity in a ram-rocket combustor. Sislian et al.<sup>20</sup> employed it to measure mean velocity components, turbulence intensity, velocity PDFs and spatial turbulence macroscale. Timnat and Levy<sup>21</sup> used the so-called pedestal method for the simultaneous measurement of particle diameters and velocities in two-phase flows. This method is based on the linear relation existing between the particle diameter and the pedestal amplitude characteristic of the LDA signal and can be applied in a range from about 0.1 to 800  $\mu\text{m}$  with velocities up to 600 m/s. The system comprises two photodetectors, aligned on the two beams issuing from a 15 mW HeNe laser, which detect the droplet path inside the control volume (see Fig. 2) and allow only signals crossing the center of the control volume to be detected. Some measurements of the mean and r.m.s. velocities in two-phase flow are shown in Fig. 3.

Another technique for obtaining simultaneously velocity and particle size in a two-phase flow is phase Doppler anemometry (PDA), also employed by Levy and Timnat<sup>22</sup>. This method shown in Fig. 4 makes use of an interferometric pattern generated by drops crossing at the control volume, which is defined by two coherent laser beams. The shape of the pattern depends on the particle diameter and the index of refraction. Detecting some characteristics of the interferometric pattern, by recording of information in the time domain, enables the drop diameter to be determined.

When all particles fulfill the conditions of sphericity and smoothness (f.i. liquid sprays, both reacting and non-reacting) the phase Doppler technique is more accurate, it has also a wide size range, its lower limit being 1-3  $\mu\text{m}$ , due to diffraction phenomena. For particles having arbitrary shape or in the presence of impurities, the pedestal technique should be used, although its accuracy is lower.

## REFERENCES

1. Gaydon, A.G. and Wolfhard, H.G., *Flames - Their Structures, Radiation and Temperature*, Chapman and Hall, 1979.
2. Helman, D. and Timnat, Y.M., *Progr. Astron. Aeron.*, **53**, 267-277, AIAA, 1977.
3. Eckbreth, A.C. 18th Symp. (Intern.) on Combustion, 1471-1488, 1981.
4. Johnston, S.C., Dibble, R.N., Shafer, R.W., Amhurst, W.T. and Kollmann, W., *AIAA J.*, **24**, 928-937, 1986.
5. Dibble, R.W. and Hollenbach, R.F., 18th Symp. (Intern.) on Combustion, pp. 1489-1499, 1981.
6. Eckbreth, A.C. Bonczick, P.A. and Verdieck, S.F., *Prog. Energy Combust. Sci.*, **5**, 253-322, 1979.
7. Regnier, I.R. and Taran, J.P.E., *Appl. Phys. Lett.* **23**, 240-241, 1973.
8. Moya, F., Druet, S., Péalat, J. and Taran, J.P.E., *Progr. Astron. Aeron.*, **53**, 549-574, 1977.



9. Neer, M.E. and Drewry, J.F., *Progr. Astron. Aeron.*, **53**, 227-242, 1977.
10. Logan, P., *Progr. Astron. Aeron.*, **112**, 116-140, 1987.
11. Logan, P., McKenzie, R.L. and Bersheder, D., *AIAA J.*, **26**, 316-322, 1988.
12. Cattolica, R.J. and Stephenson, P.A., *Progr. Astron. Aeron.*, **95**, 714-721, 1985.
13. Cattolica, R.J. and Vosen, S.R., 20th Symp. (Intern.) on Combustion, 1273-1282, 1985.
14. Kychakoff, G., Hanson, R.D. and Have, R.B., 20th Symp. (Intern.) on Combustion, 1265-1272, 1985.
15. Lee, M.P., Paul, P.H. and Hanson, R.D., *Optics Lett.*, **12**, 15-17, 1987.
16. Ray, S.R. and Semerjian, H., *Progr. Astron. Aeron.*, **92**, 300-324, 1984.
17. Zoltani, C.K. and White, K.J., *Progr. Astron. Aeron.* **95**, 700-713, 1984.
18. Durst, F., Melling, A. and Whitelaw, J.H., *Principles and Practice of Laser Anemometry*, 1981.
19. Greenberg, J.B. and Timnat, Y.M., 5th ISABE, Paper 29a, 1981.
20. Sislian, J.P., Liang, L.Y. and Cusworth, R.A., UTIAS Rep. No. 291, 1986.
21. Timnat, Y.M. and Levy, Y., *Proc. 15th Intern. Symp. Shock Waves Tubes*, 587-593, 1986.
22. Levy, Y. and Timnat, Y.M., *Progr. Astron. Aeron.*, **113**, 387-402, 1988.

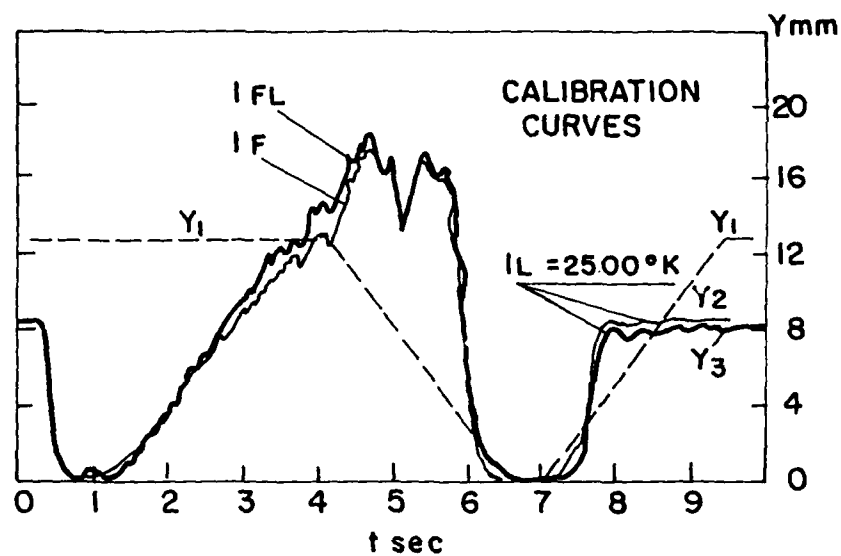


Fig. 1. Experimental radiation curve for polyester-oxygen system, utilizing the line reversal technique<sup>2</sup>.

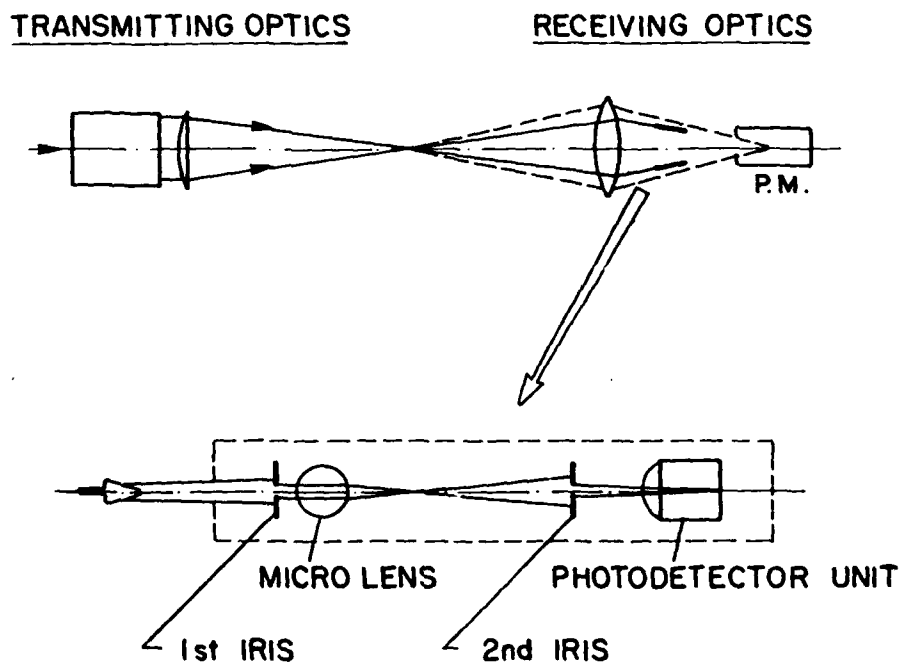


Fig. 2. LDA flow speed and particles size measurement<sup>21</sup>.

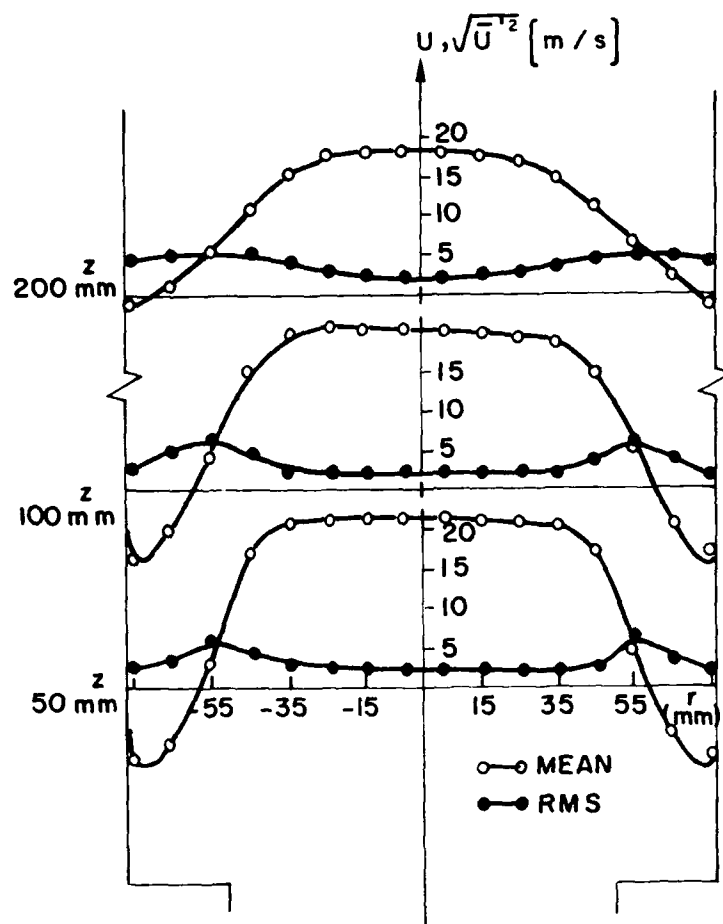


Fig. 3. Mean and r.m.s. velocity measurement by LDA<sup>22</sup>.

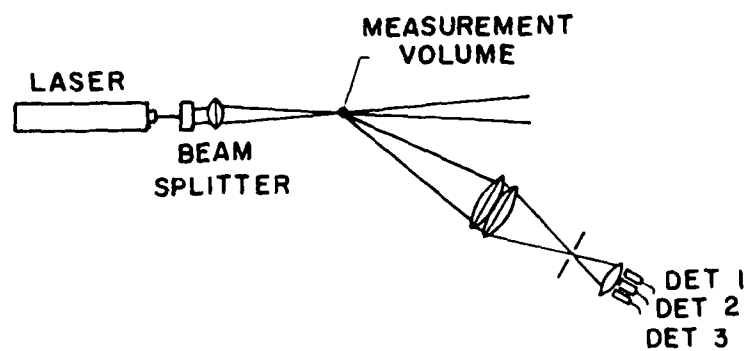


Fig. 4. PDA optical system.

# ANALYSIS OF THE IGNITION SEQUENCE OF A MULTIPLE INJECTOR COMBUSTOR USING PLIF IMAGING

Keith McManus<sup>†</sup>, Brandon Yip<sup>\*</sup>, Frédéric Aguerre and Sébastien Candel

Laboratoire EM2C, CNRS, Ecole Centrale Paris,  
92295 Chatenay-Malabry, France

**Abstract.** The ignition sequence is of critical importance in many practical devices and specifically in propulsion applications. In modern cryogenic liquid rocket engines hot gases delivered by a small solid propellant generator are exhausted into the chamber and initiate flame kernels in the injected streams adjacent to the motor axis. The flame then propagates to the surrounding injectors which are progressively ignited. As the reactant streams are successively ignited the pressure in the chamber rises and reaches the design value when all the injected streams are made to react and a flame is stabilized in the chamber. The pressure rise is often accompanied by pulsations associated with a low frequency instability which vanishes when the nominal operating point is reached. A failure in the ignition process has serious consequences. In some cases the successive rows of injectors are not only partially ignited and the motor does not reach the projected thrust. In other circumstances the ignition delay is too long and a violent pressure rise is obtained resulting in flame blow-off or engine damage. In standard practice the ignition sequence is devised according to empirical rules founded on accumulated knowledge and experiments. Indeed it has been difficult to characterize the mechanism in real engines because of the lack of access to the chamber. However it appears possible to gather fundamental ideas on the process by performing experiments on a model device allowing adequate optical access. Because the whole sequence takes only a few milliseconds and the flow velocities are high, high speed imaging techniques are required. Under these circumstances the development of the reaction zone is best characterized either by imaging the light emission from free *OH* radicals produced by the chemical reaction or by making use of planar laser induced fluorescence (PLIF) of these radicals. A research program has been recently completed with the two methods. Images of the ignition sequence were obtained on a multiple injector nonpremixed combustor fed with hydrogen and air. Reconstructed image sequences indicate how the flame kernels are initiated and successively propagate from one injector to the next. This article describes the experimental methods and a set of results obtained in this investigation.

<sup>†</sup> Current address : Physical sciences Inc., Andover MA, 01810, USA

<sup>\*</sup> Current address : Department of Mechanical Engineering, Stanford University, Stanford CA.94305, USA

# Diesel Soot Characterization Based on Simultaneous Measurement of Polychromatic Scattering and Extinction

F.E.Corcione, O.Monda, B.M.Vaglieco  
Istituto Motori, CNR-Naples-Italy

High efficiency of diesel engines and their ability to burn heavy fuels make them of great interest in transportation field. On the other hand, present exhaust emission level produced by this type of engines will not satisfy stringent international law on environment protection. The way towards the reduction of diesel particulate emissions must necessarily go through the knowledge of intrinsic structure and radiative properties of diesel soot.

In this poster we report real time and nonintrusive technique that has been applied in an undiluted exhaust volume of a d.i. diesel engine. Multiwavelength measurements of scattering and extinction coefficients from the near ultraviolet to visible are carried out to evaluate the size, concentration and volume fraction as well as spectral refractive index of diesel soot particles. The optical measurements in the near ultraviolet spectral region are particularly promising because both graphite and large aromatic molecules exhibit absorption bands between 200 and 350nm.

The spectral measurements of scattering, at  $90^\circ$ , and extinction were performed at different engine speeds and air-fuel ratios. In figure 1 the experimental set up is displayed. The scattering coefficients for different air-fuel ratios at a fixed rpm have the behaviour shown in figure 2. These spectra show a sharp peak around 250 nm, typical of carbonaceous material, and an intensity decrease at longer wavelengths. A variation in the slope was observed changing the air-fuel ratios, probably due to change in chemical composition of particulate.

An study of the growth of soot particle has been made by comparing experimental data with the numerical simulation for random shape aggregates and for equivalent diameter spheres.

Implications and limitations of both experimental technique and theoretical models have been considered.

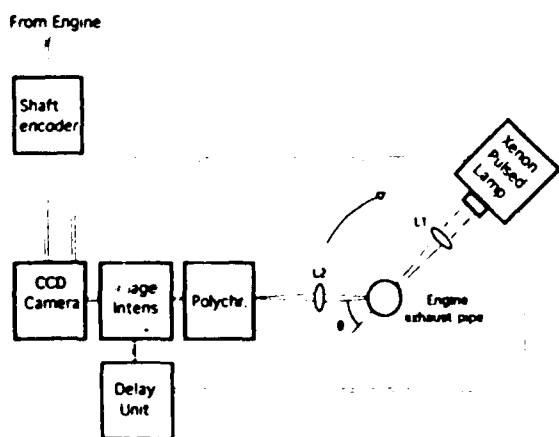


Fig.1 Experimental set-up

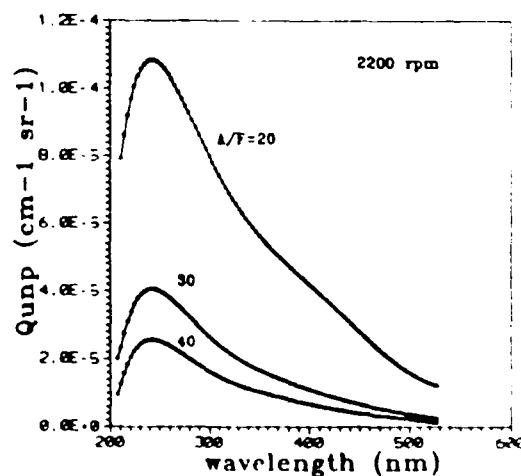


Fig.2 Spectral scattering coefficients at  $90^\circ$  for A/F

<u>Author</u>	<u>Session Number / Paper Poster Number</u>	<u>Page Number</u>
Abrukov, V. S.	PP-2.8	177
Abrukov, S. A.	PP-2.8	177
Aguerre, F.	PP-4.4	213
Akiba, R.	R-7	87
Al'tman, I. S.	PP-3.11, PP-3.12	200, 202
Arkipov, V. A.	PP-3.3	183
Assovskii, I. G.	R-7, PP-3.4	85, 185
Asthana, S. N.	R-5	52
Bar-Ziv, E.	R-2	22
Belozerova, E. V.	PP-2.3	168
Beyer, R. A.	R-6	59
Bezprozvannykh, V.A.	PP-3.1	179
Birk, A.	R-10	138
Bodart, V.	R-2, R-7	26, 90
Böhm, M.	R-3	32
Bombach, R.	PP-1.2	153
Bouchardy, P.	PP-1.6	160
Brill, T. B.	I-6	7
Brüggemann, D.	R-3	39
Burch, R. L.	R-8, R-10	95, 139
Candel, S.	PP-4.4	213
Cauty, F.	R-5	53
Char, J.-M	PP-2.1	162
Chastenet, J. C.	R-7	90
Chen, D. M.	R-3	35
Chen, S.	R-2, PP-3.5	30, 186
Cheung, F. B.	R-8, R-10	95, 139
Clauß, W.	R-3	32
Collin, K. H.	R-2	20
Collin, G.	PP-1.6	160
Corcione, F. E.	PP-4.5	214
Cottureau, M.-J	R-4	45
Darabiha, N.	PP-2.6	173
de Goey, L.P.H.	R-9	131
Démarais, J. Cl.	R-5	53
Deniges, Y.	R-10	143
Dhar, S. S.	R-5	52
Dibble, R.	I-8	10
Djavdan, E.	PP-2.6	173
Domingues, E.	R-4	45
Durst, F.	I-2	3
Dyakov, I. V.	PP-2.3	168

<u>Author</u>	<u>Session Number / Paper Poster Number</u>	<u>Page Number</u>
Eckbreth, A.C.	I-3	4
Eckl, W.	R-7, PP-3.2	89, 182
Eisenreich, N.	R-7	89
Erades, Ch.	R-5	53
Fedorov, E. Yu.	R-8	107
Feikema, D.	R-4	45
Felder, W.	R-2	23
Ferrão, P.	R-9	116
Fischer, M.	PP-1.3	154
Florko, A. V.	PP-3.11, PP-3.12	200, 202
Frolov, S.M.	PP-2.7	176
Fujiwara, T.	PP-1.5	158
Gany, A.	R-2	28
Gelfand, B. E.	PP-2.7	176
Giesen, U.	R-3	39
Gimbre-Celerg, M.	R-10	143
Grisch, F.	PP-1.6	160
Gröbel, V.	PP-3.2	182
Guerra, R.	R-9	113
Hadar, I.	R-2	28
Haibel, M.	R-9	109
Hanson, R. K.	I-1	2
Hanson-Parr, D. M.	I-7	8
Hardalupas, Y.	PP-3.10	194
Hassel, E. P.	R-9, PP-1.1	120, 150
Haug, M.	PP-4.1	205
Heitor, M. V.	R-9	116
Hemmerling, B.	PP-1.2	153
Heshe, S.	R-3	39
Hirleman, E.	PP-3.6	187
Hsieh, W. H.	R-2	23
Hsu, Y. T.	R-3	35
Huang, J.	PP-3.5	186
Huang, I. T.	R-8	100
Huigen, G.	PP-4.2	207
Ilyin, S. V.	PP-2.8	177
Ineichen, B.	R-8, R-9, PP-1.4	98, 129, 156
Janicka, J.	R-9, PP-1.1	120, 150
Kadota, T.	R-1	16
Kato, K.	R-5	48
Kienle, R.	R-4	42, 43

<u>Author</u>	<u>Session Number / Paper Poster Number</u>	<u>Page Number</u>
Kimura, M.	R-5	48
Klein-Douwel, R.	PP-4.2	207
Kline, M. C.	R-8	95
Kneer, R.	R-2	20
Knystautas, R.	R-6	80
Kobayashi, K.	R-5	48
Kodimer, K. A.	R-10	142
Kohno, M.	R-5, R-7	48, 87
Kohse-Höinghaus, K.	I-4, R-1, R-4, R-4	5, 14, 42, 43
Kondakov, I. V.	PP-3.7, PP-3.8, PP-3.9	188, 190, 192
Konnov, A. A.	PP-2.3	168
Kotlar, A. J.	R-6	59
Kreutner, W.	PP-1.2	153
Krishnan, T.E.	R-7	82
Kuo, K. K.	I-5, R-2, R-5, R-8, R-8, R-10	6, 23, 49, 95, 100, 139
Kurian, A. J.	R-7	82
Kurtz, A.	R-3	39
Kutsenogii, K. P.	R-8	107
Lai, W. Z.	PP-1.5	158
Lamarque, P.	R-10	143
Lee, J. J.	R-6	80
Lee, J.H.S.	R-6	80
Lee, Y. P.	R-3	35
Lee, M. P.	R-4, R-4	42, 43
Leipertz, A.	R-10	145
Liehmann, W.	A-7, PP-3.2	89, 182
Lipp, F.	R-9	120
Litvinov, B. V.	PP-3.8, PP-3.9	190, 192
Loboiko, B. G.	PP-3.8, PP-3.9	190, 192
Lu, Y. C.	R-5	49
Magens, E.	PP-1.3	154
Magre, P.	PP-1.6	160
Mandel, B.	R-8	98
Mann, B. A.	PP-2.4	171
Mavliev, P. A.	R-8	107
Mayinger, F.	R-9	109
McManus, K.	PP-4.4	213
McQuaid, M. J.	R-10	138
Medvedev, S. P.	PP-2.7	176
Megahed, M.	PP-4.1	205
Meier, U. E.	R-1, R-4	14, 43
Meier, W.	R-1	13



<u>Author</u>	<u>Session Number / Paper Poster Number</u>	<u>Page Number</u>
Miyoshi, K.	R-1	16
Müller, R.	R-9, PP-1.4	129, 156
Münich, K. U.	R-10	145
Nadziakiewicz	PP-2.2	165
Nazare, A. N.	R-5	52
Nelson, , R. S.	R-10	142
Neuber, A. A.	PP-1.1	150
Ninan, K. N.	R-7	82
Nisenreich, N.	PP-3.2	182
Ogden, T. R.	R-10	142
Orfanoudakis, N. G.	PP-3.10	194
Oschwald, M.	R-9	113
Parnell, L. A.	R-10	142
Parr, T.	I-7, R-8	8, 92
Pavlasek, T.J.F.	R-6	80
Péalat, M.	PP-1.6	160
Pearson, I. G.	PP-2.4	171
Perng, H. C.	R-3	35
Pestrichihin, V. A.	PP-3.8	190
Polenov, A.N.	PP-2.7	176
Proctor, D.	PP-2.4	171
Prucker, S.	R-1	13
Ramachandran, L.	R-7	82
Rao, S. S.	R-7	82
Razdobreev, A. A.	PP-3.1	179
Rolon, J. C.	PP-2.6	173
Rudolph, A.	R-3	32
Rygalov, V.A.	PP-3.7	138
Saima, A.	R-6, R-6	61, 67
Schadow, K.	R-8	92
Schneider, M.	PP-3.6	187
Schneider, H.	PP-3.2	182
Schwan, F.	R-5	49
Sennoun, M. H.	PP-2.6	173
Shaposhnikov, V. V.	PP-3.9	192
Shevchuk, V. G.	PP-3.11	200
Shibata, T.	R-7	87
Shoji, H.	R-6	67
Shrotri, P.G.	R-5	52
Singh, H.	R-5	52
Smeets, G.	R-9	126
Smirnov, N. N.	PP-2.5	172

<u>Author</u>	<u>Session Number / Paper Poster Number</u>	<u>Page Number</u>
Söntgen, R.	R-3	32
Souletis, J.	R-2	26
Stricker, W.	R-1	13
Strube, G.	R-9	109
Stufflebeam, J. H.	I-3	4
Taylor, A.M.K.P.	PP-3.10	194
ter Meulen, J. J.	PP-4.2	207
Thynell, S. T.	R-8	100
Tieng, S. M.	PP-1.5	158
Timnat, Y. M.	PP-4.3	208
Tokudome, S.	R-7	87
Tsue, M.	R-1	16
Tyurnikov, M. V.	PP-2.5	172
Vaghjiani, G. L.	R-6	78
Vaglieco, B. M.	PP-4.5	214
van de Velde, R.	R-9	131
van Walwijk, E.	PP-4.2	207
van Maaren, A.	R-9	131
Vanderhoff, J. A.	R-6	59
Vilyunov, V. N.	PP-3.3	183
Volpi, A.	R-5, R-7	55, 87
Waidmann, W.	R-9	113
Wang, H. C.	R-3	35
Wang, J.	R-2	30
Watanabe, H.	R-6	67
Weiss, Y.	R-2	22
Whitelaw, J. H.	PP-3.10	194
Wijchers, T.	R-8	104
Willmann, M.	R-2	20
Winandy, A.	PP-1.3	154
Wittig, S.	R-2	20
Woodward, R. D.	R-8, R-10	95, 139
Yeh, C. L.	R-2	23
Yeh, J.-H.	PP-2.1	162
Yermakov, V.A.	PP-3.1	179
Yim, Y. J.	R-5	49
Yip, B.	PP-4.4	213
Yoshida, K.	R-6	61
Yu, K.	R-8	92
Zanotti, C.	R-5	55
Zarko, V.E.	I-5	6
Zeitler, R.	R-2	20
Zhang, X.	R-2	30
Zolotko, A. N.	PP-3.11, PP-3.12	200, 202